ISBN 978-82-471-1283-0 (printed ver.)
ISBN 978-82-471-1284-7 (electronic ver.)
ISSN 1503-8181

Kristin Hilde Holmøy
Doctoral Thesis

Doctoral Theses at NTNU, 2008:291

Kristin Hilde Holmøy

Significance of geological parameters for predicting water leakage in hard rock tunnels

NTNU
Norwegian University of
Science and Technology

Doctoral Theses at NTNU, 2008:291

NTNU
Norwegian University of
Science and Technology
Thesis for the degree of
philosophiae doctor
Faculty of Engineering Science and Technology
Department of Geology and Mineral Resources Engineering

NTNU
Norwegian University of
Science and Technology

Kristin Hilde Holmøy

Significance of geological parameters for predicting water leakage in hard rock tunnels

Thesis for the degree of philosophiae doctor

Trondheim, December 2008

Norwegian University of
Science and Technology
Faculty of Engineering Science and Technology
Department of Geology and Mineral Resources Engineering

NTNU
Norwegian University of
Science and Technology

NTNU
Norwegian University of Science and Technology

Thesis for the degree of philosophiae doctor

Faculty of Engineering Science and Technology
Department of Geology and Mineral Resources Engineering

ISBN 978-82-471-1283-0 (printed ver.)
ISBN 978-82-471-1284-7 (electronic ver.)
ISSN 1503-8181

Doctoral Theses at NTNU, 2008:291

Printed by Tapir Uttrykk

Abstract

One of the most challenging aspects of tunnelling is prognostication of water leakages. Successful prediction of groundwater inflow would result in considerable economical saving in construction costs for future tunnel projects and give possibility for preventing potential damage to nearby environment and constructions.

The prime objective has been to test hypotheses regarding the significance of geological parameters to predict water leakage in tunnels, and the secondary objective to evaluate the ability of site investigations to prognosticate water leakage in tunnels.

Six Norwegian tunnels with different geological conditions have been selected for this research; the Romeriksporten, Frøya-, T-baneringen-, Lunner-, Skaugum- and Storsand tunnels. Based on detailed study of these tunnels, main focus has been on testing the following hypotheses:

1. The water leakage is lower in rock mass with Q-values lower than 0.1, than in rock mass with Q-values between 0.1 and 10.
2. Water-bearing joints make an angle with nearby major faults of $45° \pm 15°$.
3. Water-bearing discontinuities are sub-parallel with the largest principal stress.
4. Water leakage decreases with increasing rock cover.
5. Great thickness of permeable soil or a lake/sea above a tunnel gives high water leakage.
6. Igneous rocks give higher water leakage than other rock types.
7. Major rock type boundaries give high water leakage.
8. Large weakness zones give higher relative water leakage (inflow per 25 m) than narrow weakness zones.

Encountered water leakages along the tunnels have been calculated for each 25 m long section, and compared with relevant geological parameters, in order to test the hypotheses. Results from site investigations carried out prior to and during excavation have been compared with water leakage encountered in the 6 tunnels that have been studied. An evaluation of the ability of site investigations to prognosticate water leakage in tunnels has been made for each tunnel.

The Main conclusions regarding water inflow versus geological parameters are as follows:

- Hypotheses No. 1, 3, 5 (regarding lake above tunnel) and 7 are supported.
- Hypotheses No. 2 and 6 have low to medium support.
- Hypotheses No. 4, 5 (regarding soil thickness) and 8 are not supported.

That water leakage has been found to increase with rock cover (Hypothesis No. 4) for the tunnels studied in this thesis is rather surprising. The thickness of the weakness zones have been found to have no significance for the relative water leakage (l/min per 25). The following factors should be considered as factors increasing the risk of high water leakage; damage zones of faults (typical Q-values between 0.6 and 15), joints sub-parallel with major principal stress, magmatic rocks, major rock type boundaries, great rock cover and free water table above the tunnel.

Regarding the ability of site investigations to predict water lekage, geological field mapping with emphasis on jointing and orientation of fault/weakness zones has been found in most cases to be the most important investigation. Refraction seismic has also shown good ability for prognosticating water leakage, while 2D-resistivity has been found to give promising results for prognostication of water leakage in rock mass with high resistivity (>4000 ohmm). For the Skaugum and Storsand tunnels in particular considerable discrepancy between results and encountered water leakage has been found. Core drilling with water pressure tests has in some cases given valuable results, but for the Lunner tunnel the measured Lugeon values were not representative for high/extremely high water leakage which were encountered in the tunnel. Geophysical borehole logging with hydraulic testing has been found to give reliable prediction of high hydraulic conductivity.

Acknowledgements

This PhD work was initiated by the research- and development project "Tunnels for the citizens" which included several partners: Norwegian owners, contractors, consultants and the Research Council of Norway. This study would not have been possible without data provided from this project. The present PhD work has been financed by the Norwegian Public Roads Administration and by teaching assistance at the Department of Geology and Mineral Resources Engineering, NTNU. In addition, the project “Tunnels for the citizens” and the Geological Survey of Norway have supported financially to field work and participation on conferences. I am thankful to all these contributors for the financial support.

I am deeply thankful to my supervisor Professor Bjørn Nilsen (Department of Geology and Mineral Resources Engineering), for inspiration and encouragement when needed, and for patiently reading and commenting on my numerous drafts along the way.

Bent Aagaard, Region Manager at SWECO Trondheim, has been my co-supervisor, and I am grateful for valuable inspiration and recommendations regarding calculations and statistics he has given me.

I would like to mention friends and colleagues at the Department of Geology and Mineral Resources Engineering who have been helpful through this PhD work, especially Anne-Irene Johannessen for sketching some of the figures.

My new employer SINTEF Rock and Soil Mechanics has given me some financial support in the fini-shing stage of this PhD work, and Research Manager Eivind Grøv has been understanding and flexible, for this I want to thank him.

Finally, I want to thank Ørjan, my husband, for his understanding and belief in me, and to Martin and Jenny who will now get more play time together with their mother.

Trondheim, August 2008

CHAPTER 1 *Introduction*

1.1 Background

Groundwater inflow may cause several problems for underground excavations, such as:

- Risk of lowering the groundwater level, which can cause settlements and damage to constructions above.
- Drainage of forest land and lakes may damage recreational areas in populated areas, and sometimes the natural environment can be disturbed.
- In the planning process high uncertainty is connected to location and quantity of groundwater inflow, resulting in difficulties estimating costs concerning groundwater.
- Reduced rock mass stability and time consuming grouting (pre- and post-excavation).

The first direct result of groundwater inflow in tunnels is lowering of the groundwater table. This may cause decrease of the water pressure in soils and subsidence of soft ground (Olofsson, 1991). Buildings founded partly on hard rock and partly on soil (clay) are particularly vulnerable. In aquifers where limited amount of groundwater is available even small leakages can lower the groundwater level (Knutsson and Morfeldt, 1995). Figure 1.1 illustrates the groundwater flow path and how a combination of geological and hydrogeological conditions in addition to conditions in the overburden result in water inflow to a tunnel.

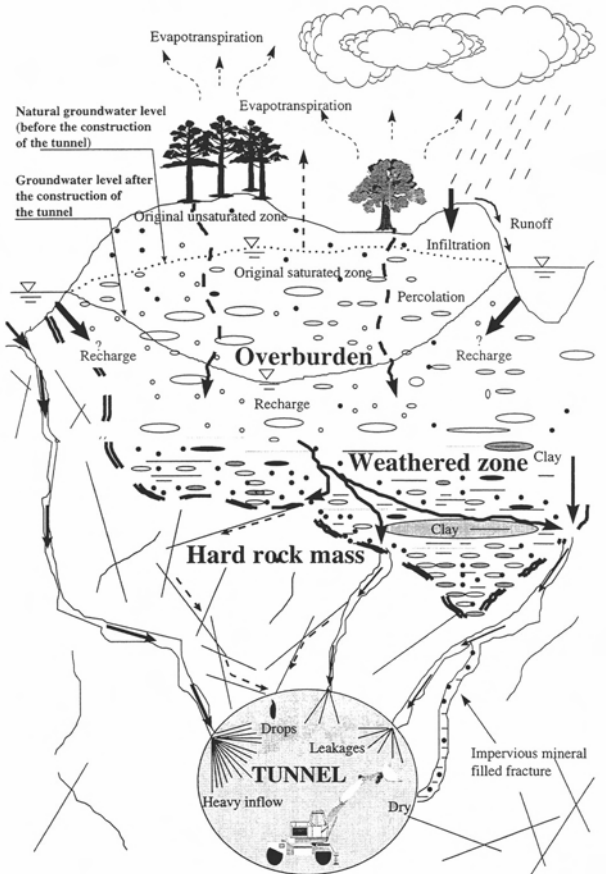

FIGURE 1.1 Principle sketch of how groundwater flow throgh jointed rock mass and into a tunnel (Cesano, 2001).

High groundwater inflow in a tunnel can cause difficult construction and working conditions, which influence the excavation rate. For sealing the rock mass pregrouting is normally used, but in some projects the rock mass has not been sealed sufficiently with pregrouting, and post-excavation grouting has been required. In the Romeriksporten tunnel (Figure 1.2) post-excavation grouting was carried out for more than one year in a section of 2.2 km of the tunnel, with a cost equal to that of excavation of the entire tunnel.

Unfortunately, several underground projects in Norway and abroad have experienced major delays, large unforeseen costs and negative attention from media, politicians and the public due to high water inflow. The partly excavated railway tunnel in Hallandsås in southern Sweden (Swedish Rail Administration, 2008) is one project with a long and

troublesome history due to difficulties caused by water leakage. The Hallandsås project consists of two 8.6 km long single-track tunnels through a horst formation, with challenging geological conditions and highly varying rock mass quality. The rock types are predominantly Precambrian gneiss and amphibolite. Tunnelling started in 1992, but in 1997 the project was stopped due to environmental pollution caused by chemical grouting used in the Hallandsås tunnel. In 2003 excavation restarted, and in May 2008 the Hallandsås tunnel project is well over halfway to completion.

In Iceland several tunnels in basalt have experienced severe difficulties due to high water inflow. In the north-west of the country a 9 km long road tunnel complex was built, the tunnelling started 1991 and was completed in 1996. The bedrock is of late Tertiary age, and the rock cover above the tunnel is 300-500 m. During excavation water leakage up to 3000 l/sec was encountered after a routine blasting round (Steingrímsson and Hardarson, 2000). The extremely high water leakage was encountered in connection with a fault and basalt dyke. The excavation was stopped for half a year before it was possible to proceed. At that point the water leakage had stabilised at 1000 l/sec, and it decreased further to 400 l/sec. Since there were no inflow criteria the tunnel profile was enlarged to make hole for water supply pipes, and Ísafjördur municipality uses this as its main water supply (Hardarson and Haraldsson, 1998). The groundwater table was lowered between 30 and 100 m.

One other example is the Kárahnjúkar hydro power project, also located in Iceland, which experienced problems with difficult geological conditions and heavy ingress of water in the 40 km long headrace tunnel (Pétursson, 2007). Excavation at Kárahnjúkar started in 2003 and was finished December 2006. For tunnelling three tunnel boring machines (TBM) were used, and one of the TBM sections had considerable problems due to extremely high water inflow; and convential drill and blast tunnelling had to be used instead.

Outside the Nordic countries several projects have also experienced extensive problems due to groundwater inflow. The 34.6 km long Løtschberg base tunnel in Switzerland (BLS AlpTransit, 2008), a two-tube single-track rail tunnel project is one example. The rock cover for that project was up to 2000 m, and the bedrock consisted of sandstone, marble, limestone, flysch, gneiss, granite and amphibolite. High water leakage with water pressure of up to 120 bar was encountered in sedimentary deposits and extensive pregrouting had to be carried out. In a section with limestone, groundwater inflow to the tunnel lowered the groundwater table below the village St. German, resulting in drying of the source for drinking water and subsidence in the centre of St. German.

The 12.9 km long Hsuehshan road tunnel in Taiwan is perhaps one of the most difficult and time-consuming tunnel projects in the world (Wallis, 2006). Tunnelling started in July

1991 and the final breakthrough was in April 2004. The slightly metamorphosed Tertiary sedimentary rocks were highly folded and jointed with several major faults. Both conventional drill and blast and TBM's were used as excavation techniques. The TBM's were forced to stop 13 times due to collapse of the tunnel face and extremely high water leakage of up to 5000 l/min.

Another relevant example is the Alfalfal hydropower project in Chile, where challenging geological conditions, high stresses (stress spalling) and water leakage with pressure of up to 100 bar were encountered (Buen et al., 1994). In granitic rock mass a concentrated water inflow of about 6000 l/min was encountered. A bypass tunnel had to be excavated, and the abandoned tunnel was used as drainage to relieve the high ground water pressure. The Andina project in Chile also experienced challenging groundwater conditions. Two tunnels were excavated in connection with treatment of waste water from a copper mine in Andina (Stefanussen, 2000). The bedrock belongs to the Cretaceous Andes mountain range. In granitic rock mass high stresses combined with major joints gave high water leakage, and in February 1997 a major cave in combined with water leakage of up to 600 l/sec stopped the tunnelling. Also in this case a bypass tunnel was used as a solution.

Finally, the Arrowhead water supply tunnels in the United States in southern California may be mentioned as projects with a difficult history and delays due to high water inflow (Burke, 2004). These two tunnels are located in the San Bernardino Mountains, which have been elevated by faulting and folding in late Tertiary period. The bedrock mainly consist of granite and gneiss. In early 2000, after excavation of 2.4 km, large ingress of water with pressures up to 17 bar was encountered. Pregrouting was started, and water leakage reduced to 946 l/min. In the fall of 2000 it was decided to terminate the ongoing contract, and engineering studies to determine the best excavation method, including a plan for pregrouting for the remaining excavation, were initiated. New contractors started the detailed planning in January 2002, and in July 2003 two new TBM's arrived to the project.

As illustrated by the cases described above water inflow is definitely one of the biggest challenges for the tunnel industry.

The problems in the Romeriksporten tunnel was one of the reasons for initiating the Norwegian research project "Tunnels for the citizens", financed by Norwegian owners, contractors, consultants and the Research Council of Norway. This research- and development project (R&D project) started in 1998-99 and the final report was completed in 2005 (Lindstrøm and Kveen, 2005). The project was organized in the following three sub projects:

- A: "Pre-investigations".
- B: "Environmental concerns".
- C: "Techniques for ground water control".

The main goal for sub project A was to work out guidelines for site investigations. The authors PhD work was initiated as part of sub project A, and is focusing on regional- and structural geological parameters importance for water leakage in hard rock tunnels. Better understanding of the geological parameters significance for groundwater flow is of great importance in identification of areas with high hydraulic conductivity and for planning and optimisation of site investigations.

Successful prediction of groundwater inflow may give considerable economical saving in construction costs due to optimization of the construction techniques, including pregrouting effort. Also, a better understanding and prognostication of the groundwater flow into underground constructions may facilitate the possibility to prevent potential damage to nearby environment and constructions.

The geological mapping for the 6 tunnels studied in this thesis was done by several persons, and the quality of the geological mapping varied. In most cases the weakness zones were not described in detail with correct structural geological definitions. Since the term “weakness zone” is inaccurate, it can be difficult in some cases to interpret if the mapped “weakness zone” is a fault zone, a section of weak rock mass or perhaps a jointed zone. Selmer-Olsen’s (1971) description of various types of weakness zones are presented in Nilsen and Palmstrøm (2000). Three main groups are defined; zones of weak material (including weathered rock mass), faults and fault zones, recrystallized and cemented or welded zones.

In this thesis, the term weakness zone refers to a part of the rock mass where mechanical properties are significantly poorer than for the surrounding rock mass, and may be either of the types described in Nilsen and Palmstrøm (2000). However, in cases where a more exact description of a specific zone is known this will be used.

1.2 Prime objectives and goals

The prime objectives have been to test hypotheses regarding water leakage and geological parameters, to evaluate the ability of site investigations to prognosticate water leakage, and based on this to contribute to improvement of the ability to make reliable prognosis for water inflow in future tunnels, and to avoid unforeseen problems with groundwater inflow in underground constructions. The results from this work hopefully will contribute to:

- Improve the understanding of different geological parameters and their relevancy for groundwater flow.
- Gain knowledge regarding potentials and limitations of relevant site investigations, and their ability to prognosticate water leakage.
- Raise the level of knowledge on groundwater prediction.

1.3 Hypotheses

The analyses and discussions in this thesis are to a great extent based on hypotheses regarding water inflow in hard rock tunnels. The hypotheses are based on the significance of different geological parameters, thoroughly presented and discussed in Secion 3.2, and the authors experience as site engineering geologist. The hypotheses are as follow:

1. The water leakage is lower in rock mass with Q-values lower than 0.1, than in rock mass with Q-values between 0.1 and 10. This is based on the assumption that the core of the weakness zone/fault consists of clay material, which will seal the rock mass. Hence, the highest water leakage will occur in the damage zone marginal to the core, where the rock mass is densely fractured but without clay filling.
2. Water-bearing joints make an angle with nearby major faults of $45° \pm 15°$. This is based on Selmer-Olsen's (1981) theory.
3. Water-bearing discontinuities are sub-parallel with the major principal stress.
4. Water leakage decreases with increasing rock cover, due to higher gravitational forces causing closing of discontinuities in the rock mass.
5. Great thickness of permeable soil or a lake/sea above a tunnel gives high water leakage, due to the reservoir capacity and the potential for good connection between the overburden and the rock mass.
6. Igneous rocks give higher water leakage than other rock types, due to their brittle character.
7. Major rock type boundaries give high water leakage, due to increased fracturing.
8. Large weakness zones give higher relative water leakage (inflow per 25 m) than narrow weakness zones.

Through analyses of 6 Norwegian tunnels the degree of support for these hypotheses has been evaluated. Sections with high water leakage in all six tunnels have been analysed, and the degree of support has been graded from "no support", "low to medium support" and "support", according to results from analyses done. See Chaper 8 for details regarding correlation values and how the degree of support has been decided.

1.4 Selected tunnels

The following 6 tunnels have been selected for the analyses, listed in order of time of excavation:

- Romeriksporten (excavation completed 1996).
- Frøya (excavation completed 1999).
- T-baneringen, stage one (Ullevål-Nydalen) (excavation completed early 2002).
- Lunner (excavation completed 2002).
- Skaugum (excavation completed 2004).
- Storsand (excavation completed 2004).

The six tunnels have been selected in an attempt to study tunnels with different geological conditions representative of Norwegian projects. Four of the tunnels were included in the research project “Tunnels for the citizens” (see Section 1.1): T-baneringen, Lunner, Skaugum and Storsand. In these four tunnels extraordinary site investigations were carried out, and data were easily available for research. The other two tunnels were selected due to their special relevancy for this study, and because the author was involved as engineering geologist on site at Romeriksporten as well as at the Frøya tunnel. The Romeriksporten tunnel is also important because extremely high water leakage was encountered, which caused considerable cost excess and time delay. For the Frøya subsea tunnel the geological conditions were particularly challenging, and high water leakage was encountered. Two of the tunnels are located on the north-west coast of Norway not far from Trondheim, and four are located in the southeastern part of Norway not far from Oslo, see Figure 1.2. More detailed descriptions of the tunnels are given in Chapter 6.

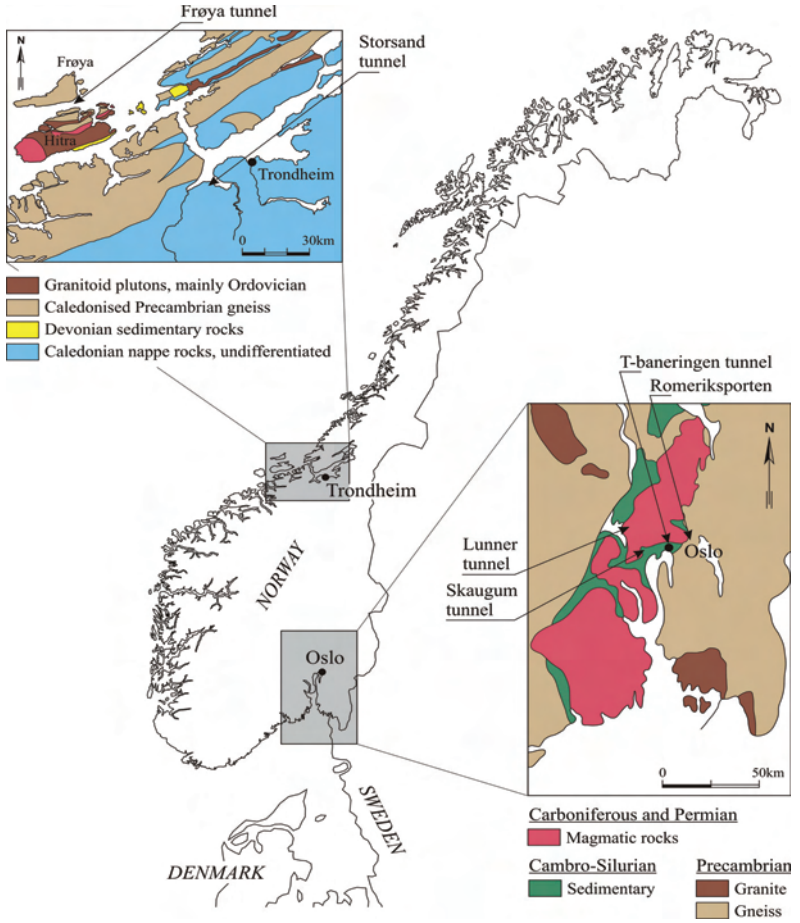

FIGURE 1.2 Map showing the location of the 6 tunnels studied.

1.5 Limitations of the work presented in thesis

This thesis is based on studies of 6 Norwegian tunnels in hard rock masses. The data are collected from contractors, owners and consultants, and collected by several persons at the tunnel projects. The author has had limited possibility for quality control of all the data used in the analyses. The data used in this study are, however, concerning quality considered to be well above average standard for tunnel projects. The analyses done are based on a limited number of tunnels, and discrepancy may result if the base of analyses is extended. The analyses are from an engineering geological point of view, focusing on geological parameters and conditions of the overburden which are well-known for engineering geologists. It also has to be realized that for some tunnel sections limited data

have been available. Particularly this applies to the Romeriksporten, Lunner and Storsand tunnels.

1.6 Thesis organization

Chapter 1 describes why it is important to study groundwater inflow to hard rock tunnels, and a short review of the background for initiating this thesis is given. Furthermore, 8 hypotheses regarding water inflow in hard rock tunnels are presented. The hypotheses are worked out based on the significance of different geological parameters, presented in Chapter 3, and the authors experience as site engineering geologist. The analyses and discussions in this thesis are to a great extent based on these hypotheses.

Chapter 2 describes principles and methods for making the available data comparable for all the tunnels studied. A description of how water leakage encountered in probedrilling and pregrouting holes is distributed in 25 m long sections along the tunnels is given.

Chapter 3 gives a review of existing theories for groundwater flow in hard rock, with emphasis on the significance of geological parameters. The review also gives the background theory for defining the 8 hypotheses presented in Chapter 1. Furthermore, the most commonly used rock mass characterization and classification systems and how water is taken into consideration are described.

Chapter 4 describes analytical, semi-empirical and empirical approximations for prediction of water inflow in hard rock tunnels. To understand the different possibilities and limitations for inflow calculations is considered to be important, and a review of the most important methods with relevant references is therefore given in Chapter 4.

In Chapter 5 a brief description of site investigation methods used to examine hydrogeological conditions in hard rock is given. Main principles, general potentials and limitations for site investigations ability to prognosticate structures with high hydraulic conductivity is emphasized. Some “extraordinary” investigation methods not commonly used in Norway are presented, and examples of the use of such methods in the R&D project "Tunnels for the citizen" are given.

Chapter 6 presents the six Norwegian tunnels selected for this study. The tunnels are described with main emphasis on geological conditions, site investigations carried out and water leakages encountered. Main emphasis is placed on investigations carried out before construction of the tunnels started.

In Chapter 7 more detailed presentations and analyses of the most interesting parts of the tunnels are carried out. The basic principles described in Chapter 2 are used in the analyses presented in Chapter 7. Analyses and evaluations of the hypotheses presented in Chapter 1 are done. Furthermore, results from site investigations carried out prior to excavation are compared with encountered water leakage in the 6 tunnels studied. An evaluation of the ability of site investigations to prognosticate water leakage into tunnels is done for each tunnel.

In Chapter 8, the degree of support for the hypotheses is evaluated based on the analyses done in Chapter 7. A discussion of correlation values found in the analyses and how the degree of support is defined is given. Based on this discussion the degree of support is graded from “no support”, “low to medium support” and “support”. Furthermore, three classes defining the ability of site investigations to prognosticate water leakage are defined. Discussions of the results for each hypothesis are presented.

Some suggestions for further research are also given in Chapter 8, and finally, conclusions and recommendations are given in Chapter 9.

CHAPTER 2 *Research methodology*

2.1 Basic approach for collecting and analysing leakage data

Main analyses have been carried out with emphasis on finding correlations between water leakage and geological parameters. For the selected cases (see Chapter 1 and 6) either a part of the tunnel or the entire tunnel has been analysed. The analyses have been based on water leakage inflow in probedrilling holes and pregrouting rounds. The idea is to measure water inflow into the tunnel in fresh rock mass, before grouting is carried out. An alternative could have been to use measurements of water leakage in the ditch, preferably with concrete barriers set up across the tunnel. However, water inflow measured after excavation is influenced by pregrouting, and for the six tunnel cases water inflow was not measured systematically or similarly. The distance between measuring points is also quite long, and thus the detailing level not high enough.

The parts of the tunnels that have been analysed were divided in 25 m long sections. 25 m long sections were chosen because the length of the probedrilling and pregrouting holes usually were between 21 and 26 m. One major problem with water leakage in drill holes is lack of control regarding where the water leakage comes into the drill holes. Therefore, it will not be correct to divide the tunnel in shorter sections than 25 m.

The uppermost drawing in Figure 2.1 shows a longitudinal section of a tunnel with two pregrouting rounds of 23 m length separated with 3 blasting rounds each of 5 m length. The grouting holes are angled outwards approximately 15°, and normal overlap between

pregrouting rounds is 6 to 8 m. The cross section in Figure 2.1 (bottom) shows a typical tunnel face with 6 probedrilling holes and 20 pregrouting holes including 7 pregrouting holes at the tunnel face. Both probedrilling and pregrouting holes are grouted. Probeholes are drilled to find rock mass quality and amount of water leakage ahead of the tunnel face. The water leakage is drained through a rubber tube into a bucket, and the water leakage is measured as liter per minute. If the measured water leakage is above a given limit value pregrouting is carried out. Six probedrilling holes is most commonly used. Experience the last 10 years has shown that sporadic pregrouting based on probedrilling as a decision tool concerning pregrouting or not, in many cases is not optimal. It can be difficult to start the grouting in time, and as a result the tunnel is not sealed well enough.

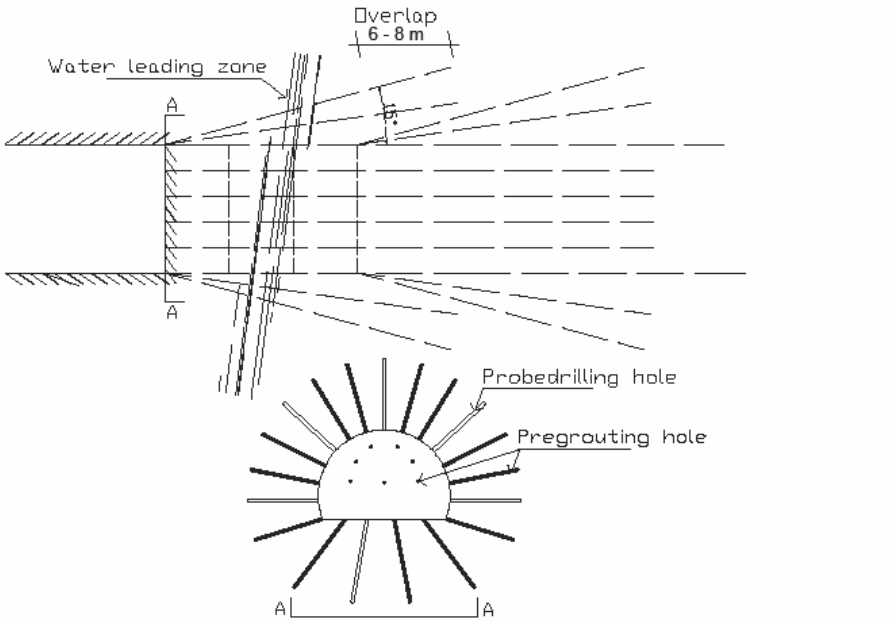

FIGURE 2.1 Principle drawing showing a longitudinal section of a tunnel with probedrilling and pregrouting holes (top), and a cross section of the same tunnel (A-A) (bottom).

Particularly the problems experienced at the Romeriksporten tunnel with high water inflow and need for post-excavation grouting, have given high focus on optimizing the grouting technique since the mid 1990's. As a result the numbers of grouting holes generally have increased, and also grouting holes at the tunnel face are more frequently used. The 6 tunnels studied in this thesis were excavated in the time span from 1995 to 2005. Therefore, the grouting techniques vary a lot. The number of pregrouting holes in one pregrouting round varied from 21 to 48, and the length of the holes varied from 18 to 24 m.

Based on measurement of water leakage in probedrilling holes and pregrouting rounds by using a bucket, calculation of water inflow into the tunnel for every 25 m has been carried out (see Section 2.2). The water leakage was measured before grouting was done in the respective drill holes. Therefore, the measured water leakage was high, and represents the amount of water that would have flowed into the tunnel in case no grouting was done.

The water leakage encountered along the tunnels has been carefully evaluated versus relevant geological parameters, to find if the hypotheses in Section 1.3 are supported or not. Particular detailed analyses have been carried out for parts of the tunnels of special interest. Each tunnel has first been studied and discussed as a separate case (see Chapter 7), and in Chapter 8 the geological parameters have been discussed jointly for all tunnels.

Spreadsheets have been used for some of the analyses mentioned above; Excel 2003 from Microsoft Office, and in addition an add-in called StatPro from Palisade (Albright et al., 2003). Diagrams showing scatterplots with correlation, trend line with mathematical function and coefficient of determination (R^2) and boxplots have been extensively used.

A boxplot clearly shows how the data set is scattered, Albright et al. (2003) explain the boxplot in StatPro as follows: “The right and left of the box are the third and first quartiles. Therefore the length of the box equals the interquartile range (IQR), and the box itself will contain 50% of the observations. The height of the box has no significance. The vertical line inside the box indicates the location of the median. The point inside the box indicates the location of the mean. Horizontal lines are drawn from each side of the box. They extend to the most extreme observations that are no farther than 1.5 IQRs from the box. They are useful for indicating variability and skewness. Observations farther than 1.5 IQRs from the box are shown as individual points. If they are between 1.5 IQRs and 3 IQRs from the box, they are called mild outliers and are hollow. Otherwise they are called extreme outliers and are solid.” Figure 2.2 shows an example from the Romeriksporten tunnel of a boxplot with one mild outlier and one extreme outlier.

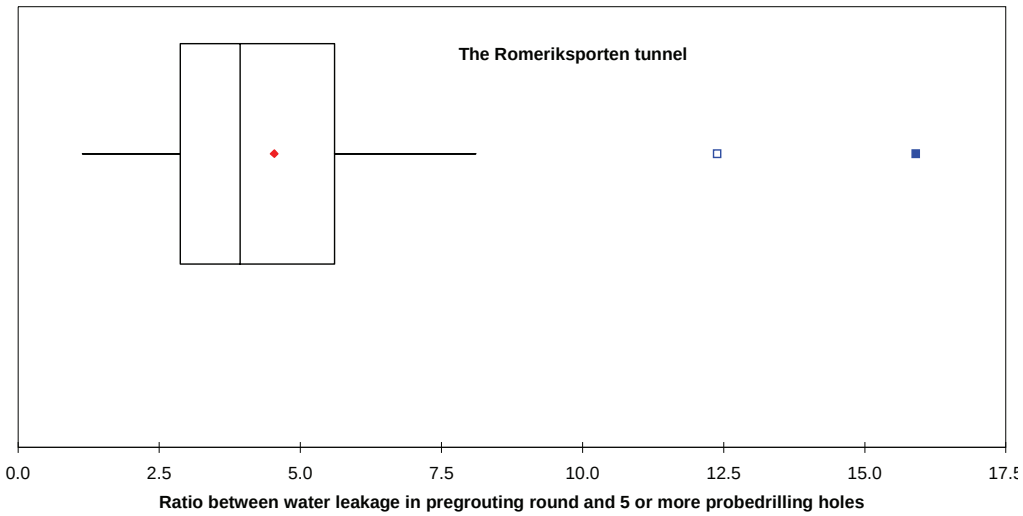

FIGURE 2.2 Example of a boxplot made in StatPro. For explanation of the values in the X-axis see Section 2.2.

In the scatterplots both correlation and the coefficient of determination R^2 have been used. In some scatterplots also a trend line is given.

The formula for correlation is as follows (Albright et al., 2003):

$$Corr(X, Y) = \frac{cov(X, Y)}{stdev(X) \times stdev(Y)} \quad \textbf{[2-1]}$$

Where the covariance, cov(X,Y), is given by (Albright et al., 2003):

$$Cov(X, Y) = \frac{\sum_{i=1} (X_i - \bar{X})(Y_i - \bar{Y})}{n-1} \quad \textbf{[2-2]}$$

Standard deviation for X or Y are the square root of the variance of X and Y.

“The correlation is unaffected by the units of measurement of the two variables, and it is always between -1 and +1. The closer it is to either of these two extremes, the closer the points in a scatterplot are to some straight line, either in the negative or positive direction. On the other hand, if the correlation is close to 0, then the scatterplot is typically a “cloud” of points with no apparent relationship. However, it is also possible that the points are

close to a curve and have a correlation close to 0. This is because correlation is relevant only for measuring linear relationships." Albright et al. (2003).

The trend line with mathematical function and the coefficient of determination R^2 is drawn and calculated in Excel and StatPro. R^2 measures the quality of a linear fit. The better the linear fit is, the closer R^2 is to 1. The coefficient of determination is given by (Albright et al., 2003):

$$R^2 = 1 - \frac{\sum e_i^2}{\sum (Y_i - \bar{Y})^2} \quad \text{[2-3]}$$

Where e_i is the difference between the observed value Y and the fitted value $\hat{Y}$. And $\bar{Y}$ is the response variable's mean. "In simple linear regression, R^2 is the square of the correlation between the response variable and the explanatory variable." Albright et al. (2003).

2.2 Principle for making the available data comparable for all the tunnels

When analyzing the data from 6 different tunnels, two principal problems were faced. First, the type and amount of data gathered from the tunnels differ. For example in the Skaugum tunnel, systematical pregrouting was carried out, and therefore no or limited probedrilling were done. In other tunnels such as the Frøya subsea tunnel, probedrilling was carried out continously below the sea. In order to compare water leakage from the different tunnels it was necessary to calculate how much water leakage could be expected in a potential pregrouting round of holes based on the results from the probedrilling holes. The second problem was caused by overlap; in some sections the pregrouting rounds were carried out with only a few metres spacing, and even at the same tunnel face. At the Romeriksporten tunnel as much as 4 pregrouting rounds were in some cases carried out at the same tunnel face before excavation could proceed. If water leakage from all pregrouting rounds were counted, the water leakage in such cases would be highly overestimated.

To explain how the problems described above have been solved, two principal drawings are used. Concerning the first problem, probedrilling versus pregrouting, Figure 2.3 shows a principle drawing of a tunnel section with moderate water leakage. Pregrouting here was carried out sporadically. In the figure the arrows to the left represent rounds of probedrilling holes (6 holes of 23 m length), and the arrows to the right represent pregrouting rounds (31 holes of 23 m length). The excavation direction was from the bottom to the top of the figure. The numbers to the right of the arrows show how much water leakage in l/min was encountered in the respective probedrilling holes and pregrouting rounds. In this principle

drawing, four cases with less than 25 l/min in the probedrilling holes were present, and pregrouting was not carried out at these tunnel faces. In order to make the data comparable, the water leakage encountered in the probedrilling holes were multiplied with a certain ratio to find what could be expected in a potential (later called imaginary) pregrouting round. How this ratio was found will be accounted for in Section 2.3. The imaginary pregrouting rounds with corresponding water leakage are given in red, as shown in Figure 2.3. The water leakage given to the right, both real and imaginary pregrouting rounds, are used when the water leakages were calculated and divided into 25 m long sections. An explanation of how the distribution along the tunnel has been done is given later in this section.

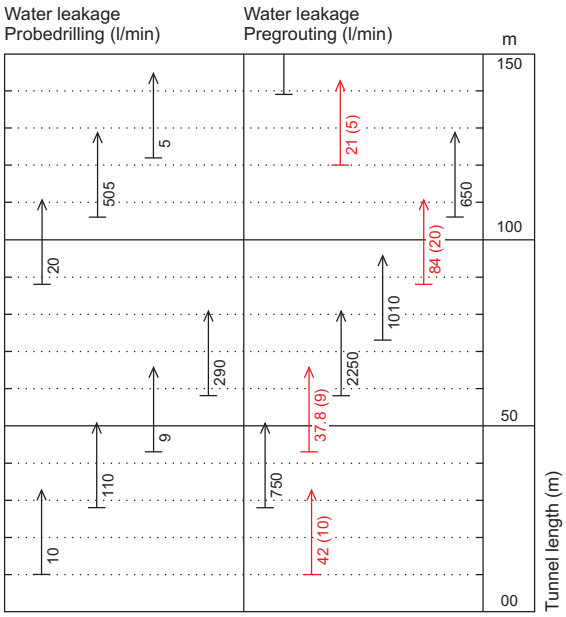

FIGURE 2.3 Principle drawing showing how the water leakage is calculated in a section without continuous pregrouting. Probedrilling rounds in left column and pregrouting rounds in the middle column. Right column shows tunnel length (m). Arrows in black represent real probe- and pregrouting rounds, while read arrows represent imaginary pregrouting rounds. The length of arrows represents lengths of the boreholes.

The second problem, overlap, occurs in sections with high water leakage, and with several pregrouting rounds necessary to seal the water inflow. Figure 2.4 shows a principle drawing of a tunnel section with high degree of overlap. In the figure the left column shows rounds of probedrilling holes (6 holes of 18 to 26 m length), and the middle column represents pregrouting rounds (31 holes of 18 to 26 m length). The column to the right shows tunnel length. As can be seen from Figure 2.4 both two and three pregrouting rounds were carried out, indicated by the overlap of the arrows. In order to reduce the overestimation of encountered water leakage, only water leakage in the first pregrouting round has been

counted. The water leakage in the first pregrouting round is written to the right of the lines in Figure 2.4. The water leakage in the probedrilling holes are not used in further analyses, they are only shown for information and comparison.

As can be seen in Figure 2.4, high degree of overlap between pregrouting rounds occurs when tunnel progress was less than 2-3 blasting rounds (10-15 m) before new pregrouting rounds were needed, and if length of pregrouting rounds are reduced compared to previous pregrouting round. Consequently the same rock mass was pregrouted several times. This technique is typically used when great problems with efficiently sealing of the rock mass are experienced.

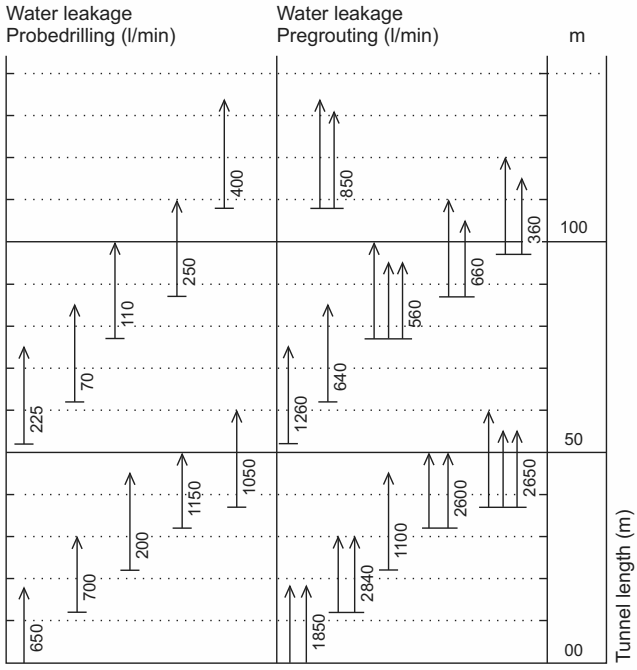

FIGURE 2.4 Principle drawing showing a section with high degree of overlap in pregrouting. The arrows represent lengths of the boreholes.

Two different methods have been used for calculating the water leakage in 25 m long sections along the tunnels:

1. Method one has been used in rock mass with low to moderate water leakage, and overlap between pregrouting rounds typically between 6 and 8 m. The water leakage has been distributed in only fresh rock mass, where no pregrouting was done.
2. Method two has been used in rock mass with high water leakage and difficult pregrouting conditions with high degree of overlap. The water leakage has been distributed in

both fresh rock mass and in the overlap section. The criteria for using method two have been as follows: tunnel progress was less than 9 m before new pregrouting round was drilled or less than 10 metre of fresh rock mass was reached with the pregrouting round.

Figure 2.5 illustrates how the calculations have been done for method one and two. Numbers in red represent metres between two subsequent pregrouting rounds. Numbers in black represent metres of overlap for method one. The water leakage in the pregrouting rounds was distributed on the sections given in blue.

For the first pregrouting round (see numbers in circles to the left in Figure 2.5) the whole length was drilled in fresh rock mass, therefore the water leakage of 1850 l/min has been divided by 18 m and evenly distributed, see Figure 2.5. For the second, third and last pregrouting round method one has been used; the total water leakage is divided by length of fresh rock mass (given in blue) and distributed in the fresh rock mass. This is done because it is most likely that the water leakage in the pregrouting round comes in fresh rock mass and not in the previous pregrouted area. This is considered most likely when the pregrouting conditions are not too complex.

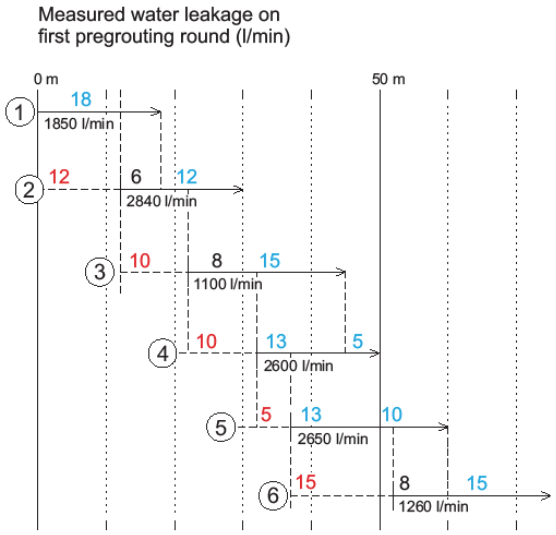

FIGURE 2.5 Principle drawing showing a section with high degree of overlap of pregrouting rounds. The numbers in circles represent pregrouting round number. The arrows represent lengths of the boreholes. Red no. is metres between two subsequent pregrouting rounds. Blue no. is metres of the boreholes where the water leakage is distributed, for method one blue no. is metres of fresh rock mass, while for method two blue no. is metres both of fresh rock mass and of overlap section. Black no. is length of overlap section for method one.

In Figure 2.5 the fourth and fifth pregrouting round are examples where method two is applied. For method two the water leakage in the pregrouting round is halved, one half is

distributed in the fresh rock mass, the other half is divided by two before it is distributed in the overlap section. The reason for dividing the water leakage in two is that it is considered likely that the water leakage in the overlap section is reduced by previous pregrouting. However, it is likely that there still is water left in the overlap section, because it is located in a section where efficient sealing is difficult. For method two, relatively higher water leakage is placed in the fresh rock mass than in the overlap section, which is considered reasonable. As a result the total water leakage in the pregrouting round was reduced to 75% of original total water leakage. Alternative approaches for distributing water inflow for the 6 tunnels studied have been evaluated, but the above explained methods (method one and two) are believed to be the best alternatives for complex cases, giving fairly realistic results for comparison between the tunnels studied.

The following example illustrates how method two has been used. The fourth pregrouting round has a water leakage of 2600 l/min, divided by two give 1300 l/min spread evenly on 5 m fresh rock mass (1300 l/min/5m=260 l/min/m). The remaining 1300 l/min is divided by two, giving 650 l/min distributed on the 13 m long overlap section (650 l/min/13m=50 l/min/m). After calculations based on method one or two, the total water leakage within each 25 m section along the tunnels was found by adding up the respective contributions. An example of a spread sheet where the water leakage per metre has been calculated for a section in the Frøya tunnel is shown in Appendix A. Water leakage per metre has been distributed on fresh rock and overlap according to method 1 and 2 and summarized for each 25 m (the latter is not shown in Appendix A, because the spread sheet is very big and difficult to follow).

Based on the methods explained above an overestimation of water leakage in sections with water leakage and complex pregrouting conditions is not fully avoided. On the other hand, the total water leakage in the tunnel in case of no pregrouting would be higher than the calculated value in this study. How much higher is difficult to estimate. Therefore, the possible overestimation of water leakage in sections with difficult pregrouting conditions is considered to be of minor importance for the main conclusions in this thesis.

Regardless of the method used, calculated water leakage may hardly be unambiguous and 100% accurate. There will always be an element of uncertainty regarding the location of water-bearing fractures. However, the calculations are believed to give clear indications on where the water leakage was high and where the water leakage was moderate to small. The chosen approach also makes sure that all tunnels are treated similar, which is considered essential for this study.

2.3 Water leakage in pregrouting rounds versus probedrilling holes

In the respective tunnels the available data for water leakage differ. In some sections water leakage was only available from probedrilling holes and in some sections only from pregrouting rounds. To make the data comparable, the water leakage encountered in the probedrilling rounds were multiplied by a certain ratio to estimate water leakage for imaginary pregrouting rounds. Analyses have been carried out for the Romeriksporten and Frøya tunnels to find the respective ratios between water leakage in actual pregrouting rounds and probedrilling rounds for the two tunnels. These two tunnels were chosen because probedrilling was actively used in both tunnels to decide whether or not to pregroute. In both tunnels a section of approximately 1.5 km was studied.

In both the Romeriksporten and Frøya tunnels 6 probedrilling holes were generally used in each probedrilling round. However, at some tunnel faces less or additional probedrilling holes were drilled. It is likely to assume that the ratio between water leakage in one pregrouting round (approx. 20 holes) and water leakage in probedrilling holes vary dependent on how many probedrilling holes are drilled. The ratio is expected to decrease with increasing number of probedrilling holes. Therefore, it was found relevant in this study to divide the calculations in two groups, one group for tunnel faces with less than 5 probedrilling holes, and one group for tunnel faces with 5 or more probedrilling holes. The latter group has 79 out of a total of 90 tunnel faces, and represent most common practice. It was considered correct to use this study to find the most appropiate ratio to recalculate water leakage to make values comparable.

The ratio between water leakage in one pregrouting round (included water leakage in probedrilling holes) and water leakage in probedrilling holes from the same tunnel face have been calculated for two selected tunnel cases. Only pregrouting rounds with minimum 15 pregrouting holes plus probedrilling holes were included in the analysis. In Table 2.1 results from the calculations are shown (for more details, reference is made to Appendix A).

TABLE 2. 1 Ratio between water leakage in pregrouting round and probedrilling holes for the Romeriksporten and Frøya tunnels. (*) = Results without outliers.

	Ratio between one pregrouting round and average water leakage in one probedrilling round (*).	Ratio between one pregrouting round and the probedrilling hole with highest water leakage.	Ratio between pregrouting round and 2, 3 or 4 probedrilling holes.	Ratio between pregrouting round and 5, 6 or 7 probedrilling holes.
The Romeriksporten tunnel.				
Minimum.	6.9 (6.9)	-	1.9	1.1 (1.1)
Maximum.	95.4 (48.6)	-	10.1	15.9 (8.1)
Mean.	26.1 (24.4)	-	5.7	4.5 (4.2)
Median.	23.4 (22.7)	-	5.1	3.9 (3.9)
St. dev.	14.5 (10.3)	-	2.9	2.5 (1.7)
Variance.	210.0 (106.8)	-	8.5	6.1 (3.0)
The Frøya tunnel.				
Minimum.	4.3	1.3	1.1	1.0
Maximum.	26.4	12.2	5.8	4.4
Mean.	11.6	4.9	3.3	2.1
Median.	11.1	4.1	3.1	1.9
St. dev.	4.8	2.5	1.95	0.8
Variance.	23.3	6.3	3.8	0.7

As shown in Table 2.1, the values in both tunnels vary considerably. This is quite logical because the geology vary considerably along the tunnel sections studied. As can be seen, there is a distinct difference between the magnitudes of the ratios for the two tunnels. For the Romeriksporten tunnel the mean ratio between water leakage in one pregrouting round and average water leakage in one probedrilling round is 26.1, and for the Frøya tunnel 11.6. See Figure 2.6 for boxplots.

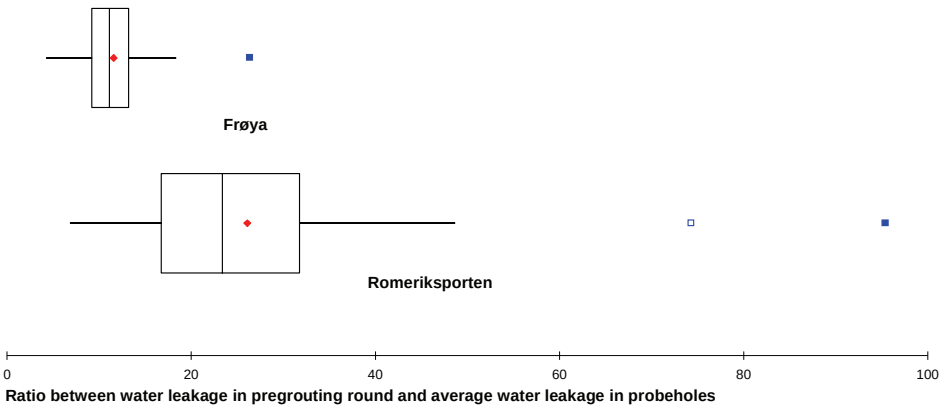

FIGURE 2.6 Boxplot showing the ratio between water leakage in pregrouting round and average water leakage in one probedrilling hole for the Romeriksporten and Frøya tunnels.

Hence, at the Romeriksporten tunnel more than twice as much water leakage was encountered in the pregrouting round compared to the Frøya tunnel with same average water leakage in the probedrilling holes. As can be seen from the boxplots, the variance is higher for the Romeriksporten tunnel. In addition, one mild and one extreme outlier are evident. If both outliers are taken out of the data set the variance is reduced considerable, and the variance is almost halved. The revised calculations without the outliers are given in brackets in Table 2.1.

Figure 2.7 and 2.8 show scatterplots for total water leakage in pregrouting rounds versus average water leakage in probeholes for the Romeriksporten and Frøya tunnels. Both plots show high and positive correlation, particularly the Frøya tunnel with correlation 0.934.

For the Frøya tunnel, the ratio between water leakage in one pregrouting round and the highest registered water leakage in one probedrilling hole has been calculated. This reduces the mean ratio from 11.6 to 4.9, see Table 2.1. As expected, the ratio between water leakage in one pregrouting round versus inflow in probedrilling holes decreases when the numbers of probedrilling holes increase. In the data available there are not many cases with less than 5 probedrilling holes. Nevertheless, the tendency is clear; the mean ratio is higher than for comparable ratios of 5 or more probedrilling holes, see Table 2.1.

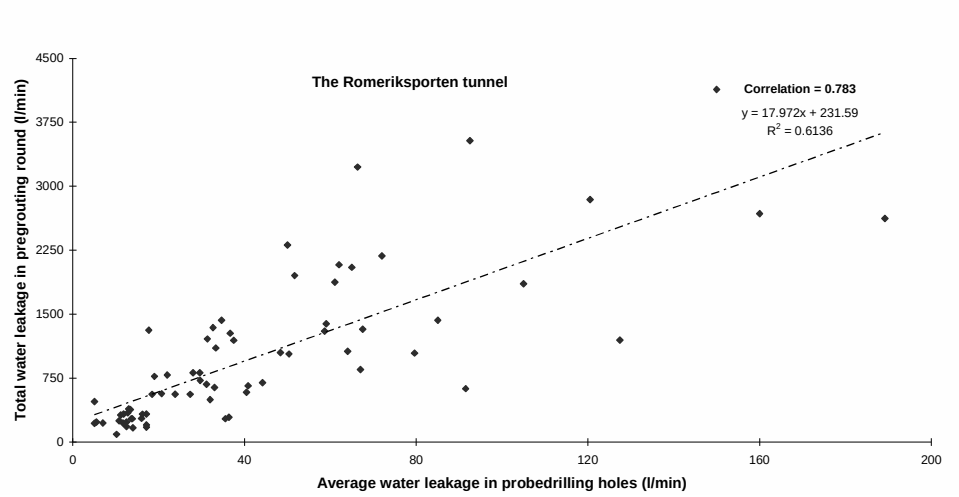

FIGURE 2.7 XY-plot showing total water leakage in pregrouting round versus average water leakage in probedrilling holes for the Romeriksporten tunnel.

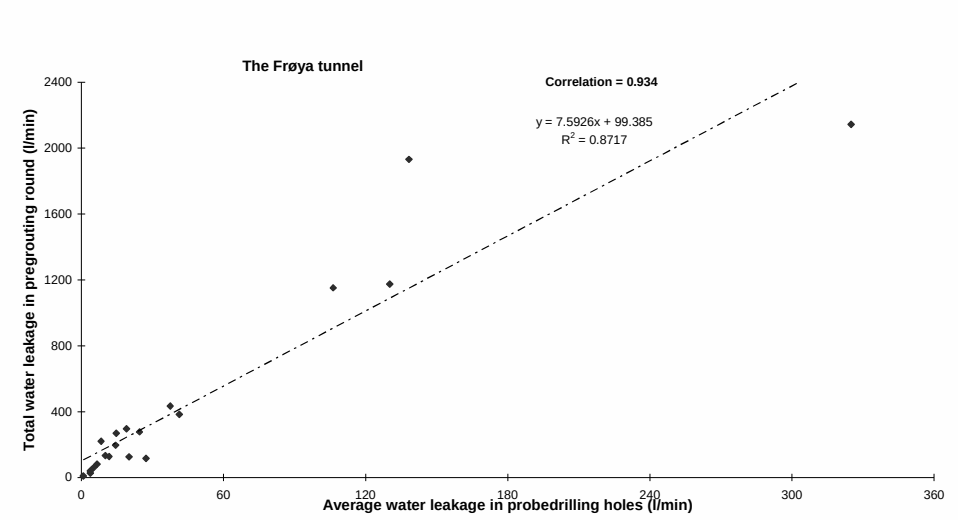

FIGURE 2.8 XY-plot showing total water leakage in pregrouting round versus average water leakage in probedrilling holes for the Frøya tunnel.

For the Romeriksporten tunnel the ratio between one pregrouting round and 5 or more probedrilling holes is approximately 4 and for the Frøya tunnel approximately 2. In Figure

2.9 this is illustrated with boxplots. In the Romeriksporten tunnel the water leakage encountered in 6 probedrilling holes was approximately 25% of the water leakage encountered in one pregrouting round, and for the Frøya tunnel around 50%.

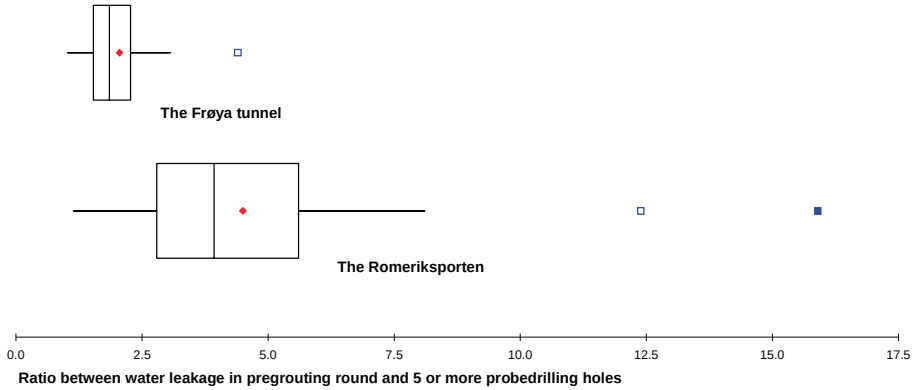

FIGURE 2.9 Boxplot comparing the ratio between water leakage in pregrouting round and probedrilling holes (5 or more) for the Romeriksporten and Frøya tunnels.

This analysis for both tunnels gives much higher ratio between one pregrouting round and probedrilling holes than the commonly used theoretical calculations such as the equation for radial flow, Karlsrud (2002), defining inflow of water as:

$$Q = \pi k h \frac{2}{\ln\left(2\left(\frac{h}{r}\text{-}1\right)\right)} \qquad \textbf{[2-4]}$$

Where:

k is hydraulic conductivity ($1 \cdot 10^{-7}$ m/s for water)

r is radius of drainage hole (varies)

h is water column above test length (m)

Equation 2-4 has been used for finding the theoretical ratio between water leakage into a borehole versus a tunnel section. Hydraulic conductivity equal to $1 \cdot 10^{-7}$ m/s and 100 m water column has been used in the calculations, which is representative for many tunnels. It is of no significance what hydraulic conductivity and water column above test length are, as long as they are constant. For k = $1 \cdot 10^{-7}$ m/s and h = 100 m, the water leakages as shown in Table 2.2 can be calculated for different hole radius.

TABLE 2. 2 Calculated water inflow for holes with varying radius (m).

Radius (m).	0.045	0.45	4.5	6.5
Q (l/min/m).	0.45	0.62	1.0	1.1

The results show that based on Equation 2-4, water leakage into a tunnel with radius 4.5 m (diameter 9 m) will give approximately twice as much water leakage as a borehole with radius 0.045 m (45 mm). If we compare these theoretically results with the analyses done previous in this section (see Table 2.1); one pregrouting round will in average give 26 (26.1) and 12 (11.6) times more water than one probedrilling hole for the Romeriksporten and Frøya tunnel respectively. It should also be taken into account that the measured water leakage in one pregrouting round is less than actual water inflow into the equivalent long excavated tunnel section assuming no pregrouting was done. Therefore, the measured values of 26 (26.1) and 12 (11.6) for the Romeriksporten and Frøya tunnels are too low. This illustrates that the conditions in the Romeriksporten and Frøya tunnels are more complex than the theory represented by Equation 2-4 assumes. The theory is based on idealised conditions like homogenuous rock mass with same hydraulic conductivity in all directions. This idealisation is not relevant for jointed rock.

Based on litterature search almost no information has been found regarding the ratio between pregrouting and probedrilling holes. According to Heuer (1995) “Theory and experience suggest the tunnel will commonly encounter in the range of 2 to 5 times the flow from a probe hole.” Heuer’s (1995) estimate is low compared to the results from the analyses done previous in this section, see Table 2.1. For the Romeriksporten and Frøya tunnels an excavated tunnel will give 26 and 12 times more water leakage than average water leakage in one probedrilling hole. The same ratios are reduced to 5 (4.5) and 2 (2.1) if considering the ratio between water leakage in one pregrouting round and water leakage encountered in 5 or more probedrilling holes.

In some tunnel sections only probedrilling has been carried out, and in order to make the data comparable, the water leakage in the probedrilling holes was multiplied by a suitable ratio in order to calculate how much water leakage could be expected in an imaginary pregrouting round. Based on the analysis and discussion presented here, ratios as shown in Table 2.3 have been used.

TABLE 2. 3 Ratios used for estimating water leakage in imaginary pregrouting round when only probedrilling has been carried out.

	Ratio for < 5 probedrilling holes.	Ratio for 5 or more probedrilling holes.
Romeriksporten.	**5.7**	**4.2**
Frøya.	**3.3**	**2.1**

2.4 Summary

In this chapter the principles for making the available data comparable for all the tunnels studied have been described, and it has been discussed how water leakage encountered in probedrilling and pregrouting holes have been distributed in 25 m long sections along the tunnels. Two methods, which consider both sections without continuous pregrouting and sections with high degree of overlap of pregrouting have been described.

The ratios between water leakage encountered in pregrouting rounds versus water leakage in probedrilling holes have been calculated for the Romeriksporten and Frøya tunnel. These ratios (see Table 2.3) will be used for estimating water leakage in imaginary pregroting rounds in sections where only probedrilling has been carried out. The ratios found studying the Romeriksporten and Frøya tunnel were high compared to other litterature (Heuer, 1995) and theoretical calculations (Karlsrud, 2002) done in Section 2.3.

The basic principles in Chapter 2 will be used in Chapter 7, for analysing possible correlations between water inflow and geological/engineering geological parameters for 6 relevant Norwegian tunnels.

CHAPTER 3

Groundwater inflow in hard rock tunnels

3.1 Flow theory

In this section main hydrogeological terms and parameters needed to understand groundwater flow in hard rock are presented.

3.1.1 Hydraulic conductivity and permeability

Groundwater flow in hard rock is controlled by primary and especially secondary porosity (Fetter, 2001). Primary porosity is made up of the pore volume in the bedrock, while secondary porosity is commonly due to discontinuities. The effective porosity, θ_{eff}, in rock mass is defined as follows:

$$\theta_{eff} = \frac{V_{sat}}{V_{tot}} \quad \text{[3-1]}$$

Where

θ_{eff} = effective porosity

V_{sat} = volume of saturable pores

V_{tot} = total rock volume

The communication between individual pores is poor, and the capacity for transmitting a fluid through intact rock is normally very low. In Norwegian intact rocks the effective

porosity is normally under 1%, but Permian and Jurassic sandstones may have effective porosity of 15 to 30% (Broch and Nilsen, 1996). In most rock types the permeability of joints and other discontinuities define the rock mass permeability. Hydraulic conductivity, k (m/s), also called coefficient of permeability is the most commonly used parameter for characterising hydrogeological conditions. The parameter represents the coefficient of proportionality of Darcy's equation:

$$v = \frac{Q}{A} = k \times i \qquad \textbf{[3-2]}$$

Where

v = flow velocity (m/s)

Q = flow rate (m^3/s)

A = flow area (m^2)

i = hydraulic gradient

k = hydraulic conductivity (m/s)

The hydraulic conductivity, k, depends on the nature of the rock mass as well as the nature of the fluid. Typical hydraulic conductivity of rocks and soils are given in Figure 3.1.

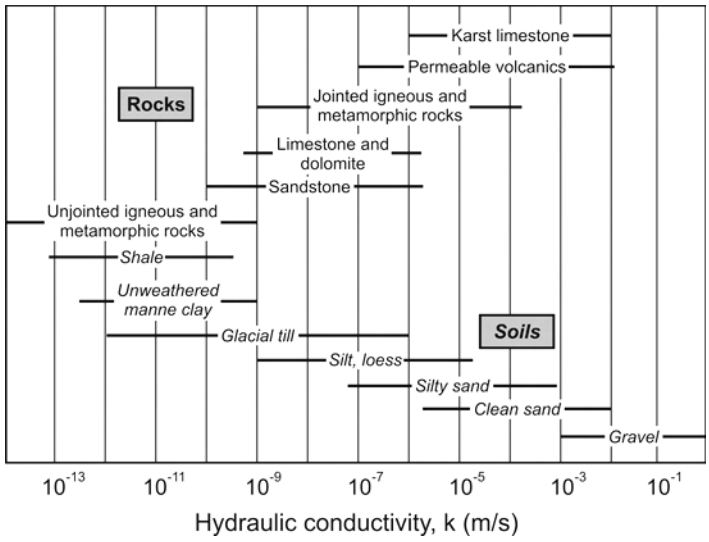

FIGURE 3.1 Typical hydraulic conductivity of rocks and soils (Freeze and Cherry, 1979)

As Figure 3.1 illustrates, hydraulic conductivity in different geological materials can vary significantly, typically from 10^{-8} to 10^{-4} m/s; with the first corresponding to no visible

water inflow or only seepage (2-3 l/min per 100 m) and the latter to several thousand l/min per 100m with regards to tunnels.

Specific permeability, K (m^2), depends on the rock mass only, and not on the nature of the fluid. Specific permeability relates to hydraulic conductivity by the following equations:

$$K = k \times \frac{\mu}{\rho \times g} = k \times \frac{\nu}{g} \quad \textbf{[3-3]}$$

Where

μ = dynamic viscosity of the fluid (=1.3 mPa×s (milliPascalsseconds) = 1.3 cP (centipoise, or g/(cm×s)) for pure water at + 10 ° C)

υ = cinematic viscosity of the fluid (=1.3×10^{-6} m^2/s for pure water at +10 ° C)

ρ = density of the fluid

g = gravitational acceleration (9.81 m/s^2)

The most frequently used method to investigate the hydrogeological conditions of the rock mass is water pressure testing. The result from water pressure tests are given in the unit Lugeon (L), where 1 Lugeon is defined as the loss of water in litres per minute and per metre borehole at an over-pressure of 1 MPa (Nilsen and Palmstrøm, 2000), see Section 5.7 for detailed definition of the Lugeon unit and description of water pressure tests. Based on a pumping test of one single borehole in isotropic conditions, the following approximate relationship between the Lugeon value and the hydraulic conductivity (k) has been published by Hoek and Bray (1981):

$$k = \left(\frac{1{,}4 \times q_c}{L \times H_c}\right) \quad \textbf{[3-4]}$$

Where

q_c = pumping rate (l/min) necessary to maintain a constant over-pressure

L = length (m) of the test section

H_c = over-pressure (constant head, given in metre)

According to this equation a water loss of 1 L corresponds to a hydraulic conductivity of $k=2{,}3 \times 10^{-7}$ m/s.

To illustrate the span of the parameters, typical values of fine sand and moderately jointed granite are indicated in Table 3.1.

TABLE 3. 1 Examples of typical values of hydraulic conductivity (L and k, related to water flow) and permeability (K) (Nilsen and Palmstrøm, 2000).

Material.	**L (Lugeon).**	**k (m/s).**	**K (m^2).**
Sand, fine-grained.	100	10^{-5}	10^{-12}
Granite, moderately jointed.	0.1	10^{-8}	10^{-15}

3.1.2 Conductivity of single joints

The aperture of joints has major influence on the flow rate. For a planar array of parallel and smooth joint the hydraulic conductivity is given by Louis (1969):

$$k = \frac{g \times e^3}{12\nu \times S} \quad \textbf{[3-5]}$$

Where

g = gravitational acceleration (9.81 m/s^2)

e = opening (aperture) of joint (m)

ν = cinematic viscosity (m^2/s)

S = spacing between joints (m)

Hence for a doubling of the joint aperture, the flow is increased by a factor of 8, this connection is called the local cubic law.

Louis' and Darcy's equations are both based on laminar flow conditions, and Louis' equation also assumes a joint geometry corresponding to a simple parallel-plate model. This is not the situation in natural rock mass. Joints are rough and often partly filled, and the flow is therefore unevenly distributed and in reality follows irregular, narrow channels. New research has supported non-Darcian flow under relatively fast flow conditions and disagree with the local cubic law, Equation 3-5 (Qian et al., 2005).

3.2 Significance of geological parameters

Groundwater flow in hard rock depends on discontinuities such as joints and their permeability. Several factors can influence on the hydraulic conductivity of the rock mass:

- Joint character, such as orientation, continuity/length, roughness and frequency.
- Stress situation.
- Faults and adjacent fractures.

- Dykes.
- Composition and thickness of the overburden.

Much research has been done on all of the factors mentioned, and brief comments on how the factors influence the groundwater flow are given. Faults and adjacent fractures will be described more thouroghly compared to the other factors, this is because faults are believed to be the most important factor influencing the hydraulic conditions of the rock mass, due to increase in fracture frequency related to faults. But all factors mentioned above are of importance and in most cases a combination of factors are significant for the groundwater flow.

3.2.1 Joint character

According to the cubic law the groundwater flow is highly dependent on the aperture of the joints (Gudmundsson, 2000). The aperture of joints depends on many different conditions. First the mechanical properties of the rock mass are important. If the rock mass is brittle and hard, such as granite, the apertures are more able to sustain wide and open. In contrast, in soft and deformable rocks, like schist and slates, the joint apertures get closed more easily. It can be difficult to measure the aperture of the joints, and according to Berkowitz (2002): "Measuring an effective fracture aperture remains a thorny and unresolved problem". Nevertheless, in Norway some geologists have gained positive experience measuring the joint apertures with thin metal sheets (thickness from 0.05 mm to 1.0 mm, at intervals of 0.05 mm), (Venvik, 2003).

Joint length, orientation and spacing define the connectivity of the joints (Odling, 1997). Many discontinuous and parallel fractures give less possibility for groundwater flow than continuous fractures of varying orientation. A combination of high connectivity and water-bearing joints give high hydraulic conductivity. Furthermore, experience and analytical models have showed that steep joints give higher groundwater than gentle dipping joints (Selmer-Olsen, 1981; Gudmundsson et al., 2001). Filling and coating of joints often tighten the joints, resulting in less hydraulic conductivity. Clayfilled joints are generally not water-bearing (Olofsson et al., 1988; Olofsson, 1991). But type of mineral coating is vital, calcite for example, can be dissolved resulting in groundwater leading channels. The joint roughness also influences the joints ability to lead water. High joint roughness can give rise to many small channels were the water can move. If the joint wall compression strength is high enough, small shear movements can lead to dilatancy, leading to even bigger voids for the water to flow (Olsson and Barton, 2001; Barton et al., 1985). These mechanisms are complicated and according to Grasselli et al. (2003) “a complete understanding of the relationship between void space geometry, contact areas, applied stress, and hydraulic conductivity has yet to be achieved.”

3.2.2 Stress situation

Generally high compressional stress perpendicular to joints tends to close the joints and reduce the hydraulic conductivity. Block tests performed by Hardin et al. (1982) and measurements carried out by Carlsson and Olsson (1986), showed that hydraulic conductivity is reduced when the stress level were raised. The rock mass overburden gives higher gravitational forces, and the vertical stress is increasing, as shown in equation:

$$\sigma_v = \rho \cdot g \cdot h \qquad \textbf{[3-6]}$$

Where

σ_v = vertical stress

ρ = density of the fluid

g = gravitational acceleration (9.81 m/s^2)

h = depth below rock surface (m)

Increasing stress with depth will close the apertures in the rock mass, resulting in decreasing hydraulic conductivity, see Figure 3.2.

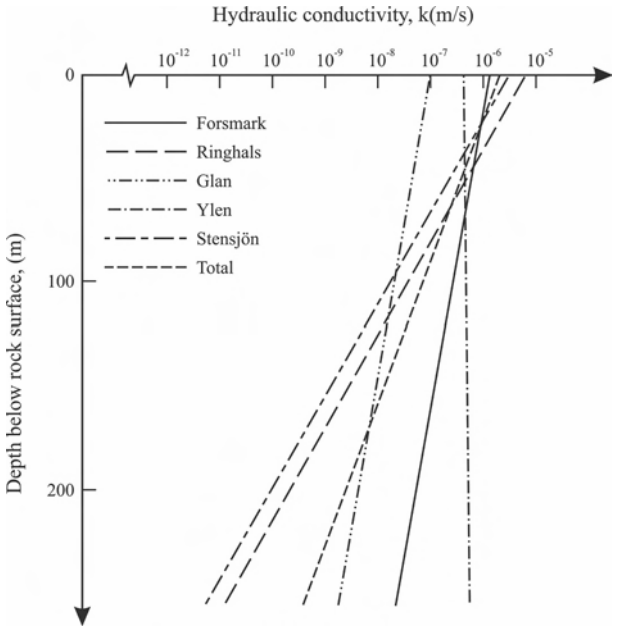

FIGURE 3.2 Hydraulic conductivity as a function of depth for Swedish test sites in Precambrian rocks (Carlsson and Olsson, 1977).

In a study of regional hydraulic conductivity data from ca. 140,000 hard rock boreholes in Norway and Sweden (Henriksen, 2008), found that flow rates were reduced with increas-

ing drilled rock depth. Most of the boreholes analysed by Henriksen (2008) were drilled to find sufficient water yield for the user. Hence, shallow holes tend to have higher flow rate than deeper holes, and the results agree with the trend shown in Figure 3.2.

High compressional stresses parallel with fractures will, however, tend to open it (Mazurak and Bossart, 1996; Singhal and Gupta, 1999; Silva and Jardim de Sá, 2000). Recent research shows that fractures approximately parallel with highest compressional stress, $\sigma_H \pm 30°$, are most likely to develop shear failure (Barton et al., 1995; Ferril et al., 1999; Rogers, 2003). Hence, it is likely that ground water flow will be encountered in fractures oriented close to parallel with major principal stress $\sigma_H \pm 30°$. Results in Henriksen and Braathen (2006) supports this theory.

In a tension fracture the displacement is primarily perpendicular to and away from the fracture plane. Tension fractures form when the minor principal stress is negative, that is, when there is an absolute tension in the crust. They are mostly limited to areas undergoing active extension, such as areas of rifting and those of great postglacial uplift (Rohr-Torp, 1994; Gudmundsson, 1999). According to Gudmundsson et al. 2002, tension fractures propagate from the surface and down to, at most, a few hundred metres depth. In contrast to tension fractures, hydrofractures can occur at any crustal depth. Hydrofractures are developed when the fluid pressure is higher than the normal stress on fracture planes. The normal condition for hydrofracture formation can thus be given as (Jaeger and Cook, 1979):

$$P_t \approx \sigma_3 + T_0 \qquad \textbf{[3-7]}$$

Where P_t is the total fluid pressure, σ_3 is the minor compressive principal stress (normal to the hydrofracture), and T_0 is the insitu tensile strength of the rock mass.

The postglacial uplift has its maximum of about 9 mm/yr in the Gulf of Bothnia (Dehls et al. 2000), see Figure 3.3. The maximum uplift rate coincide with the maximum thickness of the ice-sheet which had its maximum about 20,000 years ago. Rohr-Torp (1994) described a relationship between current uplift rates and yield of groundwater wells in Norway. Rohr-Torp (1994) analysed water yields in 1278 drilled wells in Norway, and found that the water yield in the analysed wells increased with current rate of uplift. According to a model made by Gudmundsson (1999) the total postglacial uplift can give maximum tensile stresses in the centre of the upliftet area of nearly 30 MPa. This is a magnitude higher than typical tensile strength of rock masses, hence tension cracks may be generated. Gudmundssons (1999) model showed that it is likely that postglacial uplift gives increased hydraulic conductivity, and corresponds well with the results found by Rohr-Torp (1994).

.

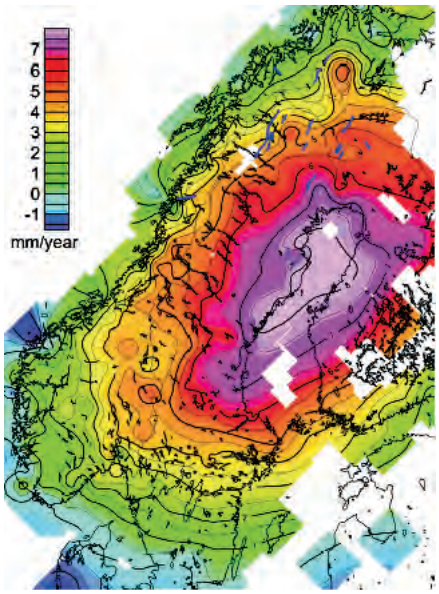

FIGURE 3.3 Map of the vertical uplift of Fennoscandia (Olesen et al. 2004).

The relationship between uplift rate and hydraulic flow rate from ca. 140,000 hard rock boreholes in Norway and Sweden have been analysed by Henriksen (2008). He found that the positive correlation was not as systematic as believed earlier (Rohr-Torp, 1994). Henriksen (2008) suggests that other factors than uplift rate may be better predictors of flow rate in rock masses, and also found that abrupt changes in uplift rates (differential uplift) may explain some of the variations in hydromechanical properties in hard rock.

Hence, the stress situation clearly has a major effect on the hydraulic conductivity of joints. Major fault zones and adjacent joints are also a result of stress and stress related movements in the rock mass.

3.2.3 Faults and direction of adjacent fractures

Experience has shown that highest risk for encountering high-volume water leakage is connected to fault zones (Barton et al., 1995; Caine et al, 1996; Evans et al., 1997; Ganerød, 2008). Results in Barton et al. (1995) indicate that the permeability of potentially active faults in todays stress field are the most water-bearing faults. From the engineering geological point of view the Norwegian professor Selmer-Olsen in 1981 suggested a theory, based on the assumption that tectonic stresses of relatively late geological age are

the driving forces generating fractures giving high water leakage into deep tunnels. He studied 11 hydropower tunnels located in mid and southern Norway. All tunnels had rock cover over 100 m and had high water leakage, from 1 l/s to 100 l/s. In one of the tunnels, water leakage of 18.000 l/min was experienced. The tunnels were typically in silicate rocks (gneiss and granite). After studying the fractures that had a greater volume of water leakage than seepage Selmer-Olsen (1981) concluded that:

- 85% of the fractures had dip angle greater than 70º.
- The angle between fractures with high water inflow and near by major faults was 45º ±15º (see Figure 3.4).
- Usually, only one joint set gave high water leakage.
- Continuous joints and fractures/crushed zones gave high water leakage.
- Measured water pressure corresponded to the rock cover.
- Highest leakage in brittle rock mass.
- The highest water leakage came in channels on joints with calcareous fillings.

In this list, most of the points are "common knowledge" today, and the same experiences have been confirmed in many tunnels. However, the relationship between the orientation of fractures with high conductivity and major faults is not well known among engineering geologists. Furthermore, the theory was not supported by Birkeland (1990), when he studied water leakage in subsea tunnels.

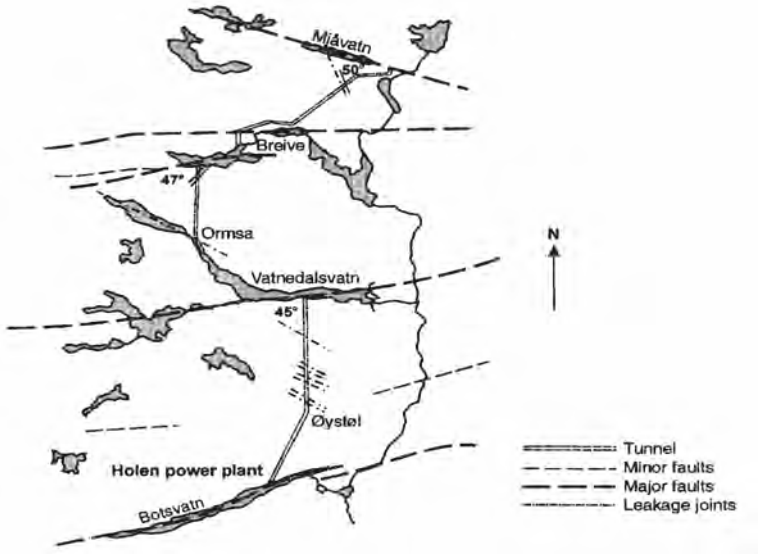

FIGURE 3.4 Major shear faults and leakage joints at the Otra Hydropower Project (Selmer-Olsen, 1981).

Recent research within structural geology concerning fracture trends and lineaments permeability focuses mostly on how the permeability changes close to fault zones (Ganerød, 2008) and how the permeability is related to the stress situation (Gudmundsson, 2000; Lie and Gudmundsson, 2002). The angle between regional faults and water-bearing fractures, including fractures outside fault zones, have not been in focus. Therefore it is relevant to check if the old theory of Selmer Olsen (1981) regarding angle between major faults and water-bearing fractures is correct.

3.2.4 Dykes

Igneous dykes are generally fine grained and brittle, and the adjacent rock mass is often more jointed than the rock mass in general. The dyke itself can be tight and work as a ground-water barrier, enabling the groundwater pressure to build up on either side of the dyke (Babiker and Gudmundsson, 2004). In contrast, a dyke can be highly fractured and water-bearing. Both possibilities give raise to higher groundwater inflow than in the surrounding rock mass. In the Oslo Region, the igneous dykes are known to be water-bearing (Løset, 1981, 2002; Boge et al., 2002).

3.2.5 Composition and thickness of the overburden

According to Cesano et al. (2000), the major leakage is clearly associated with parameters of the overburden, such as soil thickness and type, steepness of topography (ground and bedrock, topographical high and low areas). From studying the Bolmen tunnel in southern Sweden, they found that major leakage in the tunnel was clearly influenced by the topography, thickness and property of the overburden, and rock cover above the tunnel. Storage of groundwater in porous soil combined with good connection between the soil and rock mass will influence and increase potential groundwater inflow into tunnels in hard rock (Olofsson, 1994). This often occurs in valleys and depressions where the rock mass are more fractured, and therefore act as recharge zones for the rock mass. Cesano et al. (2000) found that 15% of the major leakages could be explained with only soil and topographical parameters. Areas of peat gave a weak correlation to increased numbers of major leakages. In the same analysis Cesano et al. (2000) found that tunnel sections with high rock cover gave the highest possibility of encountering large inflows, but not the small ones. According to Cesano et al. (2000) this is: “probably because deeper tunnel sections have a larger ray of influence and a larger cone of drainage, which increases the overall number of leakage.”

Other natural sources of groundwater recharge to hard rock are streams and lakes. Mabee et al. (2002) studied lineaments and groundwater inflow into a 9.6 km long tunnel located in eastern Massachusetts (USA). According to Mabee et al. (2002) lineaments identified by black and white aerial photographs (1:80.000) intersecting the tunnel less than 500 m

from a water body gave more water inflow than lineaments further away from water bodies. Furthermore, lineaments situated in valleys close to water bodies with permeable sand and gravel overlain the rock mass, gave high possibility for major water leakages (Mabee et al., 2002).

3.3 Rock mass characterization and classification systems which emphasize on water

As described in Section 3.2 several factors are affecting groundwater flow in hard rock. Furthermore, the factors are related to each other, and a full understanding is therefore very difficult to achieve. Still, rock mass characterization and classification systems also include some important aspects of the groundwater flow. In the following sections particular emphasis is placed on describing how groundwater is taken into consideration in such systems.

3.3.1 Rock mass characterization based on pregrouting

Based on experience gathered over the last 30 years from excavating tunnels in Norway, Klüver (2000) divides the rock mass into four rock mass classes. He describes typical rock mass properties for each class and suggests method and procedure for pregrouting. In Table 3.2, a summary of the rock mass properties for each rock mass class are given.

TABLE 3. 2 Typical rock mass properties for rock mass type A, B, C and D (Klüver, 2000).

Rock mass classes.	Aperture of joints.	Filling / coating of joints.	Hydraulic conductivity.	Typical rock types.
A	Open.	No or only thin coating.	High.	Sandstone, quartzite, igneous rock from the Oslo Region, syenite, and granite.
B	Partly open, water flow in channels.	Partly filled (clay, silt and rock mass fragments).	Medium to high.	Precambrian gneisses and similar metamorphic rocks.
C	Only small channels.	Highly filled (clay, silt and rock fragments).	Low.	Metamorphic rocks like shales, phyllite, mica shist, greenstone and greenschist.
D	Extremely open and/or caves.	No or only thin coating.	Extremely high.	Rock masses influenced by tectonic movements or karst phenomena (calcareous rocks).

The classification described in Table 3.2 shows four rock mass classes with very different hydrogeological proporties, and a good basis for understanding the general trends. This classification reflects that the hydrological property alters with rock types and their

properties. But all factors are not possible to cover in a simplified characterization like this four class division. For instance, rock mass type D will include a variety of geological properties, including karst phenomena in calcareous rocks, which is common in northern Norway.

3.3.2 Schematic model of a major fault zone

In Braathen and Gabrielsen (2000), a model showing typical structures of a major fault zone is described. The Geological Survey of Norway has written several reports in recent years, supporting this model (Elvebakk et al., 2002; Elvebakk and Rønning, 2002).

The model consists of five different zones, (A-, B-, C-, D- and E-zone), as shown in Figure 3.5. The A- and B-zone comprise the fault core, and is from a few cm up to 20 m wide. The fault core is highly jointed with 5-100 fractures per metre, and the A-zone consists of fault rocks, such as breccia and secondary minerals for instance clay. The C- and D- zone are together called the damage zone, and is between 5 and 50 m wide. The C-zone contains long parallel fractures, and in the D-zone two fracture sets intersects each other with an angle of 60°. The E-zone is a transition zone to the host rock with only background fracturing. The E-zone can be up to 200 m wide. According to preinvestigation and Braathen and Gabrielsen (2000), the C-zone, with long and parallel discontinuities potentially will give highest groundwater inflow in tunnels.

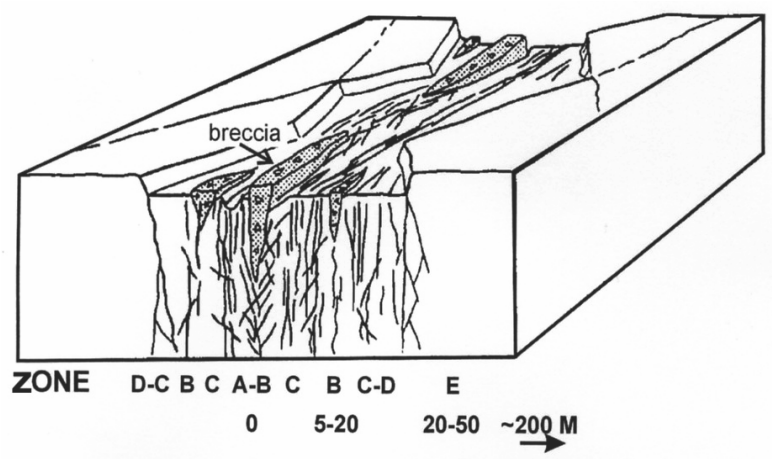

FIGURE 3.5 Typical structure of a major fault (Braathen and Gabrielsen, 2000).

Gudmundsson et al. (2001), describes faults in a similar way: "Fault slip occurs mostly along the core, which consists primarily of breccia and other cataclastic rocks. The damage zone contains numerous faults and fractures. For a major fault zone, the core thickness

is up to several tens of metres and the damage-zone thickness up to several hundred meters." Caine et al. (1996) also describes fault zone architecture and related permeability structures. He describes the faults with the following architectural components; fault core where most of the displacement occurs, damage zone with strucutures enhancing permeability compared to the core and protolith which is undeformed.

3.3.3 Groundwater flow and rock mass classification systems

In the following, the commonly used Q-method, RMR and RMi rock mass classification systems are discussed with particular emphasis on how groundwater conditions are incorporated in the systems.

The Q-system, developed at the Norwegian Geotechnical Institute (Grimstad and Barton, 1993), is the most frequently used rock mass classification system around the world. It is a quantitative classification system for estimates of tunnel support, based on a numerical assessment of the rock mass quality using the following six parameters:

- Rock quality designation (RQD).
- Number of joint sets (Jn).
- Roughness of the most unfavourable joint or discontinuity (Jr).
- Degree of alteration or filling along the weakest joint (Ja).
- Water inflow (Jw).
- Stress condition given as the stress reduction factor (SRF).

The Q-value is calculated to give the overall rock mass quality:

$$Q = \frac{RQD}{J_n} \times \frac{J_r}{J_a} \times \frac{J_w}{SRF} \qquad \textbf{[3-8]}$$

The parameter for water inflow, J_w, varies between 0.05 to 1. Highest values are given for dry excavations or minor inflow, i.e. <5 l/min locally, and lowest for exceptionally high inflow or water pressure continuing without noticeable decay (can also be rated from groundwater pressure). The variation is considerable and water inflow influence the Q-value to a great extent.

The RMR (Geomechanics) system, developed by Bieniawski in 1973, and updated in 1989 (Bieniawski, 1989), utilises the following six rock mass parameters:

- Uniaxial compressive strength of intact rock material (rating 0-15).
- Rock quality designation RQD (rating 5-20).
- Spacing of discontinuities (rating 5-20).

- Condition of discontinuities (rating 0-30).
- Groundwater conditions (rating 0-15).
- Orientation of discontinuities (rating adjustment -60-0).

The total RMR rating is given by summarizing the ratings given for each of the parameters above. Highest value is 100, and is equivalent with very good rock mass, while rating less than 20 is equivalent to very poor rock mass. When applying the RMR system, the typical, rather than the worst, conditions are evaluated. Groundwater conditions are rated from; no inflow to greater than 125 l/min per 10 m tunnel length (can also be based on groundwater pressure divided by major principal stress).

The RMi system (Rock Mass index) is a rock mass characterization system for rock engineering purposes developed by Palmstrøm (1995). The rock mass index (RMi) is given by:

$$\text{RMi} = \sigma_c \times JP \quad \textbf{[3-9]}$$

Where σ_c is the uniaxial compressive strength of intact rock measured on 50 mm samples. JP is the jointing parameter, i.e. the reduction factor from jointing. It consists of:

-The degree of jointing (given as block size), and

-The joint characteristics, representing the joint wall roughness and alteration, as well as the size of the joint

$$\text{JP} = 0.2\sqrt{jC} \times Vb^{D} \quad \textbf{[3-10]}$$

Where jC = the joint condition factor, Vb = the block volume, and D = 0,37 $jC^{-0.2}$

jC = jR · jL / jA, where

jR=Joint roughness factor

jL=Joint size factor

jA=Joint alteration factor

Figure 3.6 shows how the main inherent parameters of the RMi-system are combined. Based on the Continuity Factor (CF=tunnel diameter/block diameter), Palmstrøm (1995) divides the ground into continous or blocky material, and different charts are used for the two groups to estimate rock support method. More details and recent developments of the RMi system are given in Palmstrøm (2000).

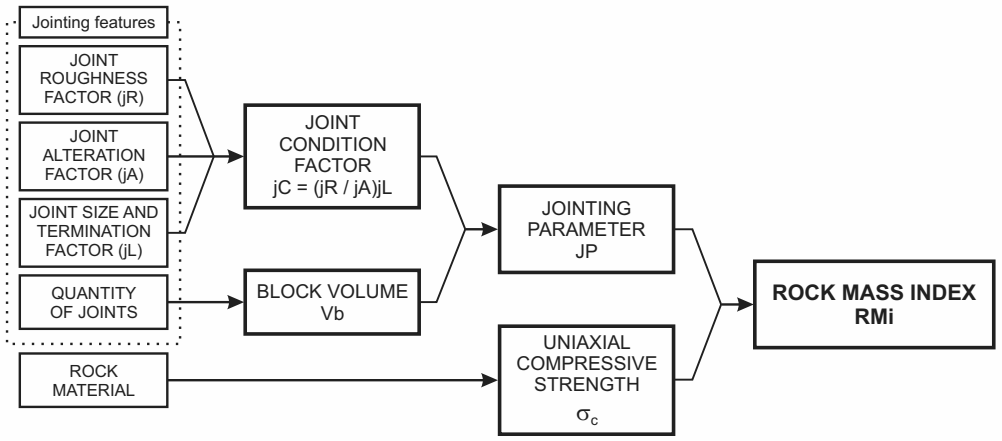

FIGURE 3.6 Combination of the selected parameters in the Rock Mass Index (Palmstrøm, 1995)

Groundwater conditions were only partly accounted for in the first version of the RMi system (Palmstrøm, 1996). In 2003 a spreadsheet was available from: www/rockmass.net, (Palmstrøm, 2007). This spreadsheet is helpful for users calculating the Rock Mass index and estimating rock support method. Among other factors applied for in the calculation of rock support, the effect from ground water was rated based on descriptions of joints, softening of clay and water pressure build-up, resulting in minor, moderate or major influence on stability. In the RMi system, the influence of groundwater is considered as one of the external forces acting on the ground, and only applied for in the estimation of rock support, and not when calculating the value of Rock Mass index.

3.4 Concluding remarks on groundwater inflow

Several parameters influence on the hydraulic conductivity of the rock mass. In many underground constructions with high water leakage several of the geological parameters mentioned are present and working together. This is maybe the most important reason why we have yet to achieve a good understanding of which parameters is the most important controlling the groundwater flow. However, as discussed in this chapter, research has shown that many of the parameters are dependent on the structural geology in the area and the movements induced by the stresses acting on the rock mass over time.

It is therefore considered important to continue the research searching for correlation between geological parameters and groundwater inflow. As a basis for further research in this field, the eight hypotheses in Section 1.3 have been defined.

CHAPTER 4

Prediction of water inflow in hard rock tunnels

4.1 The common approach and its limitations

In Norway, estimating water inflow in tunnels has to a large degree been based on general knowledge about rock types, faults, weakness zones and comparisons with other, nearby underground structures. Site investigations are important sources for information, and results from core drilling with water pressure tests are commonly used when estimating water inflow in future tunnels. To some extent analytical approaches have been used as a first approximation of how much water leakage to expect in tunnels.

The approach has however several limitations:

- Limited knowledge of how the geological, hydrogeological and hydraulic factors should be collected and used. The different factors are inter-related, and the comprehension of how to use them in predictions of groundwater inflow is still limited.
- Due to high investigation costs, only a limited amount of geological and hydrogeological information are collected. The degree of geological complexity has to be considered to decide the extent of site investigations.
- Uncertainty regarding how to interpret the limited information collected.

Numerical modelling is also one approach for estimating groundwater inflow in underground structures. Modelling is not commonly used in Norway, but has been used in a few cases as a tool to estimate groundwater flow into tunnels (Kitterød et al., 1998; Cuisiat et al., 2003). However, in both cases referred to the modelling was done after high water

leakage was encountered, and not as a tool to predict future water inflow. In this thesis, numerical modelling will not be discussed in detail. It is considered to be more important to understand the hydrogeological factors, and techniques to interpret this information making reliable predictions for water leakage in tunnels. "If numerical representations of rock masses often proved to be inadequate for predictions, it is implied that some important factors have been missed in the prediction of the inflows." (Cesano et al., 2000).

Prediction of groundwater inflow in hard rock tunnels has been a time-consuming and cumbersome problem which engineering geologists have struggled with for decades. Basically three main approaches are used, in addition to numerical modelling; 1) analytical, 2) semi-empirical and 3) empirical approaches.

1. In analytical approaches, formulas deduced through theory are used to calculate the water inflow into tunnels. Hydraulic conductivity of the rock mass is needed in the formulas, and the biggest challenge is therefore to measure the hydraulic conductivity. It is important to bear in mind that simplifications are necessary to derive the formulas used in the estimations.
2. In semi-empirical approaches, experience from several previous tunnel projects are combined to find correlations useful for estimating possible water inflow, usually the results are combined and compared with analytical formulas.
3. In empirical approaches, estimations of groundwater inflow is based solely on experience from previous underground constructions. And the results are not given exact, but in an expected range of water leakage.

In the following sections a review of the different approaches with relevant references is given. It is considered important to understand the different possibilities and limitations for estimating water inflow to hard rock tunnels.

4.2 Analytical approaches to prediction of groundwater inflow in hard rock tunnels

As a simple example a tunnel in a semi-infinite rock mass with a horizontal water table is considered. The depth of the tunnel centre from the water table is h and the tunnel radius r, see Figure 4.1

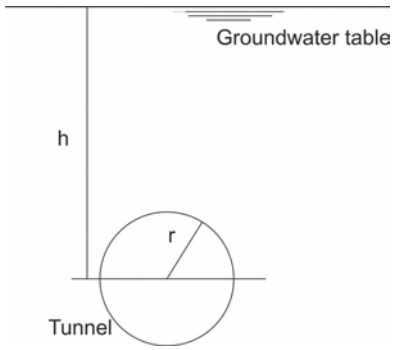

FIGURE 4.1 Circular tunnel in a semi-infinite rock mass with a horizontal water table.

Assuming isotropic and homogeneos conditions the water inflow may be calculated according to several alternative approximations, see Table 4.1.

TABLE 4. 1 Alternative approximations for the gravity water inflow (El Tani, 2003).

$Q_{MG} = 2\pi k \frac{h}{\ln\left(\frac{2h}{r}\right)}$	**[4-1]**	(Muskat, 1937) and (Goodman et al.,1965).
$Q_{Ka} = 2\pi k \frac{h}{\ln\left(\frac{2h}{r}-1\right)}$	**[4-2]**	(Karlsrud, 2002).
$Q_{SL} = 2\pi k \frac{h}{\ln\left(\frac{h}{r}+\sqrt{\left(\frac{h^2}{r^2}\right)-1}\right)}$	**[4-3]**	(Rat, 1973); (Schleiss, 1988) and (Lei, 1999).
$Q_{Lo} = 2\pi k \frac{h}{\left(1+0{,}4\left(\frac{r}{h}\right)^2\right)\ln\frac{2h}{r}}$	**[4-4]**	Lombardi (2002).
$Q_{T2} = 2\pi k \frac{1-3\left(\frac{r}{2h}\right)^2}{\left[1-\left(\frac{r}{2h}\right)^2\right]\ln\frac{2h}{r}-\left(\frac{r}{2h}\right)^2}$	**[4-5]**	(El Tani, 1999).

El Tani (1999) compared the different approximations, Q_{ap}, with exact water inflow, Q, and calculated the relative differences from formula:

$$\Delta = \frac{Q_{ap}-Q}{Q} \qquad \textbf{[4-6]}$$

The graph in Figure 4.2 illustrates the relative differences. It is evident that the approximations have improved over time, and the first approximations clearly overestimated the ground water inflow. Goodman et al. (1965) and Muskat (1937) approximations are generally differentiated in the litterature. Goodman et al. are referred to in many recent papers, therefore a more detailed description of Goodman's approach follows. In addition the approximation published by Tokheim and Janbu (1984) is described because their approach is to some degree used in Norway for estimations of groundwater inflow into tunnels.

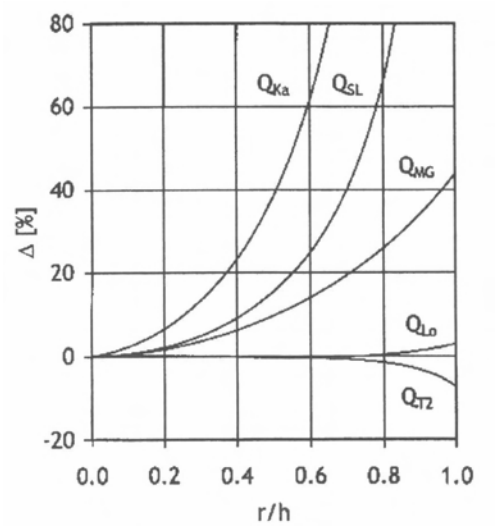

FIGURE 4.2 Relative difference of the diverse approximations in Table 4.1 with the exact gravity water inflow (El Tani, 1999)

Based on a combination of theoretical and mathematical models and model studies, Goodman et al. (1965) provided an approach for estimating permeability from single hole water pressure tests. The theory builds on several simplifications and assumptions, such as Darcy's law, and that the permeability can be measured or reasonably assumed. Goodman et al. discussed two different scenarios; inflow through tunnel walls without drawdown and face flush resulting in transient heading flows. An example of the first scenario is when a tunnel completely penetrates a leakage zone, and there is so much water that drawdown is impossible. The approximate expression for rate of inflow per unit length of tunnel is then:

$$Q = \frac{2k(h+H)}{2{,}3\log\left(\frac{r}{2h}\right)} \qquad \textbf{[4-7]}$$

Where

h = distance from the tunnel to the top of the ground (m)

r = tunnel radius (m)

H = depth of the standing water (m)

According to El Tani (2003) Equation 4-1 and 4-7 are the same when transforming the natural logarithm in Equation 4-1 into a decimal one.

The other scenario is when a tunnel face suddenly breaks into a water-bearing zone (face flush flow) such as a fault, resulting in transient heading flows. As water drains into the tunnel, the pressure declines, eventually reaching a steady state of water leakage. In the case where there is a constant upper water level, for example a large surface or ground water supply, the diffusion equation can be used to study the face discharge and potential distribution (Goodman et al. 1965):

$$\frac{\partial^2 p}{\partial x^2} + \frac{\partial^2 p}{\partial y^2} + \frac{\partial^2 p}{\partial z^2} = \frac{nc\Upsilon_w}{k}\frac{\partial p}{\partial t} \qquad \textbf{[4-8]}$$

Where

n = porosity

c = compressibility of the system (rock + water)

Υ_w = unit weight of water

k = hydraulic conductivity (m/s or cm/s)

A computer program was used to solve this equation, which allows for the calculation of the total discharge into the tunnel at any given time for typical cases. In this calculation tunnel size, fault zone thickness, hydraulic conductivity, porosity, vertical distance to impermeable layer from surface, and depth to top of tunnel were all varied. Figure 4.3 illustrates the situation as calculated with the computer program.

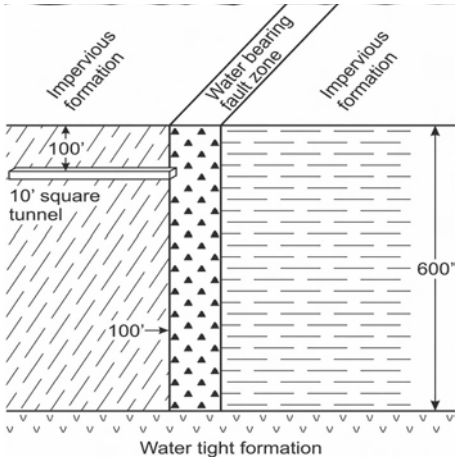

FIGURE 4.3 The situation of face discharge investigated by using a computer solution for the diffusion equation (Goodman et al., 1965).

Tokheim and Janbu (1984) wrote a paper with straightforward, approximate formulas estimating flow rates of air (gas) and water (incompressible liquid) from or into a cavern, the cavern may act as a source or a sink. According to Tokheim and Janbu, the water inflow into a tunnel or cavern is defined by the following equation:

$$Q_w = \frac{2\pi \times K \times L \times p}{\mu_w \times G} \quad \textbf{[4-9]}$$

Where

Q_w = inflow rate (m^3/s)
K = specific permeability (m^2) ($K=k\left(\frac{\upsilon}{g}\right)$)
L = length of tunnel or cavern (m)
μ_w = dynamic viscosity of water (kg/m) = density × cinematic viscosity
G = geometry factor

The geometry factor (G) describes the flow pattern relatively to the geometry of the tunnel or cavern, and is given by:

$$G = \ln\frac{(2D\text{-}r)(L+2r)}{r[L+2(2D\text{-}r)]} \quad \textbf{[4-10]}$$

Where

D = distance between the centre of the excavation and the groundwater table (m).
r = "equivalent radius" of idealised geometry, i.e., the radius of a cylinder with a surface area equal to that of the actual excavation (m).

As can be seen from the inflow equation, hydraulic conductivity, k, is needed to calculate the groundwater inflow. Hence, to obtain a reliable input, permeability testing (water pressure tests) of boreholes must be carried out.

In Norway, Tokheim and Janbu's approach is sometimes used for a first estimate of groundwater inflow into tunnels. However, this method is based on simplifications, like assuming isotropic conditions, and best estimates are obtained when L>>r (Nilsen and Palmstrøm, 2000). An example of its use is given in Holmøy (2002).

Raymer (2005) suggested simple analytical equations to estimate inflow and water table drawdown around the tunnel. One of the models was based on a conceptual model of lateral flow toward a tunnel, see Figure 4.4.

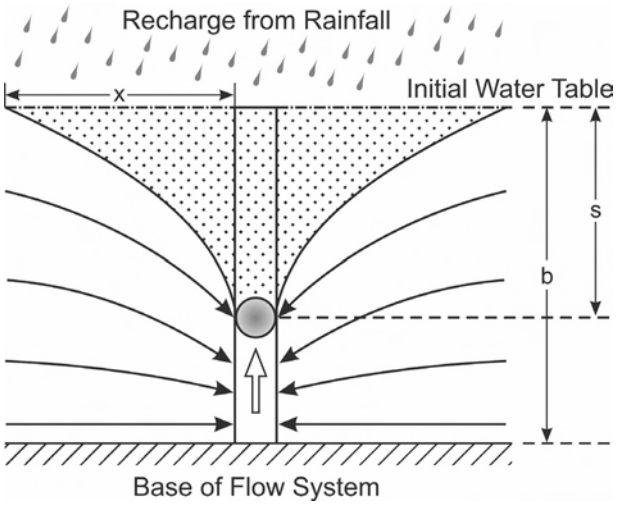

FIGURE 4.4 Conceptual model of lateral flow toward a tunnel. Shaded area is theoretically dewatered zone along tunnel (Raymer, 2005).

The lateral model considers drawdown (s) of the water table, as shown in Figure 4.4; hence, the thickness of the flow system (b) becomes smaller. The reduction in thickness of flow system further influences on the transmissivity (T), which is equal to the permeability integrated over the thickness of the flow system. Raymer (2005) solved this by using the "corrected drawdown" (s') in the equations involving water table drawdown (Lohman, 1972):

$$s' = s - \left(\frac{s^2}{2b}\right) \quad \textbf{[4-11]}$$

If long term inflow (when recharge balance the flow into the tunnel) is considered, the following equation can be used for estimation of water inflow (Raymer, 2005):

$$Q = 2L\sqrt{RTs'} \quad \textbf{[4-12]}$$

Where

L = Tunnel length (m)

R = Recharge rate (mm per year)

T = Transmissivity (m^2/s)

s' = Corrected drawdown (see Equation 4-11)

As can be seen from Equation 4-12 the water inflow is not directly proportional to hydraulic conductivity, but is a function of both recharge and permeability (in transmissivity), and varies with the square-root of permeability.

4.3 Semi-empirical approximations

Heuer (1995) described a semi-empirical method for estimating possible water inflow based on borehole water pressure test results. In his opinion estimates can be made only based upon previous tunnelling experience at a given location, or elsewhere in identical geologic settings. Heuer correlated observed water inflow in two tunnels during construction with water pressure test results available from the site. The tunnels were located in fractured dolomite formations in Milwaukee, within the state of Wisconsin in the United States. A graph based on the correlations found was defined, see Figure 4.5. Results from

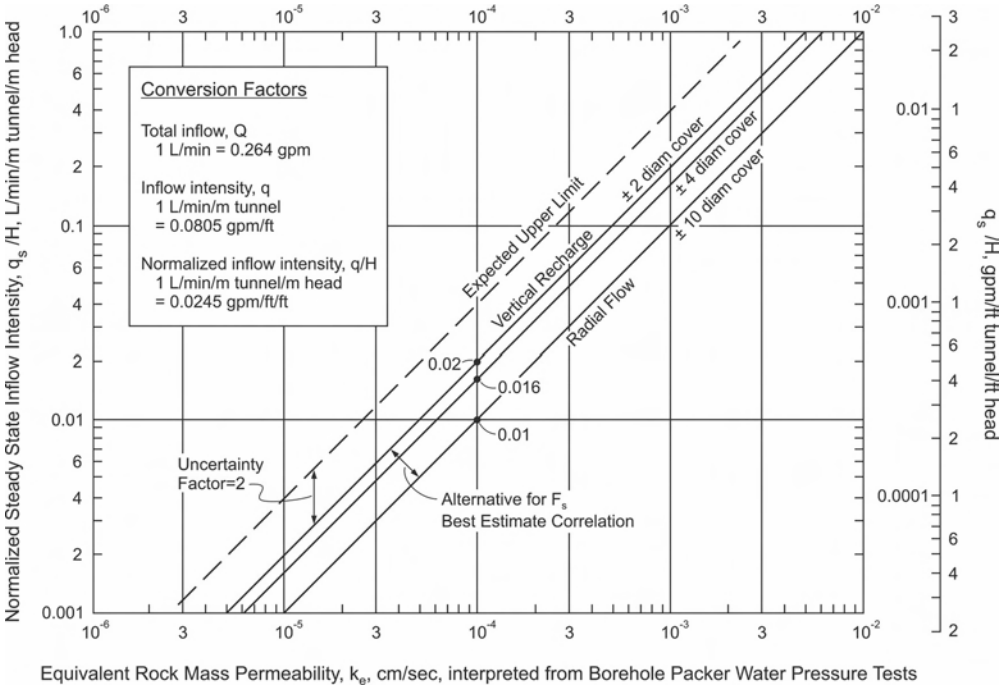

FIGURE 4.5 Relationship between steady state inflow and hydraulic conductivity interpreted from water pressure tests (Heuer, 1995)

water pressure tests can be used directly in this graph to find the steady state inflow intensity (l/min/m tunnel/m head). The phrase “long term steady state” refers to conditions which exist during time of construction, a period of several months to a couple of years.

For steady state inflow the graph considers two different boundary conditions; vertical recharge and radial flow. Vertical recharge is applied when a recharge source of large water volume at constant head is close to the tunnel, for example under a lake, or under a highly permeable aquifer. For radial flow the recharge source is far away. Also the rock cover given in tunnel diameters are considered, when the rock cover is over 10 diameters, vertical recharge and radial flow are approximately the same. The graph was made based on data from only two tunnels, but according to Heuer the data have been compared with data from other tunnels in igneous, metamorphic and other sedimentary rock types.

To give a prediction of water inflow for an entire tunnel, Heuer (1995) calculated the water inflow as explained above and assumed that the results from the water pressure tests gave a correct percentual distribution of the hydraulic conductivity along the entire tunnel. Examples of estimation of long term steady state inflow is given in Heuer (1995). The major disadvantage is the need to determine how many water pressure tests will be required to give a correct distribution for good estimations of water inflow. Heuer suggested that actual inflow can be expected to vary from one half to two times of the predicted value if his method was applied. The correlations also showed that inflows into hard rock tunnels were typically about 1/8 of those predicted by Goodman et al.'s (1965) equation.

Raymer (2001), published a paper predicting groundwater inflow into the Chattahoochee Tunnel, a deep sewer tunnel located in Cobb County, Georgia, United States. The rock in the project area consists of medium-grade metamorphic rock overlain by progressively weathered rock. Water pressure tests were carried out to determine the hydraulic conductivity in the rock mass. Fifty boreholes and 298 water pressure tests were used in his estimation. His calculations are based on Goodman et al.'s (1965) equation with Heuer's (1995) reduction factor (1/8), to calculate inflow into the Chattahoochee Tunnel:

$$Q_L = \frac{2\pi kH}{\ln\left(\frac{2z}{r}\right)} \times \frac{1}{8} \qquad \textbf{[4-13]}$$

Where

Q_L = Inflow rate per unit length of tunnel

k = Hydraulic conductivity (cm/s)

H = Groundwater head (m)

z = Thickness of the bedrock above the tunnel (m)

r = Tunnel radius (m)

The statistical distribution of the pressure tests, indicated that most of the inflow into hard rock tunnels typically comes from a small percentage of the tunnel length, see Figure 4.6.

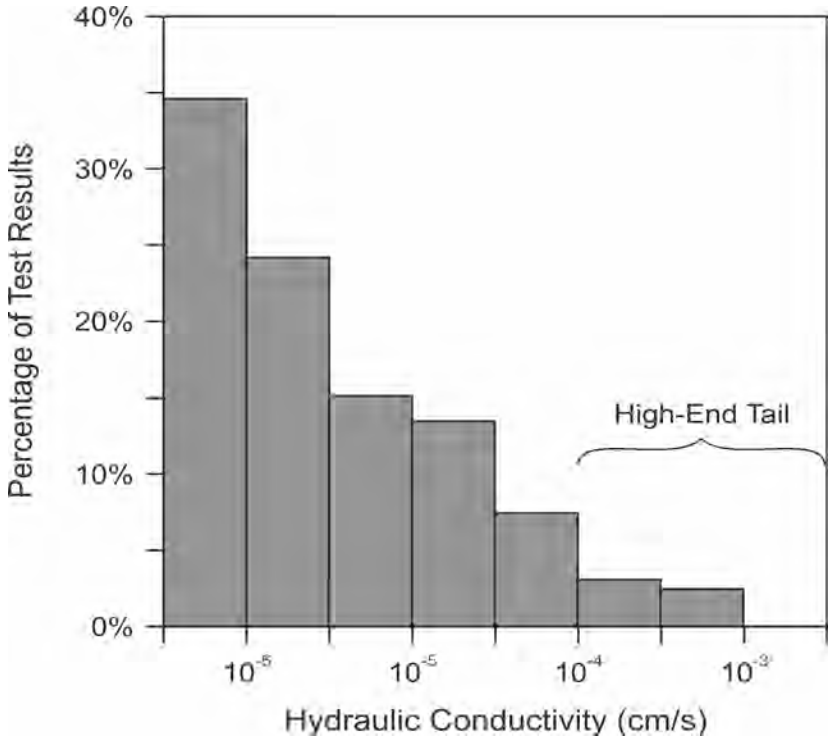

FIGURE 4.6 Histogram of 298 water pressure test results from the Chattahoochee tunnel (Raymer, 2001)

When Raymer made a cumulative curve of the same 298 water pressure test results, the pattern of points appeared to follow a log-normal distribution, with the exception of those points representing tests below 1 x 10^{-6} cm/s. It is not practical nor reasonable to measure lower hydraulic conductivity than 1 x 10^{-6} cm/s, and besides, a hydraulic conductivity this low will give no visible water leakage in the tunnel.

Raymer also made a log-normal plot of the same data as in Figure 4.6, but with the y-axis transformed to a logarithmic scale and the x-axis transformed to a normal distribution (probability) scale. The result of these transformations was a straight line, see Figure 4.7.

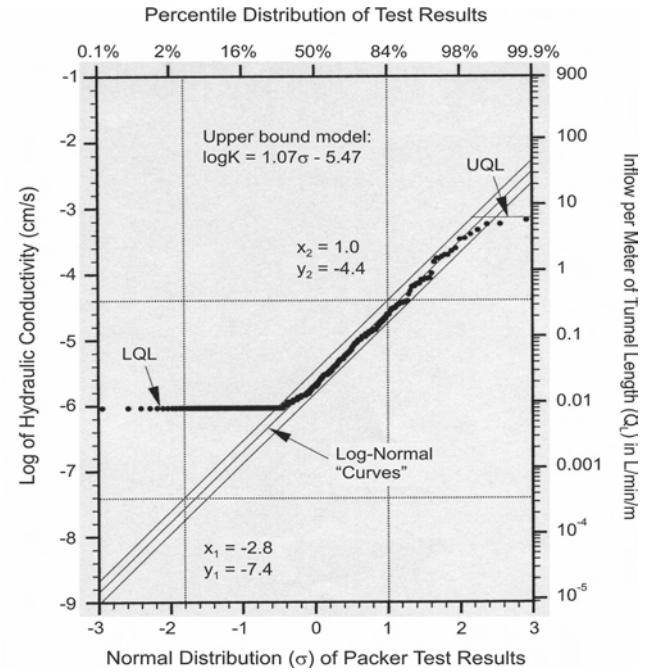

FIGURE 4.7 Log-normal distribution of same test results as Figure 4.6 (Raymer, 2001).

The log-normal plot revealed an Upper Quantitation Limit (UQL) in the data at about 7 x 10^{-4} cm/s. Raymer considered this UQL may be caused by resistance in the test equipment under high flow rates. Hence, it is very likely that the high end of the hydraulic conductivity distribution would be missed if the analysis were based on the data itself (like Heuer), rather than on a model of the data. The result would be a large underestimate.

Based on the log-normal plot, Raymer drew three correlation lines, a median correlation in the middle, flanked by upper and lower bounding lines. The median line represents an equal likelihood that the value is overestimated or underestimated. The upper bounding represents a small chance that the inflow is underestimated. Raymer calculated the total inflow for the entire tunnel (15.126 m); Q_{upper} = 8738 l/min and Q_{median} = 6045 l/min.

The Chattohoochee tunnel was under construction when Raymer wrote his paper in 2001, and the tunnel was scheduled for completion in 2004. According to Raymer (2005) the total inflow for 14.720 m of the tunnel (flow around the end of the tunnel was not included) was 5400 l/min. This corresponds well with the calculated median inflow for the entire tunnel.

Shamma et al. (2003) published a paper describing groundwater analyses for estimating the level of conservatism in the specified construction measures used to comply with the strict inflow requirements for the Arrowhead East Tunnel (AET) a water supply tunnel situated in southern California in the United States. The tunnels were excavated through hard, igneous and metamorphic rocks.

An attempt was made during the excavation of the AET to use probe hole inflow data to find which analytical approach (Goodman et al. (1965) or Heuer (1995)), would give the best estimate for tunnel inflow. This comparison gave mixed results. Goodman et al.'s face flush equation with a constant head over the entire length of the heading gave results that overestimated flow, while Heuer's approach led to results that generally underestimated flows. Therefore, Shamma et al. (2003) used the average between the two approaches to calculate the "best" estimate of heading inflows.

Thapa et al. (2003) published an interesting paper comparing predictions and actual water leakage into two tunnels in the United States, the Borman Park Intake Tunnel extending under Lake Michigan in Gary, Indiana, and the Upper Diamond Fork Tunnel in Utah. Inflow predictions for the Borman Park Intake tunnel were made using the procedure described by Heuer (1995) and augmented by Raymer (2001). One inflow estimate was based on water pressure test data applied directly assuming the tests represent the entire range of conductivities the tunnel will encounter. A second estimate was made by using the water pressure test data as a partial sample from a population of conductivities the tunnel will encounter. In the second approach a log-normal distribution was chosen, see Figure 4.8.

Both methods indicated that the inflow will be dominated by relatively high hydraulic conductivities. The high tail-end conductivities incorporated into the log-normal analysis leads to a 15% higher total inflow estimate compared to the histogram estimate, 3173 l/min and 2682 l/min, respectively. The observed inflow in the Borman Park Intake Tunnel had a different distribution form and higher mean than predicted by the histograms. Thapa et al. believed the discrepancy could be due to a fracture orientation sampling bias introduced by the use of vertical boreholes to represent a horizontal tunnel. This problem is increased when water-bearing fractures and faults encountered during tunnelling typically are close to vertical.

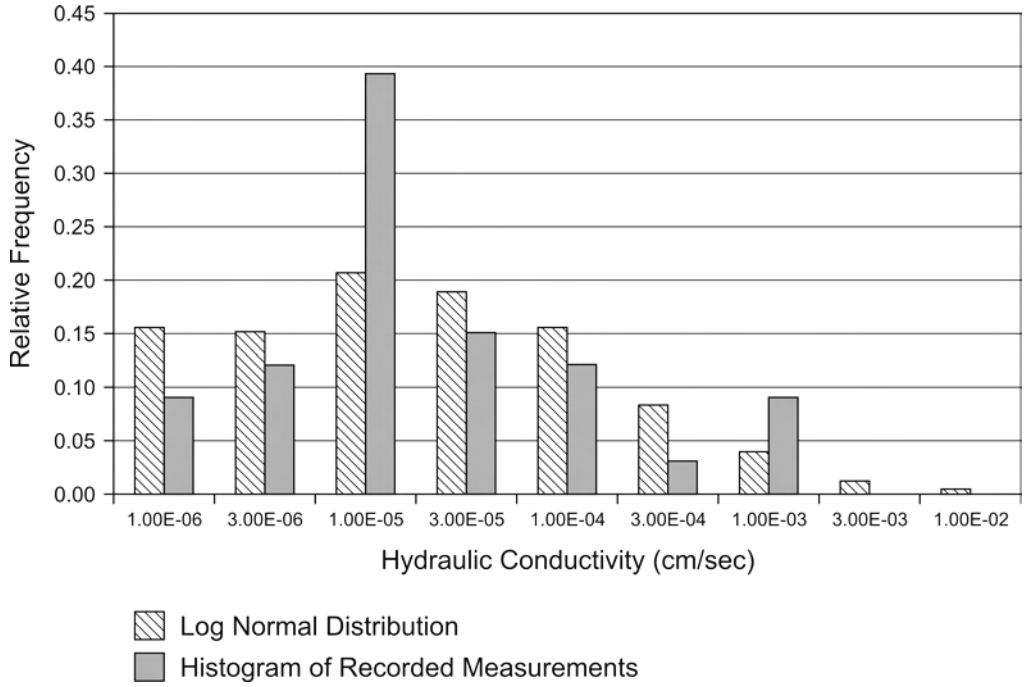

FIGURE 4.8 Histograms of Borman Park water pressure test results (Thapa et al., 2003).

At the Upper Diamond Fork Tunnel, groundwater inflows were predicted using a statistical analysis developed by Jacobs Associates and Golder Associates (2001). The method used Monte Carlo simulation to develop statistical distributions of inflow by sampling distributions of the major sources of uncertainty, and combining them using an inflow function. The equations developed by Goodman et al. (1965) were used to calculate the instantaneous heading inflow and subsequent reduction with time. For the Upper Diamond Fork Tunnel, the observed hydraulic conductivity was significantly higher than what was sampled by the water pressure test measurements. The hydraulic conductivity varied significantly with the different geological units.

Based on their analysis of the data from these two tunnels, Thapa et al. concluded that "(…) hydraulic conductivity distributions cannot be assigned a particular form (i.e., log-normal) a priori." In addition, their experience with the Monte Carlo simulation method was promising; it proved to be a useful technique for evaluating the combined effect of the factors, and the uncertainties associated with these factors, when predicting groundwater inflow.

Raymer (2005) estimated inflows for three hard rock sewer tunnels in the Atlanta area, in the United States; the Chattahoochee, Nancy Creek and Clear Creek tunnels. The latter tunnel was under construction when Raymer wrote his article, while the other two were completed. For the two completed tunnels a comparison of actual inflow and calculated inflow were done. Two different models were used; the lateral model (Equation 4-12) and Heuer's (1995) model. For both tunnels the depth of the flow system was estimated as b = 1.5s and recharge was estimated at 220 mm per year. Average permeability was calculated statistically using Raymer's (2001) log-normal method. Results from estimated inflows and actual inflow are given in Table 4.2.

TABLE 4. 2 Actual and estimated inflows using different models (Raymer, 2005).

	Chattahoochee (14.720 m).	**Nancy Creek (13.265 m).**
k (average).	3.0×10^{-5} cm/s.	6.7×10^{-5} cm/s.
	l/s	l/s
Actual.	90	88
Lateral.	89	92
Heuer.	63	96

The estimated inflows from the lateral model seem to agree well with the actual inflows in the tunnels. The results given in Table 4.2 are also plotted in Figure 4.9, which illustrates how inflow (l/s) per 1.000 m tunnel varies with average permeability, using Goodman's (1965), Heuer's (1995) and Raymer's (2005) models.

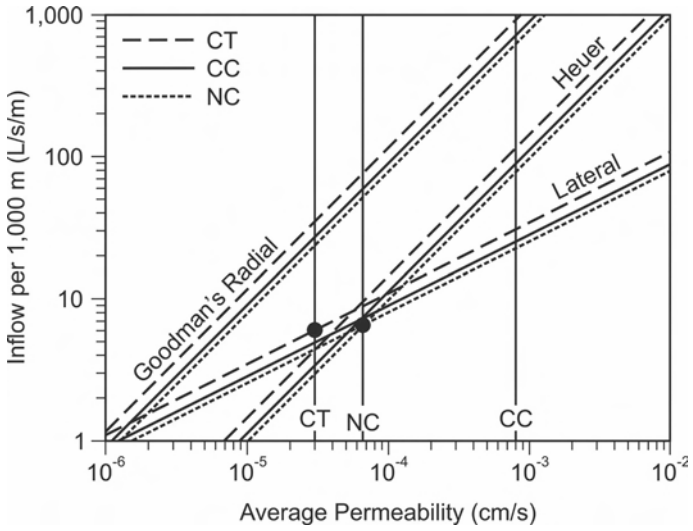

FIGURE 4.9 Inflow versus permeability for Goodman, Heuer and lateral models. Vertical lines indicate average hydraulic conductivity for each tunnel; Chattahoochee tunnel (CT), Nancy Creek tunnel (NC) and Clear Creek Tunnel (CC). Dots indicate actual inflow in CT and NC (Raymer, 2005).

4.4 Empirical approximations

Empirical approximation is most commonly used in Norway. In this method, groundwater inflow is estimated based on experience from earlier projects in identical geological setting. The problem is that the geological conditions seldom are identical and therefore the empirical approximations can only give rough assumptions.

An example of empirical approximation is given by Klüver (2000), who described four rock mass types (A, B, C and D), and based on experience from pregrouting predicted water leakage rating from low to extremely high. Another example is Rohr-Torps (1994) research showing that the hydraulic conductivity in the eastern part of Norway can be expected to be higher than in the coastal parts of Norway due to a relationship between current uplift rates and yield of groundwater wells.

Many of the relations mentioned in Section 3.2 (Significance of geological parameters) are relatively well known and in common use by planners and builders, for example the relationship between groundwater flow and stress situation. However, empirical approximations are depending on the people using them, and even for qualified and experienced people it is very difficult to give other than a qualified guess for water inflow.

Another problem is that a lot of experience gathered over time is not reported, and is therefore not easily available.

4.5 The significance of hydraulic heterogeneity for predictions on water flow

A geological formation is not homogeneous as long as the hydraulic properties vary from one place to another. The higher the degree of heterogeneity is, the larger is the variability of the hydraulic conductivity field, and the more difficult it is to make predictions on water flow, (Cesano et al., 2003). Based on this general statement, Cesano et al. described an approach to quantify the degree of heterogeneity of a fracture network. To calculate the degree of heterogeneity of a fracture network, Cesano et al. divided the fractures into a homogeneous and a heterogeneous component. Fracture sets are identified through clustering analysis of stereographic projections, and all fractures belonging to a fracture set is a part of the homogeneous component. The fractures that belong to none of the fracture sets are defined to belong to the heterogeneous component (one heterogeneous fracture set). Figure 4.10 illustrates how a network of fractures can be divided into a set of homogeneous component and a heterogeneous component.

The calculation of the heterogeneity index is based on information usually collected through a geomechanical classification of rock mass (Bienawski, 1989; ISRM, 1978 b). Before calcultion the fracture characteristics are reclassified in a non-dimensional interval (between one and zero). The heterogeneity index is a function X_i of the variance in the fracture characteristics of each fracture set i, considering the heterogeneity component also as a set on its own:

$$X_i = f(a_1 \cdot \sigma^2_{s/d}, a_2 \cdot \sigma^2_s, a_3 \cdot \sigma^2_t, a_4 \cdot \sigma^2_a, a_5 \cdot \sigma^2_r, a_6 \cdot \sigma^2_{mf}) \quad \textbf{[4-14]}$$

Where $\sigma^2_{s/d}$ is the variance of strike and dip, σ^2_s is the variance of spacing, σ^2_t is the variance of trace length, σ^2_a is the variance of aperture, σ^2_r is the variance of roughness and σ^2_{mf} is the variance of mineral filling. The coefficients a_i are weights that indicate the role that the different fracture characteristics have in relation to the specific problem in question.

The overall heterogeneity index, I_h is calculated by adding the contibution from all the fracture sets (homogeneous component) and all the fractures that do not belong to any set (heterogeneous component):

$$I_h = I_{hom} + I_{het} = \sum_{n}^{i=1} (X_i D_{hi}) + (X_h D_{hh}) \quad \textbf{[4-15]}$$

The value of D_{hi} and D_{hh} is the ratio of the number of fractures belonging to the respective fracture sets over the total number of fractures

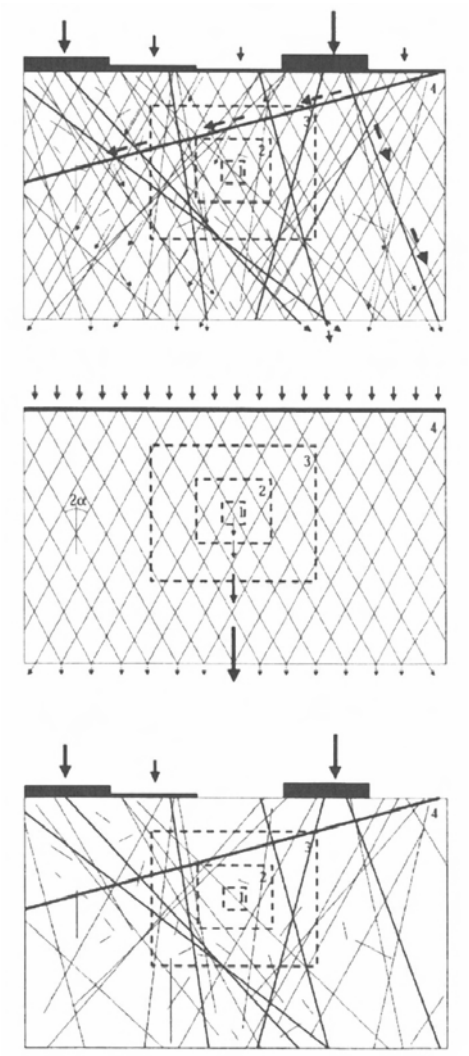

FIGURE 4.10 The homogeneous and the heterogeneous components are shown in the middle and the bottom figures respectively. The top figure results from superposition of the two bottom figures (Cesano et al., 2003).

In the approach described above, Cesano et al. assumed that all fracture characteristics play the same role in regulating fracture flow, that is $a_i = 1$ in Equation 4-14. But they stress that it is difficult to estimate the real weight that each parameter has in regulating fracture flow.

Cesano et al. carried out six synthetic experiments studying the relation between variability in fracture characteristics and flow. In addition, real fracture data along 3000 m of the Pont-Ventox tunnel was studied and compared to the variability in rate of flow. Based on this the main conclusions from Cesano et al. (2003) were:

- The degree of variability in the main direction and magnitude of flow through a fracture network increases when the overall level of heterogeneity of the network increases.
- The synthetic experiments showed that a “jump” in the variability of flow occurs in the proximity of those fractures (e.g. faults) whose characteristics differ substantially from the rest of the network.
- There exists a correlation between different fracture characteristics and the magnitude of flow.
- It is reasonable to assume that variability in such characteristics would at least play an important role in the variability of flow.
- The fracture parameters that regulate the mechanical and hydraulic aspects of the fracture network in the rock are similar in many respects.

4.6 Concluding remarks on leakage predictions

The different theoretical approximations have been developed and improved over many years and El Tani’s (1999) summary and comparison between the different approximations showed that the theoretical approach now is fairly reliable. However, in all the formulas presented, the hydraulic conductivity is an important parameter, and therefore, the real challenge is to find a realistic distribution of the hydraulic conductivity in the rock mass.

The first problem is therefore; how can we know the correct number of water pressure tests to get a reasonable statistical sampling of the tunnel length? Heuer's (1995) answer was "It depends on the nature and complexity of the geologic setting". Nevertheless, Heuer gave a hint when he said it should be in the range of 50 to 100. The second problem is that water pressure tests can easily miss the locations where the permeability is highest. The inflow prediction is sensitive to small variations in the magnitude of highest equivalent permeability or in the percentages of tunnel length in the upper ranges of equivalent permeability. The third problem is that these specific correlations may not be universally valid, even though Heuer wrote that the results were based on a variety of tunnel projects in a variety of geologic settings. Shamma et al. (2003) found that the estimations based on Goodman et al. (1965) overestimated the tunnel inflow, while Heuer (1995) underestimated the tunnel inflow.

Raymer's approach in his paper from 2001 was based on results from both Goodman et al. and Heuer, but he presented the results in log-normal curves. The graphs showed that

water pressure tests are most likely incapable of measuring the highest and lowest values of hydraulic conductivities. The high-end tail of the hydraulic conductivity distribution is particularly important when estimating inflow. Raymer (2005) proposed a lateral model for inflow estimations, which considered groundwater lowering and recharge conditions. This approach seems to be reasonable for underground projects which are likely to encounter sections with high conductivity and potentially high water inflow.

Papers like Thapa et al. (2003) and Raymer (2005) are considered particularly interesting, since water leakage actually encountered in tunnels is here compared to predicted inflow. Thapa et al. (2003) concluded that hydraulic conductivity cannot be assigned a particular preferred distribution form a priori. In fact, Thapa et al. discredit much of the work done by Raymer (2001). Thapa et al. suggest that a possible reason for underestimation of inflow is that water pressure tests often are carried out in vertical boreholes and therefore do not intersect the water-bearing fractures and faults typically oriented vertically.

Cesano et al.'s (2003) approach is different from the other prediciton methods discussed, based on the assumption that high hydraulic heterogeneity is related to high groundwater flow. The findings are promising, and somewhat attractive because the approach builds on the same information as collected for a geomechanical classification. One of the difficulties for the heterogeneity index (according to the authors) is that it is difficult to estimate the correct weight (a_i) for the different parameters characterising the hydraulic properties of the fracture sets.

Estimating ground water inflow has been one of the biggest challenges confronting the engineering geologist since tunnelling started. Goodman et al. (1965) described both the problem and what has until recently been the standard approach in Norway: "Accurate forecasts of water conditions to be expected in tunnel driving are very difficult to achieve; the best basis for prediction is often local experience in the light of geological mapping, and the presence of faults, folds and springs."

CHAPTER 5 *Investigation methods*

5.1 Introduction

In this chapter a brief description of site investigation methods used to examine geological and engineering geological conditions in hard rock is given. Main principles and potential/ limitations regarding identification of groundwater flow are emphasized. Some “extraordinary” investigation methods not commonly used in Norway are also presented, and examples of the use of such methods in the researh- and development project (R&D project) "Tunnels for the citizen" are given. The “extraordinary” investigation methods are described somewhat more detailed than well-known and more conventional methods.

Before starting an underground construction, preliminary investigations are necessary, and groundwater is only one of many factors to be examined. The investigations are usually carried out in stages. No established guidelines exist for defining the extent and types of investigations needed to establish reliable estimations of groundwater inflow into underground constructions. The standards available build on the assumption that the extent of investigations depend on the complexity of the geology and consequences in case of damage. For the time being prevailing regulations in Norway are given in the Norwegian standard NS 3480 (NBR, 1988) and the translated version of Eurocode 7, Geotechnical design, (NBR, 1997). In the future Eurocode 7 is likely to become the only prevailing Norwegian standard. Regarding investigations, several handbooks are published also by Public Road Administrations; Handbook 014 (Laboratory testing), Handbook 015 (Site investigations) and Handbook 021 (Roadtunnels) (Norwegian Public Roads Aministration,

2008). Other handbooks and guidelines are published by Norwegian and International Professional Societies.

Palmstrøm et al. (2003) suggested guidelines to find correct extent of investigations for underground constructions. Their suggestions were based on a thorough treatment of this complicated issue and many completed tunnels have been studied for establishing a good basis to suggest correct extent of investigations. Based on an evaluation of geology, weathering, rock cover, accessibility, functional requirement, risk during construction, environmental influence and risk of subsidence (damage to buildings), a project is placed in investigation class A, B, C or D, where investigation class A requires least investigation and class D most investigation. The guidelines give recommendations on how much money should be used for investigations, as percents of the blasting costs plus rig costs. The recommendations concerning investigation extent take into account the length of the tunnel, and as a consequence short tunnels require higher relative investigation costs than longer tunnels, see Figure 5.1.

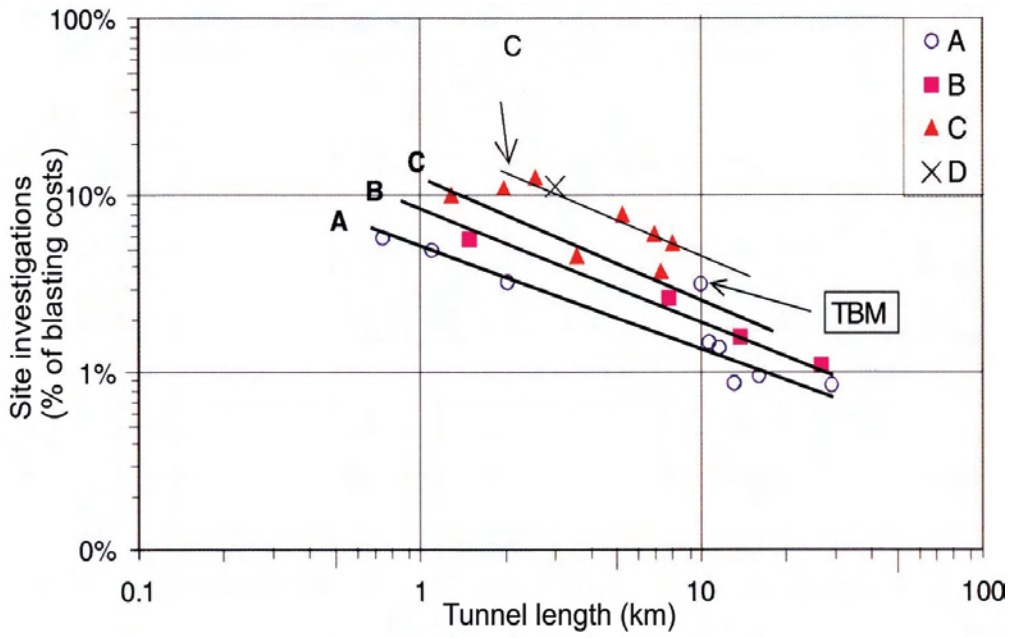

FIGURE 5.1 Recommended extent of site investigations (relative costs) as a function of tunnel length for different investigation classes. Rig costs and loading are included in the blasting costs (Palmstrøm et al., 2003).

5.2 Collection and systematizing existing geodata

The volume of rock mass involved in underground construction is large and the hydrogeological conditions are difficult to predict. Therefore, correct investigations and reliable interpretation of the results are crucial. Putting together results from different investigations, interpretations and extrapolating available information is important to achieve an optimal understanding of the hydrogeological conditions. The first stage in a high quality, cost-effective investigation plan for underground constructions is to collect and systematize existing geodata (desk studies), such as:

- Geological maps (bedrock and soils)
- Topographical maps
- Aerial photographs
- Satellite imagery
- Hydrogeology and hydrology data (yield from water wells in rock, rivers, drainage patterns)
- Results from geophysical measurements from helicopters / aeroplanes
- Results from stress measurements
- Other existing data

Collecting and systematizing existing geodata are always carried out, and are very important for future investigations. A systematic evaluation of available geodata will provide information on regional and local geology, rock types and boundaries, geophysical anomalies, structural geology such as possible weakness zones, areas covered with soil and soil types. The Geological Survey of Norway (NGU) has on their web-site (www.ngu.no) digital bedrock and lineament maps in scale 1:250.000 for downloading. The available digital maps are useful for the first stage of planning. However, more detailed maps are required for a detailed planning of the site investigations. A thorough desk study usually reveals areas that need extra attention during the field mapping, such as weakness zones/faults, geophysical anomalies and rock boundaries.

5.3 Lineament studies

An important part of the desk study is to study aerial photographs. Seen through a stereoscope, aerial photographs taken from different camera points (with an overlap of approximately 50%) will give an exaggerated relief. By analysing the relief, lineaments (structures appearing in the terrain) such as faults/weakness zones/fracture zones and bedrcok contacts can be seen. Studies of aerial photographs can also give information regarding soils and soil distribution in an area. Suitable scales are typically between 1:15.000 and 1:30.000.

During the last decade, improved computer hardware and software have made it possible to study relief and lineaments based on digital maps. Processing of maps with detailed elevation data (1m contour interval), can give images suitable for lineament studies. Figure 5.2 and 5.3 show two examples made with software from the Economic and Social Research Institute (ArcGIS).

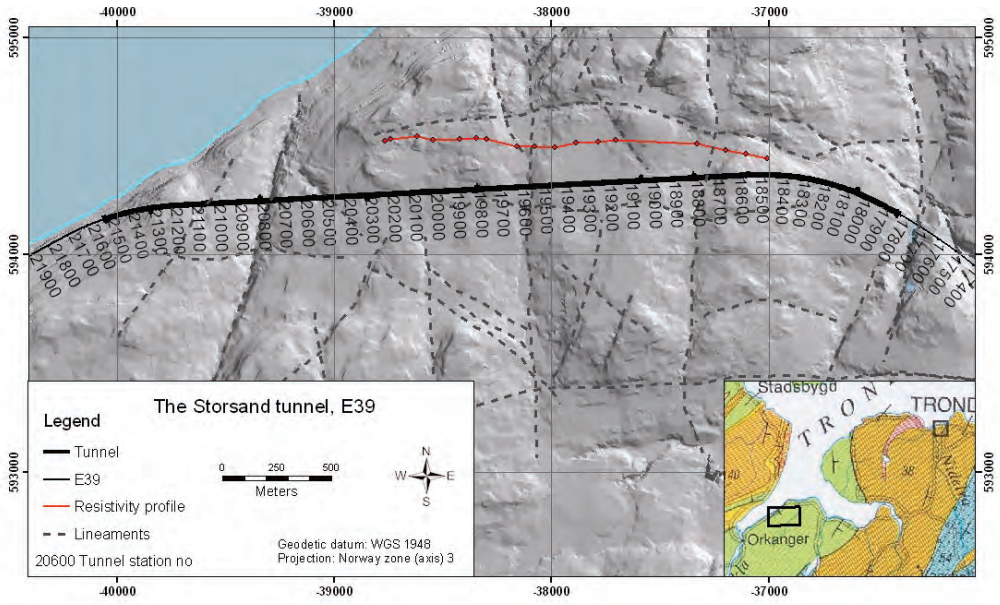

FIGURE 5.2 Example showing a lineament study at the Storsand tunnel (Ganerød et al., 2006).

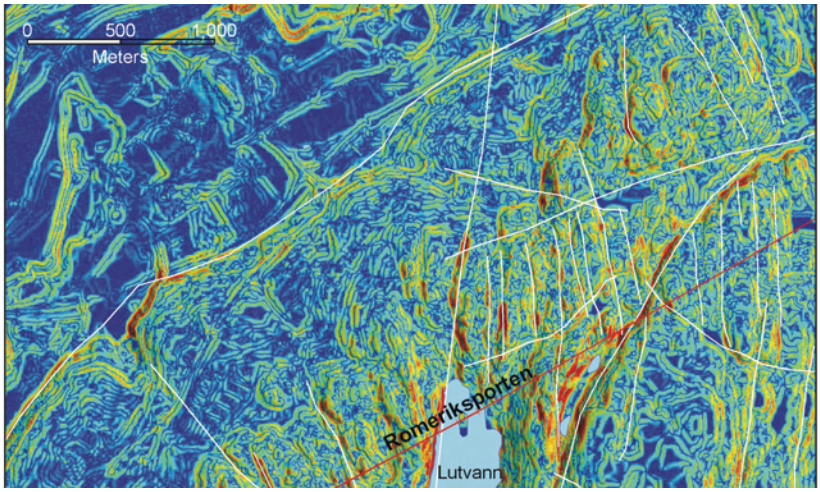

FIGURE 5.3 Example showing a study of the terrain inclination in the Lutvann-area, Romeriksporten (Nordgulen and Dehls, 2003)

Studies of aerial photographs are one of the most important preliminary investigations, and are commonly carried out in Norway before field mapping. Lineament studies based on digital maps are not commonly used in Norway today within the tunnel industry. Some of the reasons may be that the detailed maps needed for processing are expensive, processing takes time and special competence is needed. Therefore, aerial photographs still is the most commonly used alternative.

5.4 Geological field mapping

The field mapping is planned based on information gathered during the desk study and most commonly carried out as surface mapping of available outcrops. In a few cases pilot tunnels, adits or shafts are available before construction, and sometimes it may be possible to visit earlier excavated tunnels, shafts or caverns nearby the future construction.

Weakness zones/faults, dykes and rock type boundaries are of special interest. In the field, each localised weakness zone must be individually described. In addition, a description of joint characteristics along the tunnel alignment is compulsory. Main joint characteristics to map are:

- Joint orientation (strike and dip / dip and dip direction).
- Origin of joint (e.g. bedding, foliation or tectonic joints).
- Spacing (distance between adjacent discontinuities).
- Length and continuity of the joint.
- Roughness (waviness of the joint wall).
- Condition of the joint wall (alteration of wall rock or occurrence of coating).
- Filling.
- Aperture (perpendicular distance between adjacent rock walls of a discontinuity).
- Seepage (water flow or free moisture visible in individual discontinuities).
- Number of joint sets.
- RQD-value or block size.

In Norway, engineering geologists often use the Q-method (Barton et al., 1974; Grimstad and Barton, 1993) for rock mass classification. 5 out of 6 parameters included in the Q-method are mentioned in the list above (RQD, number of joint sets, joint roughness, joint alteration, seepage). The 6^{th} parameter is the stress reduction factor (SRF), this parameter is difficult to estimate from field mapping. However, in areas with high stresses it can be seen as exfoliation and large scale shear failure. To find stress magnitude and direction stress measurements are necessary. A description of stress measurements are given in Section 5.9.

The field mapping is a very crucial part of the investigations, but even for experienced engineering geologists it can be difficult to map the jointing accurately. Some form of statistical approach therefore can be beneficial. According to Villaescusa (1991) such mapping techniques can be divided into three main classes:

- Spot mapping.
- Scan line mapping.
- Area mapping.

These mapping techniques are described thoroughly in Scheldt (2002). In Norway, engineering geologists usually decide based on experience how many joints are necessary to measure for obtaining a reliable picture of which joint sets and characteristics are dominating in an area. The results are presented either as polar projections in an equal area net, (Figure 5.4), or a joint rosette.

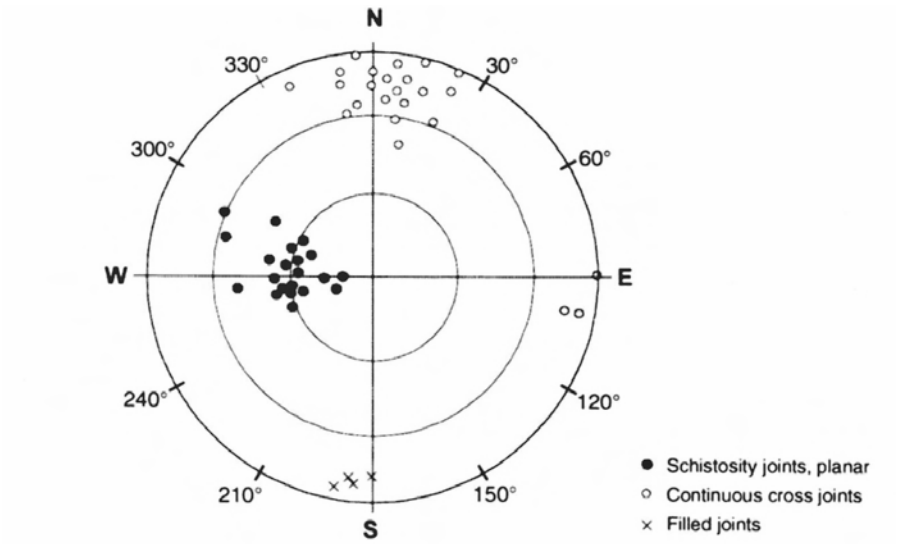

FIGURE 5.4 Presentation of joints in a polar projection (Nilsen and Palmstrøm, 2000).

In addition to measurements, collection of representative rock samples is an important part of the field mapping. Small samples may be collected to give a first overview of the distribution of the different rock types in the area, but bigger specimens (15 to 20 kg or more) need to be collected for mechanical testing. It is very important to find representative samples. In some areas blasting is necessary to avoid the effect of weathering, but blasting can induce new cracks in the specimens.

How reliable the observations of the rock mass characteristics are will depend on the complexity of the geology, and how experienced the engineering geologist is. Table 5.1 illustrates the reliability of the outcrop observations versus geological setting. Geological mapping gives a lot of information about the area, and if combined with an understanding of the regional geology, a good basis is laid for understanding the geometrical, mechanical and hydrological properties of the rock mass. Furthermore, the field mapping will also provide information for planning further investigations.

TABLE 5. 1 Classification of outcrop confidence (Kirkaldie, 1988).

Term.	Description.
High level.	Massive homogeneous rock units with large vertical and lateral extent. History of low tectonic stress level.
Intermediate level.	Rock characteristics are generally predictable, but with expected lateral and vertical variability. Systematic tectonic stress features.
Low level.	Extremely variable rock conditions due to depositional processes, structural complexity, mass movements or buried topography. Frequent lateral and vertical changes can be expected. Frequent and variable tectonic stress features.

5.5 Regional geophysical measurements

Airborne geophysics typically collect magnetic data, electromagnetic (EM) data, very low frequency EM (VLF) data and radiometric data. All the data sets mentioned have the potential to detect geological anomalies that can give important information for planners and builders of underground constructions. NGU has carried out regional geophysical measurements many areas in Norway in 1:50.000 scale. In the last few years the focus has been on Oslo and surrounding areas, where approximately 2 million people live and many new underground constructions are planned to be built in the future.

Different rock types contain different amounts of magnetic minerals, and magnetite as one of the most common magnetic minerals. For example are basic igneous rocks usually highly magnetic due to their relatively high magnetite content. While acidic igneous rocks and metamorphic rocks are less magnetic, and sedimentary rocks are usually non-magnetic. Regional measurements of magnetic fields can therefore give an overview picture of regional bedrock geology in the area. The total magnetic field is measured in nanotesla (nT) (1 nT=10^{-9} T). Anomalous magnetic properties several hundred metres deep in the ground can be detected. However, to produce a magnetic anomaly, the geological structure must have appreciable more or less magnetic material than the surrounding rock mass.

For underground constructions, anomalies representing low magnetic susceptibility are of interest. Low magnetic zones typically indicate weakness zones where magnetic minerals such as magnetite are altered to non magnetic iron-hydroxides, or silicate minerals are

transformed to clay minerals. According to Olesen et al. (2006) this transformation took place through deep weathering in Jura time in south-eastern Norway, and today only traces are left in weakness zones. There is an ongoing discussion among geologists how the clay-bearing weakness zones in south-eastern Norway most probable occurred. In addition to deep weathering in Jura time, another plausible explanation is hydrothermal alteration. However, in this connection the most interesting is not how the weakness zones occurred, but if it is possible to detect them with aeromagnetic measurements. Magnetic measurements have successfully detected many weakness zones which during construction gave unstable rock mass conditions and in some cases water leakage in tunnels in the Oslo area, such as Romeriksporten, the Hvaler and the Lier tunnels (Olesen et al., 2006).

Radiometric measurements detect variations in radiation for different rock units. Rock types such as granite, alum shale (occur in Oslo) and some pegmatite dikes have high radiation. In some cases outcropping weakness zones produce radiometric anomalies due to alteration of materials in joints. According to Beard (2001), radiometric data are sensitive to only the top few centimetres of soil or rock, and the presence of water tends to reduce the radiometric signal (zero over lakes and streams).

Electromagnetic (EM) measurements make use of the response by the ground to induced electromagnetic fields. A primary electromagnetic field is sent into the ground, and if an electric conductor, such as a clay rich or water-bearing weakness zone or an ore body is present, the electromagnetic field induces currents in the conductor. As a result, a secondary EM field is sent from the ground to the receiver. The difference between the primary EM field and the secondary EM field provides information on the geometry of the conductive rock mass, (Kearey and Brooks, 1991). The transmitters may have different coil orientations, horizontal and vertical coils are sensitive to respectively horizontal and vertical conductors. The lowest frequency normally used is 880 Hz may detect conductive faults or fractures down to a depth of about 100 m. However, lakes with moderately conductive water or several metre thick layers of conductive clay will obscure the EM signal produced by conductors below the lake or clay layer.

The VLF method uses electromagnetic radiation generated by powerful radio transmitters in long-range communications and navigational systems. Typical frequencies are between 15-25 kHz. At large distances from the source the electromagnetic field is essentially planar and horizontal. A conductor in the ground will produce a secondary electromagnetic field, changing the electromagnetic field induced from the antenna. Therefore the VLF method can detect faults or fractures that are filled with water or conductive clays. VLF data are sensitive to shallow, long, linear structures of moderate conductivity, and the method also requires transmitters providing an electromagnetic field in a suitable direction.

Geophysical measurements from helicopter and aeroplanes are not routine investigations for underground constructions in Norway. These investigation techniques are, however, under development, and may give useful information about possible weakness zones of importance. In particular, magnetic measurements and lineament studies may give useful information on where to carry out more detailed investigations.

5.6 Local geophysical measurements

Based on results from desk studies, and in some cases regional geophysical measurements, ground based geophysics such as refraction seismic and 2D-resistivity are considered.

5.6.1 Refraction seismic

Refraction seismic is used to investigate critical sections, such as tunnel entrance areas and weakness zones, or to check the thickness of soil and bed rock quality. Especially for sub-sea tunnels, refraction seismic is essential to investigate the rock mass quality along the tunnel alignment. For subsea tunnels reflection seismic is also used to map the sea bottom, and for locating the soil/rock boundary.

Seismic refraction surveys measure the time it takes for a seismic signal to travel through the ground along refracted ray paths to different distances from a known source (shot point). The seismic signal is usually initiated with an explosive source and an array of geophones receive the signals, see Figure 5.5. Based on the travel-time curves registered, the seismic velocity in respective layers can be calculated, and a geological model showing layers with different seismic velocities and thicknesses can be defined. However, it is important to be aware that this geological model is an interpretation that may, or may not, be correct. In most cases several different geological models can fit the registrations of one survey.

Best results are obtained when the seismic velocities are increasing with depth and the inclination of layers are less than $30°$. The results from refraction seismic give seismic velocity of the uppermost 5 to 10 m of the sub-surface. However, in cases with a low velocity layer below a layer of higher velocity, rays are refracted in wrong direction, and the low velocity layer will not be detected. Similarly, thin layers and layers with small increment in velocity compared to the layer above are difficult to detect. For weakness zones and/or depressions the inclination of layers with varying seismic velocity is often greater than $30°$, and this gives problems for interpretation of the results. According to Westerdahl (2003), a precise interpretation of sharp depressions and vertical weakness zones can not be expected, as long as simple interpretive programs are used and data entry is limited. Several techniques are, however, possible in such situations:

- Tomography, (i.e. seismics) either between two boreholes or between an inclined borehole and the surface.
- Reflection shots just above the depression.
- Combination of refraction seismics with control boring /core drilling.

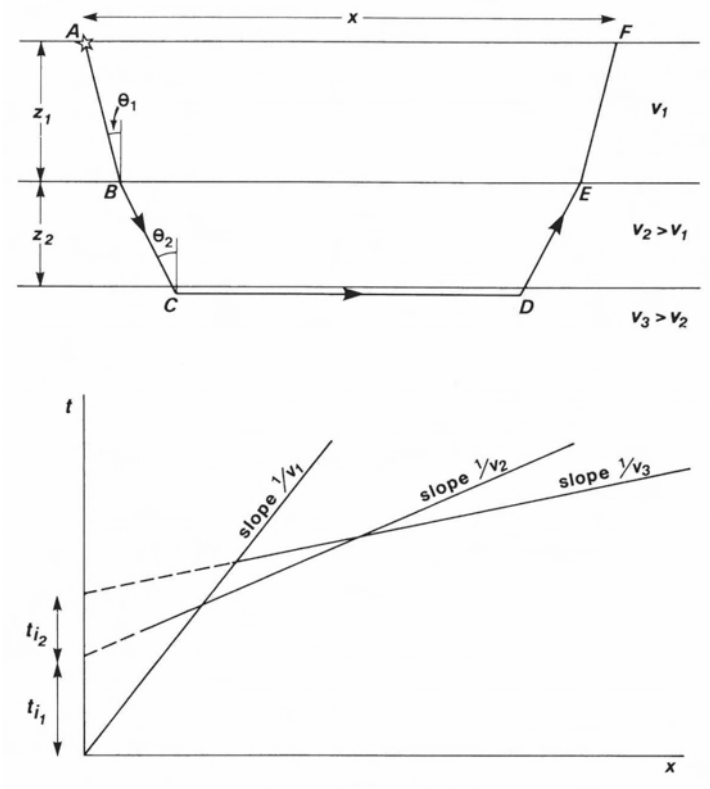

FIGURE 5.5 Refracted ray path and typical travel-time curves for a three-layer model (Kearey and Brooks, 1991).

In Norway, conventional refraction seismic has been used with good results for a long time. This may be due to favourable conditions for refraction seicmic, since a typical geological profile is comprised of a limited soil layer above bedrock with significantly higher seismic velocity, and the weathering of the bedrock is usually moderate.

Good quality rock masses below the water table generally have seismic velocities higher than 5000 m/s, while poor quality rock masses and weakness zones normally have velocities lower than 4000 m/s. Typical ranges for seismic velocities of soil and rock are shown in Figure 5.6.

The seismic velocity of rock masses depend on:

- Rock type.
- Degree of jointing, highly jointed rock mass has lower seismic velocity compared to moderately jointed rock mass. Open joints or joints with filling give lower seismic velocity.
- The stress level. The seismic velocity increase with increasing depth. This is mainly due to closing of open joints and cracks.
- The groundwater level. Higher seismic velocity below the groundwater table.

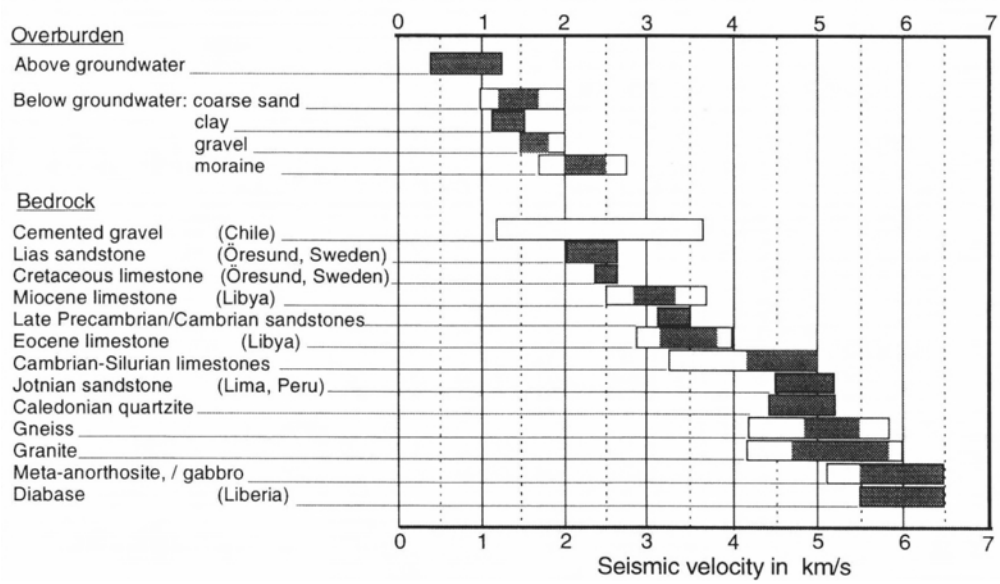

FIGURE 5.6 Characteristic seismic velocities (Sjøgren, 1984).

5.6.2 Electrical methods

Two electrical methods are commonly used and will be discussed here, the 2D-resistivity method and induced polarization (IP). Electrical methods were first used as site investigation method for tunnels in Norway during the 1980's (Pedersen et al., 1986; Veslegard, 1987). Even though the results were promising, the method was not commonly used in Norway in the 1990's. The equipment used in the 1980's was cumbersome and time-consuming, and both cable system and data collection have since been improved, (Dahlin, 1993). Typical electrode intervals are ten metres, near the centre of the composite cable, and twenty metres at the ends. When electrodes and cables are placed in the survey area, both 2D-resistivity and induced polarization can be carried out without any changes on the

electrode configurations. Therefore also IP-measurements were carried out for many of the sites involved in the project “Tunnels for the citizens”.

The purpose of 2D-resistivity is to determine the sub-surface resistivity distribution by measurements on the surface. By sending electrical current between currents (senders) and potential electrodes (receivers) and gradually increasing the distance between current and potential electrodes, information from deeper and deeper parts of the sub-surface is collected. The 2D-resistivity measurements are ploted in a pseudosection, giving an apparent resistivity of the sub-surface, which is an approximate distribution of the resistivity. To produce a 2D model with true resistivity, an inversion and iteration technique is used. A theoretical model with cells of given resistivity is made, and when the response from the theoretical model matches the measured data the true resistivity is found, (Loke, 2007).

Since the majority of rock forming minerals are insulators, the electrical current passes through the pore water. Therefore the porosity of rock mass is of major importance for the resistivity. Low resistivity in rock mass can be a result of:

- Increased porosity due to fractures.
- High electrical conductivity on the pore water.
- Electrical leading minerals, such as sulphide, graphite or magnetite.
- Clay minerals in weakness zones or high degree of weathering.

Based on different electrode configurations tested in the R&D project “Tunnels for the citizen”, the Wenner configuration seemed to be the best concerning noise and time consumption, but not on the ability to detect vertical zones (Rønning, 2003). In Figure 5.7, an example of results from 2D-resistivity measurements is shown, with high resistivity in red colours and low resistivity in blue colours. Maximum depth for the resistivity measurements is 120 m, but best resolution is achieved for the uppermost 50 to 60 m.

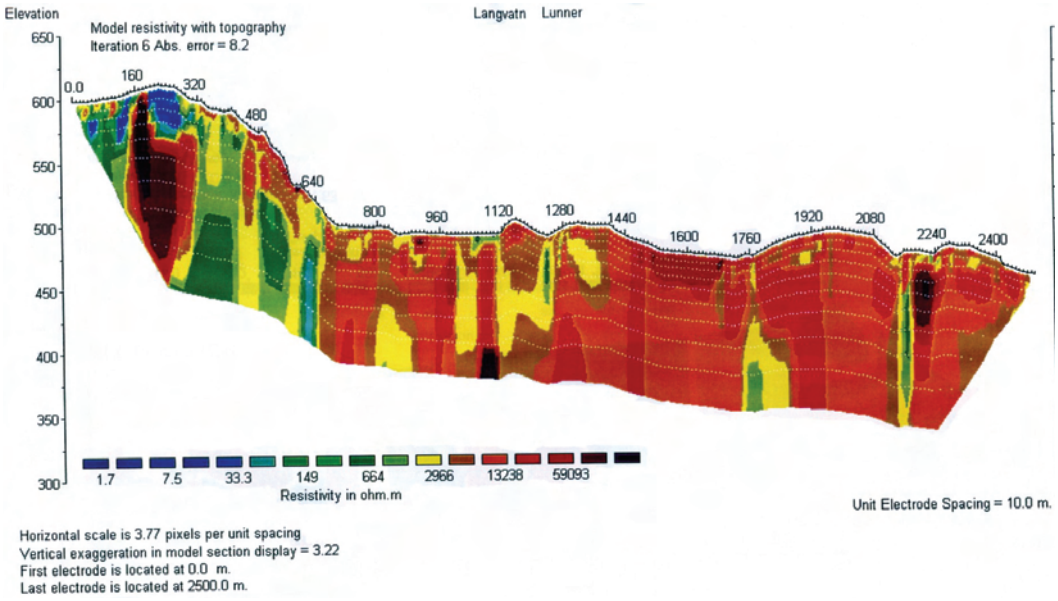

FIGURE 5.7 Result from 2D-resistivity measurements at the Lunner tunnel (Rønning and Dalsegg, 2001).

One important advantage with resistivity measurements is the range of depth, that is very good compared to most other investigation methods. The 2D-resistivity measurements have shown promising results for detection of fractured zones with water leakage, but some limitations are important to be aware of:

- Interpretation are ambiguous and limited to simple structural configurations (difficult to find dip of zones from 2D-resistivity profile).
- Zones parallel with the profile are difficult to detect.
- Best results are achieved in rock mass with higher resistivity than 5000 ohmm (to obtain a detectable variation), (Rønning, 2003).

For the time being, 2D-resistivity measurements are not used much, but as both measurements and interpretation are continuously improved the use will probably increase in the future.

IP-measurements register the grounds ability to store electrical charge. Two different survey methods exist for measuring this effect. It is possible to measure IP with different frequencies, (frequency domain). Another possibility is to measure the time it takes for the voltage between the potential electrodes to gradually decay when the current is abruptly

switched off (time domain). A gradual decay will take place, and the measurements are carried out in a certain time interval, (Kearey and Brooks, 1991). High content of conducting minerals or clay rich zones will give high IP effect.

In the planning of underground constructions it is important to distinguish a water-bearing weakness zone from a weakness zone with almost no water. In theory this is possible by combining resistivity- and IP measurements as illustrated in Table 5.2.

TABLE 5. 2 Interpretation of weakness type from resistivity and IP measurements (Veslegard, 1987).

Weakness type.	Resistivity.	IP effect.
Clay rich weakness zone.	Low.	Similar or higher than surrounding rock mass.
Water-bearing and clay rich weakness zone.	Low.	Lower than surrounding rock mass.
Water-bearing weakness zone.	Medium, (higher than clay rich zones).	Lower than surrounding rock mass.
Jointed rock mass no flowing water.	Higher than water-bearing zones.	Similar to massive rock mass of identical rock type.

The rules of interpretation for resistivity and IP suggested above were tested at several underground projects in southern Norway in the 1980's, and the results with combined resistivity- and IP measurements were promising, (Veslegard, 1987). However, experience from "tunnels for the citizen" have not been as promising, (Rønning, 2003). Best results for induced polarization were obtained with IP measurements in boreholes (see Section 5.8.3).

5.7 Core drilling and water pressure tests

Core drilling and logging is one of the most important methods to obtain information from the sub-surface making it possible to verify geological interpretations and supplement the information on orientation and character of weakness zones found through field mapping and earlier investigations. Another advantage is the possibility of mapping the rock mass properties and providing sample material for laboratory tests. The groundwater conditions can also be studied by water pressure tests, also called Lugeon tests after Professor Maurice Lugeon which established the unit of rock permeability (Lugeon, 1933).

Water pressure tests are carried out in either one or a system of boreholes. In Norway one borehole is normally used. Water is pumped into a section of the borehole under constant pressure, and the loss of water is measured, see Figure 5.8. One packer is used when meas-

uring the end section of a borehole; this is normally carried out while the hole is drilled. Two packers are necessary when measuring different sections down a drilled hole.

When performing the Lugeon test the section is put under constant overpressure of 1 MPa relative to the original groundwater pressure, and the loss of water after 5 minutes is measured with a flow meter. Based on a pumping test of one single borehole in isotropic conditions, the following approximate relationship between the Lugeon value and the hydraulic conductivity (k) has been published by Hoek and Bray (1981):

$$k = \frac{1{,}4 q_c}{L \times H_c} \qquad \textbf{[5-1]}$$

Where

q_c = pumping rate (l/min) necessary to maintain a constant over-pressure

L = length (m) of the test section

H_c = over-pressure (constant head, given in metre)

According to this equation a water loss of 1 L corresponds to a hydraulic conductivity of $k=2{,}3 \cdot 10^{-7}$ m/s. More information regarding Lugeon testing can be found in Boge (2002).

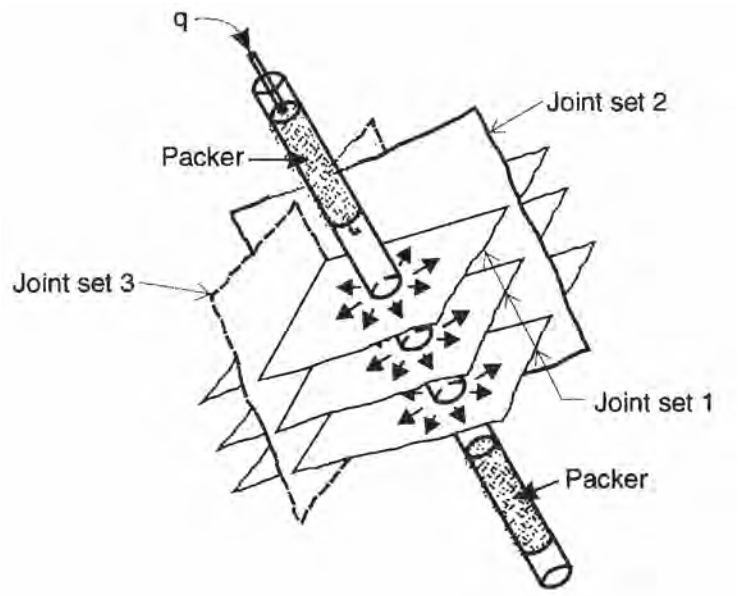

FIGURE 5.8 The principle of Lugeon pressure testing (Hoek and Bray, 1981).

It is important to be aware that the results from Lugeon tests are based on the assumption that the rock mass is isotropic. In rock mass one single joint can take a lot of water, while

next section has no water-bearing joints. There are also often uncertainties connected to the execution of the tests, for instance leakage through the packer.

Typical diameters used in diamond core drilling are 46, 56 and 66 mm. Greater diameter is possible but not conventionally used in Norway. In very poor rock mass it is advantageous to have a diameter of 56 mm or more, because the chances are higher of getting a good core recovery with greater diameters. Important parameters obtained from core logging are: degree of jointing, joint roughness, rock type, fill/gouge material, zones (jointed/ crushed), core recovery and remarks describing important observations.

Directional drilling can be favourable for boring just above tunnel level and parallel with the tunnel alignment investigating weakness zones for example below sea or lakes. This was done below the lake Langvann at the Lunner tunnel. However, in poor rock mass there will be a risk of significant less recovery of cores with directional drilling than for conventional drilling. Core loss in poor rock mass is a disadvantage with core drilling, and in worst case the drilling may even be disrupted by high swelling pressure in gouge material or cave in.

During core drilling it is important to note water ingress, colour of bore dust and comments on problems encountered during drilling. This information can be vital when studying the cores later. Core drilling is a standard investigation method in Norway for investigating weakness zones and their orientation towards the depth. Water pressure tests in the core hole are also quite often carried out, especially for underground constructions with strict inflow criteria.

5.8 Geophysical measurements in boreholes

In the R&D project "Tunnels for the citizen" geophysical logging equipment were used in several boreholes, and in this section the equipment and methods used will be discussed. Much of the information in the following sections are found on Robertson Geologging webpage, (Robertson Geologging, 2007) and Mount Sopris webpage, (Mount Sopris, 2007).

The geophysical measurements are carried out in boreholes with nominal diameter 145 mm, bored by percussive boring. Experience has shown that the boreholes should be allowed to stand for minimum 2 weeks, to reach stable conditions and obtain good visibility. In the 6 tunnels studied in this thesis four probes have been used for the geophysical measurements:

- Temperature and electric conductivity of fluid + natural gamma of rock probe (TCN-probe).

- Optical televiewer probe.
- Electrical logging probe (resistivity and induced polarization).
- High resolution impeller flow meter (location of permeable zones).

Figure 5.9 shows pictures of three of the probes mentioned above. Other relevant probes are also available, but will not be discussed here. One interesting probe is the Full-Wave-Form Sonic probe, that obtain both shear and compressional velocities along the borehole. Deviation measurements are always carried out in the boreholes, and vertical- and horizontal projection of the borehole are drawn.

5.8.1 Temperature and conductivity of fluid and natural gamma of rock

The geophysical measurements are usually initiated with a probe measuring the temperature (T) and electric conductivity (C) of the water and natural gamma radiation (N) in the rock continually down the borehole. Recommended logging speed is 3 m/min. A continuous log of the temperature and electric conductivity of the water in a borehole is a useful tool for identifying possible water-bearing fractures. Abrupt changes in temperature and fluid conductivity indicate water-bearing fractures. For example if surface water is present in the borehole, inflowing groundwater will usually have higher ionic composition and higher temperature than surface water. If changes in conductivity and temperature are registered in the same zones, this is a clear indication of water inflow. In addition, the temperature profile gives a picture of the local geothermal gradient.

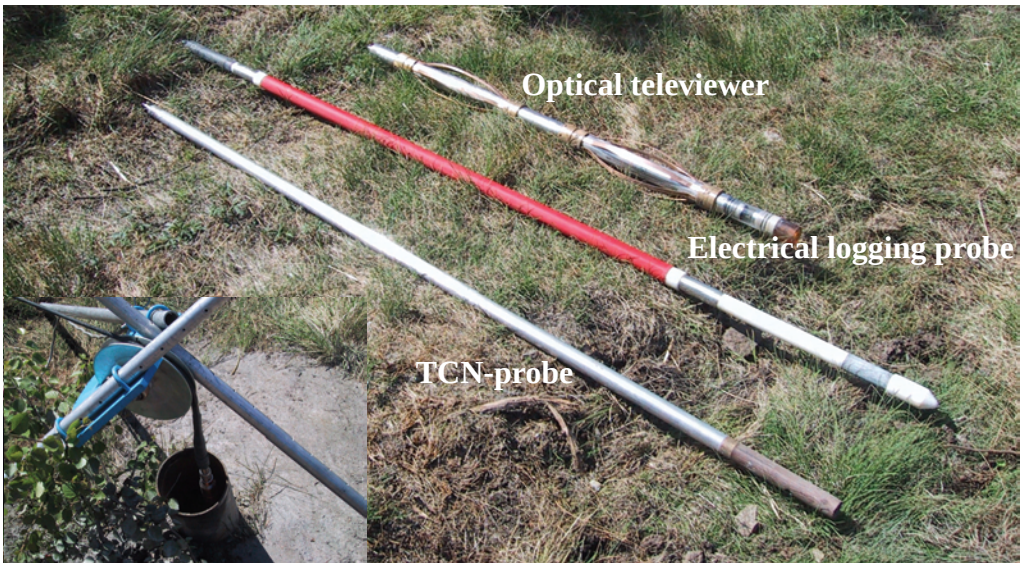

FIGURE 5.9 Three probes used for geophysical measurements in boreholes. In the lower left corner a probe is lowered into a borehole at the Storsand tunnel.

Measurements of natural gamma radiation give information about mineralogical changes in the bedrock caused by changed levels of uranium, thorium and potassium. Potassium, which is a radioactive element, is present for instance in alkali feldspar. In addition, clay-filled fractures can result in increased natural gamma due to higher potassium content than the surrounding rock mass. The gamma log together with optical televiewer makes it easier to determine the type of rock present in the borehole.

5.8.2 Optical televiewer

The optical televiewer probe (OPTV) gives a detailed and oriented recording, i.e. a video film, of the borehole wall. The logging equipment for the optical televiewer consists of a probe with the video camera unit and a personal computer recording the film. Recommended logging speed is approximately 1 m/min. The video camera unit consists of a camera, light emitting diodes, hyperbolic mirror, black needle, a brick of rubber and glass, see Figure 5.10. The images from an optical televiewer inspection have a resolution of 360 or 720 dots per circle. One row of pixels represents 1 mm depth of the borehole, and fractures with aperture from 0.5 mm and up are easily detected, (Siddans, 2002).

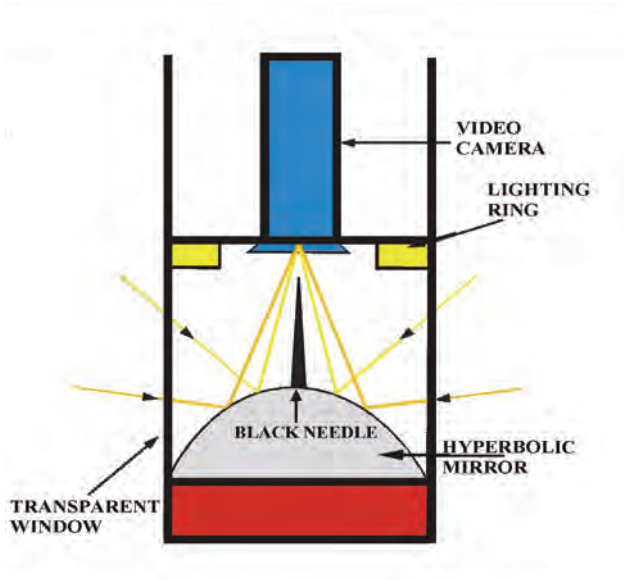

FIGURE 5.10 Sketch showing the components in the video camera unit of the optical televiewer (Rønning, 2003).

Different geological features are recorded on the imagery. For example bedding, fractures and different types of veins can be identified. Based on the registrations it is possible to

obtain a complete fracture analysis including dip, strike, frequency and fracture aperture along the borehole. Poles of all selected features for the whole log are shown on an equal-area stereogram and contoured according to pole density. Fracture groups are identified and mean strike and dip are calculated for each group, (Siddans, 2002). An example of a fracture analysis log, a whole well stereogram and an image from a section of the same borehole are given in Figure 5.11.

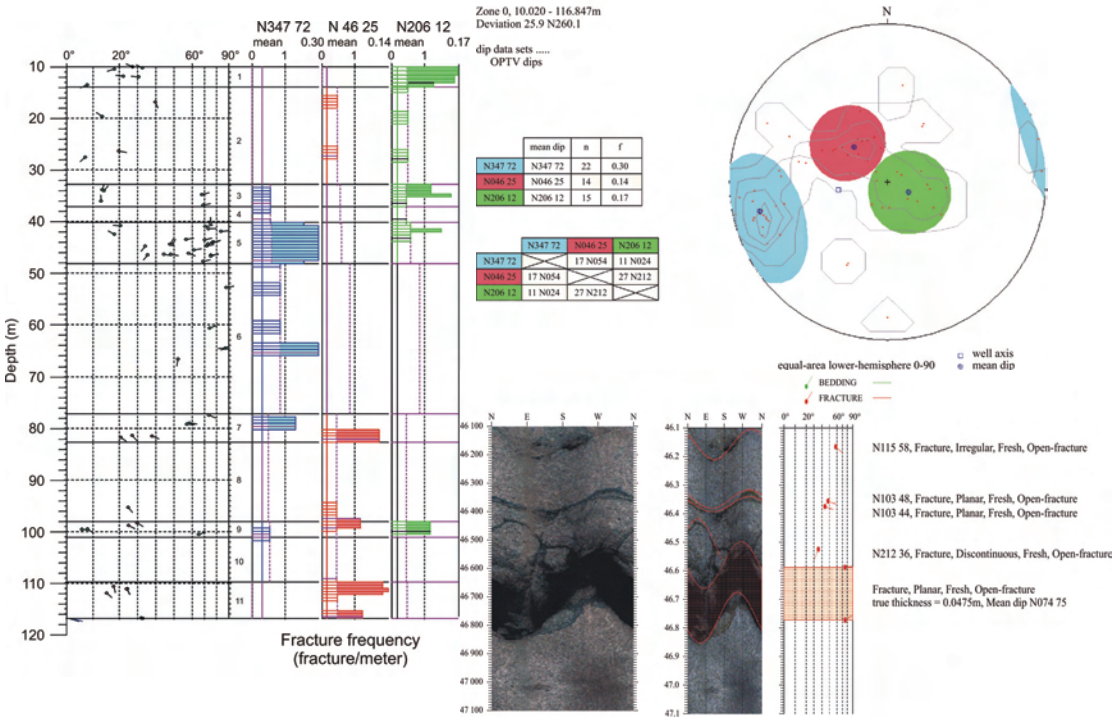

FIGURE 5.11 Example of a fracture analysis log (left), and equal-area stereogram with contoured poles (right). The image shows an open fracture at 41.8 m. All data are from borehole 6 at the Lunner tunnel, modified from (Geological survey of Norway, 2001-2002).

5.8.3 Electrical logging probe

The third probe is an electric logging probe, measuring the resistivity of the rock mass down the borehole. The probe is equipped with electrodes, measurement electronics and an insulated bridle. The measurements can only be done in waterfilled part of the borehole. Low resistivity may indicate weakness zones with highly fractured rock mass, clay filled fractures or water-bearing fractures. However, low resistivity may also be a result of high content of electrical leading minerals (sulphide, pyrite, graphite) in the rock mass.

The electrical logging probe can also measure chargeability (induced polarization) in porous, water saturated, mineralised rocks caused by the passage of a low-frequency alternating current. As mentioned in Section 5.6.2, induced polarization can be helpful to identify conductive minerals, and thereby distinguish between water-bearing zones and clay filled fractures or conductive minerals. In one borehole located at Staverhagan (above the Tanum tunnel close to the Skaugum tunnel, see Section 6.6) the contact between calcareous rock and pyrite leading schist was detected based on good correlation between IP- and resistivity measurements (low resistivity and high IP effect), (Dalsegg et al. 2003).

5.8.4 Hydraulic testing of the borehole

Groundwater inflow into the borehole can be measured using an impeller flow meter probe. The method used in "Tunnels for the citizen" has been to lower the probe with constant velocity down- and upwards the borehole. A submerged pump is placed above the probe (typically 15 to 20 m below the groundwater level). While continuously pumping, the velocity or the number of revolutions per minute (RPM) for the propeller is registered both down- and upwards the borehole. In case of inflowing water the velocity pattern in the borehole will be disturbed. The net velocity of the flow is then given by taking the difference between the up- and down velocity (Elvebakk and Rønning, 2003). The percentage distribution of water ingress along the borehole is identified. Figure 5.12 shows the principle for measurements using the impeller flow meter probe.

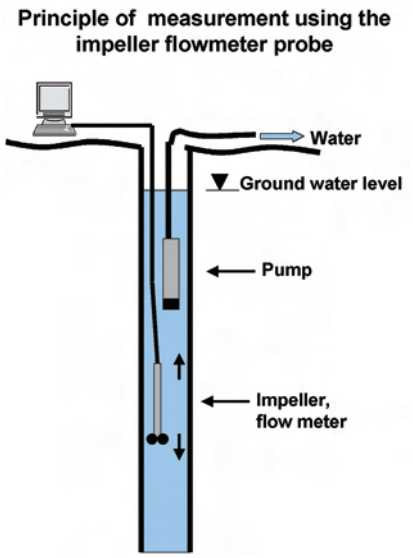

FIGURE 5.12 The impeller flow meter probe is used for identifying water-bearing fractures in the borehole (Elvebakk and Rønning, 2003).

The total water yield for the borehole is found by using data from the submerged pump (pump out rate) together with changes in groundwater level during pumping. To find the excact water yield, it is required that the pumping capacity is higher than the total water yield of the borehole.

Geophysical measurements in boreholes are quite new for this purpose in Norway, and therefore not much used. Promising results with respect to characterization of hydrogeological properties in the rock mass (Rønning, 2003) will, however, probably lead to an increase of use in the future, particularly taken into consideration that geophysical measurements and logging have only half the cost of core drilling.

5.9 Stress measurements

Stress magnitudes and directions influence also on the groundwater flow in rock mass. As earlier described in Section 3.2.2, the groundwater moves more easily in fractures with low stress (or tensile stress) perpendicular to the fracture walls. It is therefore easier to predict which fracture sets will be water-bearing, if the stress situation is known.

In the 6 tunnels studied in this thesis, unfortunately no stress measurements have been carried out. Nevertheless, rock stress is of significance here, and a brief description of the most important stress measuring methods therefore will be given. The two main methods used for in situ rock measurements are:

- Two- and three-dimensional rock stress measurements by overcoring.
- Hydraulic fracturing.

The principle for the overcoring technique is to place a measuring cell in a borehole, and afterwards overcore it so that the rock in which the measuring cell is placed is relieved from in situ stresses. Changes in strain is recorded in strain rosettes, and when the elastic constants are known, magnitude and stress directions can be calculated, (ISRM, 2003 a). Figure 5.13 shows the principle for two- and three-dimensional rock stress measurements.

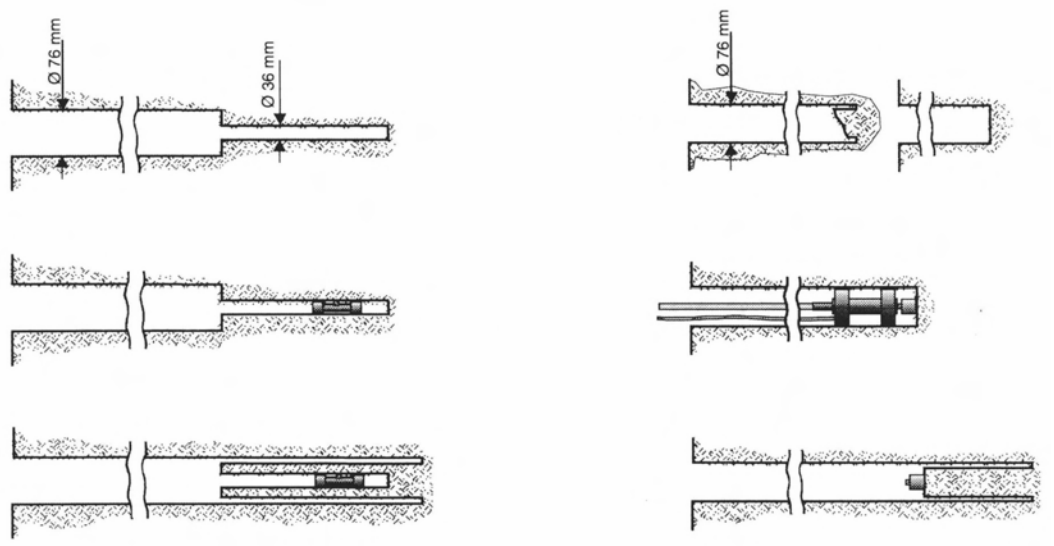

FIGURE 5.13 The principle of three dimensional (to the left) and two dimensional (to the right) rock stress measurements by overcoring (Myrvang, 1983).

The overcoring technique is normally carried out from underground constructions, and in practice maximum borehole length is 20 to 25 m. One major weakness is that the measurements can not be done in waterfilled boreholes.

Hydraulic fracturing determines magnitude and direction of the minor and major principal stresses. In a borehole a straddle packer is placed, and usually the measurements start from the bottom of the hole. Water is pumped at high pressure into the approximately 1 m long section between the straddle packers. Pressure and time progress are registered as the water pressure is increased, see Figure 5.14.

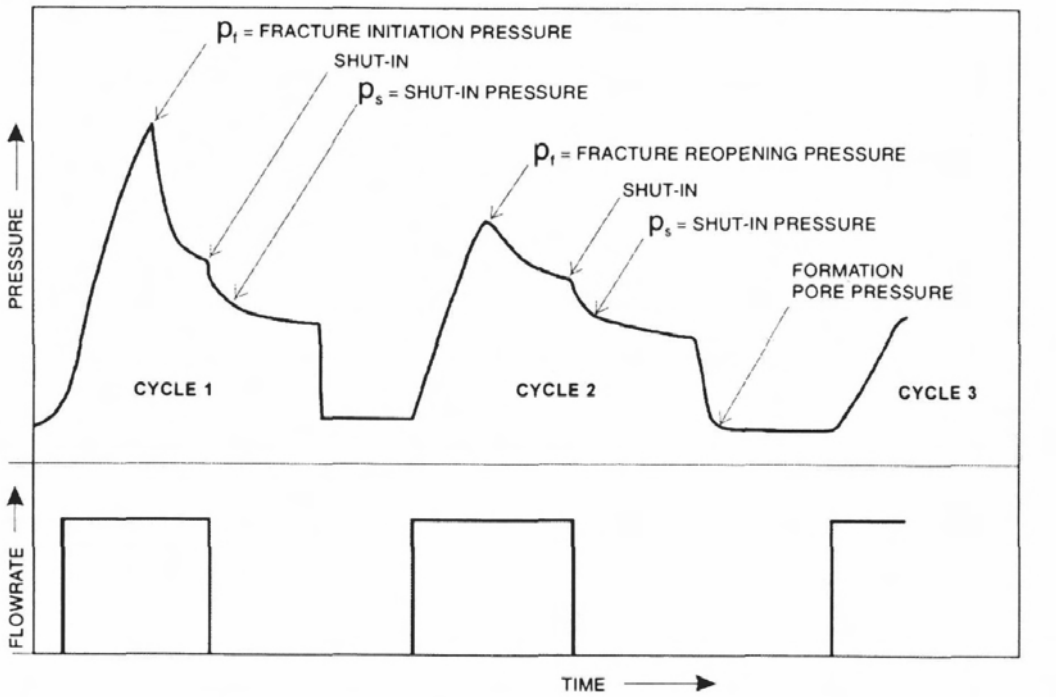

FIGURE 5.14 Idealised hydraulic fracturing pressure record (ISRM, 1987).

If the drill hole direction is assumed to be parallel with one of the principal stress directions, the vertical stress is calculated from the overburden weight, and the following expressions may be used to calculate the horizontal stresses (ISRM, 2003 b):

$$\sigma_{min} = P_s \quad \textbf{[5-2]}$$

$$\sigma_{max} = P_s\text{-}P_r\text{-}p_0 \quad \textbf{[5-3]}$$

Where p_0 is equal initial pore water pressure.

To determine the orientation of the minor and major principal stresses an impression packer is used directly after the stress measurements. Another possibility is to use an optical televiewer for registration of the fracture orientation. Major principal stress is parallel with the fracture and the minor principal stress is perpendicular to the fracture.

Stress measurements are commonly used for underground constructions such as storage halls, pressure shafts (power plant) and mines. But for tunnels, stress measurements are not usually carried out. Nevertheless, stress measurements can be useful for prediction of

possible fracture orientations expected to give water leakage (see Hypothesis No. 3 in Section 1.3). Hydraulic fracturing may in many cases be the best method for stress measurements before the construction of a tunnel.

5.10 Laboratory testing

Mechanical properties influence on the hydraulic properties of the rock mass. An overview of the most common laboratory tests are shown in Table 5.3. It is beyond the scope of this thesis to describe and discuss details for these tests. References to ISRM Standards/Recommendations or other litterature are given in Table 5.3 for more details.

TABLE 5. 3 Most frequently used laboratory tests for mechanical properties of the rock mass.

Testing/investigation of.	Method.	Sample.	Reference.
Rock strength.			
-compressive.	Uniaxial compressive strength test (UCS).	Drill cores (/cubes).	ISRM (1979).
	Triaxial strength test.	Drill cores.	ISRM (1978 a).
-tensile.	Point load test.	Drill cores (/irregular specimens).	ISRM (1985).
-brittleness.	Brittleness test.	Aggregate (11.2-16.0 mm).	Selmer-Olsen and Blindheim (1971).
Rock elasticity.			
-Young's modulus. -poisson's ratio.	Uniaxial compressive strength test (UCS).	Drill cores .	ISRM (1979).
Gouge material.			
-mineral composition.	DTA- and XRD analysis.	Powder.	ISRM (1999).
	Electron microscope.	Powder.	
-swelling.	Colour test.	Intact/powder.	
	Odometer test/free swelling.	Powder.	

It is important to be aware that the mechanical properties of rocks may have significant influence on leakage, particularly since the mechanical properties will define the character of joints. Brittle rock, for example granite, develop typically long and open joints. On the contrary, ductile/plastic rock, for example phyllite, develop typically short, non-communicating joints.

5.11 Concluding remarks on investigation methods

In Norway certain "standard" investigation methods are always used before the construction of a tunnel starts. In Table 5.4 the investigation methods described in this chapter are divided into "standard" and "extraordinary" according to Norwegian tunnel investigation practise.

TABLE 5. 4 "Standard" and "extraordinary" investigation methods.

"Standard" investigation methods.	"Extraordinary" investigation methods.
Collection and systematizing of existing geodata.	Lineament studies based on digital data.
Lineament studies based on aerial photographs.	Measurements from helicopter and aeroplane.
Field mapping.	Electrical methods.
Refraction seismic.	Geophysical measurements in boreholes.
Core drilling with water pressure tests.	Stress measurements.

The project "tunnels for the citizen" gave an excellent opportunity to test and gain experience with some of the "extraordinary" investigation methods.

Lineament studies based on digital data have given promising results, even in highly populated areas. The technique will probably become more common in the future. Until detailed digital maps are more commercialised, aerial photographs probably will remain the most used alternative among engineering geologists. Therefore, lineament studies based on digital maps are not studied any further in this thesis.

Airborne geophysics give information that can be of importance for further planning of investigations. Magnetic measurements have given promising results in detecting fracture zones (Olesen et al., 2006). The magnetic measurements and interpretation of their results are controversial, and not all engineering geologists believe that magnetic measurements can provide as much information as presented in Olesen et al. (2006). The magnetic measurements are interesting, but due to limited time it will not be studied further in this thesis. Other measurements carried out from aeroplane and helicopter will neither be studied in this thesis.

In the project "Tunnels for the citizen" 2D-resistivity measurements and geophysical measurements in boreholes gave promising results concerning water-bearing rock mass. Even though the methods are somewhat controversial, both methods are believed to have good potential for increased use in the future.

Stress measurements have not been carried out for any of the tunnels studied, and are normally not carried out in Norway only to get information about the hydrogeological condi-

tions of the rock mass. However, stress measurements will be further discussed because it is relevant for Hypothesis No. 3, and since it is believed that stress measurements in general can give valuable information for predicting groundwater flow in the rock mass.

Based on the review in this chapter, results from the following investigation methods are evaluated in Chapter 7 and 8 for their ability to prognosticate water leakage; desk studies, geological mapping, refraction seismic, 2D-resistivity, core drilling and geophysical measusements in boreholes.

CHAPTER 6 *Selected case studies*

6.1 Introduction

In this Chapter the selected cases, representing six Norwegian tunnels are described with main emphasis on geological conditions, site investigations carried out and water leakages encountered. All results from the site investigations are not described in detail. Investigations carried out before construction of the tunnels started are emphasized. A more detailed presentation and analysis of the most interesting parts of the tunnels is presented in Chapter 7.

The six tunnels were selected in an attempt to study tunnels with varying geological conditions representative for Norwegian tunnelling projects. Four of the tunnels were included in the research project "Tunnels for the citizens": the T-baneringen-, Lunner-, Skaugum- and Storsand- tunnel. In these four tunnels some extraordinary site investigations were carried out, and data are easily available for research. The other two tunnels were chosen because of their relevancy for this study, and the author has been working as engineering geologist at site both on the Romeriksporten and Frøya tunnels. The Romeriksporten tunnel is an important case to study because the water leakage caused considerable cost excess and time delay. Figure 1.1 shows the location of the tunnels.

The Q-method (Grimstad and Barton, 1993) has been used for mapping the rock mass quality. Different approaches for pregrouting have been used in the different tunnels. In some tunnels continuous pregrouting has been carried out, and no probedrilling was

required to decide whether or not to pregrout. In other tunnels pregrouting has been carried out sporadically, and probedrilling rounds (for example 6 holes each of 24 m length) have been necessary to decide whether it has been necessary to pregrout or not. Here, the water leakage has been measured prior to pregrouting, and the results have given a good indication of the conductivity of the rock mass.

When presenting data from the tunnels, some parts of the tunnels are of more interest and therefore will be more thoroughly described and discussed compared to other parts. This is necessary in order to limit the amount of data presented.

6.2 The Romeriksporten tunnel

Romeriksporten is a part of the 42 km long high speed railway link from the City of Oslo to Gardermoen airport. The tunnel is 13.8 km long and is located between Etterstad in Oslo and Stalsberg in the vicinity of Lillestrøm. The tunnel has two rails in a single tube, and a cross section of 110 m^2. The overburden varies from 10 to 250 m. Tunnelling started in the summer of 1994, and in August 1999 the first express train to the airport passed through the Romeriksporten tunnel.

Two adits were used during construction, one located at Starveien, one at Jernbane-veien. In the section between the two adits high amounts of water leakage were encountered, and the contractor experienced problems with pregrouting. The water leakages lowered the groundwater table, and caused settlement of buildings in an urban area and damage to a nearby forest. Also the small lake Puttjern was partly drained. To seal the rockmass in a 2.2 km long section of the tunnel, post-excavation grouting had to be carried out for more than one year. The consequences were a major delay, unforeseen cost and a lot of negative attention.

6.2.1 Geological conditions

The southern part of the Romeriksporten tunnel is located in the Oslo Region with sedimentary rocks of Cambrian to Silurian age, predominantly shales and limestones. Approximately 1500 m from the southern tunnel portal, the tunnel is crossing a major fault zone, the Bryn zone, representing the boundary to Precambrian rocks consisting of granites and gneisses. In the fault zone, alum shale is found. Maenaite and diabase are typical intrusives of Permian age, and the thickness of the dykes varies from a few decimetres to several metres. In the sedimentary rocks the foliation joints are close to horizontal with strike direction NE-SW. The main fault zone, the Bryn zone, at the boundary to the Precambrian rocks has a WNW-ESE direction, and was expected to be the most challenging weakness zone to pass.

The rest of the tunnel is located in Precambrian bedrock. The supracrustal gneiss is the oldest rock unit in the area, and is intruded by several generations of granitic and basic plutonic rocks. The intrusive events were separated by major deformation episodes. Four fold episodes of regional importance have been distinguished (Graversen, 1984). This has resulted in rapidly varying bedrock, with alternating rocks like augen gneiss, biotite gneiss, metatonalite/granite and supracrustal gneiss. In addition to these rocks, dykes consisting of pegmatite, diabase etc. are common. The thickness varies from less than one metre up to tens of metres. See Figure 6.1 for an overview of the geological conditions.

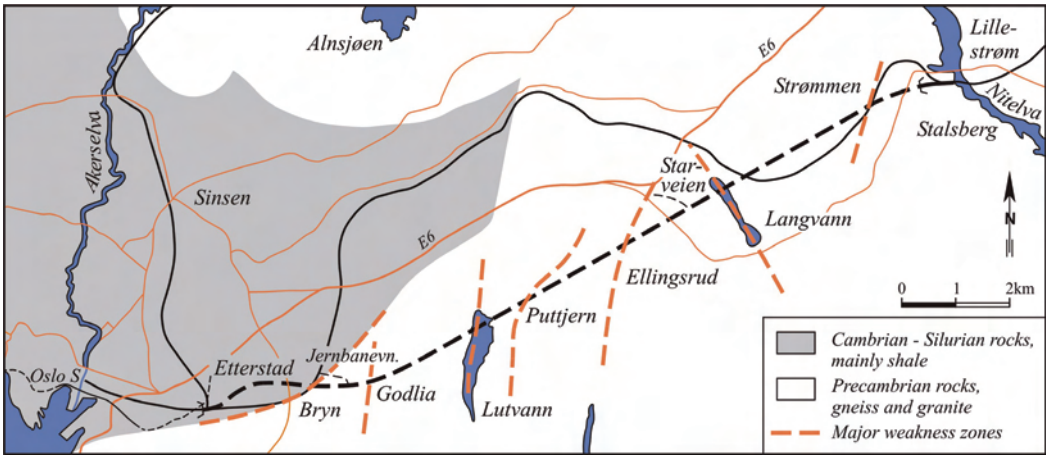

FIGURE 6.1 Simplified geological map for the Romeriksporten tunnel, modified from Bollingmo (1994).

Many of the weakness zones registered in the Precambrian bedrock are fracture zones parallel with the foliation of the rocks. The dominating strike direction for the foliation fractures are N-S. Besides the fracture zones, some of the registered weakness zones are fault zones. One of the most evident fault zones starts just North of the adit at Starveien, and strikes WNW-ESE, and crosses the tunnel alignment in a depression where the small lake Puttjern is located. Another fault zone strikes parallel with the latter and ends in the north-eastern part of the Lutvann lake. Generally the area West of the adit at Starveien has more weakness zones than the eastern part of the tunnel, and the area has more varying rock types with several fold structures, including two synclines (Lutvann and Godlia) and one anticline (Hellerud), reflecting the folding of the Precambrian rock.

The soil cover above the tunnel varies from sparsely cover to 30-40 m thickness. The area is partly under marine limit, and the soil therefore consists of Quaternary clay and silt, usually with gravel and sand covering the bedrock. In some areas moraine is dominating. The thickest soil cover was registered in Godlia, Ellingsrud, Fjellhamar and Strømmen.

6.2.2 Investigation results

The preinvestigations were focused initially on geological mapping and study of aerial photographs to identify weakness zones, faults, joint patterns and for describing the rock mass quality, (Bollingmo, 1994). Core drilling was carried out to find the rock mass quality and rock cover at the weakness zone near Bryn. No special mapping of the hydrogeological conditions was done before tunnelling started, but a total of 334 total sondings were carried out to find type and depth of soil in the residential areas of Godlia and Hellerud. In addition piezometres were set up to register the groundwater level in the areas with high potential of soil settlement.

High water leakage during construction initiated extra investigations in the area of Lutvann and Puttjern. The investigations were done to collect more information about rock mass quality and water conditions, and to improve the prognosis for the remaining excavation. Two refraction seismic profiles were shot, and several low seismic zones identified (Paulsson, 1996). Table 6.1 shows a summary of the investigations carried out. In addition to the investigations mentioned above, core drilling, probedrilling, testing of gouge materials and of course geological mapping were carried out during tunnelling.

Due to the high water leakages encountered at the Romeriksporten tunnel, additional investigations were done after excavation was completed, including acoustic and optical televiewer logging in boreholes (Elvebakk and Rønning, 2001a and b), magnetic measurements from plane followed up by gravimetry and 2D resistivity (Rønning et al., 2007). In this thesis main emphasis will be on investigations carried out before or during tunnelling.

TABLE 6. 1 Investigations carried out for the Romeriksporten tunnel.

Investigation method.	Investigation results.	Comments.
Preliminary studies (literature) and detailed field mapping.	Geological report with descriptions of rock types, orientation of joint sets and major weakness zones.	No detailed prognosis for water leakage. In contract, high amounts of pregrouting masses indicated that water leakage was expected.
4 core drilling holes, total 122 m.	Rock cover and rock quality control for the Bryn zone (major fault).	Thin rock cover and poor rock mass quality in the Bryn zone.
Geotechnical investigations to find thickness and type of soil cover along the tunnel alignment, 334 total sondings.	Map showing type and thickness of the soil cover along the tunnel alignment.	Based on the results, piezometres were placed in areas to follow up the groundwater level .
Two refraction seismic profiles, P1-325 m by Lutvann, P2-225 m by Puttjern.	Lutvann: 4 low velocity zones, velocities between 2000 and 2700 m/s. Puttjern: two low velocity zones (approx. 3500 m/s).	Carried out in July 1996, during construction. The seismic velocity for the surrounding rock mass was approx. 5000 m/s.

6.2.3 Geological conditions and water leakage encountered during construction

Many weakness zones were encountered, but no unexpected problems with extremely poor rock mass quality occurred. The Bryn zone was passed with careful excavation and full concrete lining as originally planned. A total of 619 m of concrete lining were used in the tunnel. The biggest problems were connected to high water inflow, and highest amounts of water leakage were encountered in the sections below Lutvann and Puttjern (Station No. 7000-8500). High groundwater pressure (12-13 bar), combined with highly fractured rock mass and partly clayey gouge material, resulted in difficult pregrouting conditions. Problems with sealing the rock mass were experienced especially below Lutvann and Puttjern. Figure 6.2 shows a longitudinal profile where major weakness zones and sections with high water leakage are indicated.

In Romeriksporten pregrouting was carried out sporadically. Based on measured water inflow from one probedrilling round it was decided whether it was necessary to pregrout or not. One probedrilling round consisted of 2 to 6 holes of 21 to 30 m length, and 6 holes each of 24 m length were mostly used.

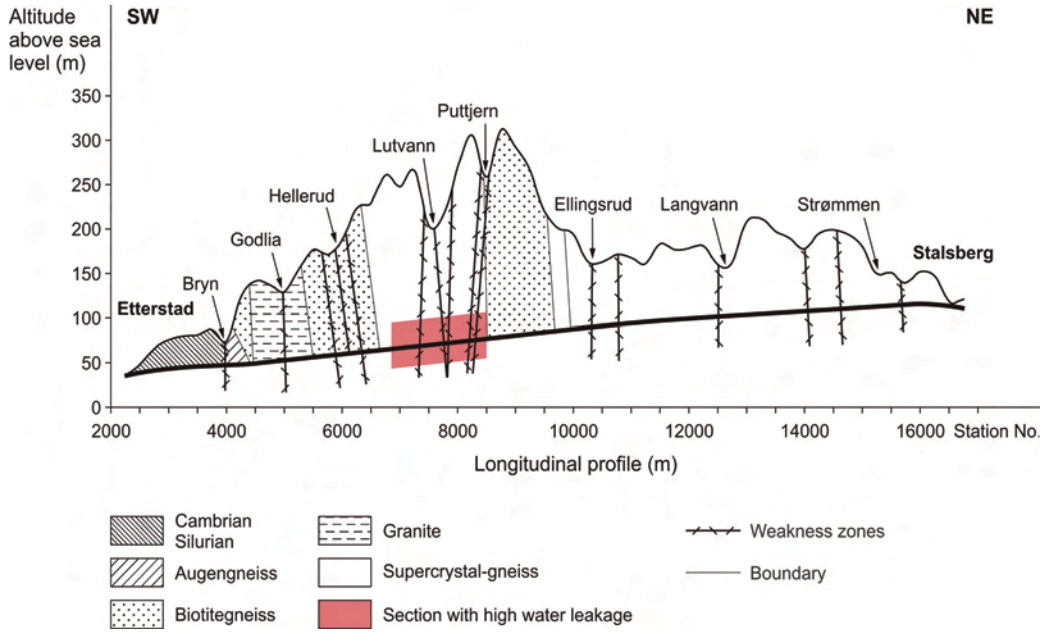

FIGURE 6.2 Longitudinal profile for the Romeriksporten tunnel (exaggerated vertical scale), modified from Beitnes (2002).

Based on geology and water leakage measured in probedrillingprobedrilling rounds the tunnel may be divided into four sections (from West to East). A simplified summary of geological conditions and water leakages is given in Table 6.2.

TABLE 6. 2 Geological conditions and water leakage encountered in the Romeriksporten tunnel.

Station no .	Rock types.	Rock mass quality.	Water leakage.
2640 - 4025 (Etterstad-Bryn zone).	Shale and limestone, maenaite, alum shale in the Bryn zone.	Q-values 2-15 in shale / limestone. In Bryn zone Q-value 0.05, 2-3 m zone consists of mostly clay, alum shale 2-7 m thick.	Small leakages, varying from 0 to 20 l/min in probedrilling rounds.
4025 - 6870 (Bryn zone - West of Lutvann).	Augen gneiss, amphibolitic gneiss, granitic gneiss, quartz diorite, pegmatite and diabase dykes.	Generally good rock mass quality, typical Q-values: 3-25. Some weakness zones with clay filled fractures, 1-6 cm clay.	Some water leakage (5-15 l/min in probedrilling rounds) connected to pegmatite/diabase dykes and fracture zones. Long sections with no water.
6870 - 8500 (West of Lutvann - East of Puttjern).	Granitic-, mica-, amphibolitic- and migmatitic gneiss. Pegmatite and diabase dykes.	Several weakness zones with Q-values 0.3-4. Often crushed with open fractures and some clay.	High water leakages, typical 400 l/min in probedrilling rounds, also sections with 1000 l/min in one probedrilling round.
8500 - 16,450 (East of Puttjern - Stalsberg).	Augen-, amphibolitic-, mica- and mylonitic gneiss, quartz diorite. Pegmatite and diabase dykes.	Mostly good rock mass quality, Q-values: 5-40. Some weakness zones, 1-10 m, with crushed rock mass and 5-25 cm clay.	Long sections with no water leakages. Locally small water leakage, 5-10 l/min registered in probedrilling rounds.

6.3 The Frøya tunnel

The Frøya subsea tunnel is located on the northwest coast of Norway, West of Trondheim, and links the Hitra and Frøya islands. The Frøya tunnel is 5.3 km long with its deepest point at 155 m below sea level. It has a major part (3.6 km) below the sea, where the rock overburden varies between 37 m and 155 m. The two-lane road tunnel has a cross sectional area of 50 m². The maximum gradient is 10 %. Tunnelling started in February 1998, breakthrough was in September 1999, and opening of the tunnel for traffic in June 2000. The station numbers in the Frøya tunnel start at 3000 (Hitra) and end at 8279 (Frøya). The breakthrough was at Station No. 5641.

6.3.1 Geological conditions

The area has been exposed to major faulting and brecciation due to Devonian to Tertiary movements. The main geological feature is the Tarva fault, which can be followed more than 150 km towards ENE on the Norwegian mainland. Based on studies of drill cores

from fault zones in the Frøya tunnel, Bøe et al. (2005) state that it is possible that late Paleozoic and Mesozoic sediments are present. One possibility is that sediments were incorporated into faults during their reactivation in Mid Jurassic and later times.

At the tunnel entrances on both Hitra and Frøya, metamorphic rocks of Precambrian age are dominating. The rock types below the Frøyfjord are gradual transitions between various gneisses, such as granitic gneiss, mica gneiss and migmatite. A few bands or layers of limestone/marble also occur. The foliation of the rocks is mainly oriented with strike ENE-WSW and steep dip towards NW. Figure 6.3 shows the tunnel alignment and the main weakness zones as interpreted from geological maps, aerial photos and field investigations.

6.3.2 Investigation results

The preinvestigations started in 1982, and were carried out in several stages (Lien et al. 2000). Compared to other similar projects very comprehensive preinvestigations were carried out. The refraction seismic measurements showed many low velocity zones. Table 6.3 show a summary of the investigations carried out.

The investigations revealed challenging geological conditions for tunnelling between Hitra and Frøya, detailed studies of the structural geology in the area therefore were carried out (Braathen, 1996). Furthermore, two groups of engineering geological experts were independently studying all available results from investigations carried out, and evaluated feasibility and recommended tunnelling methods, (Nålsund et al., 1996; Nilsen et al., 1997). Both groups concluded that it was possible to excavate the tunnel with drill and blast as the tunnelling method.

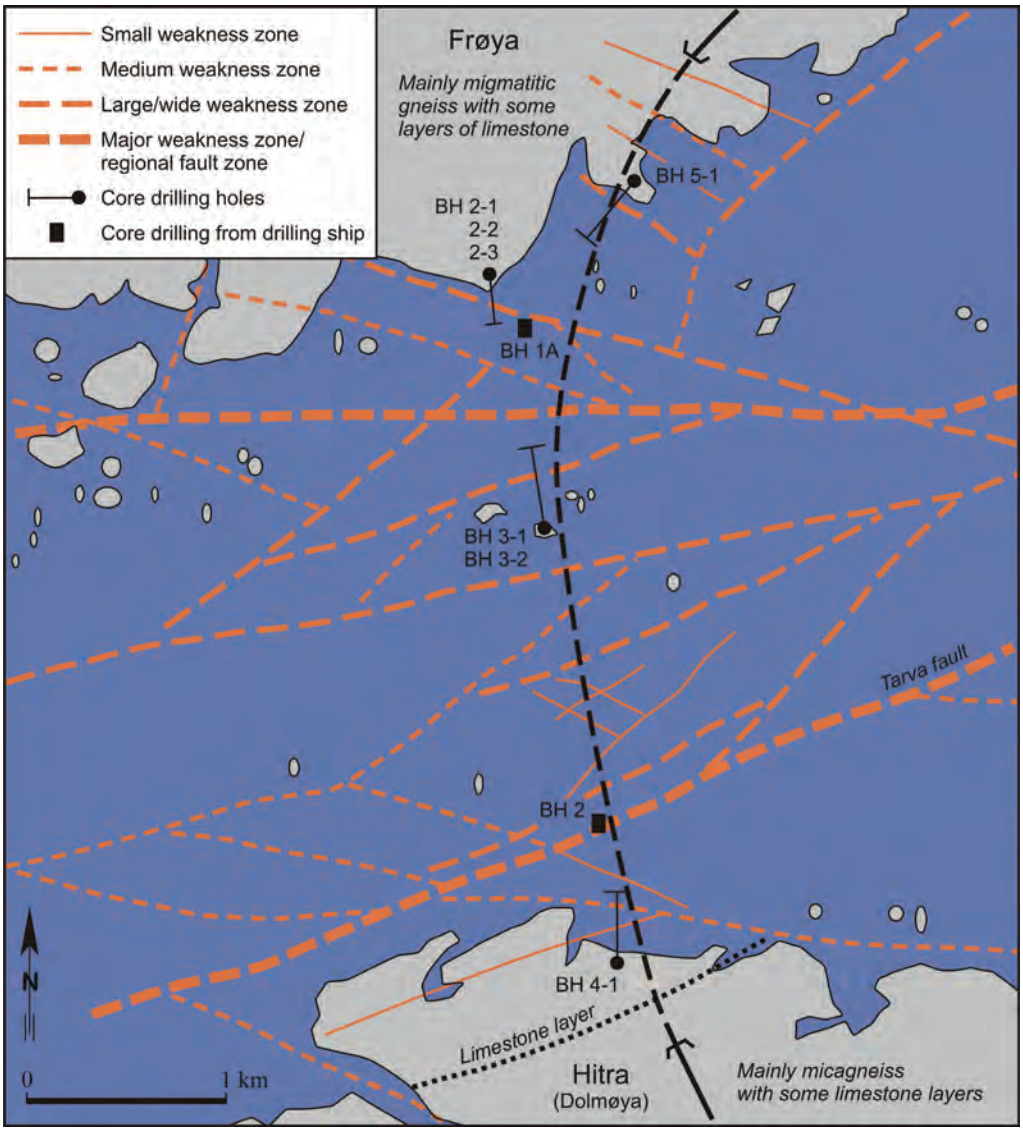

FIGURE 6.3 Geological map with main weakness zones for the Frøya tunnel (Nilsen et al., 1997).

TABLE 6. 3 Investigations carried out for the Frøya tunnel.

Investigation method.	Investigation results.	Comments.
Studies of literature and aerial photos, detailed field mapping.	Descriptions of rock types, orientation of joint sets on the islands, plans for further investigations.	First suggestion for alternative alignments.
Reflection seismic in three stages.	Better knowledge of the depths of water and soil. Indication of depressions and possible weakness zones.	Normal procedure for subsea tunnels.
Refraction seismic in five stages, a total of 10.450m with 935 m onshore.	20% of the registered profiles had seismic velocity lower than 3500 m/s. This indicated many weakness zones.	Difficult rock mass conditions were expected. Good basis for planning core holes and discussing final alignment.
13 core drilling holes, 1850 m in total, with 103 m from a drilling ship.	Difficulties with core drilling in some of the weakness zones, core loss, swelling clay and weathered rock mass. Extremely poor rock mass quality in some sections.	Weakness zones registered and more investigations ordered to decide final alignment.

6.3.3 Geological conditions and water leakage encountered during construction

Due to the challenging tunnelling conditions, the owner had always one engineering geologist at site during construction, and geological mapping was continually carried out. In many of the weakness zones core drilling was carried out and gouge material was tested to check swelling capacity. In total 30 swelling pressure tests were executed, and 73 % of them gave more than 0.3 MPa swelling pressure. Highest swelling pressure was measured to 1.05 MPa at Station No. 5622. 36 % of the tunnel length can be described as weakness zones or very poor rock mass with Q-values lower than 1. The rock mass quality between the weakness zones was not as good as the prognosis had estimated, only 32 % of the tunnel length had fair to very good rock mass quality, (the prognosis said 56 %). Figure 6.4 shows a longitudinal profile of the Frøya tunnel, with weakness zones and sections with water leakage indicated.

The rock mass quality varied a lot, and sudden changes in rock mass quality were often registered. In sections outside the weakness zones, the joints typically had 0-10 mm clay filling. In the weakness zones clay thicknesses often were 10 to 20 cm, and in some sections even more.

.

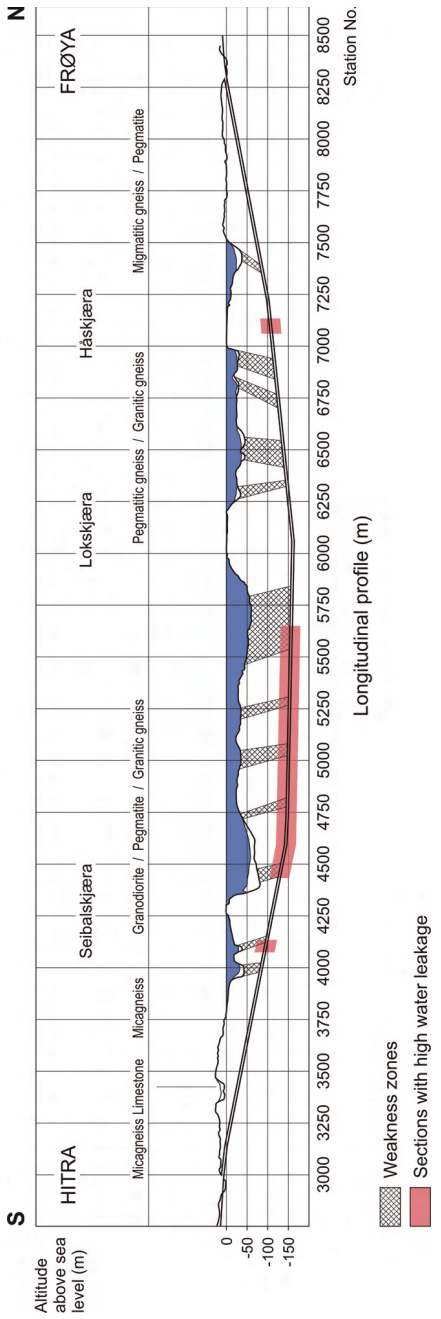

FIGURE 6.4 Longitudinal profile for the Frøya tunnel, modified from Lien et al. (2000).

Probedrilling was carried out systematically below sea level, one probedrilling round consisted of 2 to 6 holes of 21 to 30 m length, and 6 holes each of 30 m length were mostly used. Based on water inflow from a probedrilling round, it was decided whether or not pregrouting was necessary. Pregrouting has been carried out on both sides, but most frequently on the Hitra side. The pregrouting rounds varied from 10 to 22 holes of 18 to 24 m length, and commonly 20 holes of 21 m length were used. The water leakage referred to is water leakage encountered in the drillhole of one pregrouting round before any pregrouting was carried out. In Table 6.4, the Frøya tunnel is divided into sections based on water leakage encountered for the pregrouting rounds (p.g.rounds) or probedrilling rounds (p.d.rounds), and brief descriptions of geological conditions and amount of water leakage are given.

TABLE 6. 4 Geological conditions and water leakage encountered in the Frøya tunnel.

Station No.	Rock types.	Rock mass quality.	Water leakage.
3000-4073	Mica- and granitic- gneiss, limestone and pegmatite dykes.	Two weakness zones with Q-values 0.01-0.3; Station No. 3380 - 3470 (limestone) and 3979 - 4022. Outside weakness zones, Q-values from 0.3 to 18.	Generally small leakages. From 0 to 6 l/min in p.d.rounds. One p.g.round with 60 l/min at Station No. 3724.
4073-4133	Mica- and granitic- gneiss.	One major weakness zone with Q-values 0.01-0.02 at Station No. 4122 - 4149. Very poor to fair rock mass quality in rest of the section, Q=0.1 - 2.8.	Some water leakages, 40-278 l/min per p.g.round, 278 l/min at p.g.round at Station No. 4110.
4133-4431	Mica- and granitic- gneiss and limestone.	Poor to good rock mass quality, Q-values 1.1 - 25.	Generally small water leakages, 0-33 l/min on p.g.rounds / p.d.rounds.
4431-5490	Mica- and granitic- gneiss, migmatite, limestone and pegmatite dykes.	Many weakness zones, among them the Tarva fault; Station No. 4438-4505. Q-values 0.007-0.5, Weakness zones also at Station No. 5003-5080, 5197-5210 and 5265-5304.	Moderate to high water leakages. Especially high inflow between Station No. 4,521 - 4,665, highest registered water leakage was 2144 l/min in one p.g.round (Station No. 4535).
5490-6086	Gneiss, weathered gneiss, migmatitic gneiss and pegmatite dykes.	Long weakness zone, Station No. 5535-5770 with Q-values 0.009 - 0.8, fractured and crushed zones, 1-3 m weathered zones, 30 cm clay. Gradually better to very good rock mass quality, Q-values 1-45 toward Station No. 6086.	Small to moderate water leakages, 0-21 l/min on p.g.rounds/ p.d.rounds. One p.g.round at Station No. 5525 had 45 l/min.
6086-7060	Migmatitic gneiss and pegmatite dykes.	Many weakness zones, Station no; 6325-6350, 6418-6550, 6610-6640, 6675-6768 and 6841-6940.	Small to moderate water leakage, 0-32 l/min per p.g.round/ p.d.round, with one exception; p.g.round at Station No. 6116 gave 630 l/min.
7060-7132	Migmatitic gneiss.	No major weakness zone, poor to good rock mass quality, Q-values 2.1-30.	Some water leakage, 50-71.5 l/min per p.g.round.
7132-8279	Migmatitic- and mica-gneiss and pegmatite dykes.	Many weakness zones with Q-values 0.008-0.2; 7350-7390, 7422-7426, 7910-7925, 7979-7989 and 8270. Between the weakness zones varying rock mass quality, Q-values 0.2-35.	Small water leakages, no pre-grouting rounds.

6.4 The T-baneringen tunnel, stage one (Ullevål - Nydal)

The T-baneringen tunnel is stage one of a circular metroline in northern part of Oslo. The tunnel links Ullevål to Nydal, see Figure 6.5, and is 1264 m long with a cross section of 65 m^2. The station numbers in the tunnel start at 400 and ends at 1664. During excavation high water leakage was encountered in a zone between Station No. 700 and 750. The tunnelling was completed in January 2002.

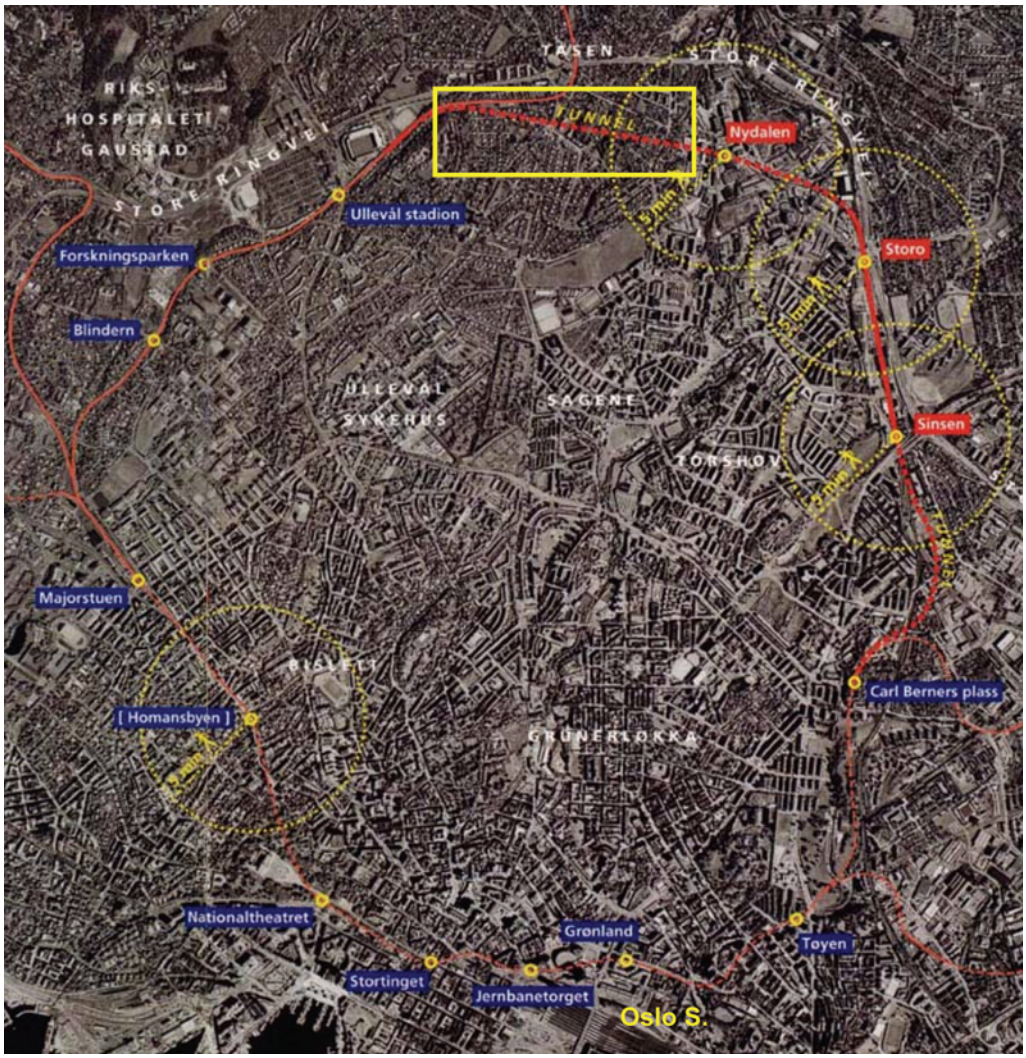

FIGURE 6.5 The circular metroline, with the T-baneringen tunnel in the northern part of Oslo (Agency for Road and Transport, 2000).

6.4.1 Geological conditions

The predominant rocks in the area are shale, nodular limestone and ordinary limestone of Ordovician age. Most important dyke rocks are syenite porphyry, syenite and diabase. During the Caledonian folding, the sediments were compressed from NW, resulting in fold axes striking ENE, with bedding dipping 30 degrees towards NNW. The sediments are cut by Permian igneous dykes, with thickness from one decimeter to several metres. Figure 6.6 shows a longitudinal profile of the T-baneringen tunnel.

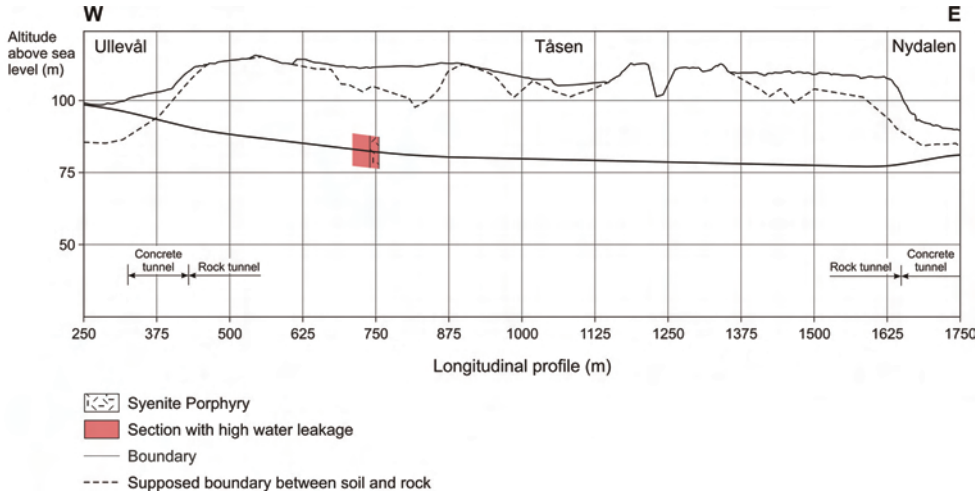

FIGURE 6.6 Longitudinal profile of the T-baneringen tunnel (exaggerated vertical scale), modified from Boge et al. (2002).

Three joint sets are distinguished; one parallel with the bedding of the sediments, the second with similar strike and dip as the dykes (NE and steep), and the third striking perpendicularly to the dykes.

The rock cover varies between 5 and 29 m above the tunnel. The area is below marine limit, and the soil cover along the tunnel varies from 0 to 17 metres. More considerable soil thicknesses were registered not far from the tunnel alignment. The soil consists of a firm toplayer with sand, gravel and dry clay, and below this medium firm clay with thin sand and silt layers. At a few locations with great soil thickness, weak and sensitive clay exists. Just above the bed rock is a layer of glacial deposits. The area above the tunnel is urban, with small houses and blocks of flats. To avoid settlements of buildings, strict inflow criteria varying from 7 to 14 l/min per 100 m were set. During construction sporadic pregrouting was tested out in the first section (Station No. 440-616), but the experience was not too good and it was decided to use continuous pregrouting for the rest of the tunnel.

6.4.2 Investigation results

The area close to the T-baneringen tunnel is thoroughly investigated. Moreover, many investigations carried out for the Tåsen road tunnel located just North of the T-baneringen tunnel are valid also for the T-baneringen tunnel. Since the excavation of the Tåsen tunnel was finished before the tunnelling of the T-baneringen tunnel started, the experience from the Tåsen tunnel regarding rock mass quality and water leakage gave valuable information. More investigations than usual were carried out to investigate soil thickness, soil types, rock cover and pore pressure for evaluating what inflow criteria were needed to avoid dangerous settlements of buildings, (Kveldsvik et al., 1999).

Investigations carried out for the T-baneringen are summarized in Table 6.5. The data are based on the geological report and tender documents, (Løset and Kveldsvik, 2003; Agency for Road and Transport, 2000).

TABLE 6. 5 Investigations carried out for the T-baneringen tunnel and brief comments on the results.

Investigation method.	Investigation results with comments.
Preliminary studies (literature) and detailed field mapping.	Geological report with descriptions of rock types, orientation of joint sets and major weakness zones /dykes.
Refraction seismic, 11 profiles: 1750 m in total (Pedersen, 1999) In addition 3 profiles: 285 m in total (Pedersen, 1996; 1997a).	Low velocity zones are registered close to trenches (depressions) with great soil thickness, such as Maridalen (Station No. 1500-1600) Tåsen (approximately Station No. 800) and around Station No. 1225.
5 core drilling holes, including Lugeon testing. (Investigation for the Tåsen tunnel).	Mean Lugeon value and /RQD values in respective rock types: shale 3,0 L / RQD 74, nodular limestone 3,4 L / RQD 82 and dykes 8,2 L / RQD 38.
Geotechnical investigations of thickness and type of soil along the tunnel alignment, including 67 total sondings.	Map showing type and thickness of the soil along the tunnel alignment. Based on the results, inflow criteria were suggested and supplementary piezometres (34 in total) were placed in areas to follow up the groundwater level.

Based on the site investigations, the rock mass quality varied from very poor to good, and one major weakness zone connected to the syenite porphyry dyke at Station No. 710-750 was expected. Water leakage was foreseen in the syenite porphyry dyke, since water leakage was encountered in syenite porphyry dykes during tunnelling of the Tåsen tunnel.

6.4.3 Geological conditions and water leakage encountered during construction

The water leakage is given in l/min per pregrouting round (p.g.round). Number of holes in one p.g.round varied from 10 to 50, and the length of the holes varied from 6 to 28 m. Between Station No. 710 to 750 high water leakage and difficult conditions for pregrouting were encountered in connection with a syenite porphyry dyke. This dyke came

not as a surprise, but the amount of water and difficulties with pregrouting were somewhat bigger than expected. Some extraordinary pregrouting rounds with high amounts of pregrouting cement and many short pregrouting holes were necessary to seal the zone. Outside this problematic zone an average p.g.round, consisted of 31 pregrouting holes of 21 or 24 m. A summary of geological conditions and water leakage along the T-baneringen tunnel is given in Table 6.6.

TABLE 6. 6 Geological conditions and water leakage encountered in the T-baneringen tunnel.

Station No.	Rock types, joint filling.	Rock mass quality.	Water leakage.
400 - 710.	Shale, nodular limestone and diabase. Calcite-, pyrite- and clay filled joints.	Very poor to fair rock mass quality, Q-values 0.1-10. Extra jointed in connection with diabase dykes. No major weakness zones.	Generally small leakages. 0-21 l/min in p.g.rounds.
710 - 780.	Shale, nodular limestone, diabase and syenite porphyry (Station No. 740-755). Calcite-, pyrite- and clay filled joints.	Extremely poor to poor rock mass quality, Q-values 0.01-3. Station No. 720-755; crushed with clay, 50 cm clay at Station No. 755.	High water leakage between Station No. 710 - 755, 30-1440 l/min per p.g.rounds.
780 - 1664.	Shale, limestone, nodular limestone, diabase, syenite and syenite porphyry. Calcite-, pyrite- and clay filled joints.	Extremely poor to fair rock mass quality, Q values 0.02 - 8. Weakness zones registered at Station No. 920, 1110 and 1225, highly jointed zones with 10-30 cm clay + diabase.	Low to moderate water leakage, 0-35 l/min per p.g.rounds.

6.5 The Lunner tunnel

The Lunner road tunnel is located approximately 40 km North of Oslo, and is a part of the new highway No. 35, between Lunner and Gardermoen airport. The 62 m^2 and 3.8 km long tunnel had breakthrough in October 2002. The rock cover varies between 20 and 230 m. For environmental reasons some sections of the tunnel had strict inflow criteria of only 10 or 20 l/min per 100 m. During excavation large water leakages were encountered.

6.5.1 Geological conditions

Geologically the Lunner tunnel is located in the Oslo Region, at the boundary between the Hadeland sedimentary sequence (Cambro-Silurian rocks) and the Nordmarka plutonic and volcanic rocks (late Carboniferous and Permian age). The heat from the syenite magma resulted in a contact metamorphism of the sediments into a hard, fine-grained and banded hornfels. The bedrock along the tunnel can be divided into four rock types from West to

East: hornfels, syenite, different volcanic rocks and sandstone/conglomerate. The syenite has an irregular boundary towards the volcanic and sedimentary rocks in the eastern part of the tunnel. In addition, some Permian intrusive dykes cut through the rock mass, especially in the hornfels area.

The hard and fine-grained hornfels is heavily jointed compared with the blocky and moderately jointed syenite. Regionally, N-S striking joints with steep dip are dominating. In the syenite and volcanic rocks a joint direction with NW-SE strike and steep dip is, however, almost as frequent as the N-S joints. Several weakness zones have been identified, all with the same directions as the dominating joint directions. A major zone of weakness (fault) is connected to the boundary between hornfels and syenite. The soil cover above the tunnel consists of a thin and discontinuous layer of moraine material. Figure 6.7 shows a simplified geological map with weakness zones as interpreted from geological mapping and site investigations.

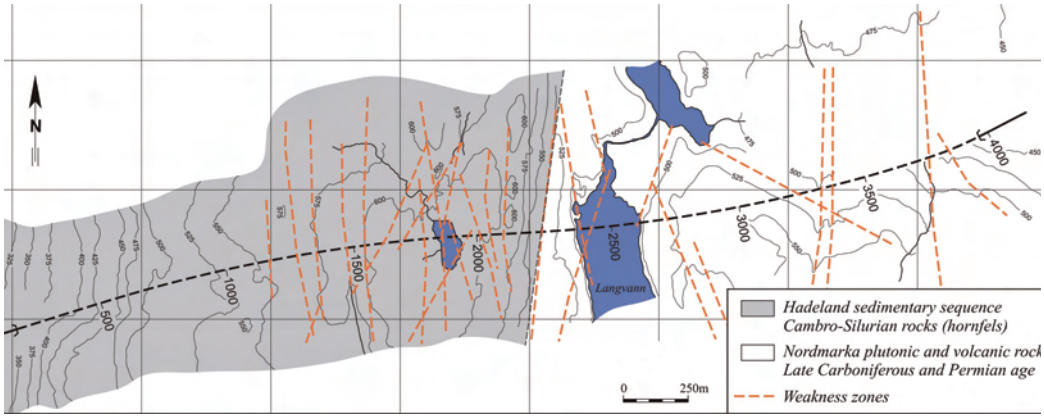

FIGURE 6.7 Simplified geological map with weakness zones for the Lunner tunnel, modified from Rønning and Dalsegg (2001).

6.5.2 Investigation results

A lot of pre-construction investigations were carried out for this tunnel project, including geological mapping (Kirkeby and Iversen, 1996), refraction seismic (Pedersen, 1997 b) and core drilling (Iversen, 1998). In addition, the R & D project "Tunnels for the citizen" organized some extra investigations to test and gain experience with different investigation methods, (Geological Survey of Norway, 2001-2002; Pedersen, 2003).

A summary of the investigations are given in Table 6.7. The section between Station No. 2220 and 2561 is particularly interesting because of the weakness zones connected to the

boundary between hornfels and syenite. Therefore a lot of the investigations were focusing on this site.

TABLE 6. 7 Investigations carried out for the Lunner tunnel.

Investigation method.	Investigation results with comments.
Preliminary studies (literature) and detailed field mapping.	Geological report with descriptions of rock types, orientation of joint sets and major weakness zones.
Refraction seismics, 4 profiles of 115 m. 2 additional profiles of 115 m in the eastern part of the tunnel.	2 low velocity zones (3300 and 3900 m/s) in the western part of Langvann and close to the western shore. In the eastern part of the tunnel alignment (Station No. 3750) a low velocity zone of 3000 m/s was registered.
Directional core drilling hole, including Lugeon testing, 1 hole ~450 m. Offset 130 m West of Langvann, the core hole ends deeper than the tunnel level below the eastern shore of Langvann.	100 m of poor to extremely poor rock mass and 250 m of good quality rock mass. Lugeon values up to 4.25, but mostly lower than 1. Rock boundary between hornfels and syenite is intrusive and not particularly jointed. Weakness zone in the syenite. Poorest rock mass quality expected between Station No. 2250 and 2400.
5 profiles with 2D resistivity measurements. 2 of the profiles cross the boundary between hornfels and syenite.	Several low resistivity zones seem to reach the tunnel depth. One zone (40 ohmm) correlate with the boundary between hornfels and syenite, the other (1000 ohmm) is in the northern part of Langvann. In addition two zones East of Langvann (around Station No. 3375 and 3750).
Borehole logging and hydraulic test pumping. 4 of 8 boreholes located close to the boundary between hornfels and syenite.	Poor rock mass quality, with jointed and crushed zones at the boundary between hornfels and syenite. Two boreholes collapsed at the lowest parts. 250 ohmm registered just above the collapsed section, and well capacity were 7 and 13 m^3 /hour.

The resistivity measurements show different resistivity levels for syenite and hornfels. In syenite the resistivity is 5000 ohmm or higher, and in hornfels it is lower than 5000 ohmm. This most likely is due to the fact that the hornfels is much more jointed than the syenite.

A more detailed description of most of the investigation results are given in Holmøy (2002), which summarises all investigation results available at an early stage of tunnelling. Based on the results in that report a prognosis or “best estimate” for water leakage was made for the part of the tunnel that was not yet excavated (Station No. 1700-3250).

The results from the site investigations point to the boundary between hornfels and syenite as the most problematic weakness zone to pass. In addition, one zone West of Langvann (Station No. 1750) and two zones East of the Langvann (Station No. 3375 and 3750) gave low resistivity, indicating poor rock mass quality or water leakage.

6.5.3 Geological conditions and water leakage encountered during construction

The hornfels section was almost completely dry; only between Station No. 1780 and 1820 water leakages were encountered in a jointed zone. Just after passing the boundary between hornfels and syenite a major weakness zone (fault) with clay filled joints was encountered in the syenite. Connected to the fault zone (Station No. 2220) one pregrouting round gave as much as 2500 l/min. The water leakage came in small channels in the clay filling, causing a lot of water inflow and difficult conditions for pregrouting. High water leakage was encountered in the syenite throughout the section below Langvann (Station No. 2220-2561). In the eastern part of the tunnel water leakage was encountered in some sections, but not as much as in the section between Station No. 2213 and 2561. The water leakage is given in l/min per pregrouting round (p.g.round). Number of holes in one p.g.round varied from 10 to 55, and the length of the holes varied from 8 to 24 m. An average p.g.round consisted of 25 pregrouting holes of 24 m length. A summary of geological conditions and water leakage along the Lunner tunnel is given in Table 6.8.

TABLE 6. 8 Geological conditions and water leakage encountered in the Lunner tunnel.

Station No.	Rock types.	Rock mass quality.	Water leakage.
157 - 2213.	Jointed hornfels, some dykes (syenite porphyry).	Q-values 1-7. Some weakness zones (Station No. 700, 1565-1580) with clay filled fractures, 1-3 cm clay.	Generally small leakages. In one fracture zone (1780-1820) 88 and 92 l/min in two p.g.rounds.
2213 - 2561.	Jointed hornfels, syenite.	Major weakness zone (Station No. 2220-2270) close to the boundary between hornfels and syenite, Q- values 0,1-1. Below Langvann (2270-2561) rock mass quality is poor to fair (Q-values 1-6).	High water leakages at Station No. 2220 as much as 2500 l/min in one p.g. round. Varying leakages below Langvann (50-1000 l/min per p.g.round).
2561 - 3950.	Syenite, various volcanic rocks and sandstone/conglomerate, rhomb porphyry, syenite porphyry.	Long sections with Q-values 5-25, Some weakness zones, Q-values 0.1-3 (Station No. 2915-3060, 3130-3190, 3370-3410, 3715-3770).	Moderate leakages; lower than 50 l/min per p.g.round. Some water leakages; 2930 - 3000 (70-400 l/min per p.g.round).

Figure 6.8 shows a longitudinal profile with weakness zones and sections with high water inflow in the tunnel.

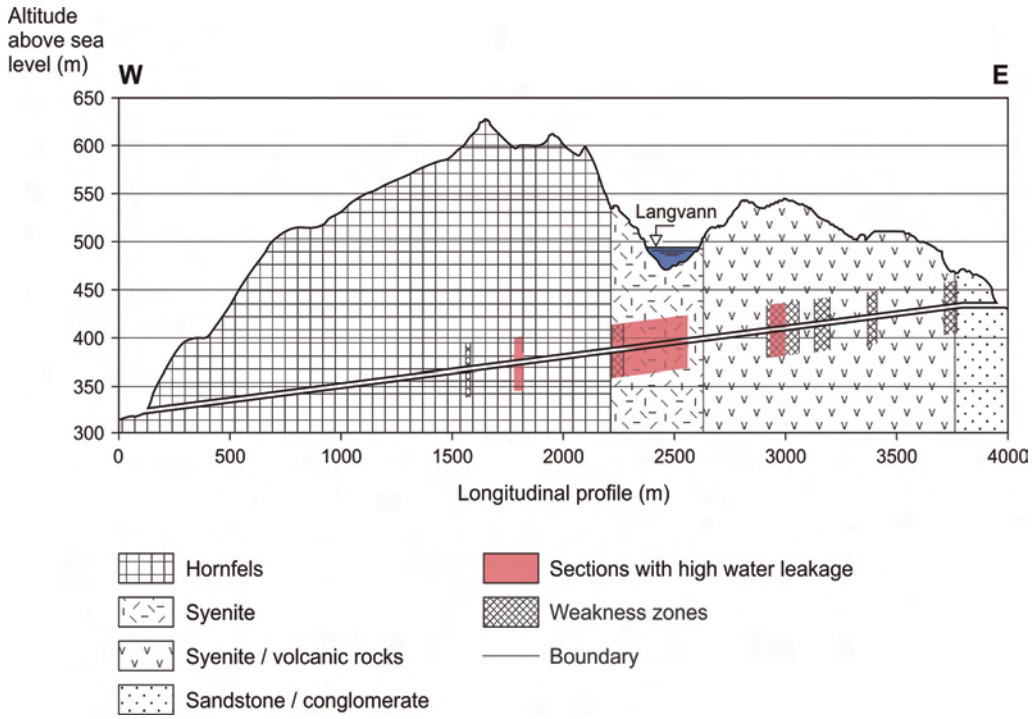

FIGURE 6.8 Longitudinal profile of the Lunner tunnel (exaggerated vertical scale), modified from Hagen (2003).

6.6 The Skaugum tunnel

The 104 m^2, 3.6 km long Skaugum railway tunnel had breakthrough in May 2004. The tunnel is one of two tunnels between Jong and Asker in the western part of Oslo. The rock cover varies between 3 and 100 m. The area is located below marine limit, and depressions are filled by marine deposits. Approximately half of the tunnel alignment has more than 5 m of clay on top of the bedrock. For environmental reasons and due to the risk of harmful settlement of buildings on the surface (densely built-up areas), very strict criteria concerning water inflow in the tunnel were defined. Inflow criteria varied from 4 to 16 l/min per 100m (water leakage after pregrouting). To meet these inflow criteria it was decided to carry out continuous pregrouting through the entire tunnel.

6.6.1 Geological conditions

Geologically, the Skaugum tunnel is located in the Ordovician and Silurian sediments (470-415 Ma), predominantly shales and limestones of the Oslo Region. Based on age, the rock mass is divided into the Oslo group (Ordovician) and the Bærum group (Silurian). The eastern part of the tunnel is dominated by the Oslo group and Permian igneous dykes, and in the western part by the Bærum group. The rock type is predominantly limestone/ shale in both groups, see Figure 6.9.

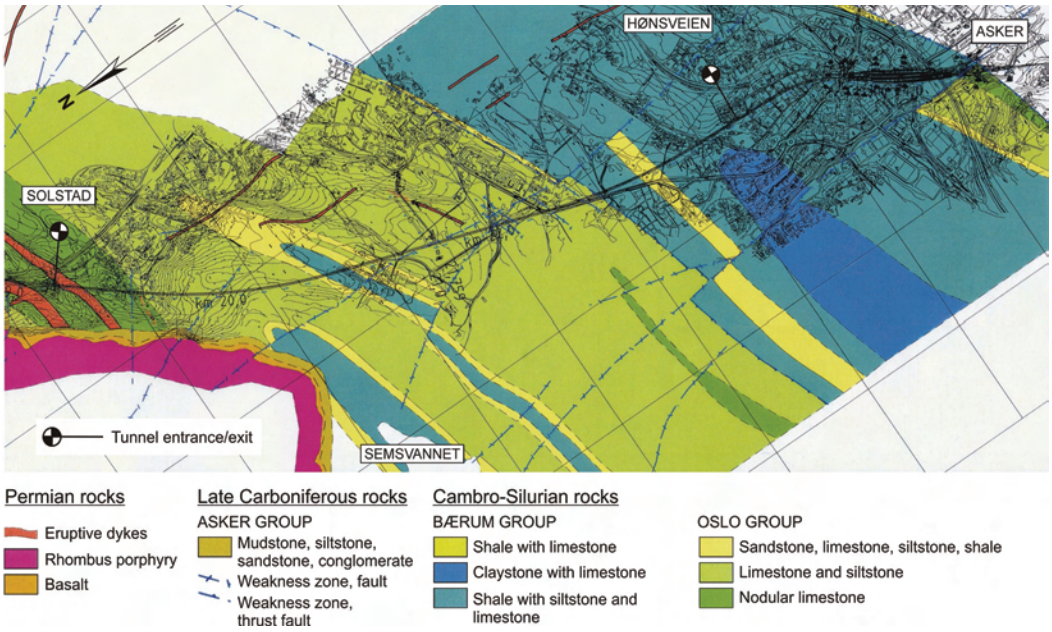

FIGURE 6.9 Geological map for the Skaugum tunnel (Norwegian National Rail Administration, 2001).

The sediments were compressed from NW during the Caledonian folding, and folds and faults were formed with gently dipping fold axis towards ENE or WSW. The foliation joints therefore have strike ENE-WSW and dip towards NW. Reverse faults developed when the NW part of the anticline fold moved up in relation to the SE part. Clay thickness of several decimetres sometimes occur in these reverse faults.

Furthermore, a dominating joint and fault direction, perpendicular to foliation, has strike NW-SE with near vertical dip. Permian igneous dykes (diabase and porphyritic syenite) cut through the sediments, with thickness varying from a few centimetres up to several tens of metres.

6.6.2 Investigation results

The Skaugum tunnel was thoroughly investigated over many years before the exact alignment was decided. The investigations presented here are based on the Geological Report (Norwegian National Rail Administration, 2001) and the investigations carried out by the Geological Survey of Norway through the R & D project "Tunnels for the citizen" (Dalsegg et al., 2003). Table 6.9 gives a brief summary of the investigations. The Station No. goes from 19.255 (Solstad) to 23.640 (Hønsveien/Asker). There is a chainage discontinuity at Station No. 21.000.

TABLE 6. 9 Investigations carried out for the Skaugum tunnel.

Investigation method.	Investigation results with comments.
Preliminary studies (literature and aerial photographs) and detailed field mapping.	Descriptions of rock types, with the orientation of joint sets and major weakness zones. Fault zone parallel with the tunnel in the Skaugum area (Station No. 22.000-22.500). Tunnel entrances also considered critical sections. Thin rock cover (Asker).
7 refraction seismic profiles, 945 m in total, length of profiles varying from 60 to 225 m.	Several low seismic vel. zones (2500-3500 m/s) between Station No. 22.000 and 22.500. Solstad: three low seismic vel. zones (2000 - 2700). Asker: one low seismic zone (3800 m/s).
5 core drilling holes with Lugeon measurements, 680 m in total.	Lugeon values varying from lower than 0.1 to over 100L. Only 10 % of the measurements from 3 core holes were higher than 10L, and the highest values registered close to the top of the core holes.
3 resistivity profiles, 2200 m in total.	General resistivity level from 1000 to 4000 ohmm. 5 low resistivity zones apparently reaching tunnel level, particularly low resistivtiy (20 ohmm) registered between Station No. 22.120 and 22.200.
Borehole logging and hydraulic test pumping of one 118.5 m long borehole (Skaugum area)	Borehole located 75 m West of Station No. 22.030, ending a few metres above tunnel level. General resistivity 500-600 ohmm, with local zones down to 200-300 ohmm. Optical log verified joints and fractured zones. Well capacity around 2 m^3/hour.

Based on the field mapping a main fault zone was expected to cross the tunnel around Station No. 20.960. The same fault zone was expected to have a branch crossing the tunnel around Station No. 22.030. Two refraction seismic profiles were shot in this area, but no major fault zone recognised. Instead several low seismic velocity zones were registered (velocities between 2500 to 3500 m/s).

Based on the results from the refraction seismics a 200 m long core drilling hole perpendicular to the tunnel was carried out. The hole is crossing the tunnel at Station No. 22.025, and showed bedrock of alternating shale and limestone. Joint filling was found to consist of calcite and silt, and some clay was registered in the lowest 50 metres. No major weakness zone was registered.

Three resistivity profiles were carried out in the Skaugum area. The results showed a general resistivity level from 1000 to 4000 ohmm. Several low resistivity zones seeming to reach the tunnel level were registered. The weakness zones indicated from the refraction seismic are within the same area as the low resistivity zones.

6.6.3 Geological conditions and water leakage encountered during construction

The rock mass quality is in average poor to fair, with Q-values between 2.5 and 10. Fractured rock mass with some clay and calcite was encountered, and in a few weakness- and fault- zones the rock mass was crushed in the central part (2-5 cm). Generally, the central parts of the fault zones had some clay filling, and water came in the fractured zones adjacent to the fault. No major stability problems were experienced.

In the Skaugum tunnel it was decided to carry out continuous pregrouting. The amounts of water given below therefore refer to water leakage from pregrouting holes in one pregrouting round. One pregrouting round consisted of 38 to 56 holes of length 21 to 28 m length, most common was 48 holes with 24 m length. Thus, water leakage is water encountered before any pregrouting was carried out. Generally, the water leakages of the pregrouting rounds (p.g.rounds) were lower than 75 l/min, but in some sections more water was encountered. A summary of geological conditions and water leakage along the Skaugum tunnel is given in Table 6.10.

TABLE 6. 10 Geological conditions and water leakage encountered in the Skaugum tunnel.

Station No.	Rock types.	Rock mass quality.	Water leakage.
19.255-19.900 Solstad.	Shaly limestone, shale, syenite, diabase, nodular limestone and pegmatite dykes.	Q-values 0.6-13.3. Some clay-zones, 2-5 cm clay, close to fold axis (Station No. 19.390) and crushed zone (Station No. 19.540). Q-values 0.6-0.8 in weakness zones.	Generally small leakages. 3 p.g.rounds with 105, 178 and 206 l/min. One at the boundary between syenite and shale, two adjacent to fold axis and diabase dyke.
19.900-20.520	Shaly limestone, nodular limestone, shale (blocky).	Q-values 3.3 to 18.8, some clay on joints.	Some water leakage. 14 p.g.rounds with 120 to 860 l/min. (Station No. 19.900-20.000, 20.305-20.350 and 20.440-20.512).
20.520-21.950	Nodular limestone, shale (some places blocky).	Q-values 3 to 10. One 3 m thick crushed and folded zone with clay, Q-value 0.1 at Station No. 20.640.	Generally small leakages. 3 p.g.rounds with 76, 90 and 100 l/min. One close to crushed zone and two in connection with a fault zone.
21.950-22.810	Nodular limestone, silt-/sandstone, shale.	Q-values 2.2-12. No weakness zones.	High water leakage in sections.19 p.g.rounds with 75 to 1285 l/min. (Station No. 21.960-22.040, 22.375-22.435, 22.700-22.810 and 23.270-23.340).
22.810-23.640 Asker / Hønstad.	Shaly limestone, shale, nodular limestone.	Q-values 0.2-17. Weakness zone close to tunnel entrance (rock cover < 3m). Crushed zone with clay (Q-value 0.2-0.4).	Moderate water leakage. 5 p.g.rounds with 85 to 299 l/min. (3 out of 5 p.g.rounds were located between Station No. 23.270-23.342, vertical clay filled joints).

Four of the sections with high water leakage were connected to boundaries between different geological formations, the Bærum group and the Oslo group. The rock mass is predominantly limestone/shale in both groups, in the Oslo group the limestone is often nodular and somewhat more jointed than the limestone in the Bærum group. Water leakage was also encountered in intensely folded areas, close to the fold axis. Figure 6.10 shows a longitudinal profile of the Skagum tunnel with encountered weakness zones and sections where high water inflow were encountered.

.

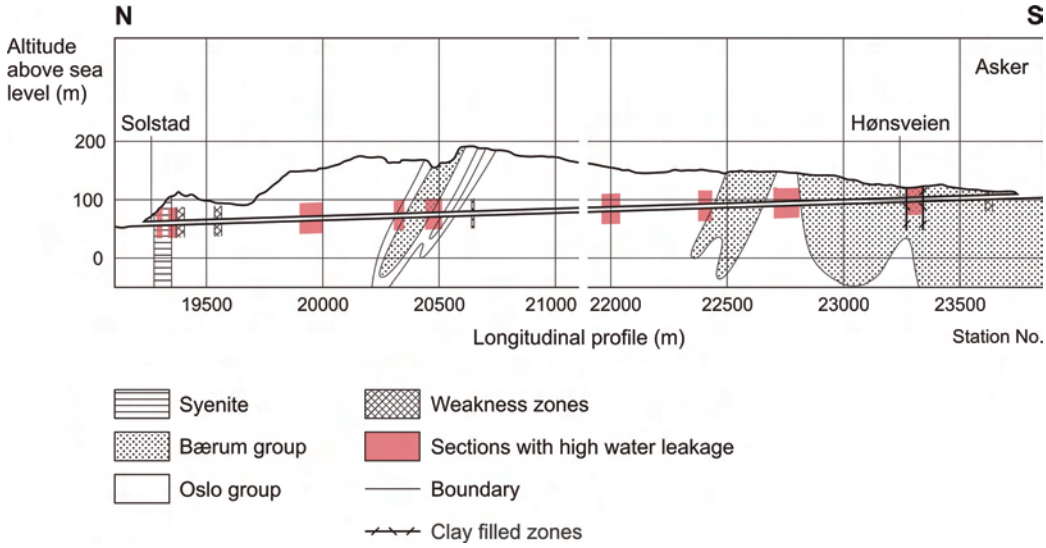

FIGURE 6.10 Longitudinal profile of the Skaugum tunnel (exaggerated vertical scale), modified from Norwegian National Road Administration (2001).

6.7 The Storsand tunnel

The Storsand tunnel is one of 7 tunnels along the new Highway E39, between Øysand and Thamshavn, southwest of Trondheim. The new highway improves safety and accessibility for more than 10.000 persons using the road daily. Excavation of the Storsand tunnel was completed late October 2004, and the new highway project was opened for public use in July 2005, two months ahead of original plans. This highway project is the first Public Private Partnership (PPP) contract organised by the Norwegian Public Roads Administration.

The tunnel is 3654 m long with a cross section of 67 m^2. The Station No. in the tunnel, from East to West, is 17.831 to 21.485. Among the 7 tunnels excavated on E39, the Storsand tunnel was the only tunnel where pregrouting was utilized. Post-excavation grouting was carried out in one section to minimize water inflow. However the water leakage in the tunnel was small compared to the other tunnels studied.

6.7.1 Geological conditions

The Storsand tunnel is located in the oldest unit of the Trondheim Nappe Complex (late Precambrian to Cambrian age) and is a part of the Caledonian mountain chain (Wolff,

1976). The bedrock consists of alternating gneisses like biotite amphibolite, granitic gneiss (quartz-/feldspar gneiss) and granodioritic gneiss. In some sections the gneiss is banded. The foliation joints have strike E-W with dip varying from 20 to 45 degrees towards South. In the tunnel, bands enriched in quartz and feldspar occur parallel with the foliation. In addition, two other joint directions are present. The predominant joint set has strike NNE-SSW and steep dip. In the landscape, gullies and canyons typically follow the same direction. Another joint direction, almost parallel with the foliation joints, has strike about WNW-ESE and steep dip. 6 steep faults or weakness zones striking NNE were expected to cross the tunnel, the two most distinct at Station No. 19.625 and 20.730. The latter is located at Storsandbekken where the tunnel has only marginal rock cover (5.5 m registered by total sondings). One weakness zone striking WNW-ESE is parallel with the tunnel alignment in the eastern part of the tunnel, but the zone was not expected to affect the tunnelling conditions. Figure 6.11 shows a simplified geological map with weakness zones as interpreted from geological mapping and site investigations.

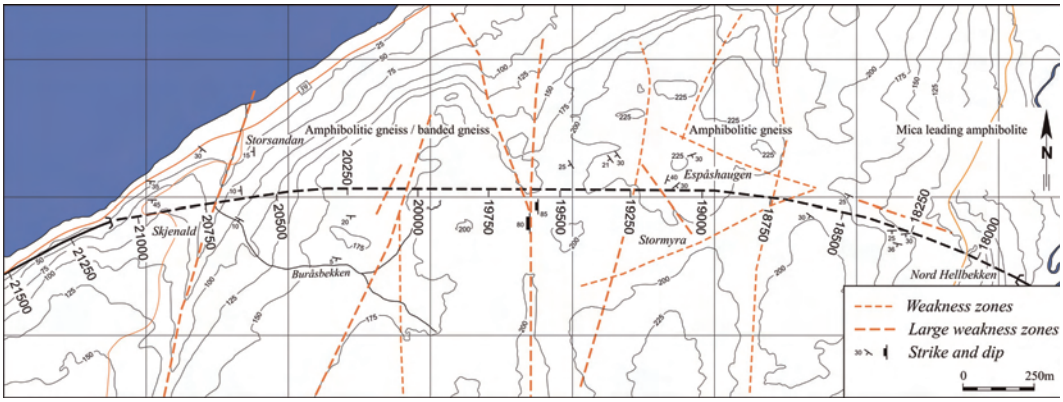

FIGURE 6.11 Simplified geological map with weakness zones for the Storsand tunnel, modified from Hagelia et al. (2001).

The rock cover varies between 5 and 160 m. The area is partly below marine limit (165 m above sea level), but the soil cover is generally less than 5 m. Greatest soil thickness is probably under the crop fields in areas close to the tunnel entrances. Above marine limit (165 m above sea level), the rock surface is hardly exposed, and the surface is covered mostly with forest and peat banks. The area above the tunnel is sparsely populated, only three farms are close to the tunnel alignment.

6.7.2 Investigation results

The site investigations for the Storsand tunnel were carried out in several stages. All investigations were summarized by the Norwegian Public Road Administration as a basis for

the tender documents (Hagelia et al. 2000; Hagelia et al. 2001). In addition, some extra investigations were carried out by the Geological Survey of Norway through the R & D project "Tunnels for the citizen" (Dalsegg et al. 2004). A brief summary of the investigations carried out are given in Table 6.11.

TABLE 6. 11 Investigations carried out for the Storsand tunnel.

Investigation method.	Investigation results with comments.
Preliminary studies (literature) and detailed field mapping.	Descriptions of rock types, orientation of joint sets and major weakness zones / faults.
Geotechnical investigations of soil thickness and rock cover at Storsandbekken, around Station No. 20.710-20.760.	A weakness zone crosses the tunnel at an angle of 70 degrees at Station No. 20.725. A soil filled ravine was registered, with minimum rock cover of 5.5 m.
1 profile (2000 m) with 2D resistivity measurements.	General resistivity level 2000-8000. 5 low resistivity zones (<2000 ohmm) registered. 3 zones coincident with weakness zones mapped in the field, one at Station No. 18.800 was not registered before. One long section with low resistivity (500-2000 ohmm) was registered between Station No. 19.600 and 20.080.
Borehole logging and hydraulic test pumping of one borehole.	Borehole located at Station No. 18.680. General resistivity in the borehole is high, 10.000-20.000 ohmm, with local zones down to 100-200 ohmm (leading minerals/fractured zones). No distinct water-bearing zones. Well capacity around 0.5 m^3/hour.
Refraction seismics, 2 profiles. 1 profile (92 m) 14 m South of the eastern tunnel entrance. 1 profile (110 m), Station No. 18.640-18.750.	2-5 m soil thickness, rock cover of more than 5 m a few metres into the tunnel. High velocity in the rock mass (5150 m/s). One low velocity zone (3500 m/s), around Station No. 18.700-18.710. Outside this zone velocity of 5150 and 5400 m/s.

6.7.3 Geological conditions and water leakage encountered during construction

The rock mass quality varied between poor and good, i.e. Q-values between 1 and 20. A few zones with fractured and crushed rock mass were encountered, and in some weakness zones 5 to 10 cm clay filling was registered. The fractures usually had no filling, but in the highly fractured zones thin filling of chlorite and/or clay was common. No major stability problems were experienced.

Because of the contract form (PPP), no inflow criteria were defined by the owner, but the contractor, together with their engineering geological consultants, evaluated the precipitation areas and sensitivity of the area concerning groundwater drainage, and based on this divided the tunnel into sections with guiding inflow criteria of 10 or 20 l/min per 100 m. Most of the tunnel has guiding inflow criteria of 20 l/min per 100 m, but sections below bogs and some weakness zones had guiding inflow criteria of 10 l/min per 100 m. In

addition, a program for follow up of groundwater level in boreholes in bedrock and inspection of the groundwater level in bogs and lakes was initiated.

During tunnelling, highest ground water inflow was encountered between Station No. 18.850 and 18.960 and post-excavation grouting was sporadically carried out between section 18.728 and 19.135. One bog area and a small stream showed a lowering of the groundwater level; as a result a farmer got a new water well to supply his animals with water during dry summer months. Figure 6.12 shows a longitudinal profile of the Storsand tunnel with weakness zones and sections with moderate water inflow in the tunnel.

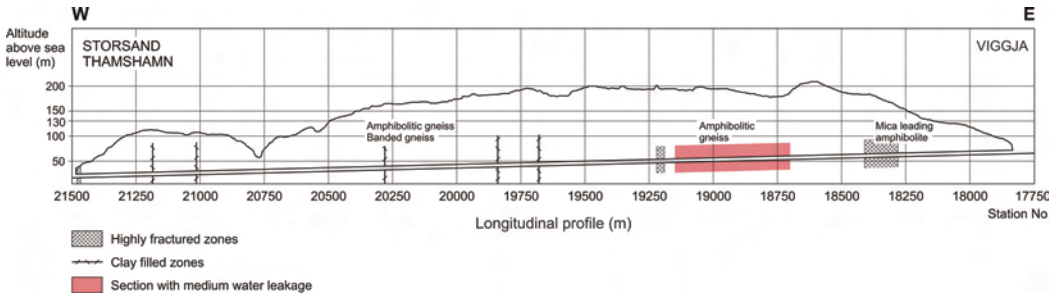

FIGURE 6.12 Longitudinal profile of the Storsand tunnel, modified from Hagelia et al. (2001).

Probedrilling was carried out sporadically. One probedrilling round consisted of 2 to 5 holes of 24 to 30 m length, most common was 2 holes each 27 m long. Based on water inflow from each respective probedrilling round, it was decided whether pregrouting was necessary or not. The pregrouting rounds varied from 10 to 22 holes of 18 to 24 m length. An average pregrouting round consisted of 21 holes with 21 m length. A brief description of geological conditions as mapped in the tunnel and amount of water leakage measured for probedrilling rounds are given in Table 6.12. The tunnel is divided into sections based on water leakage encountered in probedrilling rounds and water inflow measurements carried out in the tunnel.

TABLE 6. 12 Geological conditions and water leakage encountered in the Storsand tunnel.

Station No.	Rock types.	Rock mass quality	Water leakage
17.835-18.500	Mica gneiss (mica leading amphibolite), gneiss, quartz-, feldspar- and pegmatite dykes, amphibolitic gneiss.	Q-values 2.2-16.7. Between Station No. 18.280-18.410 highly fractured zone with 5-10 cm clay (almost parallel with tunnel).	Only seepage in probedrilling holes.
18.700-19.150	Amphibolitic gneiss, garnet amphibolite, quartz-, feldspar- and pegmatite dykes.	Q-values 2.8-22.5. Station No. 19.190-19.220 one clay filled (5-10 cm) joint crossed the tunnel.	Moderate water leakage, from 0 to 80 l/min for probedrilling rounds. Highest water leakage Station No. 18.850-18.960. Post-excavation grouting; Station No.18.728-19.135.
19.400-21.485	Amphibolitic gneiss, quartz-, feldspar- and pegmatite dykes, garnet amphibolite, banded gneiss, granodioritic gneiss.	Q-values 0.7-20. Jointed and clay filled zones at Station No. 19.680, 19.840, 20.280, 21.015 and 21.185; One weakness zone close to the tunnel entrance, weathered rock (clay and chlorite), rock cover 4m.	Only seepage in probedrilling holes.

CHAPTER 7

Analyses of water leakage versus geological parameters and site investigations

7.1 Introduction

In this chapter results and analyses concerning water leakage, geological parameters and site investigations for the selected tunnels are presented. The analyses are based on the hypotheses described in Section 1.3, and the main target is to check whether the hypotheses are supported or not. The degree of support is graded as; “no support”, “low to medium support” and “support”, see Chapter 8 for details regarding grading of support.

For each tunnel either a part (or parts) of the tunnel or the entire tunnel is analysed. Table 7.1 gives an overview of the parts that have been selected, and an explanation of why these have been chosen. Encountered water leakage in probedrilling holes and/or pregrouting holes before pregrouting, has been used as a basis for all analyses. Total water leakage for 25 m long sections have been calculated as described in Section 2.2. To make sure that narrow weakness zones do not “disappear” in an average Q-value it has been decided to use the minimum Q-value for every 25 m section in the following analyses.

Based on results from spreadsheet analyses, and distribution of calculated water leakage along the selected parts of the tunnels, further analyses have been carried out for sections of special interest. The sections have been selected based on criteria such as high amounts of water leakage and/or special geological features.

TABLE 7. 1 Parts of the tunnels that have been analysed in this thesis.

	Part of tunnel studied	Reasons for selection
The Romeriksporten tunnel.	Station No. 6850-8475. (1625 m).	Water leakage in pregrouting rounds were available in this section only.
The Frøya tunnel.	Station No. 3750-5650. (1900 m).	The part of the tunnel with highest water leakage (the Hitra-side).
The T-baneringen tunnel.	Station No. 400-1425 (1025 m) Data missing between Station No. 1425 and 1664.	The part of the tunnel with available data on water leakage and geological mapping.
The Lunner tunnel.	Station No. 1725-1850. Station No. 2200-3425. Station No. 3800-3950. (1500 m in total).	Most interesting parts of the tunnel regarding water leakage with available data on water inflow and Q-value (Q-value missing 250 m out of 1500 m).
The Skaugum tunnel.	Station No. 19.250-23.650. (4400 m).	Available data for water leakage and geological mapping for the entire tunnel.
The Storsand tunnel.	Station No. 17.831-21.485. with emphasis on station No. 18.850-18.960. (3654m/110 m).	The section between station No. 18.850 and 19.960 was the only section with water leakage.

An evaluation of the ability of site investigations to prognosticate water leakage has been carried out. It would be too comprehensive to look into all the details; and a limited number of zones therefore have been selected for each tunnel. Since the interpretations were done before the tunnels were excavated, only investigations carried out before or during tunnel construction are considered. The comments are given based on what would be expected interpretation in the light of today's knowledge.

In this chapter each tunnel is studied as separate case. An overall review of the results is given in Chapter 8 as introduction to the discussion.

7.2 The Romeriksporten tunnel

For the 13.8 km long Romeriksporten tunnel the section between Station No. 6850 and 8475 has been analysed. This section was chosen for two reasons; because of high water leakage, and because registered water leakage encountered in probe drilling and pregrouting holes were available from spreadsheets.

7.2.1 Water leakage versus geological parameters

The geological mapping was incomplete for 677 m out of 1625 m analysed. This means that the Q-value was not registered, but geological mapping was partly done. For these sections it therefore has been difficult to give unambiguous conclusions for Hypothesis No. 1 (Section 1.3).

A boxplot of calculated water leakage (l/min per 25 m) between Station No. 6850 and 8475 is shown in Figure 7.1. High water leakage was encountered, and varied from 0 to 5027 l/min per 25 m with 1249 l/min per 25 m as an average. Four mild outliers with water leakage between 3376 and 5027 l/min per 25 m can be seen from the boxplot.

Based on overall evaluation of the boxplot and the variation of water leakage along the tunnel (Figure 7.3), the following definitions for water leakage are used for the Romeriksporten tunnel:

Small water leakage: 0-500 l/min per 25 m
Medium water leakage: 500-1600 l/min per 25 m
High water leakage: 1600-3000 l/min per 25 m
Extremely high water leakage: 3000-5100 l/min per 25 m

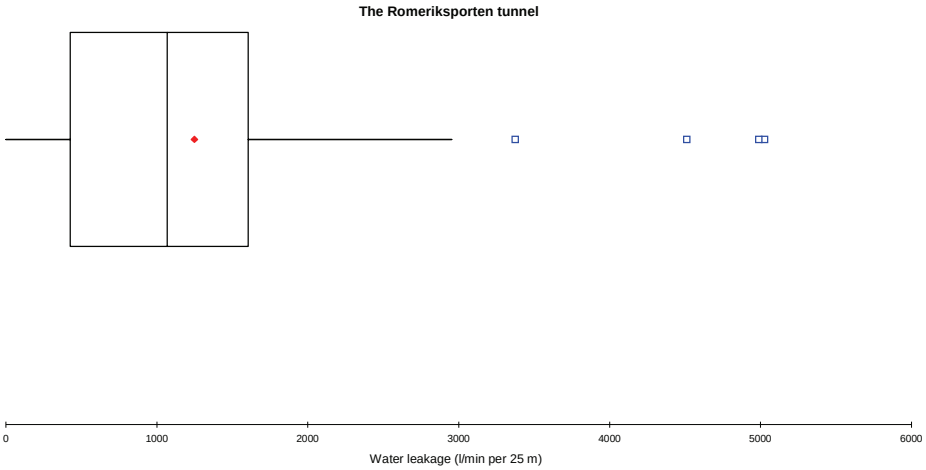

FIGURE 7.1 Boxplot of water leakage per 25 m for the Romeriksporten tunnel, Station No. 6850 - 8475.

Hypothesis No. 1; *The water leakage is lower in rock mass with Q-values lower than 0.1, than in rock mass with Q-values between 0.1 and 10.*

As a first approach a XY-plot has been made of water leakage per 25 m vs. minimum Q-value registered for each 25 m section between Station No. 6850 and 8475, see Figure 7.2. It can be seen that there is a negative correlation of -0.2, this factor indicates close to no correlation. Lack of Q-values in some sections may here be a reason for ambiguous results.

If information from the boxplot is compared with the XY-plot, it can be seen that the sections with extremely high water leakage have corresponding Q-values between 1.1 and 13.4. Therefore, it can be argued that extremely high water leakage is most likely in rock mass with Q-values between 1.0 and 15. This supports Hypothesis No. 1.

For the Romeriksporten tunnel Q-values lower than 0.1 were registered in eight sections, these 25 m long sections had water leakage between 1283 and 2927 l/min. This is higher than average water leakage, which is 1249 l/min per 25 m, and does not support Hypothesis No. 1. High variability in rock mass quality is however not easily identified

when analysing 25 m long sections. Therefore, a more detailed analysis of how the water leakage varied in and nearby sections with Q-values lower than 0.1 has been done.

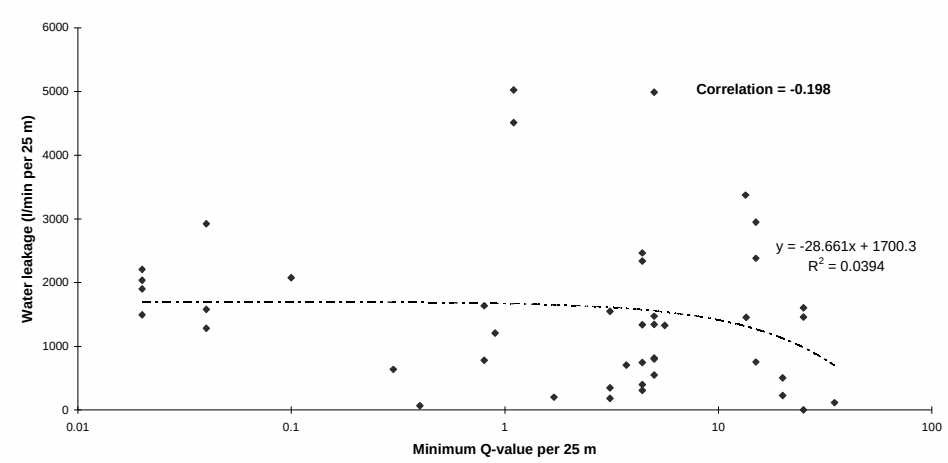

FIGURE 7.2 Water leakage versus minimum Q-value per 25 m for the Romeriksporten tunnel.

Figure 7.3 shows water leakage and minimum Q-value between Station No. 6850 and 8475. Q-values lower than 0.1 were registered between Station No. 7425-7625 and 8125-8300. Unfortunately the Q-value has not been registered in sections with low water leakage; between Station No. 7490-7525 and 8190-8250. Even though the Q-value has not been registered, geological mapping has been done, (Moen and Holmøy, 1997). The results from geological mapping between section 7490 and 7525, indicate high variability in the rock mass quality. Some areas have quite good rock mass quality and some parts have poor rock mass quality (most probably with Q-values lower than 0.1). The water inflow came near the clay filled joints, and it is not possible to say that the drop in water leakage in this 25 m long section is due to particularly low Q-value. It seems like the water sealing effect of clay was very local, and high water leakage came near and in between clay filled joints.

For the other section with low Q-values, between Station No. 8125 and 8300, the water leakage was varying a lot, and lowest water leakage was 1084 l/min per 25 m. According to the geological mapping (Moen and Holmøy, 1997) the section with lowest water leakage had good rock mass quality (approximately Q-values between 1 and 10), while the water leakage was high in the sections with Q-value lower than 0.1. Also in this section the highest water leakage was registered close to clay filled fracture zones.

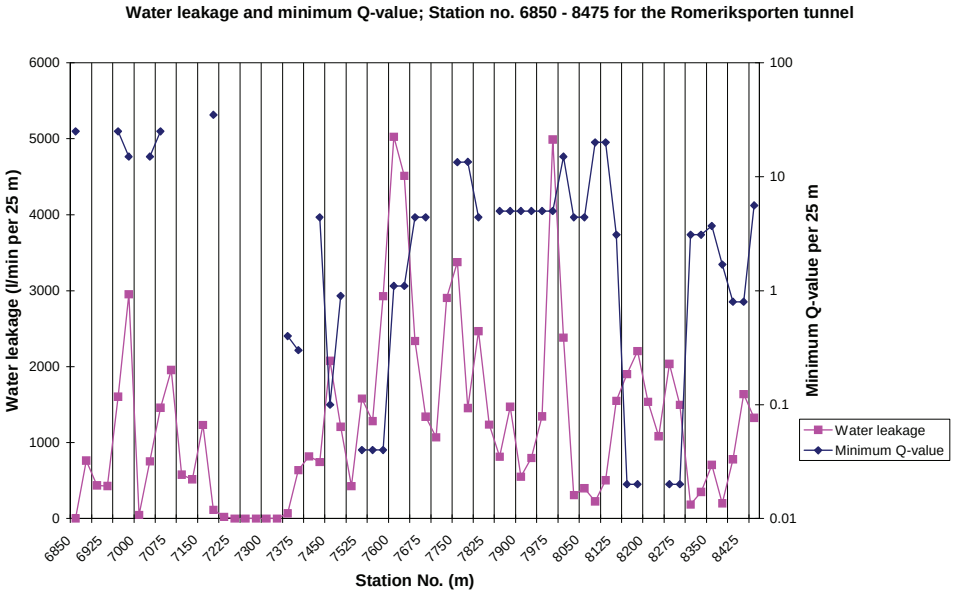

FIGURE 7.3 Diagram showing water leakage (l/min per 25 m) and minimum Q-value between Station No. 6850 and 8475.

Between Station No. 7575 and 7600 the Q-value and water leakage both increase gradually. The highest registered water leakage in the entire tunnel, 5027 l/min, was encountered between Station No. 7600 and 7625. A plausible explanation of the high water leakage can be damage zones related to several fault zones between Station No. 7525 and 7600. The Q-value between 7600 and 7650 is 1.1. Hence, Hypothesis No. 1 is partly confirmed for the Romeriksporten tunnel; the damage zones with typical Q-values between 1 and 15 gave highest water leakage.

However, the analyses do not confirm that the water leakage was decreased when the Q-value was lower than 0.1. Locally the water leakage was somewhat reduced, but for the Romeriksporten tunnel the clay filled part of the fault zones normally was less than 0.5 m thick, and highly jointed zones with thin clay filling on the joints were typical. In addition, the water came close to the clay filled joints and in good rock mass quality in between the clay filled joints.

Hypothesis No. 2; *Water-bearing joints make an angle with nearby major faults of* $45° \pm 15°$.

Figure 7.4 shows a longitudinal profile and simplified geological map for the section between Station No. 6850 and 8475. A detailed study of the sections with high and extremely high water leakage has been done. The tunnel has been divided into four sections of different length; R1, R2, R3 and R4 (see Figure 7.4). Relevant geological information for these sections is given in Table 7.2.

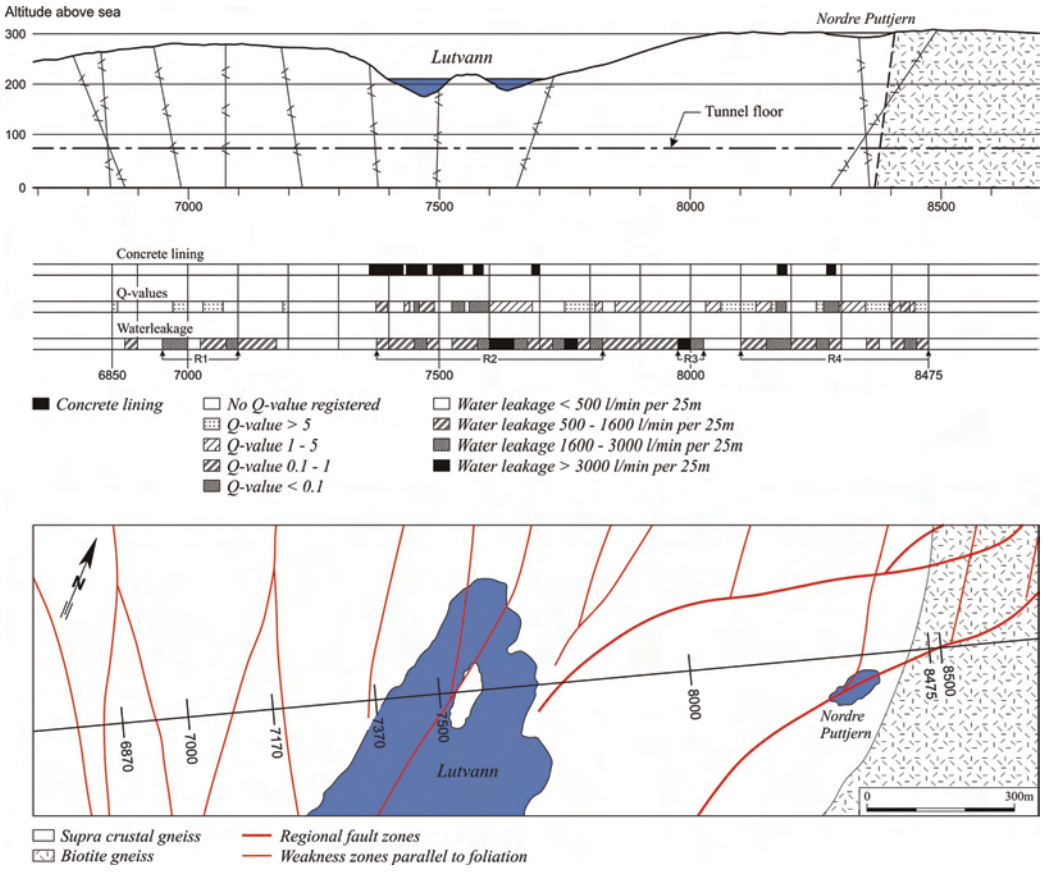

FIGURE 7.4 Longitudinal profile and engineering geological map with locations of concrete linings, Q-values and calculated water leakages. Map and profile modified from Bollingmo (1994).

TABLE 7. 2 Geological character of sections R1, R2, R3 and R4. ("JS" mean Joint Set, with No. 1 as the predominant etc.).

Station No.	Rock type / dykes.	Dominating joint sets. Direction of water-bearing joints.	Description of weakness zones / Q-value.
6950-7100. Section R1. (150 m).	Migmatitic-gneiss. Pegmatite, amphibolite with garnets and syenite porphyry dykes.	JS1: (fol.) N130-170E/60-80NE. 2 sporadic joint sets: N10-20E/20E and N30E/50-90NW. No dominating water-bearing joint set. Increased water leakage near/in pegmatite dykes.	Q-values were not registered for 80 m. In the sections where the Q-values were registered, the Q-value varied between 15 and 35. Rough and undulating joint walls. Mineral filling such as chlorite,quartz and clay was regi-stered.
7375-7825. Section R2. (450 m).	Migmatitic-, amphibolitic-, granitic-, mylonitic- and mica-gneiss. Diabase and pegmatite. Frequent variations of rock types.	JS1: (fol.) N130-170E/60-80NE. Some of the steepest were water-bearing. JS2: N70E/50N. JS3: N55E/70S. (JS3: N40E with varying dip dominated in the eastern parts). JS2 and JS3 were often registered together resulting in unstable blocks and water leakage. Water leakage in migmatite and pegmatite. Sporadic joints: N150E/20-40SW combined with foliation joints gave in some sections water leakage.	Q-values were not registered for 153 m. In the sections where the Q-values were registered, the Q-value varied between 0.04 and 13.5. Generally many weakness zones, with highly jointed rock mass/partly crushed with clay on joints. Chlorite and calcite registered on joints.
7975-8025. Section R3. (50 m).	Migmatitic gneiss. Some amphibolitic and pegmatitic dykes.	JS1: (fol.) N140-160E/60-70NE. JS2: N70E/90. Major joint (J4): N115E/70N. J4 and JS2 were water-bearing.	Migmatitic gneiss. Some amphibolitic and pegmatitic dykes. 2-5 cm clay on joints. Black coating on joints.
8100-8475. Section R4. (375 m).	Migmatitic-, amphibolitic-pegmatitic- and mica gneiss. Pegmatite and amphibolite dykes. Frequent variations of rock types.	JS1: (fol.) N-S/70-90E. Some with dip towards West. JS2: Flat joint set, often small dip towards south. JS3: N20-40E/60-90S. (JS3: N30E/60-75N, dominated in the eastern parts). JS3 and foliation joints were water-bearing.	Q-values were not registered for 60m. The Q-values varied from 0.02 to 20. Many weakness zones, clay filled joints. Some clay filled zones (0.2-0.7m thick). Clay, chlorite and mica coating registered on joints.

The analysis of the four sections shows that the foliation joints often were water-bearing, particularly when combined with other joint sets. In addition to the foliation joints, two joint sets with small angle to the tunnel alignment were dominating in the sections with high water leakage. These are shown in Figure 7.5. Joint set 2 (JS2) is oriented N70E/50-90N and joint set 3 (JS3) is oriented N20-55E/60-90SE. In the eastern part close to Station No. 8475, JS3 has dip towards N. A major water-bearing joint in section R3 (J4) is also drawn in Figure 7.5.

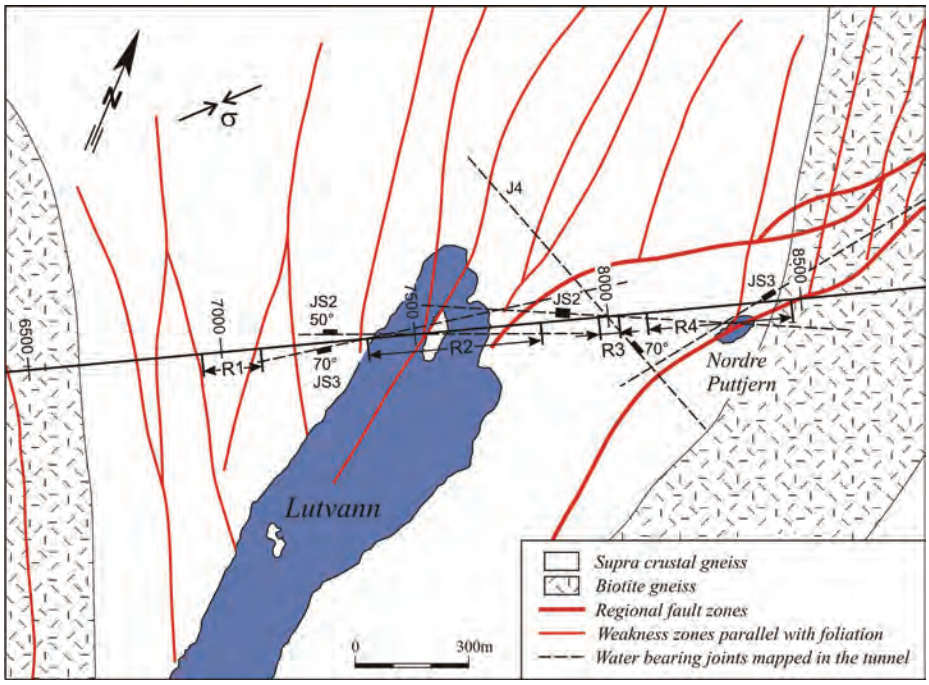

FIGURE 7.5 Details from engineering geological map, modified from Bollingmo (1994).

In this area two regional faults oriented NE-SW are dominating; one strikes through Lutvann lake and the other through the small lake Nordre Puttjern, see Figure 7.5. The geological mapping carried out in the tunnel showed that several foliation joints together with parallel weakness zones were water-bearing. It can be seen from Figure 7.5 that the angle between the weakness zones (and foliation joints) and the regional fault zones striking through Lutvann and Puttjern is approximately 45°. This is in accordance with Hypothesis No. 2.

Joint set 2 strikes N70E and makes an angle of approximately 30° to the regional faults, while joint set 3 strikes N20-55E and is almost parallel with the regional faults. Both joint sets are water-bearing, but according to Hypothesis No. 2, joint set 2 should be the most

water-bearing. The orientation of the major joint in section R3 (J4) does not agree with Hypothesis No. 2, but the analyses still support Hypothesis No. 2 since the most water-bearing joints and weakness zones make an angle with nearby faults of $45° \pm 15°$.

Hypothesis No. 3; *water-bearing discontinuities are sub-parallel with the major principal stress.*

The orientation of major principal stress in the area East of Oslo is likely to be NE-SW to NNE-SSW, (Myrvang, 2008). The regional faults and joint set 2 and 3 are sub-parallel with the assumed major principal stress (N20-70E/with varying dip). Hence, this supports Hypothesis No. 3.

Another theory is that low or even tensional stress in E-W direction during Permian age, probably leaded to open joints in N-S direction. This corresponds well with water-bearing foliation joints and weakness zones with strike close to N-S.

Hypothesis No. 4; *Water leakage decreases with increasing rock cover.*

The rock cover in the area varies from 90 to 229 m. Figure 7.6 shows a XY-plot of water leakage (l/min per 25 m) vs. rock cover (m).

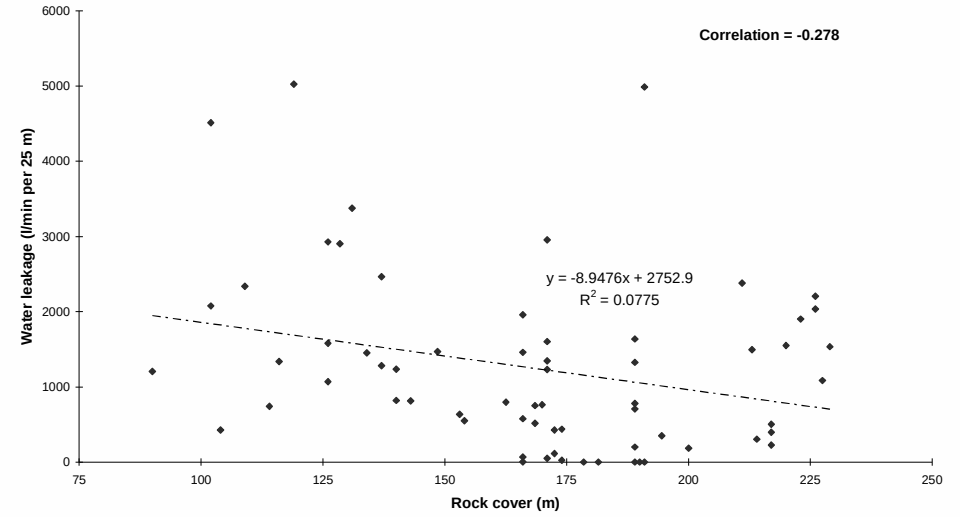

FIGURE 7.6 Water leakage (l/min per 25 m) versus rock cover (m) between Station No. 6850 and 8475 for the Romeriksporten tunnel.

The XY-plot gives a correlation of -0.278, indicating that water leakage decreases when tunnel depth is increasing. Even though the correlation is relatively poor, it gives low to medium support to Hypothesis No. 4.

Hypothesis No. 5; *Great thickness of permeable soil or a lake/sea above a tunnel gives high water leakage.*

For the Romeriksporten tunnel between Station No. 6850 and 8475 the soil cover above the tunnel is sparse, with exposed bedrock in sections. In the northern part of Lutvann lake a thin cover of till was registered. Peat and bog was registered in small areas just North and South of the tunnel alignment. Since no thick layer of soil was registered above the tunnel alignment, it is most relevant to analyse the possible effects that a lake above the tunnel may have. The lakes Lutvann and Nordre Puttjern are located in depressions in connection with fault zones, and are therefore potential recharge zones.

The influence of a lake is assumed to decrease with increasing distance, and horizontal distances of more than approximately 200 m therefore are not considered in this analysis. When the tunnel is just below a lake the horizontal distance is zero. The horizontal distance to lake versus water leakage (l/min per 25 m) is shown in Figure 7.7. A correlation of -0.35 indicates that the water leakage decreases when the horizontal distance to a lake increases. This means that it is more likely to get high water leakage just below or close to a lake. Hence, the analysis supports Hypothesis No. 5.

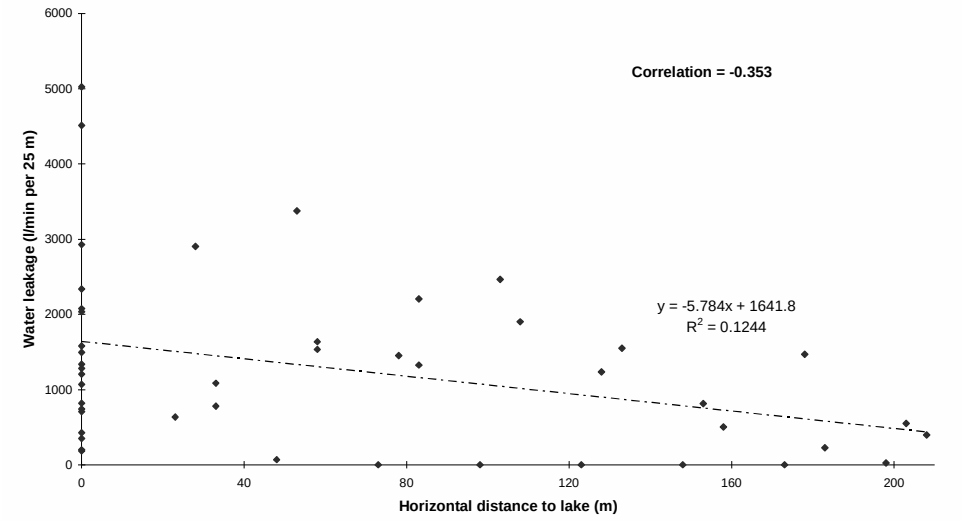

FIGURE 7.7 Water leakage versus horizontal distance to lake for the Romeriksporten tunnel (Station No. 6850 and 8475).

Hypothesis No. 6; *Igneous rocks give higher water leakage than other rock types.*

At the Romeriksporten tunnel between Station No. 6850 and 8475 various gneiss types like mica-, migmatitic-, amphibolitic-, mylonitic- and pegmatitic gneiss are dominating. No large body of igneous rocks exists, but igneous dykes consisting of diabase, pegmatite and syenite porphyry occur in the tunnel, pegmatite was present in all the 25 m sections with extremely high water leakage. Often the water leakage came locally in the transition between pegmatite and jointed gneiss. Hence, Hypothesis No. 6 is supported.

Hypothesis No. 7; *Major rock type boundaries give high water leakage.*

For the section between Station No. 6850 and 8475 of the Romeriksporten tunnel no increased water leakage related to the boundaries between different types of gneiss was registered. But as mentioned above, examples of water leakage in the transition between dykes and gneiss were registered. This supports Hypothesis No. 7.

Hypothesis No. 8; *Wide weakness zones give higher relative water leakage (inflow per 25 m) than narrow weakness zones.*

Weakness zones with Q-value lower than 1.0 were studied. The section between Station No. 7361 and 7600 (below Lutvann lake) was dominated by clay filled and highly jointed rock mass. Particularly between Station No. 7525 and 7580 the rock mass quality was extremely poor. The joints were partly clay filled and partly filled with crushed rock giving water inflow in channels and difficult conditions for pregrouting. The weakness zones had no sharp start or ending, and all had major clay filled joints parallel with the foliation. Nevertheless, highest water leakage was not encountered in the cores of the weakness zones but in the damage zone, with Q-value higher than 1.0.

Additional three weakness zones with Q-value lower than 1.0 were registered in the eastern part between Station No. 8170 and 8440. All the weakness zones were dominated by clay filled major joints, typically with 2-5 cm clay in the core and up to 1 m total width. The major joints strike approximately N-S parallel with the foliation. For all three weakness zones high water leakage was encountered. The amount of water leakage encountered varied from 1638 to 2206 l/min per 25 m, and the weakness zones were all approximately 20 m wide. Based on this analysis it seems like the width of the weakness zones has no importance for the relative water leakage. Hence, this does not support hypohtesis No. 8.

7.2.2 Water leakage versus site investigations

In the geological pre-construction report, no prognosis was made for amount of water leakage or where to expect water leakage (Bollingmo, 1994). Only general comments regarding bedrock types and weakness zones were given. In the contract (NSB Gardermoen A/S, 1994) four sections where systematic pregrouting was to be expected were described; Bryn (Station No. 3800-4050), Godlia (Station No. 4800-5050), Ellingsrud (Station No. 9700-10.800), Langvannet (12.350-12.500) and Strømmen (Station No. 15.200-15.500). No systematic pregrouting was described between Station No. 6870 and 8475. However, a need for high amounts of grouting cement was foreseen. A total of 1.160.000 kg of standard grouting cement (Rapid cement) was described in the contract. The resulting amount for the entire tunnel was 5.408.896 kg, i.e. 4.7 times as much as predicted. In sections below the lakes Lutvann and Puttjern, challenging conditions with high water pressure (12-13 bar), combined with difficult pregrouting conditions, resulted in particularly high pregrouting costs (around 2000 kg grouting cement per m tunnel was used during excavation).

In Table 6.1 the investigations carried out before and during excavation are described, and brief comments on the results are given. Pre-construction investigations for the section between Station No. 6870 and 8475 were desk studies, including studies of aerial photographs and geological field mapping. After excavation started, refraction seismic was done in July 1996 (Paulsson, 1996). The purpose of the refraction seismic was to make a prognosis for rock support for the remaining section of the tunnel. When the refraction seismic was carried out, approximately 2.0 km was left to excavate below the Lutvann and Puttjern area. Two profiles were carried out, 225 and 325 m long, see Figure 7.8.

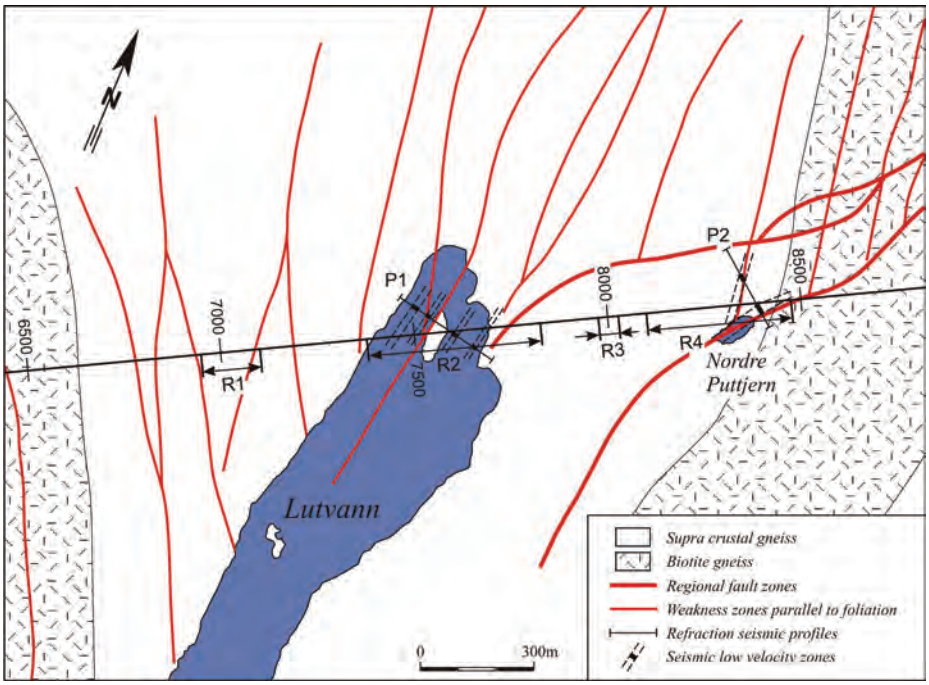

FIGURE 7.8 Location of refraction seismic profiles with registered low seismic velocity zones.

The pre-construction investigations revealed several weakness zones between Station No. 6870 and 8475, as drawn in the geological map, see Figure 7.8. In the geological report (Bollingmo, 1994) both the Lutvann area and the area just northeast of Nordre Puttjern (around Station No. 8500) were described as areas with weakness zones. In the Lutvann area several weakness zones were expected, and one weakness zone crossing the tunnel alignment at around Station No. 8500 was described as a crushed zone of 5 to 10 m width. The other weakness zones were described as highly jointed rock mass, and some of the zones parallel with the foliation were not expected to give rock stability problems. Weakness zones registered in the tunnel during excavation were located almost as expected, but width and rock mass quality were worse than expected. In the geological report water leakage was not mentioned as a potential problem in the Puttjern and Lutvann area. Based on today's knowledge and focus on water leakage it seems rather strange that no evaluation of expected water leakage was made.

The refraction seimic revealed four low velocity zones below Lutvann (three with 2000 m/s and one with 2700 m/s) and two low velocity zones (both 3500 m/s) just North and East of Nordre Puttjern, see Figure 7.8. For Lutvann the low velocity zones correspond

well with weakness zones registered in the tunnel. In addition, most of the section below Lutvann had high water leakage. Particularly below the eastern part and just East of Lutvann high water leakages were encountered. The two low velocity zones near Nordre Puttjern correspond well with the regional fault zone striking NNE-SSW, and a weakness zone oriented N-S which merge into the fault zone below Puttjern, see Figure 7.8. In the tunnel poor rock mass quality and high water leakage were encountered between Station No. 8265 and 8300 close to Puttjern. This fits well with results from refraction seismic. The major fault zone was expected to have a dip towards NW. Also West of Nordre Puttjern (Station No. 8100-8265) poor rock mass quality and high water leakages were encountered, but the refraction seismic did not cover this area.

In Table 7.3 a brief summary is made on the ability of the different investigation methods to prognosticate the encountered water leakage.

TABLE 7. 3 Ability of site investigations to prognosticate water leakage for section R1, R2, R3 and R4 of the Romeriksporten tunnel.

Station No.	Desk studies and geological mapping (prior to excavation).	Refraction seismic (during excavation).
Section R1. (6950-7100).	Two weakness zones parallel with foliation indicated. Water leakage not prognosticated.	Not carried out for this section.
Section R2. (7375-7825).	Several weakness zones and highly jointed rock mass including one regional fault passing below Lutvann.Water leakage could be expected, but not prognosticated.	Low velocity zones measured, which correspond well with high and extremely high water leakage.
Section R3. (7975-8025).	No weakness zones described in this section. Water leakage not prognosticated.	Not carried out for this section.
Section R4. (8100-8475).	One regional fault and one weakness zone identified, both running through Puttjern. Water leakage could be expected, but not prognosticated.	Low velocity zones measured, which correspond well with high water leakage.

For section R2 and R4 desk studies, geological mapping and refraction seismic detected fault zones and weakness zones below Lutvann and Nordre Puttjern. Even though the results from the investigations gave indications of potential water leakage, no prognoses for water leakage were made. Based on knowledge gained in this thesis, factors such as joint orientation and major principal stress (Hypothesis No. 2) clearly indicate probable water leakage in section R2 and R4.

As mentioned in Section 6.2.2, additional investigations were carried out in the Lutvann and Puttjern area after completion of the tunnel. However, in this thesis only investigations carried out before and during construction are considered relevant.

7.3 The Frøya tunnel

For the 5.3 km long Frøya subsea tunnel the subsea section between Station No. 3750 and 5650 has been analysed. This section was chosen because most of the water leakage in the Frøya tunnel was encountered on this side (the Hitra side) of the tunnel.

7.3.1 Water leakage versus geological parameters

The geological mapping data are incomplete for 347 m out of the 1900 m analysed (Q-value not registered, but geological mapping carried out some places).

A boxplot of calculated water leakage (l/min per 25 m) between Station No. 3750 and 5650 is shown in Figure 7.9. High water leakage was encountered, varying from 0 to 2734 l/min per 25 m with 160 l/min per 25 m as mean value. Four mild outliers with water leakage around 300 l/min per 25 m and 7 extreme outliers with water leakage between 461 and 2734 l/min per 25 m can be seen from the boxplot. 50% of the 25 m long sections had water leakage between 5 and 111 l/min, and the median value is as low as 27 l/min. The water leakage distribution is highly skewed to the right.

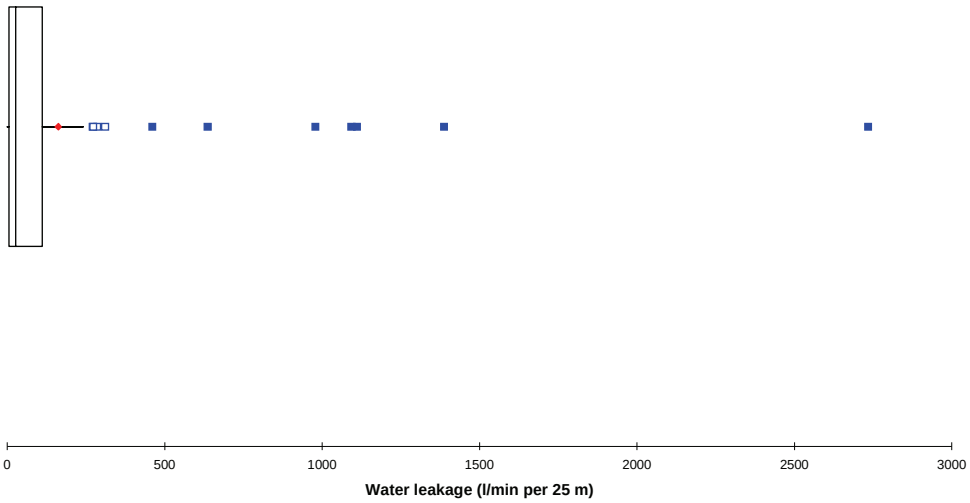

FIGURE 7.9 Boxplot of water leakage per 25 m for the Frøya tunnel, Station No. 3750-5650.

Based on overall evaluation of the boxplot and the variation of water leakage along the tunnel (Figure 7.11), the following definitions for water leakage are used for the Frøya tunnel:

Small water leakage: 0-50 l/min per 25 m

Medium water leakage: 50-200 l/min per 25 m

High water leakage: 200-500 l/min per 25 m

Extremely high water leakage: 500-3000 l/min per 25 m

Hypothesis No. 1; *The water leakage is lower in rock mass with Q-values lower than 0.1, than in rock mass with Q-values between 0.1 and 10.*

As a first approach a XY-plot has been made of water leakage per 25 m vs. minimum Q-value registered for each 25 m section between Station No. 3750 and 5650, see Figure 7.10. A correlation of 0.031 indicates no linear correlation between minimum Q-value and water leakage. It can also be seen that for the sections with minimum Q-value lower than 0.1 all had less than 286 l/min water leakage; 13 out of 16 sections had small or medium water leakage.

Figure 7.11 shows how water leakage and minimum Q-values vary between Station No. 3750 and 5650. Q-values lower than 0.1 were registered in five weakness zones, and in three of these exceptionally poor rock mass quality with Q-values lower than 0.01 were registered. Frequent variations in rock mass quality and water leakage over short distances is not easily identified when analysing 25 m long sections. Therefore, to further check if Hypothesis No. 1 is supported, a more detailed analysis of the geological mapping in the tunnel has been carried out.

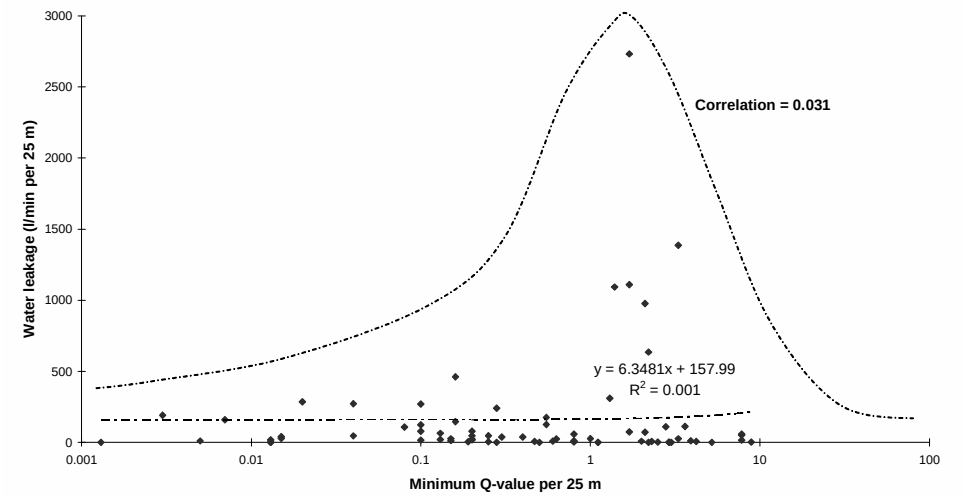

FIGURE 7.10 Water leakage versus minimum Q-value per 25 m between Station No. 3750 and 5650 for the Frøya tunnel.

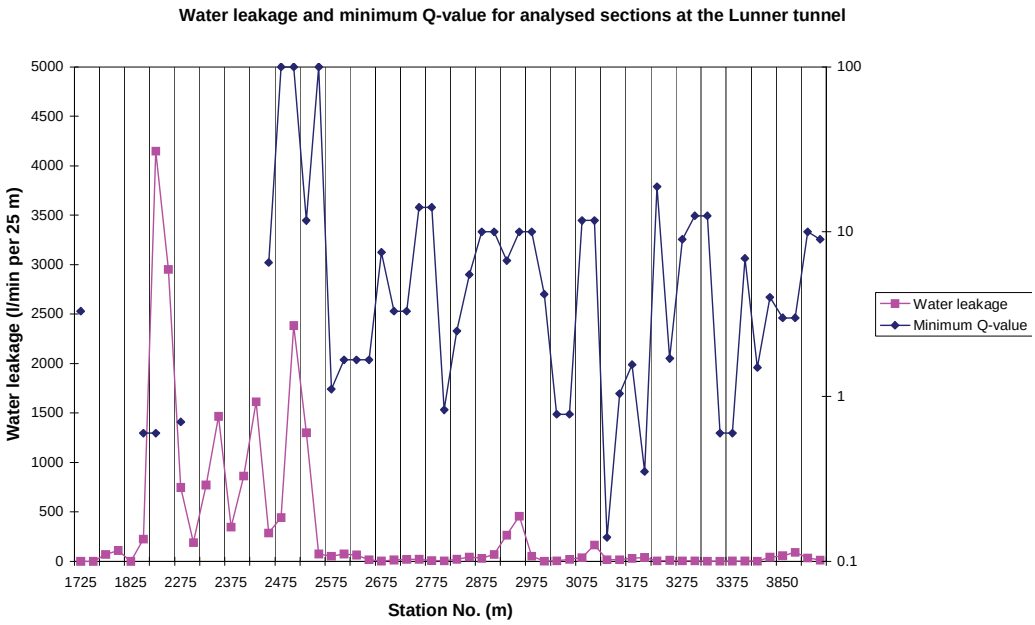

FIGURE 7.11 Diagram showing water leakage (l/min per 25 m) and minimum Q-value between Station No. 3750 and 5650.

The geological mapping shows that almost no water leakage was registered in the clay rich core of the weakness zones. The water leakage typically came in highly jointed rock mass 0-60 m away from the fault zone. Figure 7.12 shows an example of how the water leakage appeared near a weakness zone after pregrouting and excavation between Station No. 4070 and 4150.

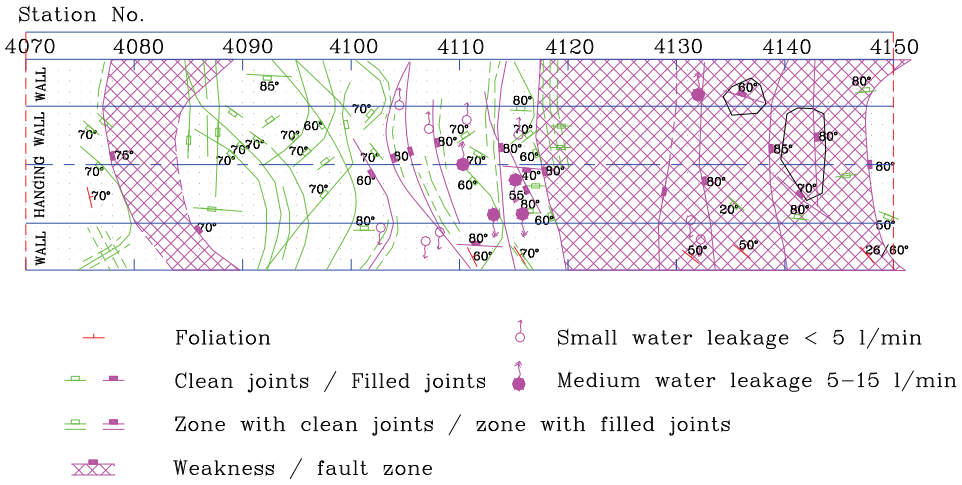

FIGURE 7.12 Geological mapping and point leakages (after pregrouting) as registered in a section of the Frøya tunnel.

Highest water leakage encountered in the Frøya tunnel came between Station No. 4550 and 4575. The extremely high water leakage can be related to the regional Tarva fault intersecting the tunnel between Station No. 4435 and 4510. The Q-value between 4550 and 4575 varied between 1.7 and 2.2 (Q-value here was only partly registered).

If information from the boxplot is compared with the XY-plot, it can be seen that the 6 highest extreme outliers with water leakage over 500 l/min per 25 m have Q-values between 1.4 and 3.3. The estimated envelope curve in Figure 7.10 further emphasizes that highest water leakage was encountered in sections with Q-values between 1.0 and 5.0. For Q-values lower than 0.1 or higher than 5.0 small to medium water leakage was encountered. This supports Hypothesis No. 1.

Hypothesis No. 2; *water-bearing joints make an angle with nearby major faults of* $45° \pm 15°$.

A detailed study of the sections with high and extremely high water leakage with nearby weakness zones has been done. The tunnel has been divided into four sections of different length; F1, F2, F3 and F4. Relevant geological information for these sections is given in Table 7.4.

TABLE 7. 4 Geological character of sections F1, F2, F3 and F4. ("JS" mean Joint Set, with No. 1 as the predominant etc.).

Station No.	Rock type / dykes.	Dominating joint sets. Direction of water-bearing joints.	Description of weakness zones / Q-value.
4050-4150. Section F1. (100 m).	Granitic and mica gneiss.	JS1: (fol.) N50-70E/70N. JS2: N40E/70SE. JS3: N120E/70SW. JS4: N0E/80-90 E/W. Weakness zone: N80E/80N. Foliation joints seems to be water-bearing.	4070-4118: Q-values varies between 0.1 and 2.8. Highly jointed with some clay filled joints, 1-5 cm clay. 4118-4150: Q-values between 0.003 and 0.3. Highly jointed and partly disintegrated, 5-10 cm clay on joints.
4400-4650. Section F2. (250 m). Tarva fault.	Marble breccia, red granitic gneiss, banded gneiss, amphibolite.	JS1: (fol.) N30-50E/50-70N. JS2: N40E/70SE. JS3: N155E/80-90SW. Sporadic joints. Weakness zone (4431-4510) N65E/50-70N. JS1 (fol.) and JS3 seem to be water-bearing.	4431-4510: Q-values vary between 0.007 and 2.2. Highly jointed, some sections with clay filled joints, 10 cm. 4510-4660: Q-values between 0.8 and 5.9. 0-5 cm clay on joints. Rough/irregular and planar joints.
4925-5100. Section F3. (175 m).	Banded gneiss.	JS1: (fol.) N35E/50-70N. JS2: N85-100E/70N. JS3: N130E/90. JS4: N50-70E/20-50S. Two narrow weakness zones one parallel with JS2 and one parallel with JS3. JS1 (fol.), JS2 and one major joint; N10E/90 seem to be water-bearing.	5000-5040: Q-values vary between 0.1 and 3.3. Highly jointed, 2-8 cm clay on joints. In the rest of section F3 Q-values varied between 0.1 and 6.7. 0-5 cm clay on joints.
5425-5650. Section F4. (225 m).	Weathered gneiss, partially altered to clay.	JS1: (fol.) N50E/40-60NW. JS2: N25E/60-80NE. JS3: N110-135E/80-90S. Sporadic joints with 10-30 ° dip. JS1 (fol.) or JS2 seem to be water-bearing.	5448-5590: Q-values 0,1-0,8. Highly jointed, 0-20 cm clay on joints. 5590-5660: Extremely poor to very poor rock mass quality, Q 0.01-0.8. Weathered gneiss partly altered to clay, 5-25 cm clay.

Figure 7.13 gives an overview of the section between Station No. 4050 and 5650. The locations of section F1, F2, F3 and F4 are shown in Figure 7.13.

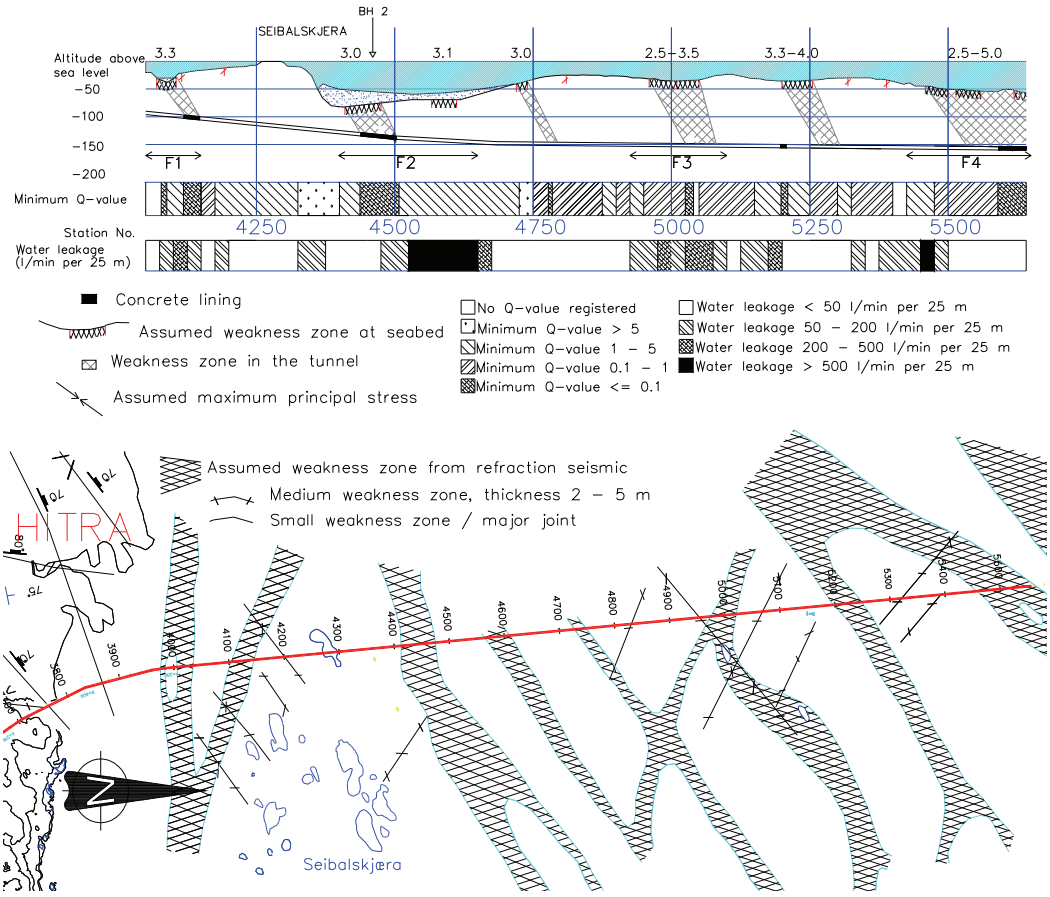

FIGURE 7.13 Longitudinal profile and engineering geological map with location of concrete linings, Q-values, calculated water leakages, registered low seismic velocity zones, etc. Modified from Lien et al., (2000).

Sections F1, F2 and F4 include three major weakness zones. The weakness zones are orientated with strike N50-80E and with varying dip. The major regional Tarva fault in section F2 strikes N65E. According to Table 7.4 the foliation joints are water-bearing and parallel or orientated with small angle to the Tarva fault. Hence, the water-bearing foliation joints do not strengthen Hypothesis No. 2. A major joint in section F3 and joint set 2 in section F4 strike N10-25E, making an angle of 45° ±15° to the Tarva fault. Furthermore, joint set 2 in section F3 with strike N85-100E also makes an angle of 45° ±15° to the Tarva fault. Thus, all the joint sets except for the foliation joints and joint set 3 in section F2 and F3 support Hypothesis No. 2. Since the analysis gave ambiguous

results, and the foliation joints which are the most water-bearing joint orientation did not support Hypothesis No. 2, this analysis gives low to medium support to Hypothesis No. 2.

Hypothesis No. 3; *water-bearing discontinuities are sub-parallel with the major principal stress.*

No stress measurements have been done in the region of the Frøya tunnel, but according to Fejerskov (1993) and Roberts and Myrvang (2004), the major principal stress is expected to be oriented NW-SE in coastal areas of central Norway. The estimation is based on borehole breakout and earthquake focal mechanism solution data acquired offshore (Roberts and Myrvang, 2004). Most likely it is related to a ridge-push force arising from divergent spreading along the active axial ridge of the North Atlantic Ocean. On the other hand, stress measurements done in Støren and Orkanger (Roberts and Myrvang, 2004; Myrvang, 1991) gave major principal stresses close to NE-SW. Accordingly, the major principal stress direction is uncertain, but after discussions with Prof. Myrvang (2008), the major principal stress in the following analysis is assumed to be oriented NE/SW.

In the Frøya tunnel two distinct joint sets were water-bearing: JS1 and JS3. JS1 is parallel the foliation (N50-70E/70N) and is the most water-bearing. The major principal stress oriented NE-SW correspond well with high water leakages encountered in joints and weakness zones which are sub-parallel with the foliation. On the other hand, joint set 3 striking N120-155E is also present in the sections with high water leakage, particularly in section F2. This is parallel with the assumed major principal stress orientation NW-SE (Fejerskov, 1993; Roberts and Myrvang, 2004). Consequently, both of the water-bearing joint sets can be explained by one of the possible stress orientations. But since the most distinct water-bearing joint set (JS1) is sub-parallel with the most likely major principal stress orientation, Hypothesis No. 3 is supported.

Hypothesis No. 4; *Water leakage decreases with increasing rock cover.*

Between Station No. 3750 and 5650 the Frøya tunnel is below the sea level, and the rock cover varies from 42.6 to 125.9 m, with the lowest rock cover at Station No. 4000. The XY-plot in Figure 7.14 shows water leakage (l/min per 25 m) versus rock cover.

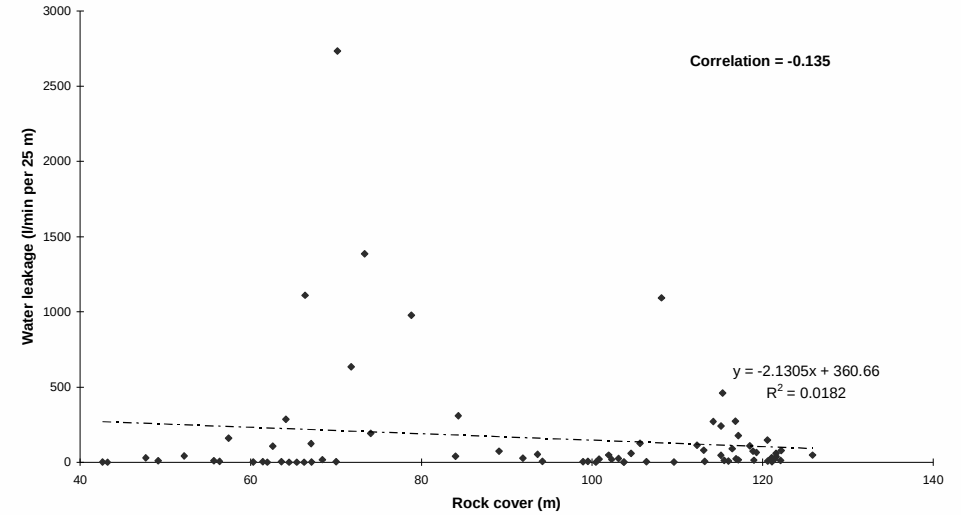

FIGURE 7.14 Water leakage (l/min per 25 m) versus rock cover (m) between Station No. 3750 and 5650 for the Frøya tunnel.

The XY-plot gives a correlation of -0.135, indicating no linear correlation between water leakage and rock cover for the Frøya tunnel, and does not support Hypothesis No. 4.

Hypothesis No. 5; *Great thickness of permeable soil or a lake/sea above a tunnel gives high water leakage.*

For the Frøya subsea tunnel analysis of the latter is irrelavant, since the the entire analysed part of the tunnel is below the sea.

The soil thickness on the seabed varies from 0 to 32 m, and greatest soil thickness was registered above the Tarva fault (section F2). Figure 7.15 shows a XY-plot of water leakage (l/min per 25 m) vs. soil thickness. A correlation of 0.232 indicates that water leakage increases when the soil thickness increases. However, it can be seen that highest water leakage was registered for soil thicknesses between 10 and 15 m. For the Frøya tunnel, medium soil thickness of 10 to 15 m is located just above damage zones nearby fault zones. Soil thickness higher than 15 m give almost no or medium water leakage. This actually supports Hypothesis No. 1, and not Hypothesis No. 5. Apparently, there exists no clear connection between soil thickness and water inflow for the Frøya tunnel.

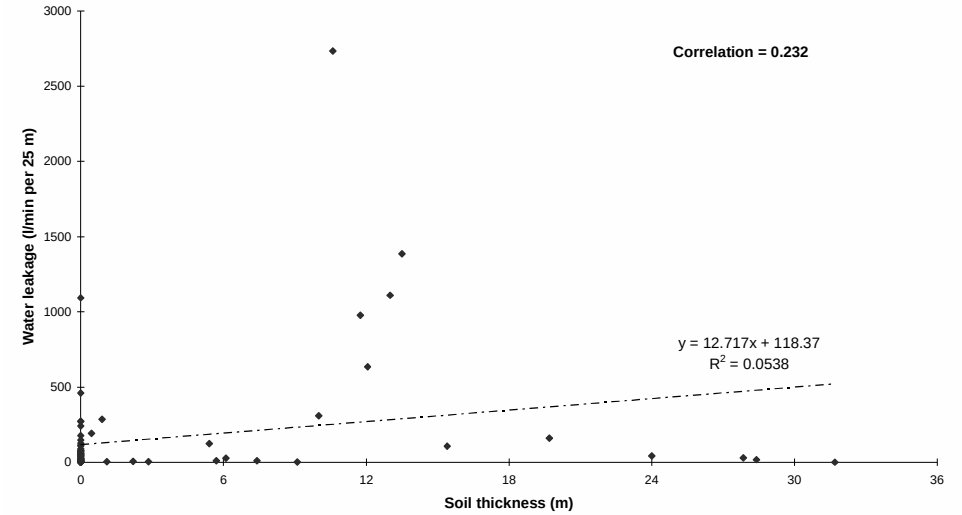

FIGURE 7.15 Soil thickness versus water leakage (l/min per 25 m) between Station No. 3750 and 5650 for the Frøya tunnel.

Hypothesis No. 6; *Igneous rocks give higher water leakage than other rock types.*

Between Station No. 3750 and 5650 in the Frøya tunnel, various gneiss types and marble were registered. Mica-, granitic- and banded gneiss were dominating. No body of igneous rock was registered, only pegmatite dykes. In a few locations the water leakage was registered locally in the transition between pegmatite and jointed gneiss. But only one 25 m section with pegmatite had extremely high water leakage, the rest had only small water leakage. Consequently, Hypothesis No. 6 is not supported by this analysis.

Another interesting question is whether there is higher water leakage in the sections with marble compared to sections with gneiss. Marble and marble breccia combined with gneiss were registered between Station No. 4190 and 4510. Figure 7.16 shows a histogram with number of 25 m sections for different rock types versus ranges of water leakage. As can be seen there was not particularly high water leakage in the sections with marble or marble breccia.

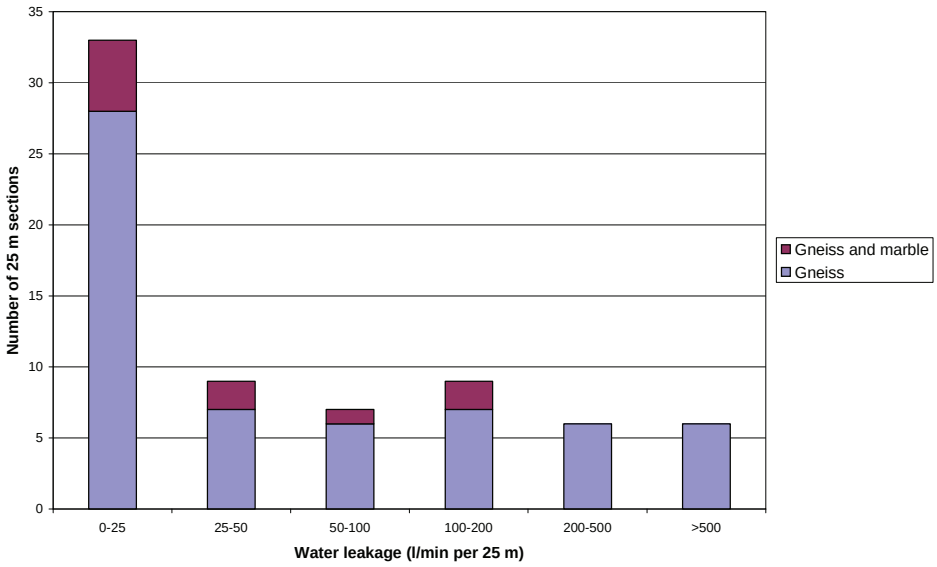

FIGURE 7.16 Distribution of ranges of water leakage (l/min per 25 m) for different rock types in the Frøya tunnel.

Hypothesis No. 7; *Major rock type boundaries give high water leakage.*

For the section between Station No. 3750 and 5650 various gneisses and marble were the only rock types registered. The marble ended at Station No. 4510 and on the following two 25 m sections water leakage of 1002 and 2734 l/min were registered. The extremely high water leakage is not necessarily due to the change of rock type, it is more likely related to the Tarva fault between Station No. 4440 and 4510. The breccia and fault zone ended both at Station No. 4510. Since this is only one single case and another plausible explanation exists, the analysis gives low to medium support to Hypothesis No. 7.

Hypothesis No. 8; *Wide weakness zones give higher relative water leakage (inflow per 25 m) than narrow weakness zones.*

Four weakness zones with high water leakage in the surrounding rock mass in the sections F1, F2, F3 and F4 have been studied. The weakness zones in section F2 (the Tarve fault) and F4 were widest, both were 72 m with Q-value lower than 0.1. Extremely high water leakage was registered in one 25 m long section in connection to section F4. For the Tarva fault in section F2, extremely high water leakage was registered for 125 m. As a result, the two longest weakness zones in the Frøya tunnel gave highest water leakage. For the Frøya

tunnel large weakness zones gave higher water leakage per 25 m than narrow weakness zones. This supports Hypothesis No. 8.

7.3.2 Water leakage versus site investigations

The Frøya tunnel was thouroghly investigated before construction started. In Table 6.3 the respective investigations are described with brief comments on the results. In addition to desk studies, and geological mapping, extensive seismic inestigation and core drilling from land, small islands and drilling ship were carried out, see Figure 6.4. Hole No. 2 was bored from a drilling ship into the Tarva fault. It was found that parts of the fault zone was dominated by crushed and altered gneiss (breccia) with high content of clay (also swelling clay) (Sættem and Mørk, 1996). Lugeon measurements gave low Lugeon values (<1L) (Heggstad and Nålsund, 1996), but highly jointed rock mass in between fault rock and in the damage zone gave indications of high water leakage near the fault zone.

The results revealed very challenging geological conditions, and two expert reports (Nålsund et al., 1996; Nilsen et al., 1997) included prognosis regarding expected rock mass quality and amount of probedrilling and pregrouting. The reports prognosticated high water leakage in the sections where extremely high water leakages were registered in the tunnel, but underestimated the length of the sections with high water leakage and also indicated high water leakage in sections where small water leakages were encountered. However, the prognoses were quite good and certainly much better than usual for a subsea tunnel in Norway.

Figure 7.13 shows a longitudinal profile for a part of the Frøya tunnel with results from refraction seismics for the weakness zones indicated. Between the weakness zones the seismic velocity was between 4.4 and 5.5 km/s. It can be seen from this figure that highest water leakages were encountered below and just outside the fault zones.

Table 7.5 gives a summary and brief comments regarding the ability of the different investigation methods to prognosticate the encountered water leakage. Reflection seismic is not included here since it is primarily giving information regarding soil thickness and indications of depressions representing possible weakness zones. This information is of considerable interest but not relevant concerning hydraulic conditions of the rock mass.

TABLE 7. 5 Ability of site investigations to prognosticate water leakage for section F1, F2, F3 and F4 of the Frøya tunnel.

Station No.	Desk studies and geological mapping.	Refraction seismic.	Core drilling.
Section F1. (4050-4150).	Gave useful information regarding regional geology.	Water leakage registered in the tunnel below low velocity zone.	Not carried out for this section.
Section F2. (4400-4650).	Gave useful information regarding regional geology.	Extremely high water leakage encountered just outside Tarva fault (3.0 km/s) and below low velocity zone (3.1 km/s).	Gave useful information regarding fault rock and probability of water flow in fault zone.
Section F3. (4925-5100).	Gave useful information regarding regional geology.	Water leakage registered in the tunnel below low velocity zone.	Not carried out for this section.
Section F4. (5425-5650).	Gave useful information regarding regional geology.	High water leakage registered outside low velocity zone.	Not carried out for this section.

The investigations carried out prior to the excavation gave a good basis for prognosticating water leakage, and both expert reports mentioned above identified the sections with highest water leakage relatively well. For the refraction seismic high water leakages were encountered both directly below and outside the low seismic velocity zones. Geological mapping combined with refraction seismic and core drilling gave good information regarding water leakage for the Frøya tunnel.

7.4 The T-baneringen tunnel stage one (Ullevål-Nydal)

In the T-baneringen tunnel, see Figure 6.6 and 6.7, water inflow from probedrilling and pregrouting holes were only registered between Station No. 400 and 1425. The following analysis therefore has been restricted to this part of the tunnel. Geological mapping was done for the entire tunnel.

7.4.1 Water leakage versus geological parameters

A boxplot of calculated water leakage (l/min per 25 m) for the analysed part is shown in Figure 7.17. High water leakage was encountered; up to 1643 l/min per 25 m with 60 l/min per 25 m as mean value. One mild and two extreme outliers with water leakage between 57 and 1643 l/min per 25 m can be seen from the boxplot. 50% of the 25 m long sections had

water leakage between 7 and 26 l/min per 25 m, and the median value was 13 l/min per 25 m. The two extreme outliers, particularly the highest, contribute to a high mean value. The water leakage distribution is highly skewed to the right.

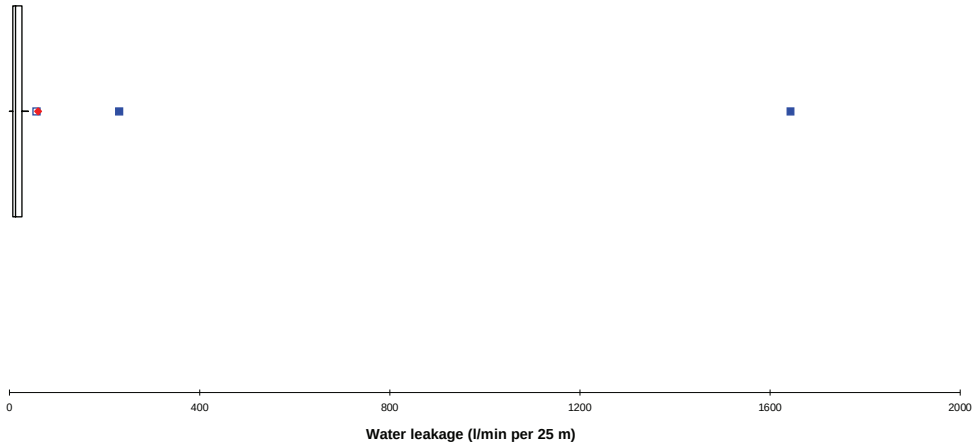

FIGURE 7.17 Boxplot of water leakage between Station No. 400 and 1425 for the T-baneringen tunnel.

Based on overall evaluation of the boxplot and the variation of water leakage along the tunnel (Figure 7.19), the following definitions for water leakage are used:

Small water leakage: 0-25 l/min per 25 m

Medium water leakage: 25-50 l/min per 25 m

High water leakage: 50-200 l/min per 25 m

Extremely high water leakage: 200-1700 l/min per 25 m

Hypothesis No. 1; *The water leakage is lower in rock mass with Q-values lower than 0.1, than in rock mass with Q-values between 0.1 and 10.*

As a first approach a XY-plot has been made of water leakage per 25 m vs. minimum Q-value registered for each analysed 25 m section, see Figure 7.18. It can be seen that there is a negative correlation of -0.178. This indicates no linear correlation between minimum Q-value and water leakage. The highest water leakage (1643 l/min per 25 m) is extremely high compared to all the other calculated water leakage values. The second largest is 231 l/min per 25 m. The six sections with highest water leakages, all had minimum Q-value lower than 0.1. Therefore, Hypothesis No. 1 is definitely not valid for the T-baneringen tunnel.

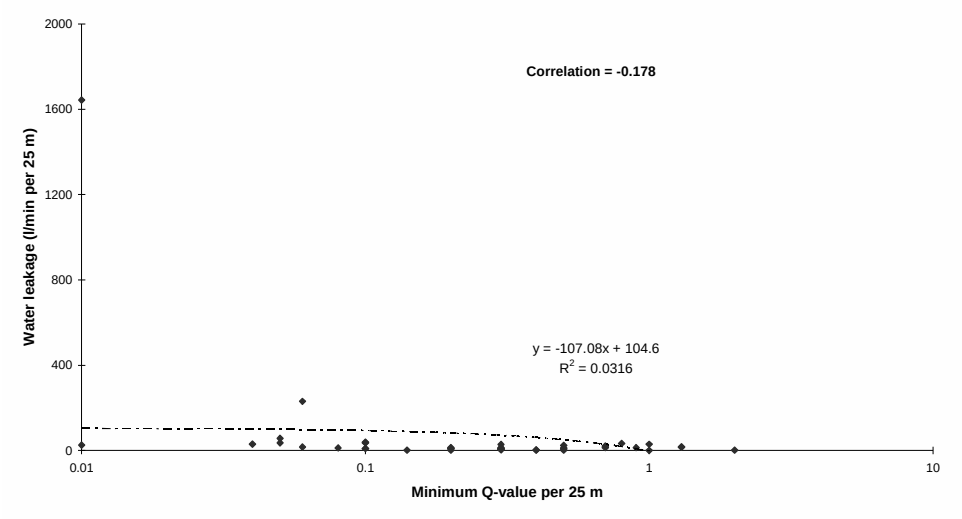

FIGURE 7.18 Water leakage versus minimum Q-value per 25 m between Station No. 400 and 1425 for the T-baneringen tunnel.

Hypothesis No. 2; *water-bearing joints make an angle with nearby major faults of* $45° \pm 15°$.

Figure 7.19 shows how water leakage and minimum Q-values varied between Station No. 400 and 1425. See also the longitudinal profile in Figure 6.6. The water leakage encountered between Station No. 700 and 775 was extremely high compared to the water leakage in the rest of the tunnel. It is therefore logical to analyse this section in particular detail. In addition, three 50 m long sections were selected based on low Q-values and small peaks of water leakage. The sections are called TB1, TB2, TB3 and TB4. Relevant geological information for these sections is given in Table 7.6.

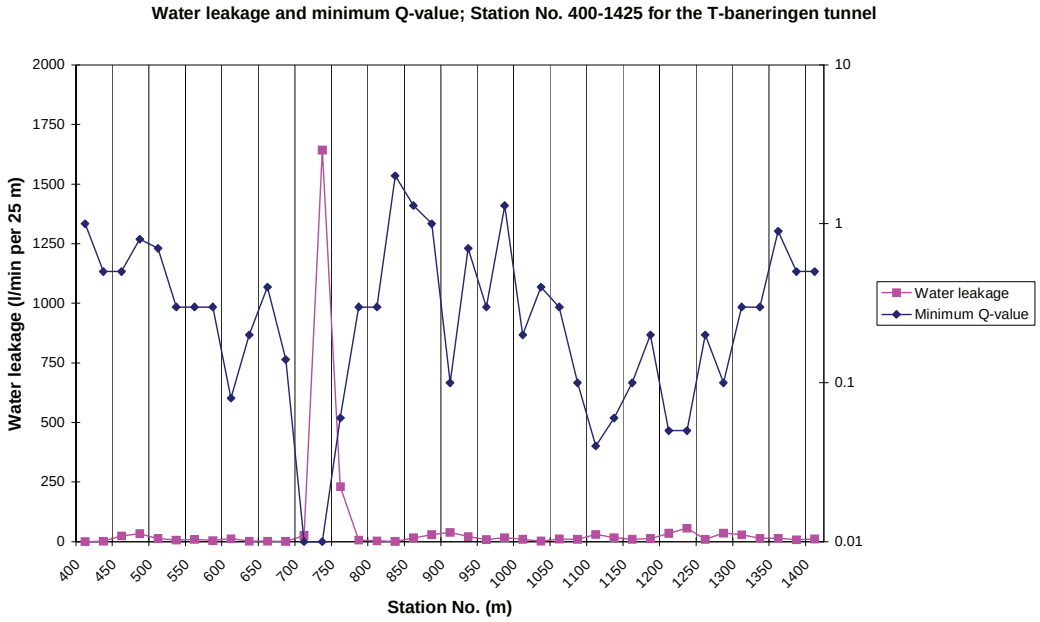

FIGURE 7.19 Diagram showing water leakage (l/min per 25 m) and minimum Q-value between Station No. 400 and 1425 for the T-baneringen tunnel.

TABLE 7. 6 Geological character of sections TB1, TB2, TB3 and TB4. ("JS" mean Joint Set, with No. 1 as the predominant etc.).

Station No.	Rock type / dykes.	Dominating joint sets. Direction of water-bearing joints.	Description of weakness zones / Q-value.
700-775. Section TB1. (75 m).	Shale and Syenite porphyry (Station No. 740-755).	JS1: (fol.) N40-80E/20-30N/S. JS2: N140-160/70-80 SE. JS3: N20-40E/60-80NE. JS4: N110E/65-80N. Some water on all joint sets. The syenite dyke was particularly water-bearing (JS3 and JS4 were dominating in the syenite).	The syenite dyke and nearby shale was a major weakness zone, Q-value 0.01-0.3. Crushed rock mass with clay (5-50 cm) in major joints. Clay, calcite and chlorite on joints.
890-940. Section TB2. (50 m).	Shale and limestone.	JS1: (fol.) N80-90E/20-36N. JS2: N110E/70-80S. JS3: N170-180E/65-80E.	Station No. 910-930 a small weakness zone parallel foliation, Q-value 0.1. 10-30 cm clay. Clay, calcite, chlorite and pyrite on joints.
1070-1120. Section TB3. (50 m).	Shale and diabase.	JS1: N115E/50-80S. JS2: N5-28E/50-75NW. JS3: (fol.) N74-108E/27-50N.	Station 1100-1120 weakness zone, highly jointed, 10 cm clay, Q-value 0.02-0.3. Clay, calcite, chlorite and pyrite on joints.
1205-1255. Section TB4. (50 m).	Shale and diabase.	JS1: (fol.) N25-50E/20-80NW/SE. JS2: N100-120E/75SW. JS3: N146E/60-80NE.	Station 1215-1230 weakness zone, highly jointed, Q-value 0.05-0.3. Clay and calcite on joints.

Section TB1 was dominated by a regional fault and a syenite porphyry dyke crossing the tunnel between Station No. 720 and 760, (Nordgulen and Dehls, 2003; Løset and Kveldsvik, 2003). Figure 7.20 shows lineaments interpreted from digital elevation data. The NE-SW lineaments represent the foliation, and the N-S lineaments (numbered 1, 2 and 3) represent jointed zones/faults (Nordgulen and Dehls, 2003). The green line shows the location of parts of the metro line and the T-baneringen tunnel is located between the two red vertical lines.

Detailed geological mapping was done in section TB1 and 3-4 joint sets identified (Boge et al., 2002; Åndal, 2001). High variation in strike and dip direction was registered for all joint sets. The foliation was oriented NE-SW with dip 25°-35° towards NW but occasionally dip towards SE was registered. In the syenite dyke a joint set almost parallel with the foliation but steeper (N20-40E/60-80NE) and a joint set oriented (N110E/65-80N) were dominating. The predominant structure in Section TB1 was, however, a regional fault with highly jointed rock mass nearby and in the syenite pophyry dyke, see

lineament No. 2 in Figure 7.20. The Q-values varied from 0.01 to 0.3. The syenite porphyry dyke was particularly water-bearing, and exceptionally high amounts of grouting cement were needed to cross this dyke (Åndal, 2001). Water leakage was registered on

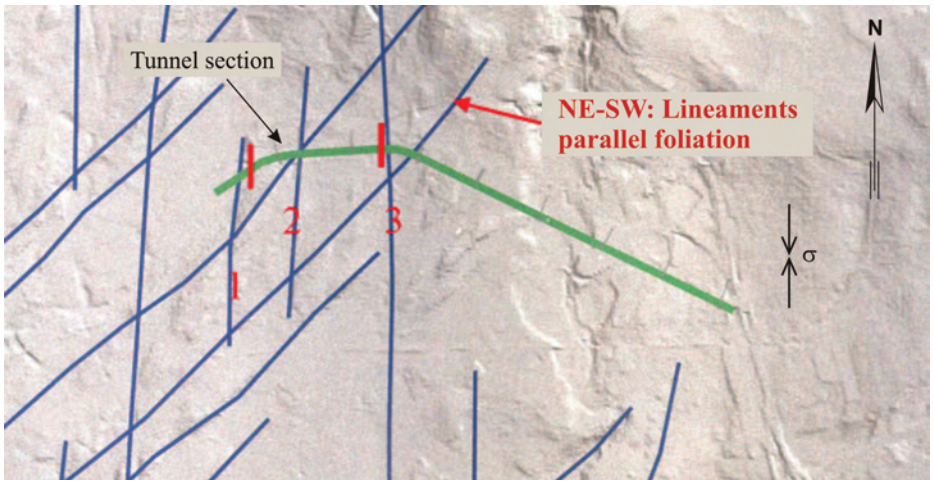

FIGURE 7.20 Lineaments interpreted from digital elevation data for the T-baneringen tunnel. Map modified from Nordgulen and Dehls (2003).

three joints oriented; N154E/78SE (JS2), N22E/60-7WNW (JS3) and N103E/60N (JS4). Hardened grouting cement was registered in both foliation joints and JS2 joints. Therefore it is not possible to recognise one or more of the joint sets to be more water-bearing than any of the other. For TB1 it is more likely that extremely poor rock mass quality due to the regional fault and syenite porphyry dyke was causing the extremely high water leakage.

For the sections TB2, TB3 and TB4 smaller weakness zones with highly jointed rock mass and Q-values varying from 0.02 to 0.1 were dominating. From the geological mapping it is not possible to locate any of the joint sets mentioned in Table 7.6 to be particularly water-bearing. It seems that generally highly jointed rock mass gave the small peaks of water leakage. In addition diabase was present in TB3 and TB4. As a result it is not possible to decide if Hypothesis No. 2 is supported or not.

Hypothesis No. 3; *water-bearing discontinuities are sub-parallel with the major principal stress.*

No stress measurements have been carried out in the area of the T-baneringen tunnel, but due to the regional fault and syenite porphyry dyke striking N-S major principal stress is likely to be close to N-S with low stress in E-W direction (Myrvang, 2008). Highest water leakage at T-baneringen tunnel came in the regional fault and syenite porphyry dyke

striking N-S. Assuming that the major principal stress is orientated N-S these results are supporting Hypothesis No. 3.

Hypothesis No. 4; *Water leakage decreases with increasing rock cover.*

In the sections analysed for the T-baneringen tunnel, the rock cover varies from 0 to 29 m. Lowest rock cover is located at the tunnel entrances, and highest rock cover was found in the eastern part of the tunnel. The rock cover is very low compared to most of the other tunnels studied in this thesis, and it may not be expected that a decrease of water leakage because of high rock cover is noticeable. Figure 7.21 shows a XY-plot of water leakage (l/min per 25 m) versus rock cover.

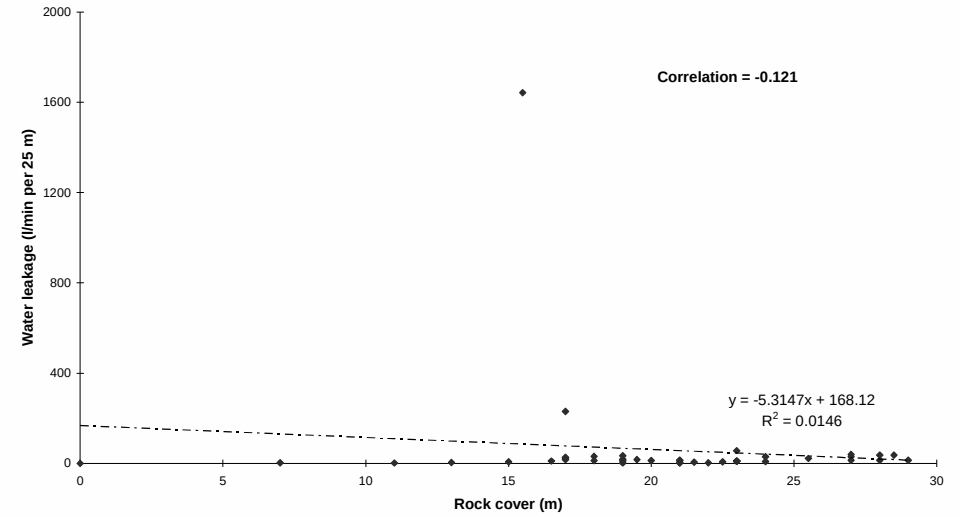

FIGURE 7.21 Water leakage (l/min per 25 m) versus rock cover (m) between Station No. 400 and 1425 for the T-baneringen tunnel.

The XY-plot gives a negative correlation of -0.12, indicating no linear correlation between water leakage and rock cover for the T-baneringen tunnel, and does not support Hypothesis No. 4.

Hypothesis No. 5; *Great thickness of permeable soil or a lake/sea above a tunnel gives high water leakage.*

The T-baneringen tunnel is located below an urban area. The soil thickness above the tunnel was thoroughly registered before excavation started, and was found to vary from 0 to 17 m, with maximum soil thickness at Station No. 817. Greatest soil thickness was found in small valleys, normally with weak rock mass or weakness zones below the soil.

The soil consists of marine deposits, mainly clay, which is more or less impermeable. As Figure 7.22 shows, and not very surprisingly, no correlation is therefore found between water leakage and soil thickness. Thus, this analysis does not support Hypothesis No. 5.

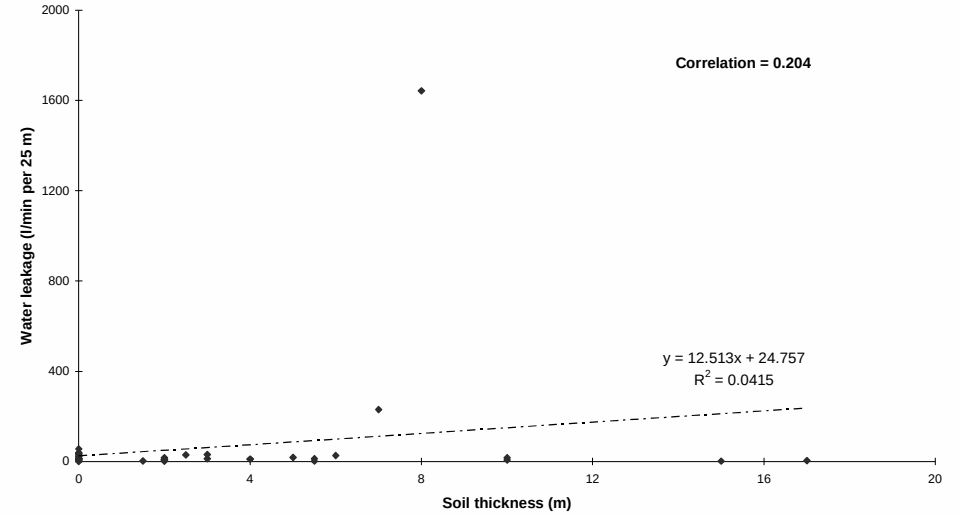

FIGURE 7.22 Water leakage (l/min per 25 m) versus soil thickness between Station No. 400 and 1425 for the T-baneringen tunnel.

Hypothesis No. 6; *Igneous rocks give higher water leakage than other rock types.*

Between Station No. 400 and 1425 in the T-baneringen tunnel, various types of limestone and shale were registered, as well as igneous dykes consisting of syenite and diabase. The syenite porphyry is approximately 15 m wide in the tunnel, and was highly water-bearing. The diabase dykes are smaller, normally around 1 m thick. Therefore, only the syenite porphyry is included in the analysis.

As explained in Section 2.2 the water leakage has been calculated for every 25 m along the tunnel. In some of the 25 m long sections both limestone and shale were registered, and it therefore has been decided to include shale as well as limestone in one of the data sets. Figure 7.23 shows a histogram with number of 25 m sections for different rock types versus ranges of water leakage. Two sections with syenite porphyry had much higher water leakage than all the other sections in the histogram. This supports Hypothesis No. 6.

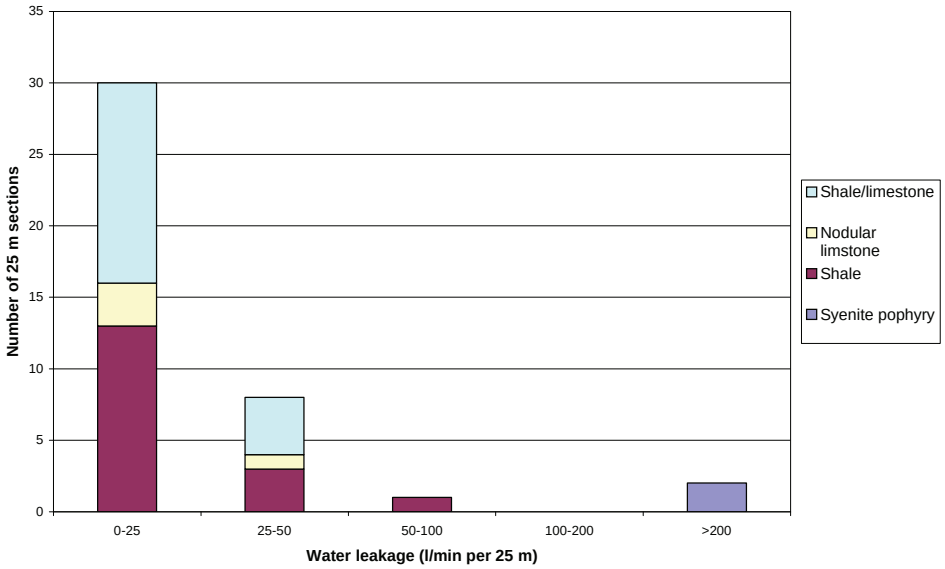

FIGURE 7.23 Distribution of ranges of water leakage (l/min per 25 m) for different rock types in the T-baneringen tunnel.

Hypothesis No. 7; *Major rock type boundaries give high water leakage.*

The T-baneringen tunnel between Station No. 400 and 1425 has considerable variation concerning rock types. The boundaries between different types of limestone and shale can not be regarded as very distinct geological boundaries, and the rock type boundary between the 15 m wide syenite porphyry and shale therefore is regarded as the most interesting. Figure 7.24 shows water leakage versus horizontal distance from the boundary between syenite porphyry and shale. A negative correlation of -0.459 indicates a distinct linear correlation; highest water leakage is expected close to a rock type boundary. This supports Hypothesis No. 7.

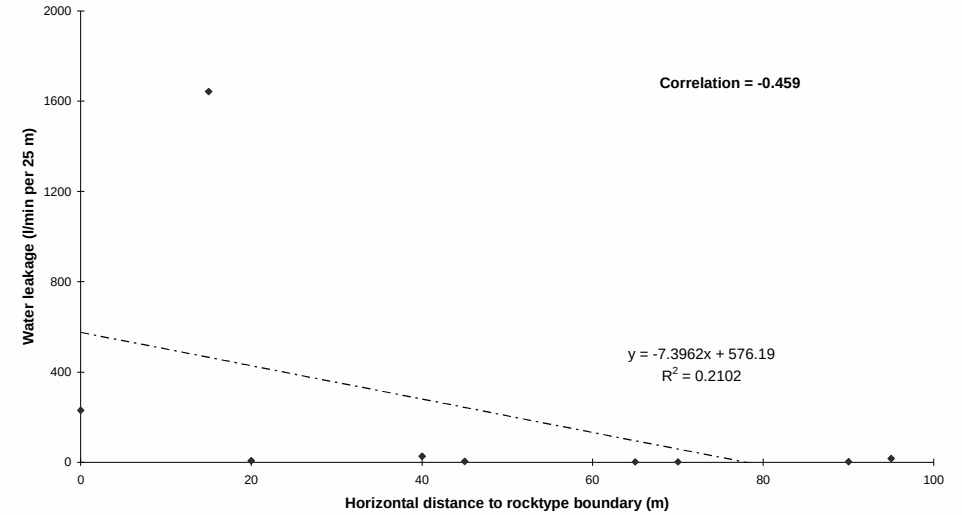

FIGURE 7.24 Water leakage (l/min per 25 m) versus horizontal distance to rock type boundary (shale-syenite porphyry) for the T-baneringen tunnel.

Hypothesis No. 8; *Wide weakness zones give higher relative water leakage (inflow per 25 m) than narrow weakness zones.*

Only one case with extremely high water leakage was registered in the T-baneringen tunnel. The smaller peaks of water leakage along the tunnel had almost the same registered water leakage (between 30 and 57 l/min per 25). Therefore, it is not possible to say if Hypothesis No. 8 is supported or not.

7.4.2 Water leakage versus site investigations

In Table 6.5 the respective investigations for the T-baneringen tunnel are described and brief comments on the results are given. In this study investigations and experience from the Tåsen tunnel, which is located just North of the T-baneringen were also important. 5 core drilling holes were carried out for the Tåsen tunnel. One of these. borehole K1, started approximately 12 m North of Station No. 660 and end 40 m North of Station No. 770. At the end of borehole K1 a dyke consisting of syenite and syenite porphyry was registered. This dyke was expected to have approximately the same rock mass quality as the syenite porphyry in the T-baneringen tunnel.

For the T-baneringen tunnel 13 refraction seismic profiles were measured along the tunnel alignment. In addition, geotechnical investigations for defining soil thickness, soil types,

rock cover and pore pressure were done, but are not considered relevant for the present analysis.

Table 7.7 summarizes the results and gives brief comments regarding the ability of the different investigation methods to prognosticate the encountered water leakage.

TABLE 7. 7 Ability of site investigations to prognosticate water leakage for section TB1, TB2, TB3 and TB4 of the T-baneringen tunnel.

Station No.	Desk studies and geological mapping.	Refraction seismic.	Core drilling (the Tåsen tunnel).
700-775. Section TB1.	Gave useful information regarding expected geology and water. (Information from the Tåsen tunnel).	Water leakage registered in the tunnel below low velocity zone (2300 m/s in 13 m wide zone). Corresponds well with syenite porphyry dyke.	Relevant information, fracturing and Lugeon values. Porphyry syenite dyke (8.4 L), shale (3.9 L) and nodular limestone (2.0L).
890-940. Section TB2.	No weakness zones identified, (covered with soil and densily built area).	Low velocity zone registered close to Station No. 925. (2200 m/s in 5.5 m wide zone).	Not carried out for this section.
1070-1120. Section TB3.	No weakness zones identified, (covered with soil and densily built area).	Low velocity zone registered 20 m North of tunnel alignment, Station No. 1100. (2400 m/s in 10 m wide zone).	Not carried out for this section.
1205-1255. Section TB4.	No weakness zones identified, (covered with soil and densily built area).	30 m North of tunnel alignment, Station No. 1250. 1700 m/s in 14.5 m wide zone. Corresponds well with water and poor rock mass quality around Station No. 1225. (Below small valley).	Not carried out for this section.

Lineament studies (digital elevation data) (Løset and Kveldsvik, 2003) identified two lineaments crossing each other in Section TB1, see Figure 7.20. The N-S trending lineament indicated a jointed zone with possible N-S movements. These results identified the porphyry syenite in this section as potentially more crushed and water-bearing than other igneous dykes in the area. Unfortunately, lineament studies were done only after excavation of the tunnel was finished.

The refraction seismic identified low seismic velocity in all the sections with high water leakage. The Lugeon values for the porphyry syenite was 8.4 and as expected higher than for shale and nodular limestone. The investigation results together with experience from the Tåsen tunnel identified the syenite porphyry dyke in section TB1 as potentially water-bearing. In the contract water tight concrete lining was described between station No. 690

and 870. Considerable amounts of grouting cement (approx. 596 ton between Station No. 700 and 750) combined with water injection kept the pore pressure stable, even though the water leakage criterion of 7 l/min per 100 m was not satisfied.

7.5 The Lunner tunnel

For the 3.8 km long Lunner tunnel geological mapping during excavation was restricted mainly to sections near the two tunnel entrances (between Station No. 160-1658 and 3321-3940), see Figure 6.8. Additional geological mapping was done after excavation, between Station No. 2340 and 3940 (Kirkeby and Kveen, 2002). Because shotcrete covered most of the tunnel roof and walls the additional mapping could not be continuous. Nevertheless, it gives useful information for the following analyses. Water leakage encountered during excavation varied a lot along the tunnel. From the western tunnel entrance at Station No. 160 to Station No. 1781 no pregrouting was necessary. Unfortunately, water inflow from probedrilling holes and pregrouting rounds was not registered between Station No. 3416 and 3815. The analyses for the Lunner tunnel therefore have been restricted to the following sections:

Station No. 1725-1850
Station No. 2200-3425
Station No. 3800-3950

Along these three sections no geological mapping has been done for 250 m out of 1500 m.

7.5.1 Water leakage versus geological parameters

A boxplot of calculated water leakage (l/min per 25 m) for the analysed sections is shown in Figure 7.25. High water leakage was encountered; up to 4149 l/min per 25 m with 330 l/min per 25 m as mean value. One mild and eight extreme outliers with water leakage between 747 and 4149 l/min per 25 m can be seen from the boxplot. 50% of the 25 m long

sections had water leakage between 8 and 199 l/min per 25 m, and the median value is 39 l/min per 25 m. The water leakage distribution is highly skewed to the right.

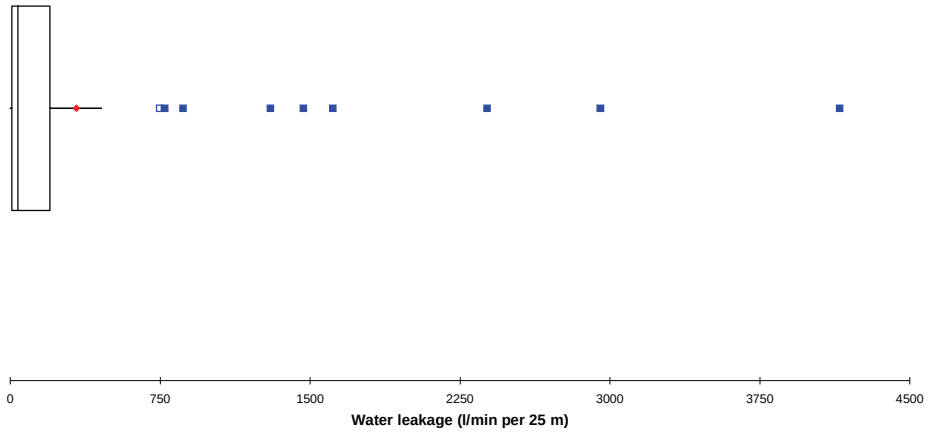

FIGURE 7.25 Boxplot of water leakage in the analysed sections for the Lunner tunnel

Based on overall evaluation of the boxplot and the variation of water leakage along the tunnel (Figure 7.27), the following definitions for water leakage are used:

Small water leakage: 0-50 l/min per 25 m
Medium water leakage: 50-200 l/min per 25 m
High water leakage: 200-500 l/min per 25 m
Extremely high water leakage: 500-4150 l/min per 25 m

Hypothesis No. 1; *The water leakage is lower in rock mass with Q-values lower than 0.1, than in rock mass with Q-values between 0.1 and 10.*

As a first approach a XY-plot is made of water leakage per 25 m vs. minimum Q-value registered for each analysed 25 m section, see Figure 7.26. A correlation of 0.249 indicates low to medium linear correlation between water leakage and minimum Q-value. The highest calculated water leakage (4149 l/min per 25 m) is extremely high compared to all the other calculated water leakage values. The second largest is 2951 l/min per 25 m. If the highest extreme outlier is taken out of the data, the correlation between water leakage and minimum Q-value per 25 m is 0.529. This means that for the Lunner tunnel it is evident that water leakages increase when Q-values increase.

Q-values lower than 0.1 were not registered in the Lunner tunnel. Therefore, it is not possible to check Hypothesis No. 1. In three sections Q-values lower than 0.5 were registered, all three had less than 40 l/min per 25 m. This shows that the water leakage seems to decrease when the Q-value is lower than 0.5. Furthermore, if we compare information from the boxplot with the XY-plot the 9 outliers with water leakage higher than 747 l/min per 25 m have Q-values between 0.7 and 100. The Q-values vary a lot and due to lack of geological mapping, only four out of nine outliers have the respective minimum Q-value registered. Therefore, the data are too sparse to decide whether Hypothesis No. 1 is supported or not.

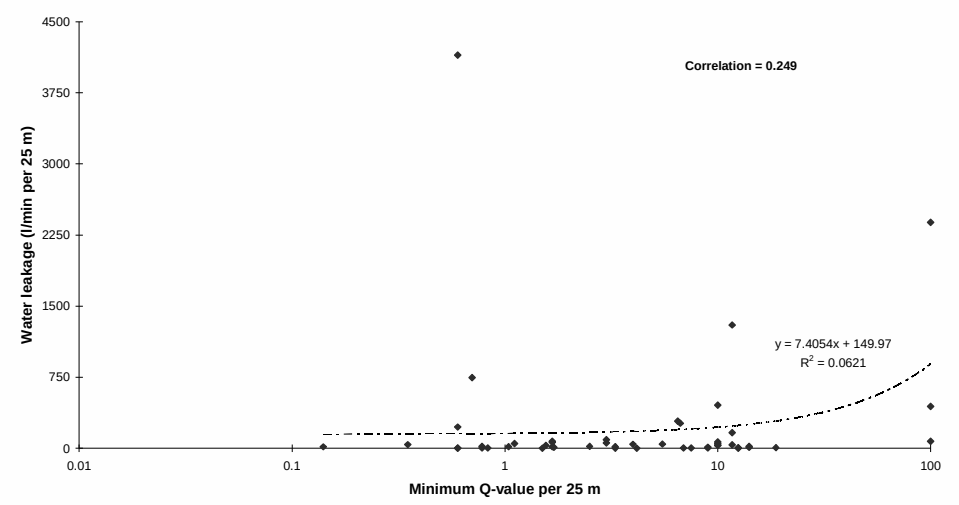

FIGURE 7.26 Water leakage versus minimum Q-value per 25 m in the analysed sections for the Lunner tunnel.

Hypothesis No. 2; *water-bearing joints make an angle with nearby major faults of* $45° \pm 15°$.

Figure 7.27 shows water leakage versus minimum Q-values for the parts of the tunnel studied. See also simplified geological map in Figure 6.7. In the diagram (Figure 7.27) two sections are missing due to lack of data; 1850-2200 and 3425-3800.

A detailed study of some sections with high and extremely high water leakage or with very poor rock mass quality (Q-value between 0.1 and 1.0) has been done. Three sections were selected; L1, L2 and L3 (see Table 7.8). The first section, L1, between Station No. 1725 and 1825 had medium water leakage. Section L1 was the first section where pregrouting was carried out during excavation from the western tunnel entrance. Unfortunately, geological mapping is lacking in most of section L1, only 5 m was mapped. The second

section, L2, between Station No. 2200 and 2550 was chosen because of obviously higher water leakage than in the rest of the tunnel. The third section, L3, between Station No. 2900-3225 was chosen because of two small peaks in water leakage and weakness zones with very poor rock mass quality, including the lowest registered Q-value for the Lunner tunnel. Relevant geological information for these sections is given in Table 7.8.

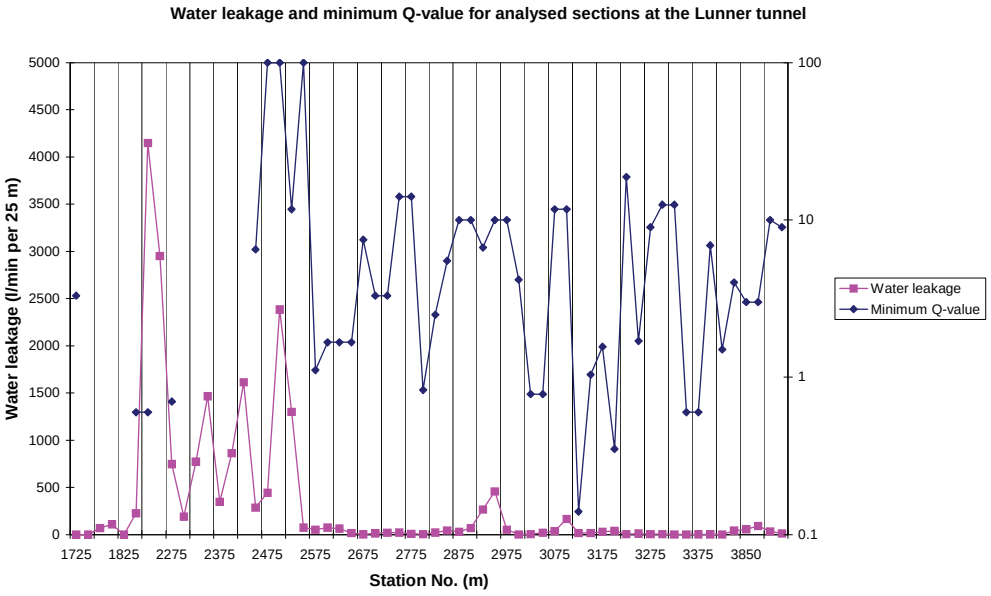

FIGURE 7.27 Water leakage (l/min per 25 m) and minimum Q-value for analysed sections at the Lunner tunnel.

TABLE 7. 8 Geological character of sections L1, L2 and L3. ("JS" mean Joint Set, with No. 1 as the predominant etc.).

Station No.	Rock type / dykes.	Dominating joint sets. Direction of water-bearing joints.	Description of weakness zones / Q-value.
1725-1825. Section L1. (100 m).	Hornfels.	JS1: N-S/80V. JS2: N60E/60-70S. JS3: N160E/10-20Ø. Cubic joint system with no clear water-bearing joints, geological mapping done for only 5 m.	Highly jointed, joint spacing 10-30 cm, Q-value 3.3-10.0.
2200-2550. Section L2. (350 m).	Mainly syenite.	JS1: N10-30E/80-90V. JS2: N75-100E/75-90N and S. JS3: Flat joints. Sporadic joints (SJ1): N136E/80NE. Some water on all joint sets. Particularly JS1 and SJ1.	Moderately jointed, Q-value 0.6-100.0. Major weakness zone Station No. 2220-2270 in connection to fault close to boundary between hornfels and syenite. 2-3 cm clay on major joints.
2900-3225. Section L3. (325 m).	Mainly syenite porphyry.	JS1: N105-120E/80-90. JS2: N45-70E/90. JS3: N-S/90. Flat joints + sporadic joints. (SJ2): N150-170E/70-90NE. Three weakness zones (WZ): N135-160E/30-60N. In highly jointed sections with JS1/JS2 and in SJ2/WZ water leakage was encountered.	Joint spacing vary a lot, from 0.1-1.0 m. Q-value 0.14-12.7. Lowest Q-value in weakness zone between Station No. 3140-3150, 2-5 cm clay, probably swelling clay. Weakness zones are 0.5-1 m wide.

Figure 7.28 shows an engineering geological map for a part of the Lunner tunnel, between Station No. 2150 and 3350. Section L2 and L3 are covered by the map.

In the tunnel one regional fault, close to the boundary between hornfels and syenite, was registered (steep and striking N10E). The highest water leakage was encountered in connection with this regional fault between Station No. 2200 and 2300 (section L2). Since geological mapping was very sparse between Station No. 2200 and 2300 (10 m) it is not possible to say that one joint set was more water-bearing than another. But the dominating joint set was oriented parallel with the fault N10E, and one sporadic joint (SJ1) oriented N136E/80NE was observed by the author to be water-bearing at Station No. 2293. In the

eastern part of section L2 (around Station No. 2500) also extremely high water leakage was encountered. In this section joints oriented N100E/90 were dominating.

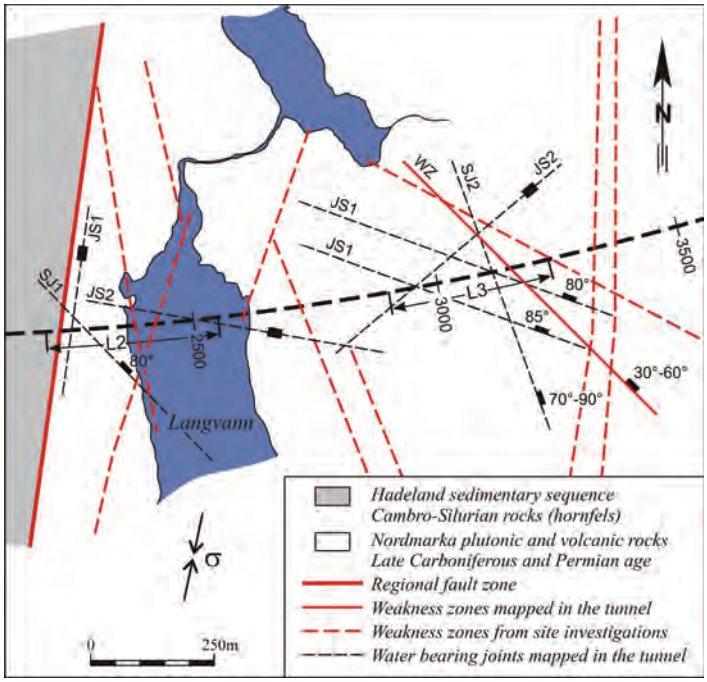

FIGURE 7.28 Engineering geological map showing regional fault, weakness zones and water-bearing joints. Modified from Rønning and Dalsegg (2001).

In section L3, moderate to high water leakage was registered between Station No. 2925-2975 and 3100-3125. In the first section the rock mass quality was fairly good, with approximately 25 m of highly jointed rock mass and two dominating joint sets: N110E/85N and N50E/90. Between Station No. 3100 and 3125 the rock mass quality was good, with one dominating joint set striking N110E and dip 80N. Some water-bearing joints (SJ2) were registered with orientation N150-170E/70-90NE. A weakness zone oriented N135E/90 with lowest registered Q-value 0.14 was registered at Station No. 3135-3150. It is likely that the water leakage encountered between Station No. 3100 and 3125 was related to the nearby weakness zone (damage zone). In addition, small water leakage was registered in two other weakness zones with Q-values lower than 1.0 strike N140-160E with varying dip from 30° to 60° NE.

From the above description, the following joint sets seem to be water-bearing: N10E/90, N110E/80N, N50E/90 and N135-170E/varying dip towards NE. The two latter joint sets both make an angle with major fault (N10E) of 45° ±15°. This supports Hypothesis No. 2.

On the other hand, the orientation of joint set parallel with the regional fault (N10E/90) and joint set N110E/80N do not support Hypothesis No. 2. Since the analysis gave ambiguous results, it gives only low to medium support to Hypothesis No. 2.

Hypothesis No. 3; *water-bearing discontinuities are sub-parallel with the major principal stress.*

No stress measurements have been carried out in the area of the Lunner tunnel, but due to the regional fault striking N10E and several close to N-S oriented weakness zones, the major principal stress is likely to be NNE-SSW (Myrvang, 2008). One of the most dominating joint sets in the Lunner tunnel is steep with strike N10E, and was registered in sections with high and extremely high water leakage. Assuming that major principal stress is orientated NNE-SSW these results are supporting Hypothesis No. 3. Thus, only the joint set oriented N110E/80N can not be explained by Hypothesis No. 3.

Hypothesis No. 4; *Water leakage decreases with increasing rock cover.*

In the sections analysed for the Lunner tunnel, the rock cover varies from 12 to 236 m. Lowest rock cover is located in the eastern part of the tunnel (Station No. 3950), and highest rock cover is located East of Langvann (Station No. 1725). Figure 7.29 shows a XY-plot of water leakage (l/min per 25 m) versus rock cover.

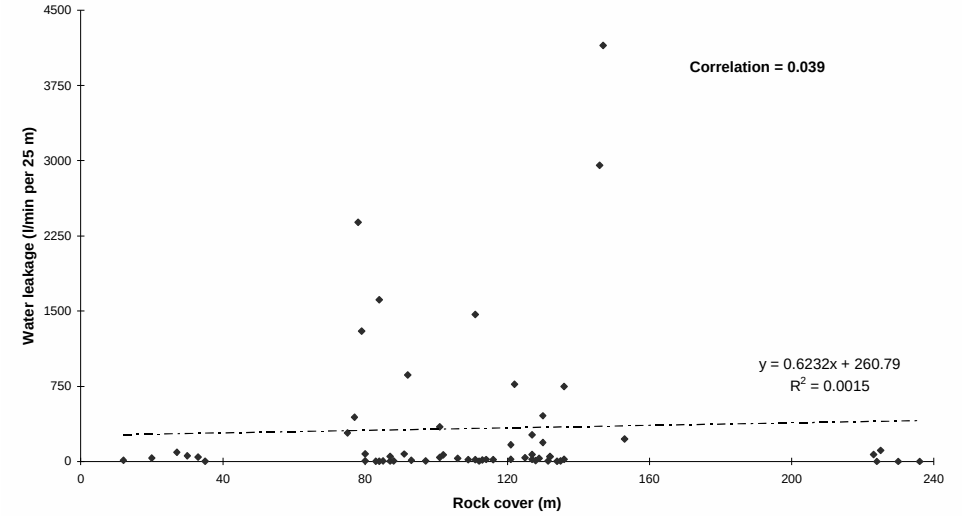

FIGURE 7.29 Water leakage (l/min per 25 m) versus rock cover (m) for analysed sections at the Lunner tunnel.

The XY-plot gives a correlation of 0.039, indicating no linear correlation between water leakage and rock cover for the Lunner tunnel, and does not support Hypothesis No. 4.

Hypothesis No. 5; *Great thickness of permeable soil or a lake/sea above a tunnel gives high water leakage.*

A thin discontinuous layer of moraine material was registered above most of the tunnel, and peat/bog occasionally West of Langvann. Since no thick layer of soil was regi-stered above the tunnel alignment it is most relevant to analyse the possible effects of the lake above the tunnel. The lakes Langvann (Station No. 2375-2610) and Nordre Munkejor-dtjern (Station No. 1825-1910) are located in connection with weakness zones registered by site investigations, and therefore represent potential recharge zones.

The influence of a lake is likely to decrease with increasing distance, and therefore horizontal distances of more than approximately 200 m are not considered in this analysis. When the tunnel is just below the lake the horizontal distance is zero. A few data points were not included due to extremely high water leakage close to the rock type boundary between syenite and hornfels. The extremely high water leakages would have given ambiguous results. The horizontal distance to lake versus water leakage (l/min per 25) is shown in Figure 7.30. A correlation of -0.41 indicates that there is a trend that the water leakage decreases when the horizontal distance to a lake increases, and supports Hypothesis No. 5.

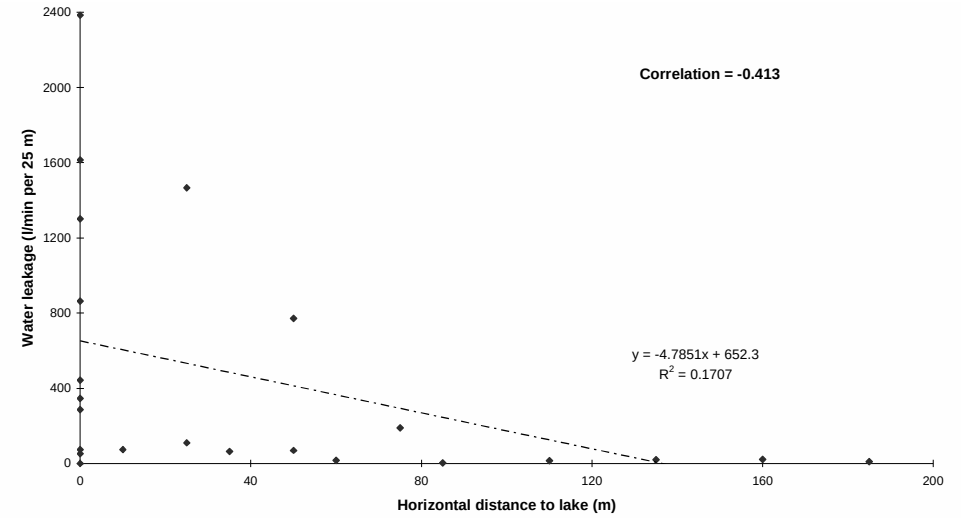

FIGURE 7.30 Water leakage versus horizontal distance to lake for analysed sections at the Lunner tunnel.

Hypothesis No. 6; *Igneous rocks give higher water leakage than other rock types.*

For the analysed sections of the Lunner tunnel several rock types were registered. Figure 7.31 shows a histogram with number of 25 m sections for different rock types versus ranges of water leakage. It has been chosen to distinguish between syenite and syenite porphyry because these rock types were located in different parts of the tunnel; the syenite between Station No. 2220 and 2580, mainly below Langvann, and the syenite porphyry between Station No. 2915 and 3200. It can be seen that syenite gave higher water leakage than all the other rock types. The histogram illustrates that all sections with higher water leakage than 200 l/min were located in syenite or syenite porphyry. This supports Hypothesis No. 6.

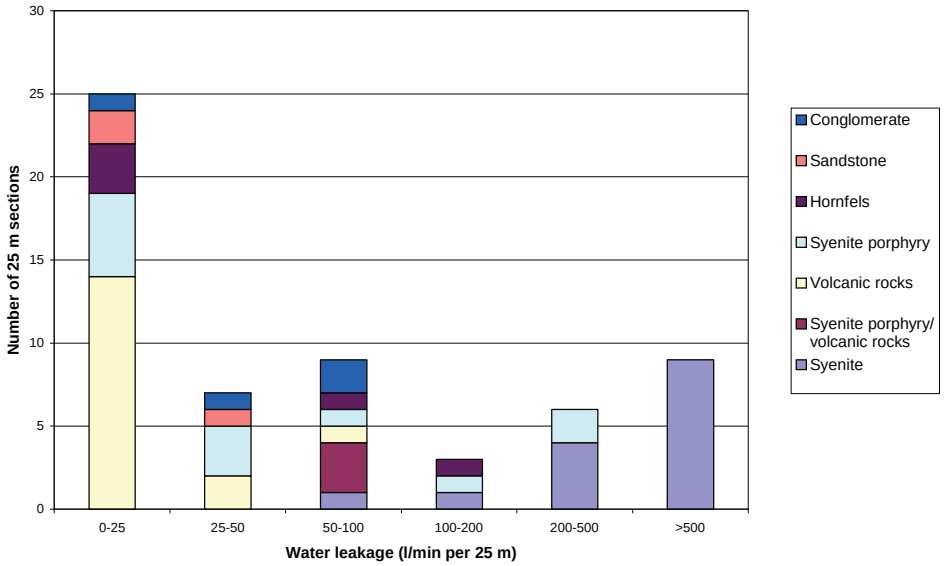

FIGURE 7.31 Distribution of ranges of water leakage (l/min per 25 m) for different rock types in the Lunner tunnel.

Hypothesis No. 7; *Major rock type boundaries give high water leakage.*

The Lunner tunnel between Station No. 2220 and 3225 has considerable variation concerning rock types. The regional geological boundary between hornfels (Cambro-Silurian rocks) in the western part and syenite (late Carboniferous and Permian age) in the eastern part of the tunnel was encountered at approximately Station No. 2220. Unfortunately, the exact boundary was not mapped, but according to people working at site, the boundary was sharp and the rock mass quality nearby was very poor to extremely poor (cubic joint system and 2-5 cm clay on major joints).

A calculated negative correlation of -0.12 between water leakage and horizontal distance to rock type boundary, indicates no correlation. Regardless of this low correlation, high and extremely high water leakage was, however, registered at the boundary between hornfels and syenite at Station No. 2220. High water leakage was also registered between Station No. 2900 and 2975, close to the boundary between volcanic rock and syenite porphyry at Station No. 2915. In addition, rock type boundaries at Station No. 2580, 3205 and 3840 locally gave moderate increase of water leakage. Thus, the hypothesis seems to be correct in some of the rock type boundaries, although increased water leakage may also be related to rock type (syenite) and distance to fault zones. Thus, the analysis is considered to give low to medium support to Hypothesis No. 7.

Hypothesis No. 8; *Wide weakness zones give higher relative water leakage (inflow per 25 m) than narrow weakness zones.*

For the Lunner tunnel the geological mapping was not continuous in sections with high and extremely high water leakage. For the parts where geological mapping was done, two locations with medium and high water leakage were, however, registered:

- Station No. 2925-2975; water leakage 266 and 457 l/min per 25 m
- Station No. 3100-3125; water leakage 166 l/min per 25 m

Between Station No. 2925 and 2975 approximately 25 m of highly jointed rock mass was registered, while between station 3100 and 3125 10-15 m of somewhat jointed rock mass was registered. Hence, highest water leakage per 25 m was registered in the widest weakness zone. Because of very scarce geological data, the correlation is, however, not very convincing, and only gives low to medium support to Hypothesis No. 8.

7.5.2 Water leakage versus site investigations

The Lunner tunnel was thoroughly investigated before construction started. In Table 6.7 the respective investigations are described with brief comments on the results. In addition to desk studies, geological mapping, refraction seismic and core drilling, 2D resistivity measurements and borehole logging with hydraulic test pumping were done. Based on the pre-construction investigation results, particularly from core drilling below Langvann, high water leakage was expected between Station No. 2280 and 2380 (Iversen, 1998).

VLF (Very Low Frequency) measurements were carried out in four profiles; the results gave anomalies on most of the already known fracture zones. The same was the case for magnetic measurements (magnetometry). Since those two methods gave almost no new information, they will not be further discussed for the Lunner tunnel. Two separate helicopter geophysical surveys were carried out (summer 1997 and 2000), and four data

types collected; magnetic, radiometric, electromagnetic and VLF data (Beard, 2001). Many anomalies seem to be related to the fault zone between hornfels and syenite, and anomalies on the western shore of the lake Langvann were also identified. Most of the anomalies were registered in the eastern part of the tunnel, and coincided with fracture zones already registered. Many anomalies were registered in the section with highest water leakage (section L2, see Figure 7.28).

In section L1 (see Table 7.8) water leakages of 70 and 110 l/min per 25 m were registered between Station No. 1775 and 1825. A steep, N-S striking fracture zone passing through the small lake Munkerudtjern just South of the tunnel alignment can be a contributing factor to water leakage. In addition, a deep low resistivity zone was registered in this section. This indicates strongly a potential water leakage in this section.

Section L2 (see Figure 7.28) includes the fault zone close to the boundary between hornfels and syenite and the section below the lake Langvann, and during excavation extremely high water leakages were encountered. All the pre-construction investigations identified this section to have fracture zones with potentially high water leakage.

In section L3 (see Figure 7.28) a steep, WNW-ESE striking fracture zone was identified by geological mapping and shallow low resistivity. This fracture zone was registered in the tunnel as a small weakness zone at the boundary between porphyry syenite and sandstone at Station No. 3210. Dripping water was registered, but only 40 l/min between Station No. 3200 and 3225 was encountered. Shallow low resistivity was also registered at Station No. 2900 and 3000 (each approximately 5 m wide). The two zones seem to disappear towards the depth, and at tunnel level the registered resistivity was 3000 ohmm or higher. During tunnelling water leakages between 51 and 457 l/min per 25 m were registered between Station No. 2900 and 3000. This means that high water leakage was encountered below an area where low resistivity was registered.

After excavation had started the author made a prognosis for water leakage for the part of the tunnel that was not yet excavated (Station No. 1700 - 3250) (Holmøy, 2002). The water leakage encountered in the tunnel was much higher than expected, particularly below the eastern part of Langvann. The locations of major water leakages were, however, mainly as expected.

Table 7.9 summarizes the results with brief comments regarding the ability of the different investigation methods to prognosticate the encountered water leakage. 2D-resistivity measurements carried out East of Langvann after excavation was completed (Dalsegg and Rønning, 2002), are also included in the Table.

TABLE 7. 9 Ability of site investigations to prognosticate water leakage for section L1, L2, and L3 of the Lunner tunnel.

Station No.	Desk studies and geological mapping.	Refraction seismic.	2D-resistivity.	Core drilling.	Borehole logging.
1725-1825. Section L1.	Several fracture zones identified.	Not carried out.	Identified zone with water leakage by deep low resistivity.	Not carried out.	Not carried out.
2200-2550. Section L2.	Potential water leakage identified by fault zone (hornfels/ syenite) + fracture zones.	Low velocity zone Station No. 2400-2455 (3300-3900 m/s), identified zones with water leakage.	Potential water leakage identified by deep low resistivity 330 m N of alignment (fault zone).	Potential water leakage identified by Lugeon values (highest 4.25 L), between Station No. 2300-2400.	Potential water leakage identified by highly jointed rock mass with low resistivity (250 ohmm), high well capacity (7/13 m^3/hour. Station No. 2200-2400
2900-3225. Section L3.	Potential water leakage identified by one fracture zone Station No. 3225. Medium water leakage encountered.	Not carried out.	Shallow low resistivity at Station No. 2900, 3000 and 3150-3225 identified to some extent water leakage.	Not carried out.	Not carried out.

Table 7.9 illustrates that the locations of water leakages to a high degree were correctly estimated, but the amount of water leakage underestimated. The borehole logging with potential well capacity gave valuable results regarding amount, since the well capacity measured was 5-10 times higher than the mean value in syenite (Storrø et al., 2002).

7.6 The Skaugum tunnel

For the 3.6 km long Skaugum tunnel pregrouting was done systematically and water inflow from pregrouting holes was registered in the entire tunnel. Geological mapping was also done for the entire tunnel. Encountered water leakage and rock quality vary a lot along the tunnel, and the analyses therefore cover the entire tunnel length (Station No. 19.250-23.650, with a chainage discontinuity of 760 m at Station No. 21.000).

7.6.1 Water leakage versus geological parameters

A boxplot of calculated water leakage (l/min per 25 m) for the Skaugum tunnel is shown in Figure 7.32. Encountered water leakage varied from 0 to 1616 l/min per 25 m with 104 l/min per 25 m as mean value. Five mild and fifteen extreme outliers with water leakage between 319 and 1616 l/min per 25 m are illustrated in the boxplot. 50% of the 25 m long sections had water leakage between 3 and 81 l/min, and the median value is 19 l/min per 25 m. The water leakage distribution is highly skewed to the right.

Based on overall evaluation of the boxplot and the variation of water leakage along the tunnel (Figure 7.34), the following definitions for water leakage are used:

Small water leakage: 0-40 l/min per 25 m
Medium water leakage: 40-250 l/min per 25 m
High water leakage: 250-600 l/min per 25 m
Extremely high water leakage: 600-1650 l/min per 25 m

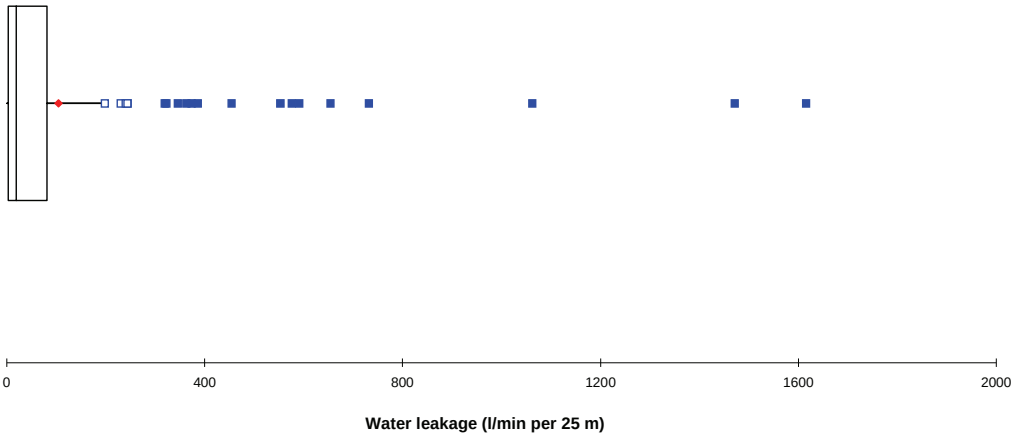

FIGURE 7.32 Boxplot of water leakage for the Skaugum tunnel

Hypothesis No. 1; *The water leakage is lower in rock mass with Q-values lower than 0.1, than in rock mass with Q-values between 0.1 and 10.*

As a first approach a XY-plot is made of water leakage per 25 m versus minimum Q-value registered for each 25 m section, see Figure 7.33. A negative correlation of -0.1 indicates no linear correlation between minimum Q-value and water leakage.

Q-values lower than 0.1 were not registered in the Skaugum tunnel. Therefore, it is not possible to check Hypothesis No. 1, but an analysis of how much water leakage was encountered close to zones with Q-values lower than 0.5 has been done. Figure 7.34 shows how water leakages and minimum Q-values varied along the tunnel. Q-values lower than 0.5 were registered in three 25 m sections, and all had lower than 82 l/min per 25 m. Two of the sections were located close to the tunnel entrance at the Asker side, between Station No. 23.600 and 23.650. Two weakness zones (2-5 m wide each) with clay filled joints were registered, and water leakages around 10 l/min per 25 m were encountered.

Between Station No. 20.635 and 20.650 a 3-4 m wide weakness zone with clay filled joints and Q-value of 0.1 was registered. Calculated water leakage between Station No. 20.625 and 20.650 was 82 l/min. Hence, small to medium water leakage was registered when the Q-value was lower than 0.5. It can also be seen that the sections with extremely high water leakages had Q-values between 2.2 and 4.2. The estimated envelope curve in Figure 7.33 further emphasizes that highest water leakage was encountered for Q-values between 1.0 and 10.0. Hence, it can be argued that extremely high water leakage is most likely in rock mass with Q-values between 1.0 and 10. This supports Hypothesis No. 1.

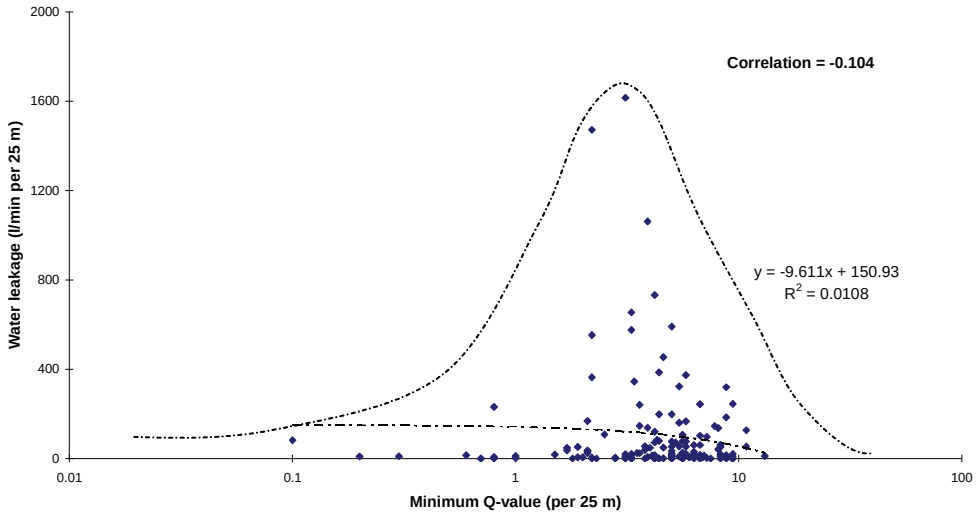

FIGURE 7.33 Water leakage versus minimum Q-value per 25 m for the Skaugum tunnel.

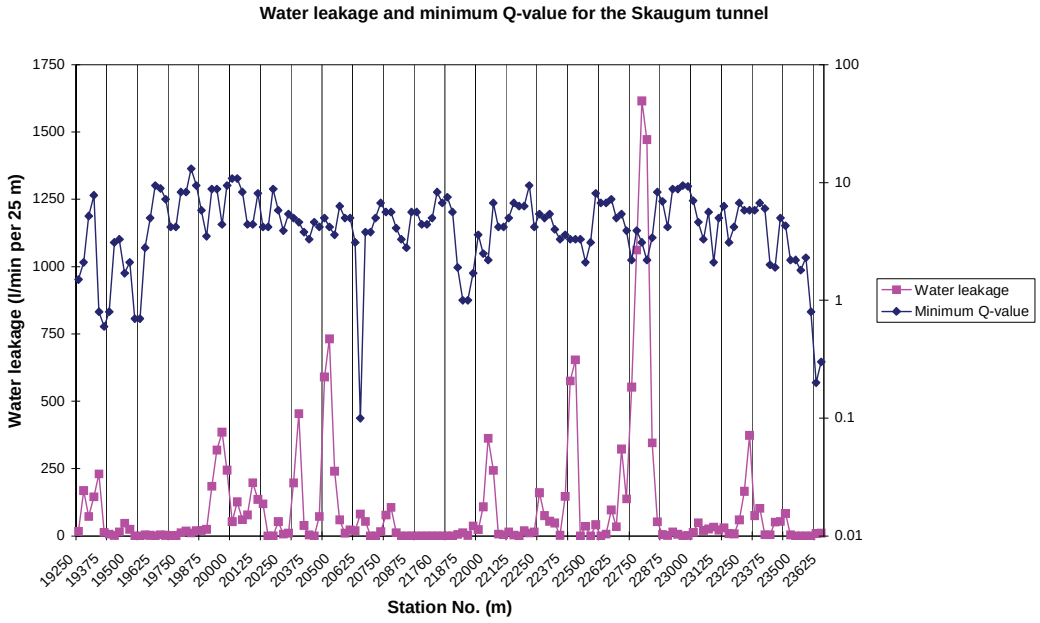

FIGURE 7.34 Water leakage (l/min per 25 m) and minimum Q-value for the Skaugum tunnel.

Hypothesis No. 2; *water-bearing joints make an angle with nearby major faults of* $45° \pm 15°$.

A detailed study of sections with high and extremely high water leakage has been done. Section S1 was extended 100 m to include a small weakness zone. Relevant geological information for four sections of different length (S1, S2, S3 and S4) is given in Table 7.10.

TABLE 7. 10 Geological character of sections S1, S2, S3 and S4. ("JS" mean Joint Set, with No. 1 as the predominant etc.).

Station No.	Rock type / dykes.	Dominating joint sets. Direction of water-bearing joints.	Description of weakness zones / Q-value.
19.900-20.650. S1 (750 m).	Nodular limestone, shaly limestone, shale and igneous dykes.	JS1: (fol.) N60-80E/varying dip. JS2: N-S/90. Sporadic joints (SJ):N115-140E/90. No clear water-bearing joints.	Q-value: 3.1-18.8. One weakness zone (3m) with Q-value 0.1; Station No. 20.635-20.650. Fold axis registered at Station No.: 19.970, 20.320 and 20.470.
21.950-22.050. S2 (100 m).	Nodular limestone, limestone, shale, sandstone and diabase dykes.	JS1: (fol.) N75-85E/50-70N(S). JS2: N-S/80-90E. Sporadic joint N98E/75. No clear water-bearing joints.	Q-value: 2.2-7.2. Several clay filled joints parallel with foliation, and several diabase dykes. Some calcite on joints.
22.375-22.825. S3 (450 m).	Nodular limestone, limestone, shaly limestone, shale, sandstone, siltstone and diabase dykes.	JS1: (fol.) N65-85E/70-90N/S. JS2: N-S/70-90E/W. JS3: N0-20E/20-45W. Sporadic joints N45E/90 and N113/65N. No clear water-bearing joints.	Q-value: 2.1-12.5. Small (0.5m) clay filled weakness zone; Station No. 22.490-22.500. Several clay filled joints. Calcite on some joints.
23.250-23.300. S4 (50 m).	Shaly limestone.	JS1: (fol.) N75-90E/10-30N. JS2:N-S/60E. Sporadic joint: N24E/60W. No clear water-bearing joints.	Q-value: 5.8-10.0. Some clay filled joints.

In the Skaugum area the major faults strike N-S to NNW-SSE (see Figure 6.9). One major fault striking NNW-SSE starts at the lake Semsvannet, and is crossing the tunnel alignment around Station No. 22.030. The same fault zone has a branch striking N-S, which is crossing the tunnel around Station No. 20.960. Another N-S oriented fault is crossing the tunnel around Station No. 20.000. In addition to the above mentioned faults, some faults oriented ENE-WSW exist in the area. However, no major corresponding fault zones were registered in the tunnel.

In the tunnel, one 3 m wide weakness zone parallel with the foliation was registered between Station No. 20.635 and 20.650. But no increased water leakage was encountered within a distance of 140 m from the weakness zone. Hence, the high and extremely high water leakages encountered between Station No. 20.450 and 20.500 were probably not related to the weakness zone between Station No. 20.635 and 20.650.

In section S1 two joint sets were dominating; 1) foliation joints striking N60-80E with varying dip and 2) steep N-S oriented joints. The dominating major faults are oriented N-S to NNW-SSE. Major faults with strike N-S and foliation joints with strike N60E make an angle of 60°, i.e. just marginal to agree with Hypothesis no. 2 (30°-60°). However, the geological mapping did not reveal the foliation joints to be more water-bearing than N-S striking joints. For the other sections the foliation joints make an even larger angle with the major faults. Joint set 2 strikes N-S and generally makes angles less than 30° with major faults. The geological mapping does not indicate any of the joint sets as particularly water-bearing. Thus, this analysis does not support Hypothesis No. 2.

Hypothesis No. 3; *water-bearing discontinuities are sub-parallel with the major principal stress.*

The major principal stress is most likely oriented N-S to NNW-SSE, (Myrvang, 2001). According to Hypothesis No. 2 joint set 2 should be more likely to be water-bearing compared to other joint sets. Analyses of sections with high and extremely high water leakages show that N-S striking diabase dykes and layers of sand- and siltstone gave high water leakage. This indicates that joints parallel with major principal stress are water-bearing. It seems, however, that other factors are more important than the orientation of the joints. Thus, this analysis does not give an unambiguous conclusion concerning Hypothesis No. 3.

When studying the sections with high and extremely high water leakage in the Skaugum tunnel, two factors seem to coincide with high water leakage; folding and geological boundaries (rock type boundaries). The latter will be discussed later in this chapter (Hypothesis No. 7). Concerning folding, it is found that 10 out of 15 sections with high and extremely high water leakage are close to a fold axis. This will be further discussed in Chapter 8.

Hypothesis No. 4; *Water leakage decreases with increasing rock cover.*

The rock cover in the area varies from 4 to 107 m. Figure 7.35 shows a XY-plot of water leakage (l/min per 25 m) versus rock cover (m).

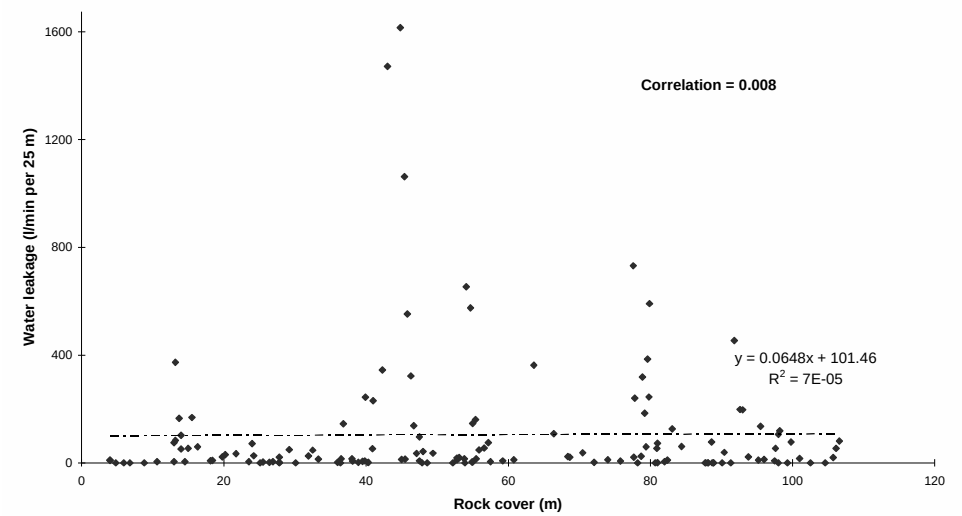

FIGURE 7.35 Water leakage (l/min per 25 m) versus rock cover (m) for the Skaugum tunnel.

The XY-plot gives a very low correlation of 0.008, representing no linear correlation between water leakage and rock cover for the Skaugum tunnel, and does not support Hypothesis No. 4.

Hypothesis No. 5; *Great thickness of permeable soil or a lake/sea above a tunnel gives high water leakage.*

There is no lake above the tunnel alignment of the Skaugum tunnel. The soil thickness varies from 0 to over 10 m, moderate soil cover of 5 to 10 m was registered in shallow valleys oriented ENE-WSW. Greatest soil thickness was above Station No. 19.525 and 19.600 (Norwegian National Rail Administration, 2001). The soil consists of marine deposits, mainly clay, which is more or less impermeable. Only small water leakage, up to 4 l/min per 25 m, was registered below the section with greatest soil thickness. An analysis of water leakage versus soil thickness gave a correlation of 0.034, indicating not very surprisingly no linear correlation between water leakage and soil thickness for the Skaugum tunnel. Hence, this does not support Hypothesis No. 5.

Hypothesis No. 6; *Igneous rocks give higher water leakage than other rock types.*

In the Skaugum tunnel limestone, shaly limestone, shale, siltstone and sandstone were encountered. No large body of igneous rocks exists, but several igneous dykes consisting of syenite, diabase and pegmatite. The main syenite dyke was approximately 85 m wide in

the tunnel and located between Station No. 19.275 and 19.360 (close to the tunnel entrance at Solstad). The diabase dykes were smaller, normally between 1 and 4 m thick. Therefore, only the syenite is included in the histogram in Figure 7.36.

As explained in Section 2.2 the water leakage has been calculated for every 25 m along the tunnel. In some of the 25 m long sections limestone (included nodular limestone) as well as shale were registered, and in such cases it has been chosen to include both in the groups representing the predominant rock type. In sections with only nodular limestone, this has been registered as nodular limestone in the histogram. Figure 7.36 shows a histogram with number of 25 m sections for different rock types versus ranges of water leakage.

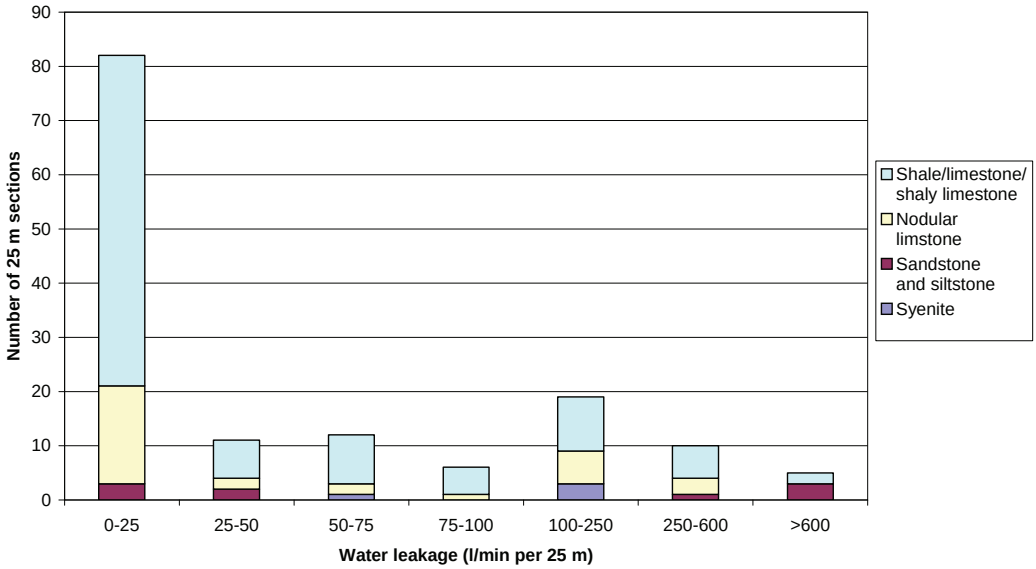

FIGURE 7.36 Distribution of ranges of water leakage (l/min per 25 m) for different rock types in the Skaugum tunnel.

From the histogram it can be seen that highest water leakages were encountered in sandstone/siltstone and shale/limestone/shaly limestone. While the syenite is represented in sections with medium water leakage. In three out of four 25 m sections with syenite represented, the water leakage was higher than 146 l/min, which is above the mean value for the Skaugum tunnel. Higher than average water leakages were also registered in several 25 m sections with diabase dykes, for example between Station No. 22.000-22.025, 22.425-22.450 and 22.700-22.725. It therefore seems that igneous rocks give higher water leakage than average, but not highest. This represents low to medium support to Hypothesis No. 6.

Hypothesis No. 7; *Major rock type boundaries give high water leakage.*

The Skaugum tunnel has considerable variation concerning rock types. The regional geological boundaries between the Bærum- and Oslo-groups (Cambro-Silurian rocks) as shown in Figure 6.9 and 6.10 were difficult to recognise in the tunnel. This is not surprising since the predominant rock types in both groups are shale and limestone. Figure 6.10 illustrates that the Bærum-group was expected in a syncline between Station No. 20.350-20.470. Based on the geological mapping done in the tunnel it seems like shale, limestone and shaly limestone dominated at Station No. 20.389-20.596, while nodular limestone and shale were dominating outside. At Station No. 20.470 a fold axis was registered in the tunnel. The water leakage between Station No. 20.300-20.525 varied a lot, with high and extremely high water leakage in three 25 m long sections, see Figure 7.34.

Furthermore, between Station No. 22.675 and 22.795 shale, siltstone, sandstone and nodular limestone were registered in the tunnel, while nodular limestone and shale were dominating before and after this section. This corresponds well with an anticline where the rock mass in the anticline belongs to the Oslo-group and the rock mass outside belongs to the Bærum-group, see Figure 6.10. The dip direction of the foliation joints changes from North to South at approximately Station No. 22.730, indicating that a fold axis is located there. High and extremely high water leakages were registered in six out of seven 25 m sections between Station No. 22.650 and 22.825.

Medium water leakage was also registered near the syenite dyke between Station No. 19.275 and 19.360. Figure 7.37 shows water leakage versus horizontal distance from rock type boundaries registered in the tunnel. A negative correlation of -0.347 indicates that based on this analysis water leakages in the Skaugum tunnel are related to rock type boundaries. Thus, Hypothesis No. 7 is supported.

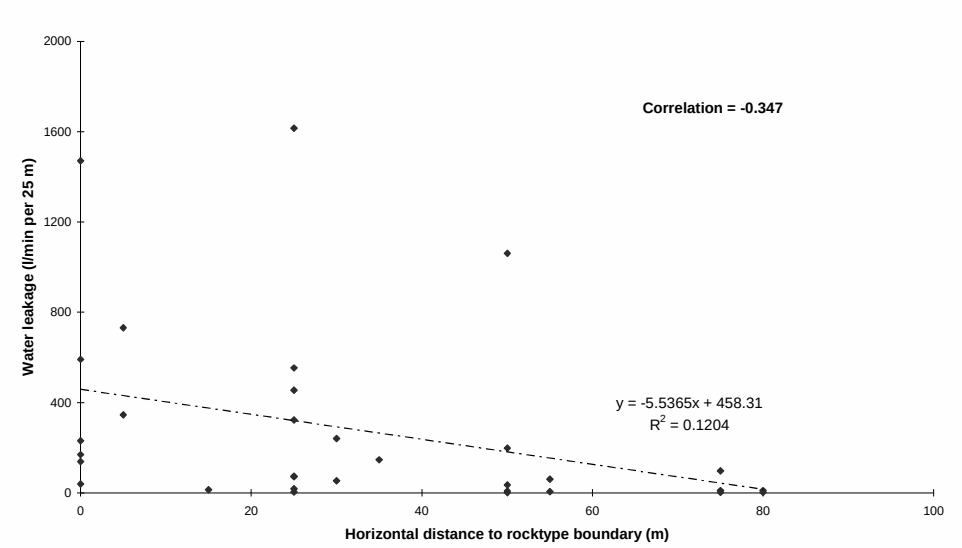

FIGURE 7.37 Water leakage (l/min per 25 m) versus horizontal distance to rock type boundaries for the Skaugum tunnel.

Hypothesis No. 8; *Wide weakness zones give higher relative water leakage (inflow per 25 m) than narrow weakness zones.*

In the Skaugum tunnel no major weakness zones with Q-values lower than 0.1 were encountered. Therefore four weakness zones with Q-values lower than 1.0 and thickness between 5 and 35 m have been analysed. See Table 7.11 and Figure 7.34 for details.

TABLE 7. 11 Description of weakness zones with Q-value<1.0.

Station No.	Registered length with Q-value<1.0.	Description of weakness zone.	Water leakage (l/min per 25).
19.350-19.410.	35 m.	Q-value 0.6-0.8. Highly jointed, several major joints with clay (swelling clay). Diabase and fold axis. Syenite.	230
19.525-19.580.	15 m.	Q-value 0.7. Highly jointed, several major joints with clay (swelling clay). Some crushed rock mass.	0
20.635-20.650.	5 m.	Q-value 0.1. Clay-rich zone.	81
23.610-23.640.	24 m.	Q-value 0.2-0.4. Two clay-rich zones, weathered rock near surface.	9

As Table 7. shows, only small to medium water leakages were registered in the four weakness zones. Even though highest water leakage was registered in the widest weakness zone, there is no evident trend that wider weakness zones give higher water leakage. In the weakness zone between Station No. 19.350 and 19.410 the increased water leakage may be caused by several other factors, such as vicinity to the boundary between syenite and shale, folding and diabase dykes. Thus, this analysis only gives low to medium support for Hypothesis No. 8.

7.6.2 Water leakage versus site investigations

The Skaugum tunnel was thoroughly investigated before construction started. In Table 6.9 the respective investigations are described and brief comments on the results are given. Desk studies, field mapping, refraction seismics, core drilling, 2D resistivity measurements and borehole logging with hydraulic test pumping were carried out.

In the Geological Report (Norwegian National Rail Administration, 2001), a prognosis was made on what pregrouting effort was believed to be necessary to satisfy the water leakage criteria along the tunnel (kg cement/m, length and number of holes). Three tightness classes were defined with class 3 as the strictest.

In section S1 (see Table 7.10) high water leakage was registered between station No. 19.925 and 20.000, which is very close to the fault zone indicated at Station No. 20.000 (see Figure 6.10). Poor rock mass quality was not registered in this section, but a fold axis was registered at Station No. 19.970. Tightness class 1 indicates that high water leakages were not expected in the area of Station No. 20.000. Another section with high and extremely high water leakages was between Station No. 20.300 and 20.525 (see Figure 6.11). The tunnel crossed a syncline with rock mass belonging to the Bærum-group. High pregrouting effort was expected (tightness class 3).

In section S2 (see Table 7.10) medium to high water leakage was encountered in the tunnel, and tightness class 2 was prognosticated. High water leakage was encountered between Station No. 21.975 and 22.050. Figure 7.38 shows an overview of investigations carried out and water leakages encountered in the tunnel for section S2 and part of section S3. A regional fault with a branch which was expected to be sub-parallel with the tunnel was mapped (field mapping) in the area. The 2D-resistivity measurements gave deep low resistivity (approx. 100 ohmm) in two 10 and 20 m wide zones at Station No. 21.960 and 22.030. Between these zones higher resistivity (1000 ohmm) was measured. The contrasts in resistivity levels were not as distinct as for the Lunner tunnel. Highest water leakage came below medium high resistivity (1000 ohmm), between the two zones with low resistivity. The refraction seismic carried out registered a low seismic velocity zone between

Station No. 22.020 and 22.150. This corresponds well with high water leakage encountered in the tunnel between Station No. 21.975 and 22.050.

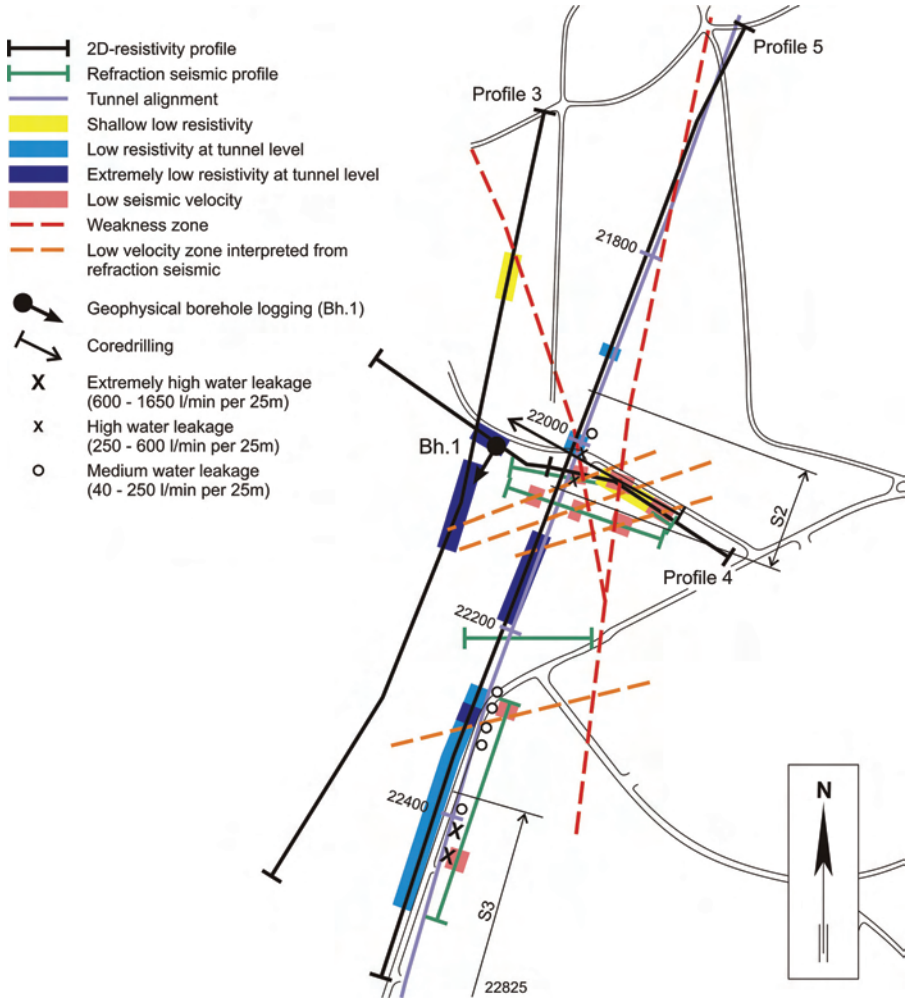

FIGURE 7.38 Overview of investigations carried out and encountered water leakages in section S2 and part of S3 for the Skaugum tunnel, modified from Dalsegg et al. (2003) and Norwegian National Rail Administration (2001).

One borehole (Bh. 1 in Figure 7.38) with geophysical logging was carried out 65 m West of the tunnel alignment. The resistivity in the borehole was generally higher (500-600 ohmm) than registered for the 2D-resistivity measurements in the area. Some sections with jointed rock mass were registered in the borehole, and highest fracturing degree was registered below 100 m. The well capacity was measured to be slightly less than 2100 l/hour. The borehole was located 65 m West of section S2, and is therefore not directly compa-

rable to section S2, although the geological conditions should be quite similar. One core drilling hole intersects the tunnel at Station No. 22.023. The core had RQD around 50 and the Lugeon values were between 3 and 9 at the tunnel level. All the pre-investigation results indicated that medium to high water leakage could be expected in section S2, which corresponds well with the water leakage that was encountered in the tunnel.

In section S3 (see Table 7.10) a considerable variation in water leakage was registered. High and extremely high water leakage was registered between Station No. 22.400-22.450 and 22.650-22.825 (see Figure 6.10). Tightness class 2 was prognosticated for the entire section S3, and the extremely high water leakages encountered were not expected. From geological mapping two fault zones crossing the tunnel approximately at Station No. 22.475 were indicated. At the same location the tunnel crosses the boundary between the Oslo- and Bærum-group (see Figure 6.9 and 6.10). This corresponds quite well with high water leakages between Station No. 22.400 and 22.450. Refraction seismic registered low seismic velocity between Station No. 22.425 and 22.450, which corresponds well with high and extremely high water leakage encountered in the tunnel.

The 2D-resistivity gave low resistivity (100-200 ohmm) between Station No. 22.375 and 22.430. Even lower resistivity was measured between Station No. 22.280 and 22.375 (40-100 ohmm), but only small to medium water leakage was encountered there. This means that for the Skaugum tunnel the lowest resistivity did not give high water leakage, high water leakage was rather characterized by medium resistivity.

In section S4 (see Table 7.10) medium to high water leakages in the tunnel were registered between Station No. 23.250 and 23.300 (see Figure 6.10). Tightness class 2 was prognosticated. No fault or fracture zone was found from the engineering geological mapping. One low seismic velocity zone between Station No. 23.225 and 23.240 was found. This corresponds quite well with the encountered water leakage. One core drilling hole intersects the tunnel at approximately Station No. 23.285, with RQD 80 and Lugeon values around 10 at the tunnel level. This indicates potential for high water leakage.

Table 7.12 gives a summary and brief comments regarding the ability of the different investigation methods to prognosticate the encountered water leakage.

TABLE 7. 12 Ability of site investigations to prognosticate water leakage for section S1, S2, S3 and S4 of the Skaugum tunnel.

Station No.	Desk studies and engineering geological mapping.	Refraction seismic.	2D-resistivity.	Core drilling.	Borehole logging.
19.900-20.650. Section S1. (750 m).	Potential water leakage identified by fault (20.000) and crossing of syncline.	Not carried out.	Not carried out.	Not carried out.	Not carried out.
21.950-22.050. Section S2. (100 m).	Potential water leakage identified by one major fault zone with one branch almost parallel tunnel.	Zones with water leakage identified by low velocity zones; Station No. 22.020-22.150 (2500-4000 m/s).	Potential water leakage identified by deep low resistivity at Station No. 21.960 and 22.030 (10 and 20 m wide).	Potential for moderate water leakage identified by Lugeon values: 1-9L. (Core drilling hole intersects tunnel at Station No. 22.023).	Well capacity ca. 2000 l/hour. 65 m West of tunnel alignment Station No. 22.050-22.100.
22.375-22.825. Section S3. (450 m).	Potential water leakage identified by two fault zones and crossing of syncline.	Zones with water leakage identified by two low velocity zones; 22.285-22.295 and 22.425-22.450. (2500 and 3200 m/s).	Partly identified section with water leakage by deep low resistivity 22.280-22.435. Water leakage encountered 22.400-22.450.	Not carried out.	Not carried out.
23.250-23.350. Section S4. (100 m).	No fault or fracture zone identified.	Potential water leakage identified by one low velocity zone: 23.225-23.240. (3800 m/s).	Not carried out.	Potential water leakage identified by Lugeon values: 7-11L. Core drilling hole intersects tunnel at Station No. 23.285.	Not carried out.

The tightness classes defined before tunnelling started in most cases corresponded quite well with the encountered water leakage, but in section S3 high and extremely high water

leakages were not expected. Concerning the refraction seismics it seems that the low velocity zones are almost straight above the sections which encountered water leakage. The two core drilling holes gave relevant information, and the Lugeon values indicated potential for water leakage for both core drilling holes. Even though the Lugeon values were considerable higher for section S4, the amount of water leakages (l/min per 25 m) were almost the same for the two sections. For the 2D resistivity measurements the results were not as easy to interpret as for the Lunner tunnel. There were cases of very low resistivity in sections that gave neither water leakage or poor rock mass quality. Highest water leakage was registered at the boundary of low resistivity zones and in sections with medium resistivity. The geophysical borehole logging gave relevant information of fracturing and well capacity, even though it was located 50 m West of the tunnel alignment.

7.7 The Storsand tunnel

The data for the Storsand tunnel are not as detailed as for the rest of the tunnels studied in this thesis. Water inflow from probedrilling and pregrouting holes were not registered in detail, and geological mapping was not carried out continuously. Therefore it has not been possible to make boxplot and XY-plot as for the other tunnels in this thesis. However, an analysis of the section in the tunnel where most water leakage was encountered will be done relatively to the hypotheses written in Section 1.3.

7.7.1 Water leakage versus geological parameters

Engineering geological map and longitudinal profile for the Storsand tunnel are shown in Figure 6.11 and 6.12. Between Station No. 18.850 and 18.960 water inflow between 10 and 80 l/min was registered in probedrilling holes (2 to 5 holes of 24 to 30 m length). Unfortunately, water inflow in pregrouting holes was not documented, but according to people working at site it was moderate. When only water leakage in probedrilling holes is known, the water leakage in probedrilling holes must be multiplied by a ratio to estimate likely water leakage in pregrouting holes. In Section 2.3 ratios between water leakage in pregrouting holes and probedrilling holes for the Romeriksporten and Frøya tunnels were calculated, see Table 2.3. The geological conditions in the Storsand tunnel are assumed to be similar as for the Frøya tunnel, and a ratio of 2.5 therefore has been used. Based on this ratio, water leakage between Station No. 18.850 and 18.960 has been calculated to between 25 and 200 l/min per 25 m. According to the data from probedrilling holes the water leakage in the rest of the tunnel was between 0 and 25 l/min per 25 m. Between Station No. 18.700 and 19.200 post-excavation grouting was done sporadically.

Hypothesis No. 1; *The water leakage is lower in rock mass with Q-values lower than 0.1, than in rock mass with Q-values between 0.1 and 10.*

No weakness zones were registered between Station No. 18.850 and 18.960, the Q-value varied between 5.2 and 11.7 and no clay was registered on joints. Thus, it is not possible to say if Hypothesis No. 1 is supported or not.

Hypothesis No. 2; *water-bearing joints make an angle with nearby major faults of* $45° \pm 15°$.

A detailed study of the section with medium water leakage has been done. Relevant geological information for the section between Station No. 18.850 and 18.960 is given in Table 7.13.

TABLE 7. 13 Geological character of one section (ST1) at the Storsand tunnel. ("JS" mean Joint Set, with No. 1 as the predominant etc.).

Station No.	Rock type / dykes	Dominating joint sets. Direction of water-bearing joints.	Description of weakness zones / Q-value.
18.850-18.960. Section ST1. (110 m).	Garnet amphibolite	JS1: (fol.) N80-110E/20-30N. JS2: N30-65E/80-90W. JS3: N93-116E/80-90NE. Generally high variation in strike directions. No clear water-bearing joint sets.	Q-values varied between 5.2 and 11.7. No weakness zones.

The most predominant faults and fracture zones in the area are oriented N-S to NNW-SSE. Joint set 2 makes an angle of 30°-65° with faults striking N-S, and should be water-bearing according to Hypothesis No. 2. This is also the case for joint set 3 which make an angle of 20-60° with weakness zones striking NNW-SSE. The foliation joints do not correspond with Hypothesis No. 2.

The geological mapping done in the section does not reveal any of the joint sets to be more water-bearing than another, and this analysis therefore does not support Hypothesis No. 2.

Hypothesis No. 3; *water-bearing discontinuities are sub-parallel with the major principal stress.*

The major principal stress is estimated to be horizontal and oriented ENE-WSW, (Myrvang, 1991 in Hagelia et al., 2000). Foliation joints and joint set 2 are both approximately parallel with the major principal stress, but both joint sets were registered in parts

of the tunnel with small water leakage as well as in sections (ST1) with medium water leakage. Thus, this analysis gives low to medium support to Hypothesis No. 3.

Hypothesis No. 4; *Water leakage decreases with increasing rock cover.*

For the section between Station No. 18.850 and 18.960 the rock cover is between 137 and 156 m, and the highest rock cover for the entire tunnel is around 160 m just West of section ST1. Hence, the highest water leakage in the Storsand tunnel came in a section with high rock cover. This does not support Hypothesis No. 4.

Hypothesis No. 5; *Great thickness of permeable soil or a lake/sea above a tunnel gives high water leakage.*

The section between Station No. 18,850 and 18,960 is located below woodland in a hillside. The soil thickness is sparse, and the highest water leakage in the tunnel did not come in a section with great soil thickness. This does not support Hypothesis No. 5.

Hypothesis No. 6; *Igneous rocks give higher water leakage than other rock types.*

No large body of igneous rocks exist, but the geological mapping prior to excavation identified one small syenite dyke that was supposed to cross the tunnel around Station No. 20.930. This dyke was not registered by the engineering geologist mapping the tunnel, probably due to incomplete mapping. However, water leakage was registered in the section where the syenite was expected, and no igneous dykes were registered in the section with medium water leakage (Station No. 18.850-18.960). This does not support Hypothesis No. 6.

Hypothesis No. 7; *Major rock type boundaries give high water leakage.*

For the section between Station No. 18.850 and 18.960 the dominating rock type was garnet amphibolite, and in the sections in the vicinity the rock type was amphibolitic gneiss. The exact rock type boundaries were not registered, and it is therefore not possible to say if Hypothesis No. 7 is supported or not.

Hypothesis No. 8; *Wide weakness zones give higher relative water leakage (inflow per 25 m) than narrow weakness zones.*

No weakness zones were registered in the section with medium water leakage, and in the rest of the tunnel the water leakage was small. Therefore, it is not possible to say if Hypothesis No. 8 is supported or not.

7.7.2 Water leakage versus site investigations

Prior to the excavation of the Storsand tunnel desk studies, field mapping, refraction seismic, core drilling, 2D resistivity measurements and borehole logging with hydraulic test pumping were carried out. Geotechnical investigations of soil thickness were also done, but are not included in the following analysis.

Based on results from the geological investigations two sections were mentioned (Hagelia et al., 2001) where pregrouting could be necessary; Station No. 19.580-19.630 and approximately at Station No. 20.725. These assumptions were based on identification of weakness zones striking NNE-SSE, but pre- or post-excavation grouting was not carried out during tunnelling.

The geological mapping indicated weakness zones on both sides of section ST1 (see Figure 6.11); one (strike N-S) crossing the tunnel alignment at Station No. 18.750 and one (strike NE-SW) crossing the tunnel alignment at Station No. 19.150. In the tunnel a major clay filled joint was registered between Station No. 19.190 and 19.220, but almost no water leakages were encountered in the tunnel.

Between Station No. 19.090 and 19.150 (just outside section ST1) the 2D resistivity measurements gave deep low resistivity (1000-2000 ohmm). In the same section (19.090-19.135) post-excavation grouting was carried out, which indicates moderate water leakages during tunnelling. On the other hand, deep low resistivity was measured for long sections particularly in the western part of the tunnel (19.600-20.100) which gave neither water leakage or poor rock mass quality. The low resistivity zone between Station No. 19.090 and 19.150 may have a connection with the major clay filled joint between Station No. 19.190 and 19.220.

The refraction seismic profiles and the borehole logging were located between Station No. 18.660 and 18.770, in minimum 80 m distance from section ST1. The refraction seismic covered two weakness zones mapped in the field. One low velocity zone was registered between Station No. 18.720 and 18.730, which corresponded well with the two weakness zones (see Figure 6.11). But no water leakage was encountered in the tunnel in this section. Geophysical borehole logging was done in the same area (crossing the tunnel at Station No. 18.710). The hydraulic testing gave less than 500 l/hour as well capacity, which is normal for amphibolite and quite small compared to the well capacity registered for example for the Lunner tunnel (7 and 13 m^3/hour). Although the results are not directly valid for section ST1 (because of 140 m distance), the results from the hydraulic testing gave useful information.

No investigations identified section ST1 as particularly water-bearing, and it is therefore difficult to explain why highest water leakages (80 l/min per 25 m) came exactly in this section of the tunnel. It has to be mentioned, however, that the amount of water leakages were considerable lower than for the other tunnels in this study. This implies that the moderate amount of water leakage was not high enough to give anomalies. Small to moderate problems with water leakage were expected in the Storsand tunnel, and this turned out to be correct.

CHAPTER 8 *Discussion*

8.1 Overall comparison of water leakage versus geological parameters for the analysed tunnels

The distributions of water leakages encountered in investigated tunnels vary considerably. All are skewed to the right, with the mean value greater than the median value, and all the outliers are greater than the mean value. Figure 8.1 shows a boxplot representing distributions of water leakages. From this boxplot it can be seen that the Romeriksporten tunnel stands out as the one with highest variation and widest span for the IQR (see Section 2.1). As can be seen from the boxplot, this tunnel had extremely high water leakages over long sections compared to the other tunnels. The opposite extremity is represented by the T-baneringen tunnel, which had small water leakages except for one 25 m section with extremely high water leakage, and the span for the middle 50% of the water leakages is small.

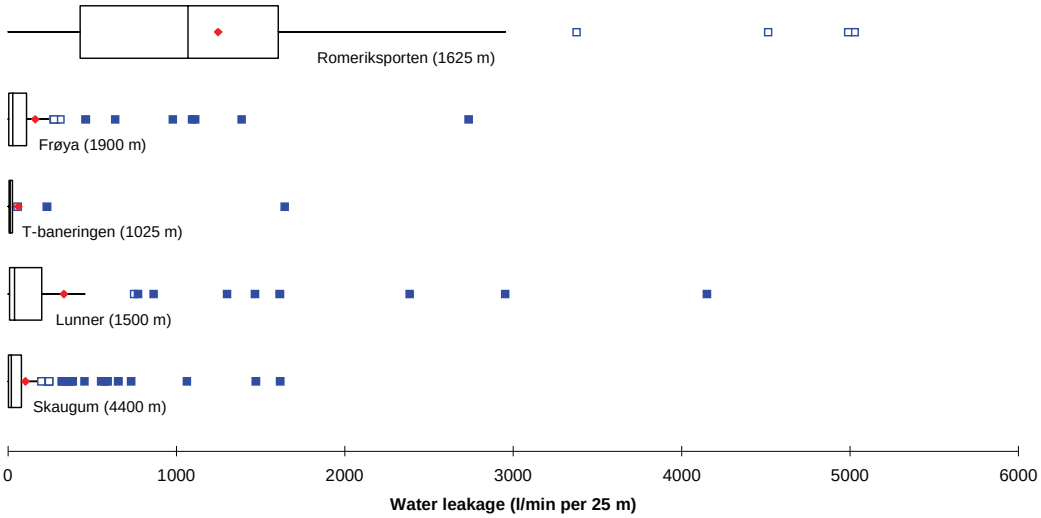

FIGURE 8.1 Boxplots of water leakages (l/min per 25 m). Total length analysed for each tunnel is in brackets.

In Chapter 7 evaluation and analyses for each of the tunnels were done. Calculated correlation values for water leakage versus rock cover, soil thickness, horizontal distance to lake and rock type boundary have been found reasonable relevant for three hypothesis; Hypothesis No. 4, 5 and 7. Also for Hypothesis No. 1 XY-plot and correlation value were calculated, primarily in order to show how water leakage varied for different Q-values. The correlation value was calculated to check whether it was correct or not that no linear correlation exists between water leakage and Q-value, as the hypothesis does not assume linear relationship, see Section 1.3. For the other hypotheses it was not feasible to make XY-plot and calculate correlation values to test the validity. A study of each tunnel with emphasis on the features relevant for the respective hypothesis was done instead.

Literature search has revealed varying limits for what is considered to be a weak correlation and what is considered to be a strong correlation within geological research; Henriksen (2008) considers correlation values, $|r| < 0.3$, as weak correlation, and Cesano et al. (2000) say that "geological or hydrogeological variables that are correlated at $\pm 0{,}5$ often can be considered as a high correlation". The interpretation of correlation values depends on the research area and the complexity. The calculated correlation values in Chapter 7 vary considerably, as illustrated for Hypothesis No. 4, 5 and 7 in Figure 8.2.

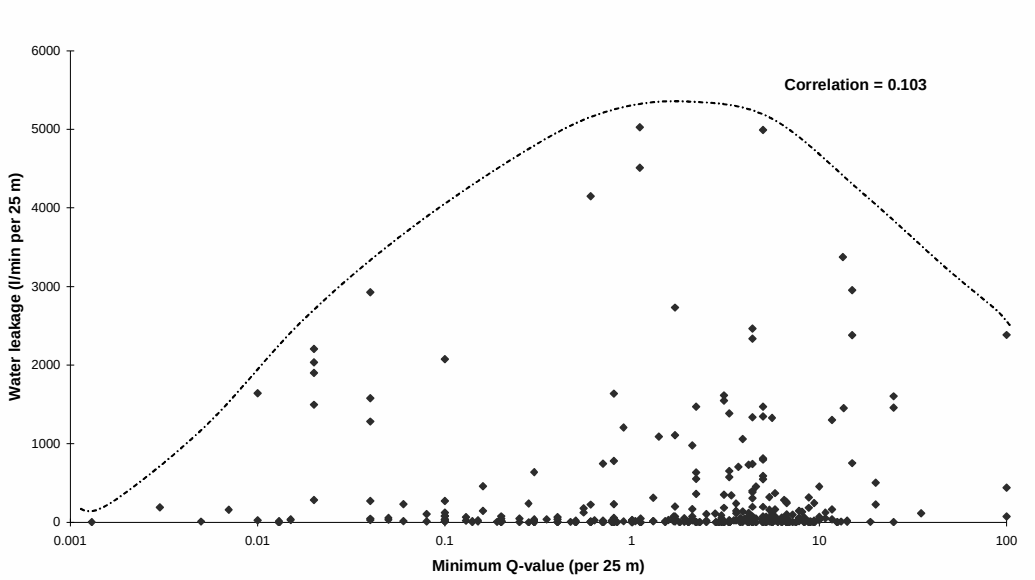

FIGURE 8.2 Distribution of calculated correlation values for all analysed tunnels.

The correlation values are generally quite low; no correlation value is higher than 0.5, and only 4 out of 13 correlation values are higher than 0.3. This illustrates that more than only one parameter is governing the water inflow in hard rock tunnels. Based on the calculated correlation values and the correlation values related to geology as mentioned by Henriksen (2008) and Cesano et al. (2000), the degree of support may be graded as shown in Table 8.1. The ranges are to be considered as guideline values.

TABLE 8. 1 Degree of support based on correlation values.

Degree of support	Negative correlation values	Positive correlation values
No support	-0.2 to 0	0 to 0.2
Low to medium support	-0.3 to -0.2	0.2 to 0.3
Support	-0.5 to -0.3	0.3 to 0.5

In some analyses it has not been possible to decide whether results supported the hypothesis or not due to missing data such as Q-value, orientation of major principale stress or problems to identify which joint set was most water-bearing. Results from analyses done in Chapter 7 with respect to degree of support for the respective hypotheses and tunnels are given in Table 8.2. Correlation values are given in brackets where relevant.

TABLE 8. 2 Summary of degree of support for the hypotheses.

	Hypotheses.							
Tunnel.	**No. 1 (Q-value).**	**No. 2 (45° ±15°)**	**No. 3 (Parallel stress).**	**No. 4 (Rock cover).**	**No. 5 (Soil/lake).**	**No. 6 (Igneous rockt).**	**No. 7 (Rockt boundary).**	**No. 8 (weaknz width).**
Romeriks-porten.	Low to med support.	Support.	Support.	Low to med support. (-0.278).	Support (lake). (-0.353).	Support (pegmatite dykes).	Support.	No support.
Frøya.	Support.	Low to med support.	Support.	No support. (-0.135).	No support (soil). (0.232).	No support.	Low to med support.	Support.
T-bane-ringen.	No support.	Not possi-ble to say.	Support.	No support. (-0.121).	No support (not rele-vant, clay). (0.204)	Support (syenite porphyry dyke).	Support (-0.459).	Not possi-ble to say.
Lunner.	Not possi-ble to say (sparse data).	Low to med support.	Support.	No support. (0.039).	Support (lake). (-0.413).	Support (syenite and syenite por-phyry).	Low to med support (-0.12).	Low to med support.
Skaugum.	Support.	No support.	Not possi-ble to say.	No support. (0.008).	No support (not rele-vant, clay). (0.034).	Low to med support.	Support (-0.347).	Low to med support.
Storsand.	Not possi-ble to say.	No support.	Low to med support.	No support.	No support. (soil).	No support.	Not possi-ble to say.	Not possi-ble to say.

Based on Table 8.2 a discussion concerning each hypothesis will be given in the following:

Hypothesis No. 1; *The water leakage is lower in rock mass with Q-values lower than 0.1, than in rock mass with Q-values between 0.1 and 10.*

For five of the six tunnels a XY-plot with water leakage versus minimum Q-value per 25 m was made as a first approach to check if hypothesis No. 1 was correct or not. The correlation value between water leakage and minimum Q-value was calculated even though Hypothesis No. 1 did not assume linear correlation. The correlation values varied from -0.198 to 0.249. This spread in correlation values clearly shows that there is no linear correlation between Q-value and water leakage. This result is not surprising, since the Q-method is primarily used for geological mapping and decision tool for rock support and not prognostication of water leakage.

Water leakage versus minimum Q-value per 25 m as one XY-plot for 5 out of 6 tunnels is shown in Figure 8.3. An envelope curve is estimated to illustrate how water leakages vary for different Q-values. This shows a slight tendency for water leakage to decrease when the Q-value is lower than 0.1, and it also shows that highest water leakages were encountered in sections with Q-values between 0.6 and 15.0.

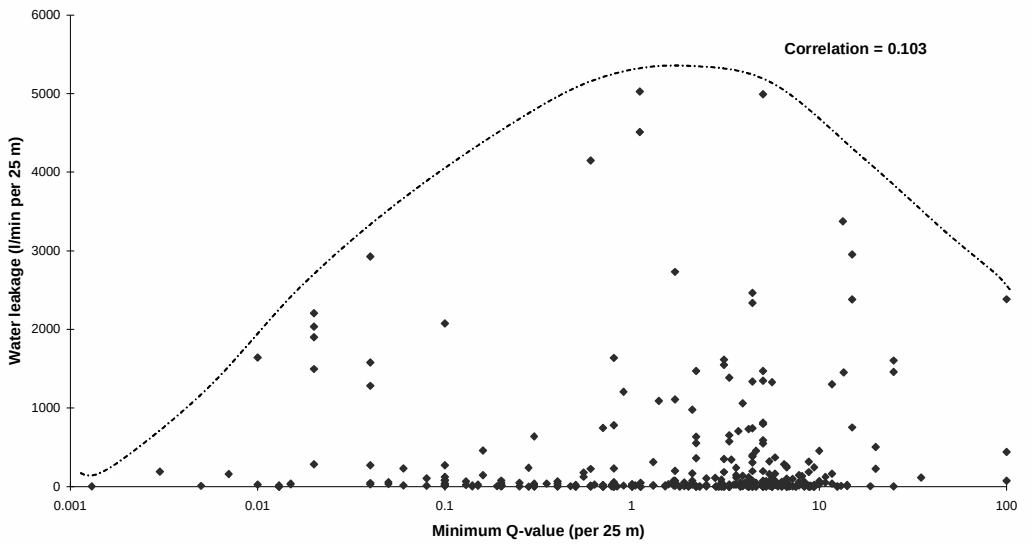

FIGURE 8.3 Water leakage versus minimum Q-value for 5 out of 6 tunnels with envelope curve.

In the Lunner, Skaugum and Storsand tunnel no weakness zones with Q-values lower than 0.1 were registered. Therefore, it was checked if the water leakage decreased in sections with Q-values between 0.1 and 1.0. It was found that water leakage decreased when the Q-value got lower than 0.5. All in all this supports the assumption of Hypothesis No. 1; the cores of weakness/fault zones are often less water-bearing due to clay gouge. The fault core often acts as a barrier for the groundwater flow; as a result the groundwater builds up and is transported along the fault. This was typical in the Frøya subsea tunnel, where major fault zones were encountered.

That highest water leakages were encountered in the damage zone marginal to the core also corresponds well with results described by Ganerød (2008), who found that the inner damage zone had highest permeability, and required twice as much grouting cement than the fault core. One of Henriksen's (2007) conclusions was that largest borehole flow-rates are in the proximal zone of lineaments. Thus, results in this thesis and recent research by Ganerød (2008) and Henriksen (2008) support earlier reports by Caine et al. (1996) and Evans et al. (1997) that the damage zone has the highest permeability within the fault zone.

Hypothesis No. 2; *water-bearing joints make an angle with nearby major faults of* $45° \pm 15°$.

Hypothesis No. 2 is based on Selmer-Olsen's (1981) theory. He studied 11 hydropower tunnels with over 100 m rock cover, and he found that highest water leakages were encountered in joints which made an angle with nearby major faults of $45° \pm 15°$. Selmer-Olsen's theory was mainly empirical, and based on the assumption that highest water leakage was encountered in joints influenced by tectonic stresses of relatively late geological age, in particular where shear faults change character or direction. This corresponds well with results reported by Barton et al. (1995), who found that potentially active faults appear to be the most important hydraulic conduits.

For the Romeriksporten, Frøya and Lunner tunnels the analyses support Hypothesis No. 2. For the rest of the tunnels it was either not possible to say, or no support was found. In the three tunnels which supported Hypothesis No. 2, relatively high water leakage was encountered compared to the other tunnels, and most of the water leakage was connected to joints in the damage zone of major faults. High water leakages were, however, also encountered in jointed rock mass outside the major fault zones.

Table 8.3 shows the predominant directions of water-bearing joints and orientations of major faults for the Romeriksporten, Frøya and Lunner tunnels. Minimum angles between strike of water-bearing joints and major faults are also given for the respective tunnels. It

can be seen from the table that 6 out of 10 water-bearing joint sets correspond well with Selmer-Olsen's theory. The foliation joints at the Frøya tunnel (N30-70E) only marginally agree with Hypothesis No. 2. Consequently, the results give medium support to Hypothesis No. 2. More cases should be tested regarding Hypothesis No. 2 before it can be considered unambiguous.

TABLE 8. 3 Summary of results from analysing Hypothesis No. 2 and 3.

Tunnel.	Direction of major fault.	Direction of water-bearing joints.	Minimum angle (°) between strike of major fault and water-bearing joints.
Romeriksporten.	N45E	N170E (N10W)	55°
		N70E	25°
		N20-55E	0-25°
Frøya.	N65E	N30-70E	5-35°
		N25-40E	25-40°
		N85-100E	20-35°
Lunner.	N10E	N10E	0°
		N110E	80°
		N50E	40°
		N135-170E	20-55°

Hypothesis No. 3; *water-bearing discontinuities are sub-parallel with the major principal stress.*

Hypothesis No. 3 was difficult to test because few stress measurement data exist for the areas in question. Based on literature review and personal discussions with Prof. Myrvang (2008), most likely directions of maximum stress have however been estimated. Results from four out of six tunnels (Romeriksporten, Frøya, T-baneringen and Lunner) support Hypothesis No. 3. For the Skaugum tunnel it was not possible to conclude, and for the Storsand tunnel the results gave low to medium support to Hypothesis No. 3. This clearly indicates that water-bearing discontinuities often are sub-parallel with the major principal stress. But it has to be mentioned that for the Skaugum and T-baneringen tunnel the stresses are most likely not high (Myrvang, 2008), the stress orientation therefore is not expected to have great significance for the conductivity of the joints.

For the Romeriksporten, T-baneringen and Lunner tunnels, the major fault(s) in the area are parallel with estimated major principal stress orientation. For the Frøya tunnel the major principal stress is most likely around N45E (Myrvang, 2008); which means that two of the water-bearing joint sets are sub-parallel with the major principal stress direction (see Table 8.3). It seems like almost all of the water-bearing joint sets can be explained either by Hypothesis No. 2 or 3.

Despite the element of uncertainty related to direction of major principal stress the results in this thesis are convincing and in accordance with earlier and recent research showing that high compressional stresses parallel with discontinuities tend to open it (Mazurak and Bossart, 1996; Singhal and Gupta, 1999; Silva and Jardim de Sá, 2000). Furthermore, recent research shows that fractures approximately parallel with major principal stress, ($\pm 30°$), are most likely to develop shear failure (Barton et al., 1995; Ferril et al., 1999; Rogers, 2003). Hence, it is likely that ground water flow will be encountered in fractures oriented sub-parallel with major principal stress. Results in Henriksen and Braathen (2006) also support this theory.

Hypothesis No. 2 and 3 can be explained by rock mass failure mechanisms; according to Mohr-Coulomb failure criteria the angle of failure is equal to $45° \pm \frac{\Theta}{2}$, where Θ is internal friction angle. The internal friction angle for rock mass varies from $0°$ to $60°$, giving an angle of failure between $15°$ and $45°$. If an in-situ situation is considered, the angle of failure is equal to the angle between fault (failure) and major principal stress. Hence, when the fault is activited, joints making an angle of $15°$ to $45°$ with the fault are parallel with the maximum principal stress, and likely to be open and water-bearing. For typical hard rocks like gneiss and granite the internal friction angle often is high resulting in an acute failure angle. With this in mind it might be that the results from Birkeland (1990); reporting that around 80% of the water-bearing joints had an acute angle with nearby major faults of $0 \pm 15°$ agree quite well with failure mechanism. But the stress situation may change over time, and therefore originally open joints may close due to higher compressional stress perpendicular to the joint. It is therefore important to find today's stress situation.

From the discussion of Hypothesis No. 2 and 3 it is evident that today's stress situation play a significant role for joints ability to lead water. In some cases both Hypothesis No. 2 and 3 can occur at the same, and in such cases it is particularly important to be aware of the risk of high water leakage. This was the case in the Romeriksporten, T-baneringen and Lunner tunnel; see Figure 7.5, 7.20 and 7.28.

Hypothesis No. 4; *Water leakage decreases with increasing rock cover.*

Hypothesis No. 4 is not supported by any of the cases studied in this thesis except for the Romeriksporten tunnel, which had a correlation value of -0.278 for water leakage versus rock cover. For water leakage versus rock cover plotted in one XY-plot the correlation value is 0.364 (see Figure 8.4). This result does not support Hypothesis No. 4, and contradicts theory (Hardin et al., 1982; Carlsson and Olsson, 1986) as well as experience from tunnel projects (Hewitt and Smirnoff, 2005; Carlsson and Olsson, 1977). To further investigate this unexpected result, more detailed analysis has been done.

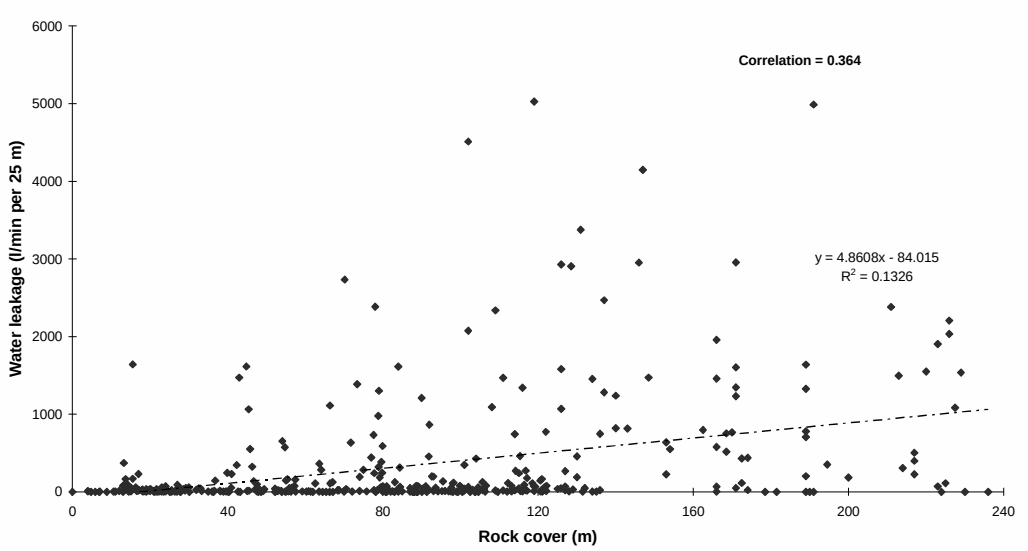

FIGURE 8.4 Water leakage versus rock cover for 5 out of 6 tunnels.

As step 1 in further investigation the correlation values for water leakage versus rock cover have been calculated for sections with different ranges of Q-value. (Q-value lower than 0.1, Q-value between 0.1 and 10.0 and finally Q-value greater than 10.0). The results are shown in Table 8.4.

TABLE 8. 4 Correlation values calculated for different ranges of Q-value.

Sections with following Q-values were included in the calculation of correlation value:	Correlation value.
Q-value < 0.1.	0.609
Q-value between 0.1 and 10.0.	0.312
Q-value > 10.0.	0.273

As can be seen, extremely poor rock mass quality (Q<0.1) gives a correlation value of 0.609, indicating a distinct trend that high water leakage is likely in case of extremely poor rock mass quality and large rock cover. The positive correlation between water leakage and rock cover decreases when the rock mass quality improves.

Step 2 in further investigation has been calculation of correlation values for water leakage versus rock cover including only sections with water leakage (l/min per 25 m) less than: 3000, 1500 and 500. The results are shown in Table 8.5.

TABLE 8. 5 Correlation values including only sections with water leakage (l/min per 25 m) lower than 3000, 1500 and 500 respectively.

Sections with following water leakages were included in the calculation of correlation value:	Correlation value.
Water leakage < 3000 (l/min per 25 m).	0.411
Water leakage < 1500 (l/min per 25 m).	0.352
Water leakage < 500 (l/min per 25 m).	0.258

As can be seen the correlation value is decreasing with decreasing amount of water leakage. Hence, water leakage is less correlated with rock cover with small water leakage.

One possible explanation for the ambiguous results regarding Hypothesis No. 4 may be that when a water-bearing discontinuity is encountered in a deep tunnel it most likely is related to a major structure such as a regional fault or highly jointed dyke oriented sub-parallel with the major principal stress. When a joint first is open at great depth, high hydraulic pressure can give large inflows. This has been experienced for example in the Løtschberg base tunnel in Switzerland (BLS AlpTransit, 2008) and in the Alfalfal hydropower project in Chile (Buen et al., 1994), where the water pressures were 120 and 100 bar, respectively. Also Cesano et al. (2000) found that tunnel sections with high rock cover gave highest possibility of encountering large inflows, but not the small ones.

Hypothesis No. 5; *Great thickness of permeable soil or a lake/sea above a tunnel gives high water leakage.*

Based on reports from Cesano et al. (2000) and Mabee et al. (2002) water leakage in hard rock tunnels is not only depending on properties in the rock mass, but also by the composition and thickness of the overburden. It was therefore considered interesting to test whether this was correct for the 6 tunnels studied in this thesis or not. Both the Romeriksporten and Lunner tunnel have lakes above the alignment, and no thick layers of soil. XY-plots were made (see Figure 7.7 and 7.30) with water leakage versus horizontal distance to lake (limited to approximately 200 m). Correlation values of -0.353 and -0.413 for the

Romeriksporten and Lunner tunnels reflect that high water leakage were encountered close to and below lakes. This supports Hypothesis no. 5, but there may also be other factors contributing to the high correlation, for example faults, stress situation and rock type boundary (the Lunner tunnel).

Possible correlation between water leakage and permeable soil were difficult to find. For the Frøya tunnel the analysis showed that the correlation was low and most likely the influence from fault zones is of greater importance than soil thickness (see Section 7.3). At the T-baneringen and Skaugum tunnels the soil mainly consists of clay and is therefore not directly relevant (impermeable sediments). Analysis also showed that no correlation existed. Likewise, no correlation was found between water leakage and soil thickness for the Storsand tunnel.

Hypothesis No. 6; *Igneous rocks give higher water leakage than other rock types.*

Hypothesis No. 6 is based on the fact that igneous rocks often are more brittle and tend to have more open channels where water can flow than other rock types. The histogram in Figure 8.5 shows the overall distributions of water leakage (l/min per 25 m) for different rock types.

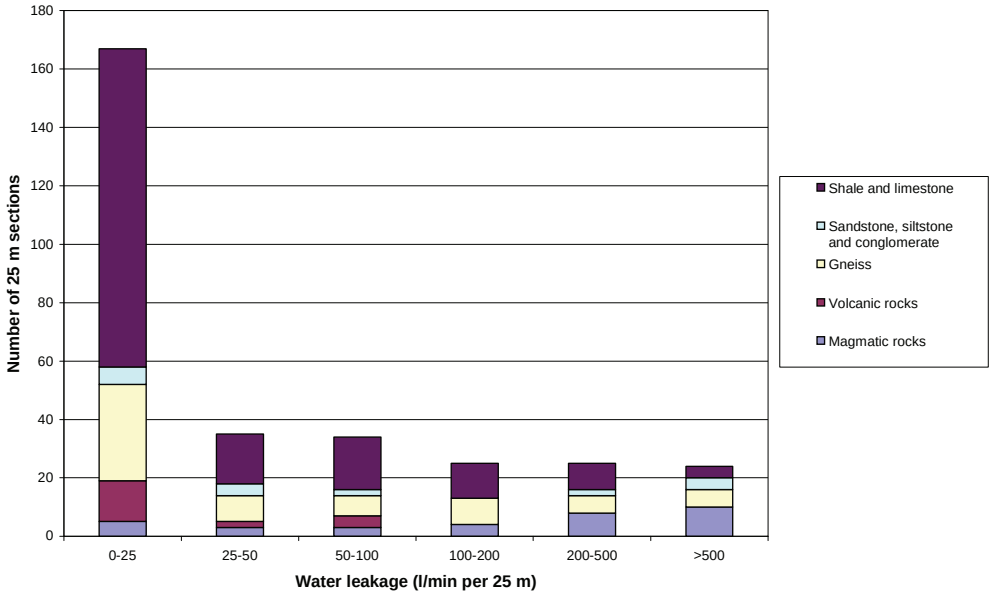

FIGURE 8.5 Number of 25 m sections for different rock types distributed on ranges of water leakage (l/min per 25 m) for all tunnels studied.

More than half of the 25 m sections in igneous rocks (i.e. syenite/syenite dykes) had leakage of more than 200 l/min (see Figure 8.5), while in the volcanic rocks no 25 m sections had more than 100 l/min. Hence, based on this study it is no general trend that igneous rocks give higher water leakage than other rock types. On the other hand the results indicate that magmatic rocks and in particularly syenite and syenitic dykes have higher hydraulic conductivity than other rock types. This agrees well with Klüver's (2000) rock mass classes, where syenite is placed in rock mass class A, representing high hydraulic conductivity.

Hypothesis No. 7; *Main rock type boundaries give high water leakage.*

Hypothesis No. 7 is based on the assumption that the rock mass will be more jointed close to main rock type boundaries than in the surrounding rock mass. In the analyses done in this thesis a distance of 100 m from the rock type boundary is considered. Rock mass further away from the rock type boundary is assumed to be unaffected by the boundary.

For the Romeriksporten-, T-baneringen- and Skaugum tunnel the analyses done in Chapter 7 support Hypothesis No. 7. For the T-baneringen- and Skagum tunnel the correlation values were -0.459 and -0.347, while for the Lunner tunnel the value was only -0.12. Regardless of this rather low correlation value for the Lunner tunnel, extremely high water leakage at the rock type boundary between hornfels and syenite plus some other examples of locally increased water leakage in connection with rock type boundaries, give low to medium support to Hypothesis No. 7.

Main rock type boundaries can typically be formed due to faults, igneous rocks in contact with sedimentary or metamorphic rocks, or boundaries between rock types of same origin; for example sedimentary layers with different composition and character. An example of the latter is the Skaugum tunnel, where high water leakages often came at the boundary between the Oslo- and Bærum groups, both containing sedimentary rocks. As discussed in Chapter 3 dykes can be either tight (water barriers) or highly fractured and water-bearing (Løset, 1981, 2002; Boge et al., 2002). In case of tight dykes groundwater pressure can build up on either side of the dyke. Highest water leakages are often encountered in the damage zone marginal to the fault core, which in some cases also is a rock type boundary. From this follows that different mechanisms can explain that it is reasonable to expect high water leakage close to main rock type boundaries.

In the Skaugum tunnel it was found that 10 out of 15 sections with high and extremely high water leakage were close to a fold axis. The increased water leakage connected to folding can be explained by increased fracturing (cleavage) close to the axial planes (Nordgulen et al., 1998). In some cases faults can be developed from these axial planes,

particularly in anticlines (Løset, 1981). The findings in this thesis thus correspond well with earlier experience in shales and limestones in the Oslo Region.

Hypothesis No. 8; *Large weakness zones give higher relative water leakage (inflow per 25 m) than narrow weakness zones.*

Hypothesis No. 8 was based on the assumption that major weakness/fault zones were formed by distinct geological incidents and therefore may lead to joints with higher hydraulic conductivity than smaller weakness zones. From the analyses done in Chapter 7 no convincing general support has been found for Hypothesis No. 8.

8.2 Water leakage versus site investigations for the 6 tunnels analysed

For each tunnel selected sections have been analysed with emphasis on water leakage and site investigations as described in Section 7.2.2, 7.3.2, 7.4.2, 7.5.2, 7.6.2 and 7.7.2. The sections were selected based on high and extremely high water leakages encountered in the tunnels. In an attempt to summarize the ability of site investigations to prognosticate water leakage three classes are defined, see Table 8.6.

TABLE 8. 6 Classes defining the ability of site investigations to prognosticate water leakage.

Class.	Ability to prognosticate water leakage.	Definition of classes.
1	Able to prognosticate water leakage.	The investigation results identified potential water leakage in the analysed section (±20 m).
2	Partly able to prognosticate water leakage.	The investigation results identified potential water leakage in the analysed section (±40 m). However, the investigation also gave anomalies indicating potential water leakage in sections which turned out to give small or close to no water leakage.
3	Incapable to prognosticate water leakage.	No anomalies indicating potential water leakage were identified in the analysed section (even though water leakage was encountered).
-	Investigation not carried out in this section.	

When the classes regarding ability to prognosticate water leakage are defined for the respective sections, knowledge gained in this thesis regarding water leakage and geological parameters is also taken into account. For example; for the Romeriksporten tunnel engineering geological mapping identified potential water leakage below the lakes Lutvann (section R2) and Puttjern (section R4) based on support by hypotheses No. 2, 3, 4 and 5. In contrast, no prognostication of water leakages was made for these sections prior to the excavation. Table 8.7 gives an overview of the ability of investigations to prognosticate water leakage for the analysed sections.

TABLE 8. 7 Ability of site investigations to prognosticate water leakage for the analysed sections. (- means investigation not carried out in the respective section).

Tunnel.	Section.	Investigation method				
		Desk studies, geol. field mapping.	Refraction seismic.	2D-resistivity.	Core drilling.	Borehole logging.
Romeriksporten.	R1	2	-	-	-	-
	R2	1	1	-	-	-
	R3	3	-	-	-	-
	R4	1	1	-	-	-
Frøya.	F1	2	1	-	-	-
	F2	1	2	-	2	-
	F3	2	1	-	-	-
	F4	2	1 (2)	-	-	-
T-baneringen.	TB1	1	1	-	1	-
	TB2	3	1	-	-	-
	TB3	3	1	-	-	-
	TB4	3	1	-	-	-
Lunner.	L1	1	-	1	-	-
	L2	1	1	1 (2)	1	1
	L3	1	-	2	-	-
Skaugum.	S1	1	-	-	-	-
	S2	1	1	1	1	2
	S3	1	1	2	-	-
	S4	3	1	-	- (1)	-
Storsand.	ST1	3	-	3	-	-

As can be seen from Table 8.7, all sections with high water leakage, except from section R2, R3 and ST1, were identified (Class 1) by at least one investigation method. Hence, most of the sections with high water leakage were, or should have been, prognosticated. It is important to notice that it varies from section to section what preinvestigations were carried out.

Desk studies and geological field mapping were done for all 6 tunnels, and for 14 out of 20 sections studied, possible water-bearing structures were identified. Due to the soil cover and densely built-up areas it was difficult to obtain any detailed geological mapping for the T-baneringen and Skaugum tunnels. A thorough desk study, including studies of aerial

photographs or digital maps is perhaps the most important investigation to identify water-bearing structures, and a good basis for planning of further investigations.

Refraction seismic has been carried out for all 6 tunnels, and for 12 out of 14 sections refraction seismic successfully identified water-bearing weakness zones. In two sections at the Frøya tunnel, section F2 and F4; highest water leakage was encountered somewhat to the side and in far longer sections than expected from the registered low seismic velocity zones, see Figure 7.13. The results from refraction seismics were in good accordance with encountered water leakage in the tunnels.

2D-resistivity has been carried out for the Lunner, Skaugum and Storsand tunnel, and for 2 sections (L1 and S2) out of 6 sections, water leakage was identified clearly by 2D-resistivity, see Table 8.7. For section L2 the fault zone (boundary between hornfels and syenite) which gave water leakage in the tunnel was registered approximately 300 m North of the tunnel alignment. Furthermore, in section L3 shallow low resistivity were registered in two 5 m wide zones, but seem to disappear towards the depth. In the tunnel high water leakage was encountered for longer sections than expected from the 2D resistivity. The results from 2D-resistivity measurements at the Skaugum tunnel were not as good as for the Lunner tunnel. Highest water leakages in the Skaugum tunnel were encountered in sections with medium resistivity (1000 ohmm). The resistivity level was generally lower in the Skaugum tunnel than in the Lunner tunnel, and the contrasts were therefore not as high. It should also be emphasized that the Skaugum tunnel is located in a highly populated area where technical installations might have disturbed the resistivity results (Dalsegg et al., 2003)

For the Storsand tunnel deep low resistivity were registered 130 m outside section ST1, in the same section moderate water leakage was encountered and post-excavation grouting had to be carried out. Deep low resistivity was measured for long sections in the tunnel, but not in section ST1 where moderate to medium water leakage was encountered. From the above summary it is evident that 2D-resistivity often identify water-bearing structures quite well, but there are also results indicating that the ability to prognosticate water leakage is not unambiguous.

Core drilling was carried out for all tunnels except for Romeriksporten and Storsand. Valuable information such as fracturing and content of clay in weakness zones were found. The Lugeon values gave correct information for the Frøya and T-baneringen tunnels. For the Lunner tunnel highest measured Lugeon value was 4.25 L which indicates medium high hydraulic conductivity, but extremely high water leakage up to 2400 l/min per 25 m was encountered in the tunnel. For the Skaugum tunnel the Lugeon values were between 3 and 9 for section S2, and between 7 and 11 for section S4. Encountered water

leakage in section S2 and S4 was 243 and 373 (l/min per 25 m) where the borehole crossed the tunnel alignment. For the Skaugum tunnel the Lugeon values were more in correspondence with the encountered water leakage. This shows that the Lugeon value is not always dependable. If Lugeon values are measured in only one coredrilling hole, the results must be used with care. More than one hole should be carried out to consider the measurements reliable. One bias that has been reported by Thapa et al. (2003) is the fact that many water pressure tests are carried out in vertical boreholes, and therefore do not intersect the most water-bearing joints. The latter was, however, not the case for instance for the Lunner tunnel; where the coredrilling hole was close to horizontal in the section of interest, intersecting the water-bearing structures close to perpendicularly.

Geophysical borehole logging was carried out at the Lunner, Skaugum and Storsand tunnels. For the Skaugum and Storsand tunnels the boreholes were located at 65 and 140 m's distance from the respective water-bearing sections. Although the results are not directly valid for the studied sections, water yields for the boreholes are of particular interest. For section L2 (the fault zone close to the boundary between hornfels and syenite) the geophysical borehole logging gave valuable results, in particular the high well capacity of 7 and 13 m^3/hour gave clear indication of potentially high hydraulic conductivity. In addition to the water well capacity, it was useful to measure by an impeller flow meter the percentage distribution of water ingress along the boreholes (See description in Section 5.8.4). The optical televiewer gave information about fractures in the boreholes (orientation and apertures) as well as rock mass distribution. Particularly, the combination of investigation results as described above gave valuabe results for prognostication of water leakage.

8.3 Recommendations for further research

During the work with this thesis many interesting aspects of engineering geology related to water leakage in tunnels have been investigated, but several complex issues still remain to be analysed. The following issues for further research are considered particularly relevant and important:

- More tunnels should be included in further study to test the reliability of the hypotheses. It would be an advantage also to include ongoing tunnel projects where particularly comprehensive geological mapping and investigation could be possible. The mapping and investigation should focus particularly on water-bearing joints and structures such as faults.
- To further check the validity of Hypothesis No. 3, rock stress measurements in the respective tunnels should be carried out. Three dimensional stress measurements with overcoring is one possibility, an alternative could be hydraulic fracturing (see Section 5.9).

- Results from airborne magnetic measurements should be further studied, to investigate in more detail whether the anomalies correspond with encountered water leakage in the tunnels.
- Multivariate analyses such as principal component analysis, multiple regression and analysis of variance (ANOVA) should be considered in order to better quantify which parameters are influencing groundwater flow the most. In such analyses, it is necessary first to identify mutually independent factors. The encountered water leakages in this analysis also should be divided in major and minor water leakages to analyse if different parameters can explain different amounts of water leakages.
- A logic continuation of the research in this thesis is also to examine rock mass groutability. Is it possible to predict groting effort needed in different sections in the tunnel based on geological parameters from geological field mapping and site investigations?
- Further research should be focused on investigation methodology that may define hydraulic conductivity cheaper and better than the conventional water pressure tests used today. Is it possible to improve the technology?
- Results from geophysical borehole logging with hydraulic testing (well capacity and percentage distribution of water ingress in the borehole) and results from water pressure tests (Lugeon values) should be correlated with encountered water leakage in future tunnels, in order to gain experience on which of the methods are most reliable for prognostication of water leakage in tunnels.

CHAPTER 9 *Conclusions*

The research in this thesis has covered to different aspects:

1. The prime objective - testing of hypotheses regarding the significance of geological parameters to predict water leakage in tunnels.
2. The secondary objective - evaluation of the ability of site investigations to prognosticate water leakage in tunnels.

The main conclusions based on the research are summarized in the following.

9.1 Conclusions regarding water inflow versus geological parameters

Based on the detailed study of 6 Norwegian tunnels, main focus has been on testing the following hypotheses:

1. The water leakage is lower in rock mass with Q-values lower than 0.1, than in rock mass with Q-values between 0.1 and 10.
2. Water-bearing joints make an angle with nearby major faults of $45° \pm 15°$.
3. Water-bearing discontinuities are sub-parallel with the largest principal stress.
4. Water leakage decreases with increasing rock cover.
5. Great thickness of permeable soil or a lake/sea above a tunnel gives high water leakage.
6. Igneous rocks give higher water leakage than other rock types.

7. Major rock type boundaries give high water leakage.
8. Large weakness zones give higher relative water leakage (inflow per 25 m) than narrow weakness zones.

Based on discussion and evaluation of results from analyses described in Chapter 7, the main conclusions are as follows:

Hypothesis No. 1: support. There was a slight tendency that water leakage decreased in rock mass with Q-values lower than 0.1. Highest water leakages were encountered in the damage zone marginal to faults/weakness zones cores, with typical Q-values between 0.6 and 15.

Hypothesis No. 2: medium support. Many of the water-bearing joints and weakness zones made an angle with nearby major faults of $45° \pm 15°$.

Hypothesis No. 3: support. Almost all water-bearing joints were sub-parallel with the major principal stress.

Hypothesis No. 4: no support. For the tunnels studied in this thesis it was found that water leakage in fact increases with rock cover.

Hypothesis No. 5: no support (soil)/support (lake). No correlation was found between great thickness of permeable soil and high water leakage, but lake above tunnels increase the risk of encountering high water leakage.

Hypothesis No. 6: low to medium support. High water leakage was encountered in syenite and syenitic dykes, but not in volcanic rocks.

Hypothesis No. 7: support. It was found that high water lekage often occured in connection with rock type boundaries.

Hypothesis No. 8: no support. No convincing support was found. It seems like thickness of the weakness zone has no significance for the relative water leakage (l/min per 25 m).

9.2 Conclusions concerning the ability of site investigations to predict water leakage

Based on the analyses in this thesis, the following main conclusions have been reached:

- Geological field mapping with emphasis on jointing and orientation of fault/weakness zones was in most cases the most important investigation.
- Refraction seismic has shown good ability for prognosticating water leakage.
- 2D-resistivity has given promising results for prognistication of water leakage in rock mass with generally high resistivity (above 4000 ohmm), but particularly for the Skaugum and Storsand tunnel there was considerable discrepancy between results and encountered water leakage. One advantage with resistivity measurements is the range of depth, which is very good compared to refraction seismic. 2D-resistivity measurements may however be disturbed by technical constructions and give ambiguous results in urban areas. Zones which are parallel with the profile are generally difficult to detect.
- Core drilling with water pressure tests has given valuable results, but for the Lunner tunnel the measured Lugeon values were not representative for high/extremely high water leakages which were encountered in the tunnel.
- Geophysical borehole logging with hydraulic testing (well capacity and percentage distribution of water ingress in the borehole) has given reliable predictions of high hydraulic conductivity.

9.3 Recommendations

Prognostication of water leakage in tunnels is generally a very difficult task. To improve the possibility of making good prognoses, the following recommendations are given based on the research in this thesis:

- The most important investigation is a thorough geological mapping. An understanding of the regional- and structural geology is very important, and particular emphasis should be put on orientation of joints and faults/weakness zones, (cf. Hypothesis No. 1 and 2).
- If possible, rock stress measurements should be carried out in order to define the orientation of the major principal stress, (cf. Hypothesis No. 3.)
- Magmatic rocks, major rock type boundaries and free water table above the tunnel combined with great rock cover should be considered factors increasing the risk of high water leakage. Refraction seismic or 2D-resistivity should be carried out in sections were one or more of these conditions exist.
- In areas where high hydraulic conductivity is expected core drilling with water pressure tests or geophysical borehole logging with hydraulic testing should be carried out . Core drilling should be used if it is considered important to collect rock or clay sam-

ples. If not, geophysical borehole logging with hydraulic testing may be a good alternative.

- It is important to be aware that borehole investigations are only covering a limited volume of the rock mass. Measurement in more than one borehole therefore should be considered, particularly for major projects in complex geology.
- If possible, the investigations should be carried out strictly above the planned tunnel, and not to far to the side. 2D-resistivity measurements should be oriented as perpendicularly to the structure in question as possible. In some cases, two profiles perpendicular to each other may be used.
- Based on available geological information and results from site investigations, a prognosis should be made (only through practice it is possible to improve). It is generally very difficult to predict exact amounts of water leakage in a tunnel, but a classification for example as small, moderate, high and extremely high should in any case be done.

References

Agency for Road and Transport, 2000: “Geotechnical and geological report. T-baneringen. Entreprise B2: Ullevål-Nydalen”, Samferdselsetaten - Oslo kommune, 6 pp. In Norwegian.

Albright, S.C, Winston, W. and Zappe, C.J. 2003: “Data Analysis & Decision Making, with Microsoft Excel”, Second Edition, 975 pp.

Babiker, M. and Gudmundsson, A. 2004: “The effects of dykes and faults on groundwater flow in an arid land: the Red Sea Hills, Sudan.” Journal of Hydrology 297. pp- 256-273.

Swedish Rail Administration, 2008: ”Våra project. Hallandsås”. Project information, http://www.banverket.se/sv/Amnen/Aktuella-projekt/Projekt/1869/Hallandsas.aspx [cited 13. May 2008] In Swedish.

Barton, N., Lien, R. and Lunde, J. 1974: “Engineering classification of rock masses for the design of rock support”, Rock Mechanics 6, pp. 189-236.

Barton, N., Bandis, S. and Bakhtar, K. 1985: “Strength, Deformation and Conductivity Coupling of Rock Joints” International Journal of Rock Mechanics and Mining Sciences, Volume 22, No. 3, June 1985, pp. 121-140.

Barton, A.C., Zoback, M.D., Moos, D. 1995: “Fluid flow along potentially active faults in crystalline rock.” Geology 23, pp. 683-686.

Beard, L. P. 2001: “Assessment of Geophysical Anomalies near Langvatnet, Lunner, Oppland Fylke” Tunnels for the citizen, Report No. 5 / Geological Survey of Norway Report No. 2001.046, 39 pp.

Beitnes, A. 2002: “Lessons to be learned from long railway tunnels” Water control in Norwegian tunnelling, Publication No. 12, Norwegian tunnelling society, pp. 51-57.

Berkowitz, B. 2002: “Characterizing flow and transport in fractured geological media: A review”, Advances in Water Resources 25, pp. 861-884.

Bieniawski, Z.T. 1989: “Engineering rock mass classifications”, New York; John Wiley & Sons. 251 pp.

Birkeland, J.P. 1990: "Relation between engineering geological parameters and water leakage in subsea tunnels" Unpublished thesis (Master Thesis), Norwegian University of Science and Technology, Trondheim, 96 pp. In Norwegian.

BLS AlpTransit, 2008: "Geology. The three geological challenges" http://www.blsalptransit.ch/en/frameset_e.htm [cited 13. May 2008].

Boge, K. 2002: "Grouting technics for rock mass", the Norwegian Tunnelling Society, Handbook No. 1. 110 pp. In Norwegian.

Boge, K., Åndal, T. and Kjølberg R. 2002: "Final report for the pregrouting at the T-baneringen tunnel (stage one, Ullevål-Nydalen)". Norwegian Public Roads Administration, Tunnels for the citizens, Report No. 16, 28 pp. In Norwegian.

Bollingmo, P. 1994: "NSB Gardermobanen -Tunnel Etterstad - Stalsberg. Geological Report", Noteby Report No. 45440-1, 12 pp. In Norwegian.

Braathen, A. 1996: "Fracture zones on Frøya and Northern Hitra." Geological Survey of Norway, Report No. 96.023, 15 pp. In Norwegian.

Braathen, A. and Gabrielsen R.H. 2000: "Fracture zones in rock - structure and definitions", Gråsteinen 7, Geological Survey of Norway, 20 pp. In Norwegian.

Broch, E and Nilsen, B. 1996: "Engineering Geology of Rocks". NTNU Trondheim, Dept. of Geology and Mineral resources Engineering. 294 pp.

Buen, B., Gausereide, L.R. and Mathiesen, C. 1994: "Engineering geology in the design and construction of the Alfalfal hydropower plant in Chile." Proceedings. Integral Approach to Applied Rock Mechanics. (IV South American Congress on Rock Mechanics) Santiago, Chile, 10 pp.

Burke, J. 2004: "Arrowhead east and west - Trying again." World Tunnelling, Volume 17, No 3, pp. 115-119.

Bøe, R., Mørk, M.B.E., Roberts, D. and Vigran, J.O. 2005: "Possible Mesozoic sediments in fault and brecciation zones detected in the Frøya tunnel, Frøyfjorden, Mid Norway", Geological survey of Norway, Bulletin 443, pp. 29-35.

Caine, J.S., Evans, J.P. and Forster, C.B. 1996: "Fault zone architecture and permeability structure." Geology, Volume 24, No. 11, pp. 1025-1028.

Carlsson, A. and Olsson, T. 1977: "Variations of hydraulic conductivity in some Swedish rock types", Proceedings of International Symposium Rockstore, pp. 257-263.

Carlsson, A. and Olsson T. 1986: "Large Scale In-Situ Tests on Stress and Water Flow Relationships in Fractured Rock" Vattenfall, Swedish State Power Board, Design and Construction, Research, Development and Demonstration, 147 pp.

Cesano, D. 2001: "Water leakage into Underground Construction in Fractured Rocks - Geological and Hydrogeological Information as a Basis for Prediction.", Doctoral Thesis, Division of Land and Water Resources, Royal Institute of Technology, Stockholm, 154 pp.

Cesano, D., Olofsson B. and Bagtzoglou A.C. 2000: "Parameters regulating groundwater inflows into hard rock tunnels - a statistical study of the Bolmen tunnel in southern Sweden.", Tunneling and Underground Space technology, Volume 15, No. 2, pp. 153-165.

Cesano, D., Bagtzoglou A.C. and Olofsson B. 2003: "Quantifying fractured rock hydraulic heterogeneity and groundwater inflow prediction in underground excavations: the heterogeneity index." Tunnelling and Underground Space Technology, Vol 18, pp. 19-34.

Cuisiat, F., Skurtveit E. and Kveldsvik V. 2003: "Prediction of leakage into Lunner Tunnel based on discrete fracture flow models." Tunnels for the citizen, Report No. 27, (NGI Report No. 20001042-2), 56 pp. In Norwegian.

Dahlin, T., 1993: "Automation of 2D resistivity surveying for engineering and environmental applications", Doctoral thesis, Lund University, Sweden, 187 pp.

Dalsegg, E. and Rønning, J.S. 2002: "Geophysical measurements Langvatnet - East, Lunner, Oppland." Tunnels for the citizen, Report No. 21 / Geological Survey of Norway, Report No. 2002.106. In Norwegian, 11 pp.

Dalsegg, E., Elvebakk H. and Rønning J.S. 2003: "Results from geophysical measurements and borehole logging. Jong - Asker." Tunnels for the citizen, Report No. 34/ Geological survey of Norway, Report No. 2003.006. 61 pp. In Norwegian.

Dalsegg, E., Elvebakk, H., Rønning J.S., Mauring E. and Tønnesen J.F. 2004: "Geophysical measurements and borehole logging, E39, Skaun, Sør-Trøndelag." Tunnels for the citizen, Report No. 36 / Geological Survey of Norway Report No. 2003.067, 80 pp. In Norwegian.

Dehls, J.F., Olesen O.,Bungum H., Hicks E.C., Lindholm C.D., Riis F. 2000: "Neotectonic map: Norway and adjacent areas, 1:3 000 000. Geological Survey of Norway, Trondheim.

El Tani, M. 1999: "Water inflow into tunnels." Proceedings of the World Tunnel congress ITA-AITES, Oslo, Balkema, pp. 61-70.

El Tani, M. 2003: "Circular tunnel in a semi-infinite aquifer.", Tunnelling and Underground Space Technology, Volume 18, pp. 49-55.

Elvebakk H., Rønning J.S., 2001a: "Borehole logging. Testing and comparison of Optical and Acoustic Televiewer." Tunnels for the citizen, Report No. 9, Norwegian Public Roads Administration, (NGU Report 2001.011), 42 pp. In Norwegian.

Elvebakk, H., Rønning J.S. 2001b: "Inspection of boreholes by optical televiewer above the Romeriksporten tunnel. Correlation to water leakages and stability." NGU Report 2001.09, 51 pp. In Norwegian.

Elvebakk, H. and Rønning J.S. 2002: "Borehole logging in rock well, Holmedal, Sunnfjord. A verification of hydrogeological model with respect to compressional stresses, fracturing and flow direction." Tunnels for the citizen, Report No. 26, Norwegian Public Roads Administration, 33 pp. In Norwegian.

Elvebakk, H., Rønning J.S., Storrø, G. 2002: "Borehole logging in rock well, Folvåg, Sunnfjord. A verification of lineament model with respect to fracturing and water yield." Tunnels for the citizen, Report No. 25, Norwegian Public Roads Administration, 39 pp. In Norwegian.

Elvebakk, H. and Rønning, J.S. 2003: "Measurements of water inflow in borehole. Identification of water ingress." Poster presentation at the 12th Seminar on Hydrogeology and Environmental Geochemistry, Geological Survey of Norway, Trondheim 4th-5th February 2003. Abstract in NGU Report 2003.015, pp. 61-62, In Norwegian.

Evans, J.P., Forster, C.B., Goddard, J.V. 1997: "Permeability of fault-related rocks and implications for hydraulic structure of fault zones." Journal of Structural Geology 19, pp. 1393-1404.

Fejerskov, M. 1993: Stress in rock mass in Norway on-shore and off-shore", Rock Blasting Conference, Norwegian Tunnelling Association, Oslo, pp. 25.1-25.17, in Norwegian.

Ferril, D.A., Winterle, J., Wittmeyer, G., Sims, D. Colton, S., Armstrong, A. and Morris A.P. 1999: "Stressed Rock Strains Groundwater at Yucca Mountain, Nevada." GSA Today 9 (5), pp. 1-8.

Fetter, C.V. 2001: "Applied hydrogeology" 4th ed. Prentice Hall, New Jersey.

Freeze, R.A. and Cherry, J.A. 1979: "Groundwater", Englewood Cliffs, NJ: Prentice-Hall, Inc. 553 pp.

Ganerød, G.V. 2008: "Predictive permeability model of extensional faults in crystalline and metamorphic rocks; verification by pre-grouting in two sub-sea tunnels, Norway." Journal of Structural Geology, In press, available online 10. April 2008, 12 pp.

Ganerød, G. V., Rønning, J.S., Dalsegg, E., Elvebakk, H., Holmøy, K.H., Nilsen, B., and Braathen, A. 2006: "Comparison of geophysical methods for sub-surface mapping of faults and fracture zones in a section of the Viggja road tunnel, Norway" Bull Eng Geol Env, pp. 231-243.

Geological Survey of Norway, 2001-2002: "Results from geophysical and geological investigations for the Lunner tunnel.", Tunnels for the citizen, Report No. 7, 10, 20 and 21. In Norwegian.

Goodman, R.E., Moye, D.G., Van Schalkwyk, A., Javendel, I. 1965: "Ground water inflows during tunnel driving", Bull. Ass. Eng. Geologists, Vol 2, No. 1, pp. 39-56.

Grasseli, G., Wirth, J., Zimmerman, R.W., 2003: "Surface parameters for quantifying the hydro-mechanical anisotropy of rock discontinuities", 10th Congress of the ISRM, Technology roadmap for rock mechanics, South Africa, pp. 415-422.

Graversen, O. 1984: "Geology and Structural Evolution of the Precambrian Rocks of the Oslofjord-Øyeren Area, Southeast Norway", Geological Survey of Norwy, Bulletin 398, 50 pp.

Grimstad, E. and Barton, N. 1993: "Updating the Q-system for NMT" Proc. Int. Symp. on Sprayed Concrete, Fagernes, Norway 1993, Norwegian Concrete Association, Trondheim: Tapir Press, pp. 46-66.

Gudmundsson, A. 1999: "Postglacial crustal doming, stresses and fracture formation with application to Norway." Tectonophysics 307, pp. 407-419.

Gudmundsson, A. 2000: "Fracture dimensions, displacements and fluid transport", Journal of Structural Geology 22, pp 1221-1231.

Gudmundsson, A., Berg S.S., Lyslo, K.B. and Skurtveit E. 2001: "Fracture networks and fluid transport in active fault zones", Journal of Structural Geology 23, pp. 343-353.

Gudmundsson, A., Fjeldskaar, I. and Gjesdal, O. 2002: "Fracture-generated permeability and groundwater yield in Norway" Geological Survey of Norwy, Bulletin 439, pp. 61-77.

Hagelia, P., Gressetvold, I. and Lynneberg, T.E. 2000: "New E39 - Øysand-Thamshamn. Geological site investigations for six tunnels", Norwegian Public Roads Administration, Oppdrag U204B, Report No. 1, 68 pp. In Norwegian.

Hagelia, P., Gressetvold, I. and Lynneberg, T.E. 2001: "New E39 - Øysand-Thamshamn. Engineering geological registrations for six tunnels. Tender report", Norwegian Public Roads Administration, Oppdrag U204B, Report No. 2, 39 pp. In Norwegian.

Hagen, K.F., 2003: "Analyses of pregrouting carried out in the Lunner tunnel." Unpublished Master Thesis at NTNU, Norwegian University of Science and Technology, Dept. of Geology and Mineral Resources Engineering, Trondheim, 104 pp. In Norwegian.

Hardarson, B.A. & Haraldson, H. 1998: "Harnessing the flood at Isafjordur." Tunnels and Tunneling International. March 1998, pp. 17-20.

Hardin, E. L., Barton, N., Lingle R., Board M. P. and Voegele M. D. 1982: "A heated flatjack test series to measure the thermo-mechanical and transport poperties of in situ rock mass" Office of Nuclear Waste Isolation, Columbus, Ohio, ONWI-260, 193 pp.

Heggstad, S. and Nålsund, R. 1996: "The Frøyatunnel - demanding site investigations of exceptionally poor rock mass conditions" Rock Blasting Conference, Norwegian Tunnelling Association, Oslo, pp. 33.1-33.20, in Norwegian.

Henriksen, H. 2007: "The role of Regional and Local Variables in the Hydrogeology of the Solid Rocks of Fennoscandia." Dissertation for the degree of philosphiae doctor, University of Bergen, Norway, 175 pp.

Henriksen, H. 2008: "Late Quaternary regional geodynamics and hydraulic properties of the crystalline rocks of Fennoscandia". Journal of Geodynamics, Volume 45, Issue 1, pp. 49-62.

Henriksen, H. and Braathen, A. 2006: "Effects of fracture lineaments and in-situ rock stresses on groundwater flow in hard rocks: a case study from Sunnfjord, western Norway." Hydrogeology Journal 14, pp. 444-461.

Heuer, R.E., 1995: "Estimating rock tunnel water inflow." Proceedings - Rapid Excavation and Tunnelling Conference, pp. 41-66.

Hewitt, P. and Smirnoff, T. 2005: "Groundwater control for Sydney tunnels." Proceedings - Rapid Excavation and Tunnelling Conference, pp. 433-445.

Hoek, E. and Bray, J.W. 1981: "Rock Slope Engineering" Revised Third Edition, Institution of Mining and Metallurgy, Elsevier Applied Science, London and New Yourk, Chapter 6: "Groundwater flow; permeability and pressure", pp. 127-149.

Holmøy, K.H. 2002: "Results from site investigations at the Lunner tunnel, and prognosis for water leakages." Tunnels for the citizen, Report No. 15. 25 pp. In Norwegian.

ISRM 1978a: "Suggested mehods for determining the strength of rock materials in triaxial compression" Int. j. Rock Mech. Min. Sci. & Geomech. Abstr. Volume 15, Issue 2, pp. 47-51.

ISRM 1978b: "Suggested methods for the quantitative description of discontinuities in rock masses" Int. J. Rock Mech. Min. Sci. & Geomech. Abstr. Volume 15, Issue 6, pp. 319-360.

ISRM 1979: "Suggested methods for determining the uniaxial compressive strength of rock materials and deformability of rock materials" Int. Soc. Rock Mech. Min. Sci. & Geomech. Abstr. Volume 16, Issue 2, pp. 137-140

ISRM 1985: "Suggested method for determining point load strength. Int. J. Rock Mech. Min. Sci. & Geomech. Abstr. Volume 22, Issue 2, pp. 51-60.

ISRM 1987: "Commision on Testing Methods - Suggested methods for rock stress determination. Int. J. Rock Mech. Min Sci. & Geomech. Abstr. Volume 24, Issue 1, pp. 53-73.

ISRM 1999: "Suggested mehods for laboratory testing of swelling rocks" Int. J. Rock Mech and Min Sci, Volume 36, pp. 291-306.

ISRM 2003a: "Suggested Methods for rock stress estimation - Part 2: overcoring methods" Int. J. Rock Mech and Min Sci, Volume 40, pp. 999-1010

ISRM 2003b: "Suggested Methods for rock stress estimation - Part 3: hydraulic fracturing (HF) and/or hydraulic testing of pre-existing fractures (HTPF)" Int. J. Rock Mech and Min Sci, Volume 40, pp. 1011-1020.

Iversen, E. 1998: "Highway No. 35 Grualia - Slettmoen, Coredrilling for tunnel below the lake Langvann, Lunner" Norwegian Public Road Authority (Laboratory), Task No. E-218 A, Report No. 3, 8 pp.

Jacobs Associates and Golder Associates, 2001: "Geotechnical Baseline Report, Upper diamond Fork Project." Report to Central Utah water Conservancy District.

Jaeger, J.C. and Cook, N.G.W. 1979: "Fundamentals of Rock Mechanics" Third Edition, Chapman & Hall, London, 593 pp.

Karlsrud, K. 2002: "Control of water leakage when tunnelling under urban areas in the Oslo region." Water control in Norwegian tunnelling, Publication No. 12, Norwegian tunnelling society, pp. 27-33.

Kearey, P. and Brooks, M. 1991: "An Introduction to Geophysical Exploration", Second Edition, Oxford, Blackwell Scientific Publications, 245 pp.

Kirkaldie, L. 1988: "Rock classification systems for engineering purposes." STP 984. Amer. Society for Testing Materials, 167 pp.

Kirkeby, T. and Iversen, E. 1996: "Highway No. 35 Grualia - Slettmoen, Tunnel through Tveitmarktoppen. Report on main geological investigations" Norwegian Public Road Authority (Laboratory), Task No. E-218 A, Report No. 2, 27 pp.

Kirkeby, T. and Kveen, A. 2002: "Geological mapping between Station No. 2340 and 3940, The Lunner tunnel." Norwegian Public Roads Administration, In Norwegian.

Kitterød, N.O., Colleuille, H., Pedersen, T.S., Langsholt, E. and Dimakis, P. 1998: "Groundwater flow in fractured rock - Numerical modelling of groundwater inflow in the Romeriksporten", The Norwegian Water Resources and Energy Directorate (NVE), Document No. 11. 42 pp. In Norwegian.

Klüver, B.H. 2000: "Pregrouting in hard rock", Internal Report No. 2151, Norwegian Public Roads Administration, Oslo, 21 pp. In Norwegian

Knutsson, G. and Morfeldt, C.O. 1995: “Groundwater - theory and applications.” Text book, Stockholm, In Swedish.

Kveldsvik, V., Hagen, A. W. and Jensen, T. G. 1999: ”T-baneringen Bergslia - Nydalen. Evaluation of inflow criteria for underground tunnel”, NGI Report No. 991010-1, Oslo, 19 pp. In Norwegian.

Lei, S. 1999: “An analytical solution for steady flow into a tunnel.”, Ground Water Vol 37 (1), pp. 23-26.

Lie, H. and Gudmundsson, A. 2002: “The importance of hydraulic gradient, lineament trend, proximity to lineaments and surface drainage pattern for yield of groundwater wells on Askøy, West Norway.” Geological Survey of Norway, Bulletin 439, pp. 51-60.

Lien, J.E., Mehlum, A., Moe, L.E., Lillevik, S. and Soknes, S. 2000: "The Frøya tunnel and adjoining road network - Final Report", Norwegian Public Roads Administration, 61 pp. In Norwegian.

Lindstrøm, M. and Kveen, A. 2005: "Tunnels for the citizen - Final Report." Norwegian Public Roads Administration, Tunnels for the citizens, Report No. 105, 62 pp. In Norwegian.

Lohman, S.W. 1972: “Ground-water hydraulics.” U.S. Geological Survey Professional Paper 708.

Loke, M.H. 2007:”Geoelectrical Imaging 2D & 3D”. Instruction manual, RES2DINV Description ver. 3.55. http://www.geoelectrical.com, [cited 1. October 2007].

Lombardi, G., 2002: Private communication with El Tani, M.

Louis, C. 1969: “A study of groundwater flow in jointed rock and its influence on the stability of rock masses” Imperial College, London, Rock Mechanics Report No. 10, 90 pp.

Lugeon, M. 1933: “Barrages et Géologie”, special edition 1979, Fourth International Congress on Rock Mechanics, Montreux (Suisse), 127 pp. In French.

Løset, F. 1981: “Geological engineering experience from the sewage tunnel Lysaker - Slemmestad.” Rock Blasting Conference, Norwegian Tunnelling Association, Oslo, pp. 31.1-31.11, in Norwegian.

Løset, F. 2002: "Geology of the Norwegian tunnels", Norwegian Geotechnical Institute, 90 pp. In Norwegian.

Løset, F. and Kveldsvik V. 2003: "Metro-line Ullevål stadion - Nydalen, preliminary investigations and pregrouting" Internal Report No. 2331; and Tunnels for the citizen, Report No. 33. 51 p. (NGI Report No. 20001042-4), in Norwegian.

Mabee, S.B., Curry, P.J. and Hardcastle, C. 2002: "Correlation of Lineaments to Ground Water Inflows in a Bedrock Tunnel." Ground Water, Volume 40, No. 1. pp. 37-43.

Mazurak, M., Bossart, P. 1996: "Structural evolution of Äspö and initial characterization of seclected water-conducting features." In Mazurek, M., Bossart, P., Eliassen, T. 1996: "Classification and characterization of water-conducting features at Äspö. Results of investigations of the outcrop scale. SKB (Swedish Nuclear Fuel and Waste Management Co) International Report ICR 97-01, Stockholm pp. 17-40.

Moen, K. and Holmøy, K.H. 1997: "Geological mapping; Romeriksporten" Unpublished project documents.

Mount Sopris, 2007: "Mount Sopris Instruments Co., Inc. Products, Downhole Tools" http://www.mountsopris.com/downhole_tools.htm [cited 1 October 2007].

Muskat, M. 1937: "The flow of Homogeneous Fluid Through Porous Media, Mc Graw Hill, pp. 175-181.

Myrvang, A. 1983: "Practical use of rock stress and deformation measurements." Norwegian Soil and Rock Engingeering Association, Publication No. 12, pp. 9-14.

Myrvang, A. 1991: "Rock stress and rock stress problems in Norway." in Hudson J.A. Comprehensive Rock Engineering, Vol 3, Rock Testing and Site Characterization. pp. 461-471.

Myrvang, A. 2008: Oral discussion with author.

NBR (Norges Byggstandardiseringsråd), 1988: "Geotechnical Design - Foundation, Ground and Subsurface Work. Norwegian Standard NS3480. Pronorm, Oslo, 11 pp. In Norwegian.

NBR (Norges Byggstandardiseringsråd), 1997: "Eurocode 7: Geotechnical design - Part 1: General Rules." Norwegian Standard NS-ENV 1997-1" Pronorm, Oslo, 107 pp. In Norwegian.

Nilsen B., Palmström A. and Stille H. 1997: "The Frøya tunnel. Analysis of excavation and rock support methods as basis for cost estimate, feasibility and risk assessments." Internal project report, 50 pp. In Norwegian.

Nilsen, B. and Palmstrøm, A. 2000: "Handbook No 2, Engineering Geology and Rock Engineering", Norwegian Group for Rock Mechanics (NBG), ISBN 82-91341-33-8, Tapir, 249 pp.

Nordgulen, Ø., Lutro, O., Solli, A., Roberts, D. and Braathen, A. 1998: "Geological- and structural geological mapping for Norwegian National Rail Administration Construction in Asker and Bærum." The Geological Survey of Norway, Report No. 98.124. 27 pp. In Norwegian.

Nordgulen, Ø and Dehls, J. 2003: "Use of digital elevation data for lineament analysis. With examples from Oslo municipal" The Geological Survey of Norway, Tunnels for the citizens, Report No. 24, 10 pp. In Norwegian.

Norwegian National Rail Administration, 2001: "Engineering geological Report, Contract JA1, Parcel Solstad-Hønsveien." Document No.: USA72-6-R-001613 Rev. 01 B, 46 pp. In Norwegian.

NSB Gardermobanen A/S, 1994: "Contract. Tunnel Etterstad-Stalsberg (Romeriksporten). Book 2. Specifications and quantities." 298 pp. In Norwegian.

Nålsund R., Heggstad S., Mehlum A. and Aagaard B. 1996: "Analysis of excavation methods and rock support." Internal project report, 21 pp. In Norwegian.

Odling, N.E. 1997: "Scaling and connectivity of joint systems in sandstones from western Norway." Journal of Structural Geology, Volume 19, No. 10, pp. 1257-1271.

Olesen, O., Blikra, L.H., Braathen, A., Dehls, J.F., Olsen, L., Rise, L., Roberts, D., Riis, F., Faleide, J.I. and Anda, E. 2004: "Neotectonic deformation in Norway and its implications: a review." Norwegian Journal of Geology, Volume 84, pp. 3-34.

Olesen, O., Dehls, J.F., Ebbing J., Henriksen, H., Kihle, O. and Lundin, E. 2006: "Aeromagnetic mapping of deep-weathered fracture zones in the Oslo Region - a new tool

for improved planning of tunnels." Norwegian Journal of Geology, Volume 87, pp. 253-267.

Olofsson, B., 1991: "Impact on ground water conditions by tunnelling in hard rock crystalline rocks." Ph.D. dissertation, Department of Land and Water Resources, Royal Institute of Technology, Stockholm, Sweden, TRITA-KUT 91:1063.

Olofsson, B. 1994: "Flow of groundwater from soil to crystalline rock." Applied Hydrogeoloy 3 (1994), pp. 71-83.

Olofsson, B., Bjarnason, B., Gustafson G., Leijon B., Stanfors R. and Wallman S., 1988: "The Bolmen tunnel research project.", Swedish Rock Engineering Research Foundation, Stockholm, BeFo 160:2/88.

Olsson, R. and Barton, N. 2001: "An improved model for hydromechanical coupling during shearing of rock joints." International Journal of Rock Mechanics & Mining Sciences 38, pp. 317-329.

Palmstrøm, A. 1995: "RMi - a rock mass characterization system for rock engineering purposes" Dissertation for the degree Doctor Scientiarum, University of Oslo, Norway, 400 pp.

Palmstrøm, A. 1996: "Characterizing Rock Masses by the RMi for Use in Practical Rock Engineering, Part 2: Some practical applications of the Rock Mass index (RMi)." Tunnelling and Underground Space Technology, Volume 11, No. 3, pp. 287-303.

Palmstrøm, A. 2000: "Recent development in estimating rock support by the RMi", Journal of Rock Mechanics and Tunnelling Technology, Volume 6, No. 1, pp. 1-19.

Palmstrøm, A. 2007: "Rockmass.net. Ground characterization and classification in rock engineering" http://www.rockmass.net/rmi/rockproperties.html [cited 9 October 2007].

Palmstrøm, A., Nilsen, B., Pedersen, K. B. and Grundt, L. 2003: "Correct extent of site investigations for underground constructions." Norwegian Public Roads Administration, Tunnels for the citizens, Report No. 101, 130 pp. In Norwegian.

Paulsson, S. 1996: "Romeriksporten, Refraction Seismic investigations by Lutvann" Oppdrag 96271, a.s. GeoPhysix, 3 pp. In Norwegian.

Pedersen, O. C. 1996: “Results from refraction seismic for the T-baneringen, Nydalen” Geomap, Job No. 96828. Report No. 1. 4 pp. In Norwegian.

Pedersen, O. C. 1997a: “Results from refraction seismic for the T-baneringen, Nydalen” Geomap, Job No. 96843. Report No. 1. 4 pp. In Norwegian.

Pedersen, O.C. 1997b: “Results from refraction seismic for the Lunner tunnel.” Geomap, Job No. 97943, Report No. 1. 5 pp. In Norwegian.

Pedersen, O.C. 1999: “T-baneringen Bergslia (ullevål) - Nydalen, Refraction seismic” Geomap, Job No. 991116, Report No. 1. 6 pp. In Norwegian.

Pedersen, O.C. 2003: “The Lunner tunnel refraction seismic profile P1/02 og P2/02.” Geomap, Job No. 221424, Research Report through R & D project “Tunnels for the citizen”.

Pedersen, O.C., Helgebostad, J. and Veslegard, G. 1986: “Measuring the geoelectrical properties of crushed zones in the rock mass - Final Report.” Research project performed by A/S Geoteam, supported by NTNF, (prosjekt BA 0442.14855), Report 9083.01, 34 pp.

Pétursson, G. 2007:”Challenges and completion phase of the Kárahnjúkar project.” http://www.karahnjukar.is/EN/article.asp?catID=434&ArtId=1879 [cited 26. May 2008].

Norwegian Public Roads Administration, 2008: “National guidelines for roads” http://www.vegvesen.no/vegnormaler/ [cited 9. June 2008]. In Norwegian.

Qian, J., Zhan, H., Zhao, W. and Sun F. 2005: “Experimental study of turbulent unconfined groundwater flow in a single fracture”, Journal of Hydrology, Volume 311, 15. pp. 134-142.

Rat, M., 1973: “Ground water flow and distribution of pressures around tunnels” Bull. Liaison du Laboratoire des Ponts et Chaussées 68, pp- 109-124. In French.

Raymer, J.H. 2001: “Predicting groundwater inflow into hard-rock tunnels: Estimating the high-end of the permeability distribution.”, Proceedings - Rapid Excavation and Tunnelling Conference, pp. 1027-1038.

Raymer, J.H. 2005: “Groundwater inflow into hard rock tunnels: A new look at inflow equations.” Proceedings - Rapid Excavation and Tunnelling Conference, pp. 457-468.

Roberts, D and Myrvang A. 2004: “Contemporary stress orientation features in bedrock, Trøndelag, central Norway, and some regional implications.” NGU Bulletin 442, pp. 53-63.

Robertson Geologging, 2007: “Borehole Logging and System Services, Products, Probes” http://www.geologging.com/english/products/probes/probes.html [cited 1 October 2007].

Rogers, S.F. 2003: “Critical stress-related permeability in fractured rocks.” In Ameen, M.S. (ed): “Fracture and In-situ Stress Characterization of Hydrocarbon Reservoirs.” Geological Society London Special Publication 209, pp. 7-16.

Rohr-Torp, E. 1994: “Present uplift rates and groundwater potential in Norwegian hard rocks”, Geological survey of Norway, Bulletin 426, pp. 47-52.

Rønning, J.S. 2003: "Sub project A, Preinvestigations - Final report." Norwegian Public Roads Administration, Tunnels for the citizens, Report No. 102, 66 pp. In Norwegian.

Rønning, J.S., Dalsegg, E. 2001: “Geophysical measurements, Langvatn, Lunner, Oppland.” Norwegian Public Roads Administration, Tunnels for the citizens, Report No. 7, 12 pp. In Norwegian.

Rønning, J.S., Olesen, O., Dalsegg, E., Elvebakk, H. and Gellein, J. 2007: “Deep weathering in the Oslo Region. Demonstration and follow up measurements.”, Geological Survey of Norway, Report No. 2007.034, 50 pp. In Norwegian.

Scheldt, T. 2002: “Comparison of Continuous and Discontinuous Modelling for Computational Rock Mechanics”, Doctoral Thesis, Department of Geology and Mineral Resources Engineering, Norwegian University of Science and Technology, Trondheim, 141 pp.

Schleiss, A.J. 1988: “Design of reinforced concrete lined pressure tunnels.” International Congress of Tunnels and Water, Madrid, Volume 2, Balkema, pp. 1127-1133.

Selmer-Olsen, R. 1971: “Engineering geology. Part 1.” Tapir press, Trondheim, 230 pp.

Selmer-Olsen, R. 1981: “Considerations of large water leakages in deep-seated tunnels.” Rock Blasting Conference, Norwegian Tunnelling Association, Oslo, pp. 21.1-21.15, in Norwegian.

Selmer-Olsen, R. and Blindheim, O.T. 1971: "On the drillability of rock by percussive drilling." Proc. 2nd ISRM Congress, Belgrade. Volume 3 : pp. 5-8.

Shamma, J., Tempelis, D., Duke, S., Fordham E. and Freeman T. 2003: "Arrowhead tunnels: assigning groundwater control measures in a fractured hard rock medium.", Rapid Excavation Tunnelling Conference, Proceedings, pp. 296-305.

Siddans, A.W.B. 2002: "Structural geology using borehole wall imagery: case study of an OPTV log in flagstones, North Scotland." First break, Volume 20, European Association of Geoscientist & Engineers (EAGE), pp. 623-629.

Silva, C.C.N. and Jardim de Sá E.F. 2000: "Fracture chronology and neotectonic control of water wells location in crystalline terranes: an example from the Equador region, north-easternmost Brazil." Revista Brasileira de Geosciências, Volume 30, pp. 346-349.

Singhal, B.B.S. and Gupta, R.P. 1999: "Applied Hydrogeology of Fractured Rocks." Kluwer Academic Publishers, Dorcrecht. 400 pp.

Sjøgren, B. 1984: "Shallow refraction seismics." Chapman and Hall, London, 270 pp.

Stefanussen, W. 2000: "Tunnel in Chile. Experience using Norwegian support methods." Rock Blasting Conference, Norwegian Tunnelling Association, Oslo, pp. 4.1-4.11, in Norwegian.

Steingrímsson, J.H. and Hardarson, B.A. 2000: "Water in basaltic tunnels. Examples from Breidadals- og Botnsheidi tunnel and Hvalfjördur subsea tunnel, Iceland." Rock Blasting Conference, Norwegian Tunnelling Association, Oslo, pp. 37.1-37.16, in Norwegian.

Storrø, G., Elvebakk, H. and Rønning J.S. 2002: "Hydraulic testing of boreholes in hard rock at Grualia, Lunner municipal." Tunnels for the citizen, Report No. 20, Norwegian Public Roads Administration, (NGU Report 2002.051), 50 pp. In Norwegian.

Sættem, J. and Mørk M.B.E. 1996: "The Frøya tunnel. Studies based on vertical borings and regional lineament information." IKU-Report 23.2574.00/01/96 35 pp. In Norwegian.

Thapa, B. B., Nolting R. M., Teske M. J. and McRae, M. T. 2003: "Predicted and observed groundwater inflows into two rock tunnels.", Rapid Excavation and Tunnelling Conference, New Orleans, Proceedings, pp. 555-567.

Tokheim, O. and Janbu, N. 1984: "Flow rates of air and water from caverns in soil and rock.", ISRM Proceeding, Symposium in Rock Mechanics related to caverns and pressure shafts. Aachen. Rotterdam, pp. 1335-1343.

Venvik, R.G.F. 2003: "Fracture systems and stresses orientation along the tunnel alignment Ringveg Vest in Bergen, Norway" ("Bruddsystemer og spenningsfelt tilknyttet tunneltraséen Ringveg Vest i Bergen") Unpublished Master Thesis in Hydrogeology, Hard Rock. Department of Geosciences, University of Bergen, 145 pp.

Veslegard, G. 1987: "Geoelectrical methods" Course in Geophysical Site Investigations, Gol, Norway, 12 pp. In Norwegian.

Villaescusa, E. 1991: "A three dimensional model of rock jointing" Doctoral Thesis, Julius Kruttschnitt Mineral Research Centre, Department of Mining and Metallurgical Engineering, University of Queensland, pp. 14-37.

Wallis, S. 2006: "Long distance TBM operations on account." Tunnels & Tunnelling International (September), pp. 22-24.

Westerdahl, H. 2003: "Seismic modelling; Modelling of seismic characteristics of soil-filled depressions, weakness zones and problems with hanging cables" Norwegian Public Roads Administration, Tunnels for the citizens, Report No. 32, 50 pp. In Norwegian.

Wolff, F.C 1976: "Geological map, Trondheim 1:250 000, Norway." In Norwegian.

Åndal, T. 2001: "Pregouting of "problematic zone" at the T-baneringe tunnel (stage one) Ullevål-Nydalen" Norwegian Public Roads Administration, Tunnels for the citizens, Report No. 3, 15 pp. In Norwegian.

Appendix A

1. Example of a spread sheet where the water leakage per metre has been calculated for a section in the Frøya tunnel.
2. Spread sheet showing how the ratio between water leakage in one pregrouting round (included water leakage in probedrilling holes) and water leakage in probedrilling holes from the same tunnel face has been calculated for the Frøya tunnel.

Table finding the ratio between waterleakage in pregrouting round and probedrilling hole.
Data from the Frøya tunnel (Hitra-side)

From Station no.	Probedrilling (m)	Number of probedrill-ing holes	Max. Water leakage for one hole (l/min)	Total water leakage for probedrilling (l/min)	Water leakage for one hole (mean) (l/min)	Total water leakage for pregrouting round (min.15 holes)	Ratio between pregrouting round and one probedrilling hole (mean)	Ratio between pregrouting round and one probedrilling hole (max)	Ratio between pregrouting round and 2, 3 or 4 probe-drilling holes	Ratio between pregrouting round and 5, 6 or 7 probe-drilling holes
3724	120	4	10	21	5,25	60	11,43	6,00	2,86	*
3969	207	7	2	6	0,86	8	9,33	4,00		1,33
4073	120	4	45	109	27,25	116	4,26	2,58	1,06	*
4100	180	6	100	121	20,17	125	6,20	1,25		1,03
4110	144	6	90	147	24,50	278	11,35	3,09		1,89
4118	126	6	5	23	3,83	40,5	10,57	8,10		1,76
4179	150	5	10	19	3,80	26	6,84	2,60		1,37
4521	162	6	120	248	41,33	384	9,29	3,20		1,55
4526	42	2	60	75	37,50	435	11,60	7,25	5,80	*
4535	51	2	400	650	325,00	2144	6,60	5,36	3,30	*
4550	180	6	240	830	138,33	1931	13,96	8,05		2,33
4560	180	6	18	50	8,33	220	26,40	12,22		4,40
4606	180	6	300	781	130,17	1174	9,02	3,91		1,50
4626	180	6	32	61	10,17	133	13,08	4,16		2,18
4645	180	6	60	114	19,00	297	15,63	4,95		2,61
4982	180	6	36	87	14,50	196	13,52	5,44		2,25
5042	180	6	84	88	14,67	269	18,34	3,20		3,06
5077	180	6	26	70	11,67	127	10,89	4,88		1,81
5123,5	180	6	22	40	6,67	80	12,00	3,64		2,00
5448	180	6	300	638	106,33	1152	10,83	3,84		1,81
						Mean	11,56	4,89	3,25	2,06
						Median	11,12	4,08	3,08	1,85
						Standard deviation	4,83	2,50	1,95	0,81
						Variance	23,29	6,27	3,81	0,65
						Maximum	26,40	12,22	5,80	4,40
						Minimum	4,26	1,25	1,06	1,03
						Numbers	20,00	20,00	4,00	16,00

Appendix A1